VOLUME 38 NOVEMBER 1960 NUMBER 11

Canadian Journal of Chemistry

Editor: LÉO MARION

Associate Editors:

HERBERT C. BROWN, *Purdue University*
A. R. GORDON, *University of Toronto*
C. B. PURVES, *McGill University*
SIR ERIC RIDEAL, *Imperial College, University of London*
J. W. T. SPINKS, *University of Saskatchewan*
E. W. R. STEACIE, *National Research Council of Canada*
H. G. THODE, *McMaster University*
A. E. VAN ARKEL, *University of Leiden*

Published by THE NATIONAL RESEARCH COUNCIL

OTTAWA CANADA

Canadian Journal of Chemistry

Under the authority of the Chairman of the Committee of the Privy Council on Scientific and Industrial Research, the National Research Council issues THE CANADIAN JOURNAL OF CHEMISTRY and five other journals devoted to the publication, in English or French, of the results of original scientific research. Matters of general policy concerning these journals are the responsibility of a joint Editorial Board consisting of: members representing the National Research Council of Canada; the Editors of the Journals, and members representing the Royal Society of Canada and four other scientific societies.

The Chemical Institute of Canada has chosen the Canadian Journal of Chemistry as its medium of publication for scientific papers.

EDITORIAL BOARD

Representatives of the National Research Council

I. McT. Cowan (Chairman), *University of British Columbia*
Léo Marion, *National Research Council*
H. G. Thode, *McMaster University*
D. L. Thomson, *McGill University*

Editors of the Journals

D. L. Bailey, *University of Toronto*
T. W. M. Cameron, *Macdonald College*
F. E. Chase, *Ontario Agricultural College*
H. E. Duckworth, *McMaster University*
Léo Marion, *National Research Council*
J. F. Morgan, *Department of National Health and Welfare, Ottawa*
J. A. F. Stevenson, *University of Western Ontario*

Representatives of Societies

D. L. Bailey, *University of Toronto*
Royal Society of Canada
T. W. M. Cameron, *Macdonald College*
Royal Society of Canada
H. E. Duckworth, *McMaster University*
Royal Society of Canada
Canadian Association of Physicists
P. R. Gendron, *University of Ottawa*
Chemical Institute of Canada
D. J. Le Roy, *University of Toronto*
Royal Society of Canada
J. F. Morgan, *Department of National Health and Welfare, Ottawa*
Canadian Biochemical Society
R. G. E. Murray, *University of Western Ontario*
Canadian Society of Microbiologists
J. A. F. Stevenson, *University of Western Ontario*
Canadian Physiological Society

Ex officio

Léo Marion (Editor-in-Chief), *National Research Council*
J. B. Marshall (Administration and Awards), *National Research Council*

Manuscripts for publication should be submitted to Dr. Léo Marion, Editor-in-Chief, Canadian Journal of Chemistry, National Research Council, Ottawa 2, Canada.
(For instructions on preparation of copy, see **Notes to Contributors** (inside back cover).)

Proof, correspondence concerning proof, and orders for reprints should be sent to the Manager, Editorial Office (Research Journals), Division of Administration and Awards, National Research Council, Ottawa 2, Canada.

Subscriptions, renewals, requests for single or back numbers, and all remittances should be sent to Division of Administration and Awards, National Research Council, Ottawa 2, Canada. Remittances should be made payable to the Receiver General of Canada, credit National Research Council.

The journals published, frequency of publication, and subscription prices are:

Canadian Journal of Biochemistry and Physiology	Monthly	$9.00 a year
Canadian Journal of Botany	Bimonthly	$6.00 a year
Canadian Journal of Chemistry	Monthly	$12.00 a year
Canadian Journal of Microbiology	Bimonthly	$6.00 a year
Canadian Journal of Physics	Monthly	$9.00 a year
Canadian Journal of Zoology	Bimonthly	$5.00 a year

The price of regular single numbers of all journals is $2.00.

Canadian Journal of Chemistry

Issued by THE NATIONAL RESEARCH COUNCIL OF CANADA

VOLUME 38 NOVEMBER 1960 NUMBER 11

NUCLEOPHILIC DISPLACEMENT OF METHYL SULPHONIC ESTERS BY HYDROXIDE ION IN WATER[1]

S. HARTMAN[2] AND R. E. ROBERTSON

ABSTRACT

Rate data for the reaction between OH^- and methyl benzenesulphonate, methyl methanesulphonate, and dimethyl sulphate in water are determined for a series of temperatures. The corresponding k_{OH^-}/k_{H_2O} ratio are found to be 3 to 6 times smaller than those values characterizing the reaction for the methyl halides, and the ratios in all cases are temperature dependent. While the stability of the initial state solvation shell undoubtedly contributes to the difference between the halides and sulphonates in these reactions, it is probable that differences in nucleophilic interaction between the oxygen of the water molecule and the partially empty p orbital of the methyl carbon is a more important factor in determining the characteristic difference.

In a recent paper (1) Fells and Moelwyn-Hughes suggested that the rough constancy of the k_{OH^-}/k_{H_2O} ratio of ~216 for the three methyl halides be taken as evidence for the similarity of the two reactions

$$R{-}X + H_2O = ROH + H^+ + X^-, \quad [1]$$

$$R{-}X + OH^- = ROH + X^-. \quad [2]$$

Extending this argument, the fact that the corresponding value for the above ratio for methyl benzenesulphonate was calculated to be 75 (2) would suggest some marked difference in mechanism between the methyl benzenesulphonate and the methyl halides in one or both of the above reactions. The aim of this work was to determine the rate of base-catalyzed hydrolysis for the methyl benzenesulphonate, methyl methanesulphonate, and dimethyl sulphate and to examine any differences in the k_{OH^-}/k_{H_2O} ratio between these values and the corresponding values reported by Moelwyn-Hughes for the methyl halides in terms of current mechanistic ideas.

EXPERIMENTAL METHOD

The experimental method adopted for the determination of the rate of bimolecular displacement of sulphonate ions from methyl esters by hydroxide was the classical one involving the use of ampoules containing a measured aliquot of the reaction mixture. Since the methyl sulphonic esters are relatively involatile at the temperatures studied, the presence of a small vapor space above the solution would not introduce the errors noted by Moelwyn-Hughes (3). There can be no doubt that there is a great need for the development of a method for obtaining bimolecular rate data such as sought here by some means which does not involve a sampling technique. However, the tube method

[1]*Manuscript received May 27, 1960.*
Contribution from the Division of Pure Chemistry, National Research Council, Ottawa, Canada.
Issued as N.R.C. No. 5954.

[2]*Summer student, 1959. Present address: Queen's University, Kingston, Ontario.*

was used in this instance in spite of its shortcomings because the rate data so obtained would be accurate enough as a basis for our conclusions. The methyl benzenesulphonate, methyl methanesulphonate, and dimethyl sulphate were from the same samples as had been purified for detailed study of the temperature dependence of the rate of hydrolysis of these compounds (4, 5, 6) and were used without further purification. The reaction mixture was made up to 0.02 N in NaOH and 0.01 M with respect to ester. Aliquots of 5 cc$\pm$0.007 were added to ampoules with a semiautomatic tube filler, the filling temperature being held at approximately 0° C in the case of the dimethyl sulphate. Rates were determined by immersing the required number of tubes simultaneously in the bath, with shaking, and, after allowing sufficient time for temperature equilibrium, initial tubes were chilled and analyzed for residual base. A series of such analysis over a suitable range of time, combined with corresponding solvolytic rates, provided the necessary data for calculation of the bimolecular rate of reaction, according to the following equation (7):

$$k_2 = \frac{1}{(a-b)t} \ln \frac{b(a-x)}{a(b-x)} - \frac{k_1}{a-x}.$$

Typical data for the hydrolysis of methyl benzenesulphonate at 30.0° C are given in Table I.

TABLE I

Typical kinetic data for the reaction of methyl benzenesulphonate and OH^- in water at 30.00° C

Time, seconds	Concentration of: Base a, moles/liter	Ester b, moles/liter	$k_2 \times 10^3$, liters/mole sec
0	0.01671	0.00646	
7200	0.01490	0.00465	1.46
9000	0.01451	0.00426	1.51
14400	0.01368	0.00343	1.37
16200	0.01339	0.00314	1.42
18000	0.01312	0.00287	1.46
19800	0.01289	0.00264	1.47
21610	0.01272	0.00247	1.42
23400	0.01254	0.00229	1.43
25200	0.01241	0.00216	1.37
27000	0.01218	0.00193	1.46
∞	0.01025	0	
	$k_1 = 2.146 \times 10^{-5}$*		
	k_2(av.) $= 1.44 \times 10^{-3}$ liters/mole sec		

*Reference 4.

RESULTS AND DISCUSSION

A summary of the rate data for the three compounds methyl methanesulphonate, methyl benzenesulphonate, and dimethyl sulphate is given in Table II for several temperatures. By combining these values with those for the hydrolytic process in the absence of base the corresponding k_{OH^-}/k_{H_2O} ratios may be calculated. In Table III these are compared with the corresponding values for the methyl halides from the work of Moelwyn-Hughes (7). The difference in the value of this ratio between the methyl halides and that for methyl benzenesulphonate from the early work of Praetorius (8) is seen to be confirmed and, if we may generalize from three examples, represents a general difference between the relative reactivity of the halides and sulphonates in respect to one or both reactions [1] and [2].

TABLE II

Summary of rate data for hydrolysis of methyl esters

Ester	Temp., °C	k_1, mole/liter sec	k_2, sec^{-1}	k_2 (average)	k_2/k_1
Me methanesulphonate	30.00	$9.32_5\times10^{-6}$	6.95×10^{-4} 7.13×10^{-4}	7.04×10^{-4}	76
	40.00	$2.93_8\times10^{-5}$	1.96×10^{-3} 1.96×10^{-3} 1.97×10^{-3}	1.96×10^{-3}	67
	50.00	$8.43_8\times10^{-5}$	5.44×10^{-3} 5.42×10^{-3}	5.43×10^{-3}	64
Me benzenesulphonate	30.00	$2.14_6\times10^{-5}$	1.437×10^{-3} 1.441×10^{-3}	1.44×10^{-3}	67
	40.00	$6.78_0\times10^{-5}$	4.27×10^{-3} 4.16×10^{-3}	4.22×10^{-3}	62
	50.00	$1.96_4\times10^{-4}$	1.09×10^{-2} 1.09×10^{-2} 1.07×10^{-2}	1.09×10^{-2}	55
Dimethyl sulphate	5.00	$1.12_3\times10^{-5}$	9.222×10^{-4} 8.94×10^{-4}	9.08×10^{-4}	81
	10.00	$2.30_5\times10^{-5}$	1.73×10^{-3} 1.62×10^{-3}	1.67×10^{-3}	73

TABLE III

A comparison of reactivity relative to methyl chloride for reactions [1] and [2]

RX	$k_X/k_{Cl}(OH^-)$	$k_X/k_{Cl}(H_2O)$
MeCl	1	1
MeBr	6.0	14.6
MeI	6.6	3.5
Me methanesulphonate	11.1	111.4
Me benzenesulphonate	22	260
Me methoxysulphonate	(363)	(3552)
Me phosphate	(13.5)	(0.36)

Normal experience would suggest that individual differences would be more apparent for reaction with the weaker nucleophile (water), and support for this conclusion may be found in Table IV where the relative reactivity of the methyl esters is compared with

TABLE IV

Dependence of relative reactivity on displaced anion for methyl compounds in hydrolysis

Anion	k_{OH^-}/k_{H_2O}*	k_H/k_D‡
Methoxysulphonate	47†	0.97
Benzenesulphonate	50	0.96
Methanesulphonate	56	0.96
Chloride	180	0.92
Bromide	226	0.90
Iodide	300	0.87

*Approximate values for 60° C.
†Estimated from data at lower temperature.
‡Secondary deuterium isotope effect from fully deuterated methyl esters (6).

that of methyl chloride for the two types of reaction. For nucleophilic displacement by OH^-, individual differences as a consequence of differences in the C—X bond being broken are surprisingly small (column 1, Table III). The differences in relative reactivity for hydrolysis show a slightly greater range of values for hydrolysis through the three halides (column 2, Table III) but a 10-fold increase in reactivity between the halides and the sulphonates. Hence, assuming that the difference is quantitative rather than qualitative, the reduced value of the k_{OH^-}/k_{H_2O} ratio noted in Table IV is the consequence of the relatively greater increase in the reactivity of the sulphonic esters for hydrolysis, in the absence of strong base.

Since a value of the k_{OH^-}/k_{H_2O} ratio > 1 indicates (9) some degree of nucleophilic interaction in the activation process for hydrolysis, the reduced values of this term for the sulphonates (Table IV) would suggest that bond making is less advanced in the transition state for these compounds than for the halides. The inverse secondary deuterium isotope effect ($k_H/k_D < 1$) recently reported by Llewellyn, Robertson, and Scott (6) for the hydrolysis of the above compounds leads to the same conclusion. Thus, the sharing of the p orbital between the entering and leaving groups leads to crowding of the transition state which will vary with the degree of overlap required of the former in the transition state and so leads to a proportional increase in the C—H bending frequencies and corresponding changes in the zero-point energy terms. Gratifying confirmation of this interpretation is seen in the linear correlation between the k_H/k_D and k_{OH^-}/k_{H_2O} ratios for a series of methyl esters (Fig. 1).

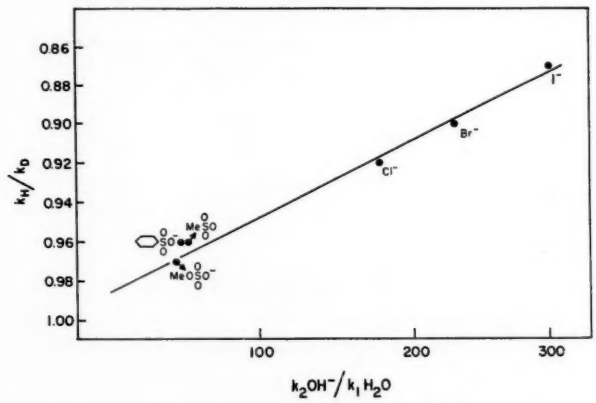

FIG. 1. A correlation of α-deuterium isotope effect with the k_{OH^-}/k_{H_2O} ratio.

The temperature dependence of the k_{OH^-}/k_{H_2O} ratio follows directly from the fact that reaction [1] is characterized by a large negative heat capacity of activation (6) while it would appear that this factor is small for reaction [2] (13).

Differences in the stability of the initial state solvation shell about the two types of esters will also contribute to the difference in reactivity but it is difficult to evaluate the relative importance of this factor. Thus the medium isotope effect which appears to depend on the relative stability of the initial state solvation shell in light and heavy water is, for the sulphonates, but one-half the average value for the halides (10, 11) and shows a much lower temperature dependence as would be expected (12). Evidence for

modification of the initial state solvation shell by the nature of the sulphonate grouping may be also obtained by considering the relative heat capacity changes (ΔC_p^*) which characterize the hydrolysis of corresponding sulphonic and halide esters (4). The latter terms, which appear to be determined to an important degree by the temperature dependence of the stability of the initial state solvation shell, have less negative values for the sulphonic esters than for the halides, a result quite consistent with the indications of the medium isotope effect and supported by the value of $\delta_X \Delta H^*$ (below). Against such arguments favoring the importance of initial state solvation differences in determining differences in reactivity must be considered the position of methyl phosphate in such reactions. Thus judging from the medium isotope effect (k_{D_2O}/k_{H_2O}) the methyl phosphate would appear to have reduced the stability of the initial state solvation shell in a manner analogous to the sulphonates (11) (k_{D_2O}/k_{H_2O} for methyl methanesulphonate and methyl phosphate being identical, 0.94). The relative reactivity of the methyl phosphate, however, is but one-third that of methyl chloride in hydrolysis, while methyl methanesulphonate reacts 100 times faster (Table III).

While no particular significance can be attached to small differences in the values of the enthalpy and entropy corresponding to the reaction of the sulphonates and the halides with hydroxide (Table V), there is, approximately, a regular decrease in enthalpy

TABLE V

Thermodynamic parameters for the reaction of a series of methyl esters with OH^- and H_2O in water

	Base attack			Hydrolysis		
MeX	ΔH^*, kcal/mole	ΔS^*, cal/deg mole	Ref.	ΔH^*, cal/mole	ΔS^*, cal/deg mole	Ref.
Chloride	22,855	−5.5	(7)	25.263	−8.89	(14)
Bromide	21,575	−3.5	(7)	24.142	−6.65	(14)
Iodide	20,795	−8.0	(7)	25.950	−3.94	(14)
Methanesulphonate	19,500	−8.72	(*)	20.441	−14.08	(15)
Benzenesulphonate	19,180	−8.30	(*)	20.597	−11.58	(4)
Methoxysulphonate	(18,500)	(−5.81)	(*)	(19.918)	(−8.87)	(5)

*This paper.

with increasing reactivity in contrast to the 4–5 kcal difference ($\delta_X \Delta H^*$) between the values for the halides and the sulphonates in the hydrolysis reactions. With the exception of the iodide, the entropy change associated with the displacement by OH^- is 3–5 e.u. more positive than for the corresponding hydrolysis, as is required by the difference in the charge distribution in the initial and transition states.

ACKNOWLEDGMENT

The authors wish to acknowledge the technical assistance received from Mr. S. Sugamori during the initial stages of this investigation.

REFERENCES

1. I. Fells and E. A. Moelwyn-Hughes. J. Chem. Soc. 398 (1959).
2. A. J. Streitwieser. J. Chem. Revs. **56**, 571 (1956).
3. E. A. Moelwyn-Hughes. Trans. Faraday Soc. **37**, 279 (1941).
4. R. E. Robertson. Can. J. Chem. **35**, 613 (1957).
5. R. E. Robertson. Unpublished work.
6. J. A. Llewellyn, R. E. Robertson, and J. M. Scott. Can. J. Chem. **38**, 222 (1960).
7. E. A. Moelwyn-Hughes. Proc. Roy. Soc. A, **196**, 540 (1949).
8. A. Praetorius. Monatsh. **26**, 1 (1905).

9. C. K. INGOLD. Structure and mechanism in organic chemistry. Cornell Univ. Press, Ithaca, N.Y. 1953. Chap. 7.
10. P. M. LAUGHTON and R. E. ROBERTSON. Can. J. Chem. **34**, 1714 (1956).
11. R. E. ROBERTSON and P. M. LAUGHTON. Can. J. Chem. **35**, 1319 (1957).
12. P. M. LAUGHTON and R. E. ROBERTSON. Can. J. Chem. **37**, 1491 (1959).
13. D. N. GLEW and E. A. MOELWYN-HUGHES. Proc. Roy. Soc. A, **211**, 254 (1952).
14. R. L. HEPPOLETTE and R. E. ROBERTSON. Proc. Roy. Soc. A, **252**, 273 (1959).
15. P. W. C. BARNARD and R. E. ROBERTSON. Unpublished work.

THE CHEMISTRY OF ETHYLENE OXIDE

VI. THE ACID-CATALYZED REACTION OF ETHYLENE OXIDE WITH ETHANOL–WATER MIXTURES[1]

R. K. Brown and A. M. Eastham

ABSTRACT

The rate of reaction of ethylene oxide with alcohol–water mixtures at 25° C has been determined. The ratio of glycol to ethoxyethanol in the product was determined for each mixture and found to be approximately equal to the molecular ratio of water to ethanol in the solvent.

Ethylene oxide reacts with water to form ethylene glycol and with ethanol to form 2-ethoxyethanol. The uncatalyzed and alkali-catalyzed reactions are very slow at ordinary temperatures but the acid-catalyzed reactions are rapid and suitable for kinetic measurements because they can be followed easily by the dilatometric method. Rate data are well established for the water reaction (1, 2, 3) but not for ethanol so this paper records the results of some measurements in ethanol and ethanol–water mixtures.

EXPERIMENTAL

Anhydrous ethanol was prepared from the commercial anhydrous material by distillation from sodium and ethyl phthalate (4). No aldehydes could be detected with Tollen's reagent.

Commercial ethylene oxide having a purity of over 99% was used as received.

Stock solutions of perchloric acid in alcohol were prepared from the 70% acid (perchloric acid dihydrate) and anhydrous ethanol and were found to be stable for several weeks. All titrations were made with a pH meter as most acid–base indicators give unsatisfactory end points.

Sodium perchlorate was dried by heating at 110° C for 24 hours, then over phosphorus pentoxide. It is sparingly soluble in dry ethanol so was used only with solutions containing at least 1% water.

Lithium perchlorate was dried under vacuum for 8 hours at 100° C, then was held for 10 hours at 160° C in a stream of thoroughly dry air. The product was immediately dissolved in dry ethanol and used as a solution.

For all reactions in aqueous ethanol the amount of glycol in the product was determined by the periodic acid – arsenite method (5). The remainder of the ethylene oxide was assumed to form ethoxyethanol.

For the rate measurements, acid and salt were dissolved in the appropriate alcohol–water mixture in a dry container attached to the dilatometer. A small glass vial containing a weighed quantity of ethylene oxide was introduced and the solution was then degassed by slight suction. The solution was brought to constant temperature (25.0° C) in a water bath, the vial of oxide was broken by means of a plunger, and the solution was then forced into the dilatometer by air pressure. The concentration of oxide in all experiments was between 0.01 and 0.06 *M* and its rate of disappearance showed excellent first-order dependence under all conditions. Rates were evaluated by the Guggenheim method (6).

[1]*Manuscript received July 7, 1960.*
Contribution from the Division of Applied Chemistry, National Research Council, Ottawa, Canada. Issued as N.R.C. No. 5944.

Can. J. Chem. Vol. 38 (1960)

RESULTS

As the acid-catalyzed hydration of ethylene oxide shows a marked salt effect, it was desirable to evaluate this effect in ethanol so a series of runs were made with varying concentrations of lithium perchlorate and a constant acid concentration of 0.0034 *M*. The results were quite erratic possibly due to traces of water (see below), but indicated a strong positive salt effect. All points within the concentration range 0.005 *M* to 0.12 *M* of perchlorate ion were accounted for within ±3% by a rate constant having the value

$$k_{H^+} = 5.9+16.\,c \text{ liter mole}^{-1} \text{ min}^{-1},$$

where c is the total concentration of perchlorate ion. However, the data suggest that the salt effect may be even greater at lower salt concentration (compare the results for reaction of acetaldehyde in ethanol – hydrogen chloride solutions (7)).

The corresponding expression for the salt effect upon the hydration of ethylene oxide at 25° C was found to be (2)

$$k_{H^+} = 0.55+0.48\,c,$$

so the rate of reaction with ethanol is much faster than with water and shows a salt effect which is in the same direction but proportionately about three times as large as that in water. The subsequent runs in water–ethanol mixtures were conducted at a constant concentration of perchlorate ion (0.055 *M*) but the magnitude of the salt effect was not determined for each composition. It cannot be assumed that salt effects do not make at least a minor contribution to the shape of the curve in Fig. 1; presumably they make a larger contribution to the rate at the higher alcohol concentrations.

TABLE I
Composition of the product in alcohol–water mixtures

Molarity H_2O	Mole% H_2O	Mole% glycol in product
1	5.7	~8
2	11	13
4	20	26
8	35	37
12	46	47
16	56	51
20	63	60.5
30	78	70
43	92	86
49	96	92
52	98	95
—	100	101

The rates of reaction of ethylene oxide with water–ethanol mixtures containing up to 95 mole % of ethanol are shown in Fig. 1. Each point represents the average of several runs at acid concentrations varying from about 0.01 to 0.06 *M*. The rates decrease to a minimum at about 40 mole % (ca. 15 wt.%) of water from either pure water or pure ethanol. Throughout this range the ratio of glycol to ethoxyethanol is approximately equal to the molecular ratio of water to alcohol in the solvent (Table I), which might indicate a reaction independent of the concentration of nucleophilic reagent. In other studies of competition between reactants for ethylene oxide in acid solution, however, it was found that the rate was markedly dependent upon nucleophilicity (2), so one must conclude that water and ethanol are about equally reactive under the present conditions.

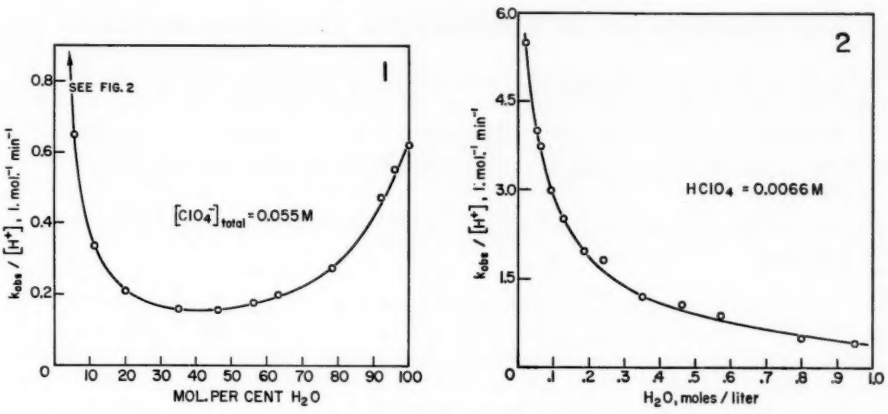

FIGS. 1 AND 2.

It follows that the shape of the curve in Fig. 1 must be determined primarily by medium effects and by variations in the acid–base equilibria due to changes in the ratio of the ions H_3O^+ and $C_2H_5OH_2^+$.

At water concentrations below about one molar, the rate increases very sharply with further reduction in the water concentration (Fig. 2). The extent of the increase cannot be estimated from the present data because solutions made up from 70% perchloric acid always contain small amounts of water, but it is at least 10-fold on reducing the water concentration from 1 *M* to about 0.015 *M*. Similar observations have been made by Deyrup (7) in studies of the acid-catalyzed reaction of acetaldehyde in ethanol solution and by Goldschmidt and his co-workers (8) in studies of acid-catalyzed esterifications in ethanol. The usual explanation is due to Goldschmidt and accounts for the decreasing rate with increasing water as due to the replacement of the ion $C_2H_5OH_2^+$ by the less acidic and therefore less catalytic ion, H_3O^+. So far as we are aware, however, this phenomenon has been observed only in ethanol; in the reaction of acetaldehyde with methanol the effect of small amounts of water ought to be very large if the above explanation is correct, because the rate in pure methanol is greater than that in water by a factor of 10^3 (9).

REFERENCES

1. J. N. BRONSTED, M. KILPATRICK, and M. KILPATRICK. J. Am. Chem. Soc. **51**, 428 (1929).
2. A. M. EASTHAM and G. A. LATRÉMOUILLE. Can. J. Chem. **30**, 169 (1952).
3. H. J. LICHTENSTEIN and G. H. TWIGG. Trans. Faraday Soc. **44**, 905 (1948).
4. H. MANSKE. J. Am. Chem. Soc. **53**, 1106 (1931).
5. ORGANIC REACTIONS. Vol. II. John Wiley & Sons, Inc., New York. 1947.
6. E. A. GUGGENHEIM. Phil. Mag. **2**, 538 (1926).
7. A. J. DEYRUP. J. Am. Chem. Soc. **56**, 60 (1934).
8. H. GOLDSCHMIDT and E. SUNDE. Ber. **39**, 711 (1906); H. GOLDSCHMIDT and O. UDBY. Z. physik. Chem. **60**, 728 (1907).
9. G. W. MEADOWS and B. DE B. DARWENT. Trans. Faraday Soc. **48**, 1015 (1952).

THE PREPARATION OF SUBSTITUTED THIONOCARBAMATES[1]

A. F. McKay, D. L. Garmaise, G. Y. Paris, S. Gelblum, and R. J. Ranz

ABSTRACT

The preparations and properties of a number of substituted thionocarbamates are described.

The thionocarbamate derivatives in Tables I–IV were prepared by one of the following three methods:

$$ROH + CSCl_2 \xrightarrow{-HCl} ROC(S)Cl + R'NH_2 \xrightarrow{-HCl} R'NHC(S)OR, \quad [1]$$

$$ROH + R'NCS \xrightarrow{(C_2H_5)_3N} R'NHC(S)OR, \quad [2]$$

$$ROH + R'NCS \xrightarrow{NaH} R'NHC(S)OR. \quad [3]$$

Route 1 was used to prepare both the aryl arylthionocarbamates and the aryl aralkylthionocarbamates. Procedure 2 gave good results with aralkyl isothiocyanates but triethylamine did not catalyze the addition of aryl isothiocyanates to phenols under the conditions employed in this study. All of the benzyl N-substituted thionocarbamates were prepared by procedure 3.

Harris and Fischback (1) reported the preparation of thionocarbamates by the reaction of amines with methyl xanthates. An attempt to prepare phenyl 3,4-dichlorobenzylthionocarbamate from S-methyl phenylxanthate by this procedure gave methyl 3,4-dichlorobenzyldithiocarbamate. Thus the phenoxy group was replaced more readily by 3,4-dichlorobenzylamine than the methylmercapto group. However, if 3,4-dichlorobenzylamine is added to S-methyl ethylxanthate the methylmercapto group is replaced and ethyl 3,4-dichlorobenzylthionocarbamate is formed. These reactions are represented by equations 4 and 5.

$$RNH_2 + \bigcirc\!\!-OC(S)SCH_3 \longrightarrow RNHC(S)SCH_3 + \bigcirc\!\!-OH \quad [4]$$

$$RNH_2 + C_2H_5OC(S)SCH_3 \longrightarrow RNHC(S)OC_2H_5 + CH_3SH \quad [5]$$

$R = 3,4\text{-}Cl_2C_6H_3CH_2-$

The thiolcarbamates in Table V were prepared by treating the corresponding phenyl chlorothiolformates with the appropriate amines. The phenyl chlorothiolformates were obtained by treating the lead salts of the thiophenols with phosgene by the method of Rivier (2).

An attempt to prepare phenyl 3,4-dichlorobenzylthionocarbamate by heating a methanolic solution of methyl 3,4-dichlorobenzyldithiocarbamate in the presence of Amberlite IRA-400 resin saturated with phenol gave methyl 3,4-dichlorobenzylthionocarbamate in 48% yield.

The aryl chlorothionoformates, which were isolated during these studies, are described in Table VI.

[1]*Manuscript received July 8, 1960.*
Contribution No. 28 from the L. G. Ryan Research Laboratories of Monsanto Canada Limited, LaSalle, Que.

EXPERIMENTAL[2]

Di-3,4-dichlorobenzylamine

A mixture of 3,4-dichlorobenzyl chloride (9.75 g, 0.05 mole) and 3,4-dichlorobenzylamine (35.2 g, 0.20 mole) was heated on the steam bath for 2 hours. Ether (200 ml) and 10% sodium hydroxide solution (50 ml) were added, and the ether layer was washed with water and dried over anhydrous sodium sulphate. Fractionation of the ether extract yielded 15 g (85.2%) of unchanged 3,4-dichlorobenzylamine (b.p. 93–100°/1 mm) and di-3,4-dichlorobenzylamine (b.p. 175–180°/1 mm, n_D^{25} 1.60665, D_4^{27} 1.3690), yield 10 g (59.7%). Anal. Calc. for $C_{14}H_{11}Cl_4N$: C, 50.20; H, 3.31; Cl, 42.34; N, 4.18. Found: C, 50.68; H, 3.44; Cl, 42.00; N, 4.13.

A solution of the amine (0.61 g, 0.0018 mole) in absolute ethanol (30 ml) was acidified with hydrogen chloride. Di-3,4-dichlorobenzylamine hydrochloride (m.p. 228–229°) was recovered by filtration, yield 0.21 g (33%). Anal. Calc. for $C_{14}H_{12}Cl_5N$: C, 45.26; H, 3.26; Cl, 47.72; N, 3.77. Found: C, 45.17; H, 3.09; Cl, 47.80; N, 3.98. N-4-Chlorobenzylaniline (3) (b.p. 155°/0.5 mm) and di-4-chlorobenzylamine (m.p. 30–32°) were prepared in the same way in 62.8% and 60% yield respectively. A melting point of 31° has been reported (4) for di-4-chlorobenzylamine.

2-(3,4-Dichlorophenyl)-acetonitrile

A solution of 3,4-dichlorobenzyl chloride (48.87 g, 0.25 mole) in ethanol (50 ml) was added during 30 minutes to a stirred solution of potassium cyanide (19.50 g, 0.30 mole) in water (15 ml) at 60°. The mixture was refluxed for 4 hours, and then cooled and filtered. The filtrate was concentrated *in vacuo* and the residue was extracted with ether (100 ml). The ether solution was dried and evaporated, and the residue was distilled to give the product (b.p. 106–108°/0.1 mm; m.p. 35.5–38.5°), yield 37.6 g (81%). Recrystallization from ether – petroleum ether raised the melting point to 39.5–40.5°. Anal. Calc. for $C_8H_5Cl_2N$: C, 51.65; H, 2.71; Cl, 38.12; N, 7.53. Found: C, 51.81; H, 2.92; Cl, 38.14; N, 7.56.

2-(3,4-Dichlorophenyl)-ethylamine

Aluminum chloride (6.66 g, 0.05 mole) in ether (150 ml) was added to a suspension of lithium aluminum hydride (1.99 g, 0.05 mole) in ether (100 ml) maintained in a nitrogen atmosphere. A solution of 2-(3,4-dichlorophenyl)-acetonitrile (9.3 g, 0.05 mole) in ether (200 ml) was added dropwise to the stirred mixture, and the stirring was continued for 30 minutes. Water was added cautiously to destroy the excess lithium aluminum hydride and after further addition of water (total 140 ml) and 6 *N* sulphuric acid (140 ml), the aqueous layer was separated and washed with ether (100 ml). The aqueous layer was basified with 40% sodium hydroxide solution at 0°, and the free base was extracted with ether (3×150 ml). Fractionation of the dried ether extract yielded the product (b.p. 100–102°/0.12 mm), yield 6.75 g (71%). Anal. Calc. for $C_8H_9Cl_2N$: C, 50.56; H, 4.78; Cl, 37.32; N, 7.37. Found: C, 50.25; H, 4.92; Cl, 37.16; N, 7.22.

The amine in aqueous ethanol was converted into its picrate (m.p. 199–200°, decomp.) in the usual manner, yield 67.5%. Anal. Calc. for $C_{14}H_{12}Cl_2N_4O_7$: C, 40.12; H, 2.89; Cl, 16.92; N, 13.37. Found: C, 40.15; H, 3.14; Cl, 17.06; N, 13.50.

3-(3,4-Dichlorophenyl)-propionic Acid

3,4-Dichlorobenzaldehyde was converted to 3,4-dichlorocinnamic acid (m.p. 214–217° C) in 69.2% yield by the method of Walling and Wolfstirn (5).

[2]*All melting points are uncorrected. Microanalyses were performed by Micro-Tech Laboratories, Skokie, Illinois.*

3,4-Dichlorocinnamic acid (58.5 g, 0.27 mole) in glacial acetic acid (1500 ml) was hydrogenated at atmospheric pressure in the presence of 5% palladium on charcoal (5.8 g). The absorption of hydrogen ceased after 10.5 hours (6 liters). The solution was filtered and evaporated, and the residue was crystallized from water to give the product (m.p. 90–93°), yield 53.0 g (90%). Recrystallization from ethanol raised the melting point to 96–97°. Anal. Calc. for $C_9H_8Cl_2O_2$: C, 49.34; H, 3.68; Cl, 32.37. Found: C, 49.07; H, 3.68; Cl, 32.41.

3-(3,4-Dichlorophenyl)-propionamide

A solution of 3-(3,4-dichlorophenyl)-propionic acid (53.0 g, 0.24 mole) and thionyl chloride (119 g, 1.0 mole) in benzene (100 ml) was allowed to stand overnight, and was then evaporated to dryness. The oily residue was added in portions to 28% aqueous ammonia (270 ml) with stirring at 20–25° and the mixture was stirred for 4 hours. The product (m.p. 76–80°) was recovered by filtration, yield 45.5 g (86.3%). Recrystallization from benzene – petroleum ether raised the melting point to 80–81°. Anal. Calc. for $C_9H_9Cl_2NO$: C, 49.56; H, 4.16; Cl, 32.51; N, 6.42. Found: C, 49.78; H, 4.22; Cl, 32.67; N, 6.42.

3-(3,4-Dichlorophenyl)-propionitrile

A solution of the amide (37.9 g, 0.174 mole) and thionyl chloride (119 g, 1.0 mole) in benzene (200 ml) was refluxed for 5 hours, and the solution was then evaporated. Distillation of the residue yielded crude 3-(3,4-dichlorophenyl)-propionitrile (b.p. 140–158°/1 mm), yield 30.8 g (88%). Redistillation gave the pure product (b.p. 121°/0.4 mm, n_D^{25} 1.55403; d_{20} 1.2742). Anal. Calc. for $C_9H_7Cl_2N$: C, 54.02; H, 3.53; Cl, 35.44; N, 7.01. Found: C, 54.24; H, 3.66; Cl, 35.38; N, 7.03.

3-(3,4-Dichlorophenyl)-propylamine

3-(3,4-Dichlorophenyl)-propionitrile (18.0 g, 0.09 mole) was reduced by lithium aluminum hydride – aluminum chloride in ether exactly as described above for 2-(3,4-dichlorophenyl)-acetonitrile. The product (b.p. 120–125°/1 mm) was obtained in 17.3 g (95%) yield. A redistilled sample (b.p. 104°/0.4 mm, n_D^{27} 1.55487, d_{20} 1.2082) was submitted for analysis. Anal. Calc. for $C_9H_{11}Cl_2N$: C, 52.96; H, 5.43; Cl, 34.75; N, 6.87. Found: C, 53.08; H, 5.45; Cl, 34.73; N, 7.09.

The picrate of the amine, which was prepared in quantitative yield from water, melted at 150–151° after recrystallization from hot water. Anal. Calc. for $C_{15}H_{14}Cl_2N_2O_7$: C, 41.59; H, 3.26; Cl, 16.37; N, 12.93. Found: C, 41.69; H, 3.21; Cl, 16.53; N, 12.84.

Preparation of 4-n-Alkylphenols

A series of 4-*n*-alkylphenols, three of which are new, was prepared by the general method of Sandulesco and Girard (6).

4-n-Hexylphenol

4-*n*-Hexylphenol (b.p. 135–136°/0.4 mm) was prepared in 72.6% yield from *p*-caproylphenol. The reported (6) boiling point at 10 mm is 146–147°.

4-n-Decylphenol

Decanoyl chloride (69 g, 0.35 mole) was heated with phenol (32.9 g, 0.35 mole) at 120° for 1 hour. The crude phenyl decanoate was added during a 30-minute period to a suspension of anhydrous aluminum chloride (56 g, 0.42 mole) in carbon disulphide (100 ml). The reaction was exothermic and the solvent began to reflux during the addition. Refluxing was continued for 2 hours. The solution was then evaporated to dryness, and the residue was heated at 150° for 2 hours. Hydrochloric acid (200 ml of 18% HCl) was added cautiously

and the mixture was diluted with water (150 ml). The oily product was extracted with chloroform (200 ml) and the chloroform solution was dried and evaporated. Fractionation of the residue yielded 2-decanoylphenol (b.p. 130–133°/0.25 mm), yield 42.8 g (49.4%), and 4-decanoylphenol (b.p. 194–195°/0.4 mm), yield 15 g (17.3%). The *p*-isomer (m.p. 59–60°) crystallized in the receiver. Anal. Calc. for $C_{16}H_{24}O_2$: C, 77.38; H, 9.74. Found: C, 77.26; H, 9.79.

4-Decanoylphenol (10 g, 0.04 mole) in ethanol (50 ml) was added to a vigorously stirred suspension of amalgamated zinc (70 g) in 18% hydrochloric acid (140 ml) and the reaction mixture was refluxed for 2 hours. The mixture was extracted with toluene (100 ml) and the toluene solution was dried and evaporated. Fractionation of the residue gave 7.8 g (83%) of 4-*n*-decylphenol (b.p. 146–148°/0.75 mm). The product crystallized (m.p. 54–56°) on standing. Anal. Calc. for $C_{16}H_{26}O$: C, 82.00; H, 11.19. Found: C, 81.83; H, 11.01.

4-n-Dodecylphenol

Phenol was heated with dodecanoyl chloride under similar conditions to form phenyl dodecanoate, which was rearranged to yield 51% of 2-dodecanoylphenol (b.p. 140–165°/0.75 mm), and 29.5% of 4-dodecanoylphenol (b.p. 198°/0.25 mm). Reduction of 4-dodecanoylphenol with amalgamated zinc and hydrochloric acid gave 4-*n*-dodecylphenol (b.p. 154°/3 mm, m.p. 65–67°), yield 81%. Anal. Calc. for $C_{18}H_{30}O$: C, 82.38; H, 11.53. Found: C, 82.48; H, 11.58.

4-n-Octadecylphenol

A mixture of stearic acid (113 g, 0.4 mole) and thionyl chloride (143 g, 1.2 mole) was refluxed for 1 hour. The mixture was distilled to give octadecanoyl chloride (b.p. 159–162°/0.1 mm), yield 87.9 g (72.5%). The acid chloride was converted to phenyl *n*-octadecanoate, which was rearranged to 31.6% of 2-*n*-octadecanoylphenol (b.p. 164–182°/0.15 mm) and 28% of 4-*n*-octadecanoylphenol (b.p. 209–212°/0.15 mm). Reduction of the para-isomer gave 4-*n*-octadecylphenol (b.p. 182–187°/0.15 mm, m.p. 65–67°) in 83% yield. Anal. Calc. for $C_{24}H_{42}O$: C, 83.18; H, 12.22. Found: C, 83.10; H, 12.00.

Aryl Thionocarbamates

Method A: 4-n-Propylphenyl 3,4-Dichlorophenylthionocarbamate

4-*n*-Propylphenol (20.43 g, 0.15 mole) in 3% sodium hydroxide solution (200 ml) was added to a stirred solution of thiophosgene (17.25 g, 0.15 mole) in chloroform (200 ml) at 0–10° during a period of 30 minutes. The stirring was continued for 30 minutes and the chloroform layer was separated, dried, and evaporated. Distillation of the residue gave 4-*n*-propylphenyl chlorothionoformate (b.p. 101–102°/0.8 mm), yield 24 g (74.7%).

3,4-Dichloroaniline (16.2 g, 0.1 mole) in chloroform (150 ml) was added to a stirred solution of 4-*n*-propylphenyl chlorothionoformate (10.73 g, 0.05 mole) in chloroform (200 ml) at 25° during a period of 30 minutes. The stirring was continued for 1 hour, and the precipitated 3,4-dichloroaniline hydrochloride (9.6 g, 97%) was removed by filtration. The filtrate was concentrated to a volume of 200 ml and petroleum ether (300 ml) was added to give the product (m.p. 150–151°), yield 12.6 g (74%). Recrystallization from the same solvents did not raise the melting point. When the phenol was insoluble in dilute sodium hydroxide, the dried sodium phenoxide was reacted with thiophosgene in chloroform suspension.

The compounds listed in Tables I and III, and those compounds in Table II for which no other method is noted, were prepared by this general procedure.

TABLE I

Aryl arylthionocarbamates, RNHC(S)OR′

R	R′	Yield, %	M.p., °C	Formula	C		H		Cl		N		S	
					Calc.	Found	Calc.	Found	Calc.	Found	Calc.	Found	Calc.	Found
3,4-Dichlorophenyl	Phenyl	44	156–157[a]	$C_{13}H_9Cl_2NOS$	52.36	52.37	3.04	3.12	23.78	24.19	4.70	4.73	10.75	10.82
3,4-Dichlorophenyl	4-Methylphenyl	53	173–174[b]	$C_{14}H_{11}Cl_2NOS$	53.86	53.63	3.55	3.84	22.71	22.83	4.49	4.62	10.27	10.18
3,4-Dichlorophenyl	4-Ethylphenyl	52	158–159[b]	$C_{15}H_{13}Cl_2NOS$	55.22	55.37	4.02	4.13	21.74	21.76	4.29	4.34	9.83	10.02
3,4-Dichlorophenyl	4-*n*-Propylphenyl	74	159–161[b]	$C_{16}H_{15}Cl_2NOS$	56.48	56.73	4.44	4.50	20.84	21.07	4.12	4.24	9.42	9.61
3,4-Dichlorophenyl	4-*n*-Butylphenyl	48	125–126[c]	$C_{17}H_{17}Cl_2NOS$	57.63	57.39	4.84	4.84	20.01	20.13	3.95	4.17	9.05	9.18
3,4-Dichlorophenyl	2,6-di-*t*-Butyl-4-methylphenyl	24	139–140[c]	$C_{22}H_{27}Cl_2NOS$	62.26	62.67	6.41	6.40	16.71	16.00	3.30	3.29	7.55	7.22
3,4-Dichlorophenyl	4-Methoxyphenyl	57	167–168[d]	$C_{14}H_{11}Cl_2NO_2S$	51.24	50.97	3.38	3.43	21.61	21.61	4.27	4.42	9.76	9.62
3,4-Dichlorophenyl	4-Ethoxyphenyl	64	173–175[a]	$C_{15}H_{13}Cl_2NO_2S$	52.64	52.46	3.84	3.92	20.72	20.73	4.09	4.45	9.37	9.48
3,4-Dichlorophenyl	3,4-Dichlorophenyl	91	142–143[a]	$C_{13}H_7Cl_4NOS$	42.54	42.16	1.92	2.02	38.65	37.68	3.82	4.23	8.74	8.38
3,4-Dichlorophenyl	3-Nitrophenyl	85	135–136[b]	$C_{13}H_8Cl_2N_2O_3S$	45.50	45.70	2.35	2.64	20.66	20.74	8.17	8.24	9.34	9.38
2,4-Dichlorophenyl	2,4-Dichlorophenyl	68	142–143[e]	$C_{13}H_7Cl_4NOS$	42.54	42.77	1.92	2.10	38.65	38.85	3.82	4.23	8.74	8.38
4-Methoxyphenyl	4-Methoxyphenyl	87	175–176[b]	$C_{15}H_{15}N_2O_3S$	62.26	62.44	5.23	5.34	—	—	4.84	4.85	11.08	11.05
4-Ethoxyphenyl	4-Ethylphenyl	61	118–119[b]	$C_{17}H_{19}NO_2S$	67.75	67.43	6.35	6.41	—	—	4.65	4.64	10.63	10.56
3-Nitrophenyl	4-Ethylphenyl	58	104–105[b]	$C_{15}H_{14}N_2O_3S$	59.58	59.66	4.67	4.62	—	—	9.27	9.13	10.60	10.49
3-Nitrophenyl	3-Nitrophenyl	67	157–158[f]	$C_{13}H_9N_3O_5S$	48.90	49.24	2.84	3.09	—	—	13.16	13.06	10.04	10.13
3-Phenyl-6-hydroxyphenyl	4-Methoxyphenyl	57	139–140[a]	$C_{20}H_{17}NO_3S$	68.36	68.28	4.88	5.12	—	—	3.99	4.18	9.12	9.41

[a]Crystallized from chloroform. [b]Chloroform – petroleum ether. [c]Petroleum ether. [d]Benzene – petroleum ether. [e]Ether – petroleum ether. [f]Benzene.

TABLE II

Aryl aralkylthionocarbamates, RNHC(S)OR′

R	R′	Yield, %	M.p., °C	Formula	C		H		Cl		N		S	
					Calc.	Found	Calc.	Found	Calc.	Found	Calc.	Found	Calc.	Found
Benzyl	Phenyl	46	82–83[b]	$C_{14}H_{13}NOS$	69.11	69.32	5.38	5.69	—	—	5.76	5.63	13.18	13.17
4-Nitrobenzyl	Phenyl	81	110–111[c]	$C_{14}H_{12}N_2O_3S$	58.32	58.36	4.20	4.32	—	—	9.72	9.65	11.12	11.15
4-Chlorobenzyl	Phenyl	82	119–120[d]	$C_{14}H_{12}ClNOS$	60.56	60.69	4.36	4.28	12.77	12.72	5.04	5.05	11.54	11.40
4-Chlorobenzyl	3,4-Dichlorophenyl	80	90–91[c]	$C_{14}H_{10}Cl_3NOS$	48.51	48.84	2.91	2.81	30.68	30.75	4.04	4.25	9.25	9.13
3,4-Dichlorobenzyl	Phenyl	89	104–105[c]	$C_{14}H_{11}Cl_2NOS$	53.85	53.98	3.55	3.70	22.71	22.48	4.49	4.31	10.27	10.06
3,4-Dichlorobenzyl	2-Methylphenyl	34[a]	89–90[b]	$C_{15}H_{13}Cl_2NOS$	55.25	55.14	4.02	4.41	21.75	21.94	4.29	4.32	9.83	9.90
3,4-Dichlorobenzyl	4-Methylphenyl	68[a]	118–119[b]	$C_{15}H_{13}Cl_2NOS$	55.25	55.08	4.02	4.10	21.75	21.60	4.29	4.17	9.83	9.75
3,4-Dichlorobenzyl	4-Ethylphenyl	59[a]	97–98[e]	$C_{16}H_{15}Cl_2NOS$	56.48	56.54	4.44	4.45	20.84	20.84	4.12	4.32	9.42	9.41
3,4-Dichlorobenzyl	4-*n*-Propylphenyl	14[a]	81[e]	$C_{17}H_{17}Cl_2NOS$	57.64	57.88	4.84	4.86	20.02	20.01	3.95	4.13	9.05	8.86
3,4-Dichlorobenzyl	4-*n*-Butylphenyl	42	90–91[b]	$C_{18}H_{19}Cl_2NOS$	58.70	58.53	5.20	5.36	19.25	19.35	3.80	3.91	8.71	8.69
3,4-Dichlorobenzyl	4-*n*-Hexylphenyl	49	87–88[e]	$C_{20}H_{23}Cl_2NOS$	60.61	60.81	5.85	6.24	17.89	17.81	3.53	3.63	8.09	8.38
3,4-Dichlorobenzyl	4-*n*-Decylphenyl	81	85–86[e]	$C_{24}H_{31}Cl_2NOS$	63.71	63.74	6.91	6.78	15.67	15.74	3.09	3.32	7.09	7.08
3,4-Dichlorobenzyl	4-*n*-Dodecylphenyl	70	87.5–88.5[e]	$C_{26}H_{35}Cl_2NOS$	64.48	64.81	7.34	7.33	14.76	14.96	2.91	3.10	6.67	6.67
3,4-Dichlorobenzyl	4-*n*-Octadecylphenyl	60	86–87[e]	$C_{32}H_{47}Cl_2NOS$	68.06	67.29	8.39	8.08	12.56	13.21	2.48	2.61	5.68	6.01
3,4-Dichlorobenzyl	2,6-di-*t*-Butyl-4-methylphenyl	65	113–114[b]	$C_{23}H_{29}Cl_2NOS$	63.01	62.92	6.67	6.67	16.17	16.22	3.19	3.03	7.31	7.26
3,4-Dichlorobenzyl	4-Methoxyphenyl	75	107–108[c]	$C_{15}H_{13}Cl_2NO_2S$	52.64	52.93	3.83	4.07	20.72	21.07	4.09	4.09	9.37	9.58
3,4-Dichlorobenzyl	4-Ethoxyphenyl	80	88–89[c]	$C_{16}H_{15}Cl_2NO_2S$	53.95	53.92	4.25	4.41	19.91	20.08	3.93	4.06	9.00	9.03
3,4-Dichlorobenzyl	3-Nitrophenyl	89	123–124[f]	$C_{14}H_{10}Cl_2N_2O_3S$	47.07	47.04	2.82	2.97	19.85	20.31	7.84	7.65	8.98	9.07
3,4-Dichlorobenzyl	β-Naphthyl	78	124–125[e]	$C_{18}H_{13}Cl_2NOS$	59.61	59.74	3.61	3.73	19.58	19.60	3.87	3.98	8.85	8.86
3,4-Dichlorobenzyl	4-Fluorophenyl	63	123–124[c,g]	$C_{14}H_{10}Cl_2FNOS$[h]	50.94	50.95	3.05	3.12	21.48	21.26	4.26	4.34	9.71	9.78
3,4-Dichlorobenzyl	4-Chlorophenyl	72	135–136[e]	$C_{14}H_{10}Cl_3NOS$	48.51	48.49	2.91	3.04	30.68	30.53	4.04	3.97	9.25	9.17
3,4-Dichlorobenzyl	2,4-Dichlorophenyl	85	154–155[e]	$C_{14}H_9Cl_4NOS$	44.13	44.13	2.38	2.55	37.23	37.46	3.68	3.70	8.41	8.26
3,4-Dichlorobenzyl	3,4-Dichlorophenyl	20	95–96[c]	$C_{14}H_9Cl_4NOS$	44.13	44.07	2.38	2.56	37.23	37.10	3.68	3.70	8.41	8.38
3,4-Dichlorobenzyloxy	Phenyl	50	67–68[b]	$C_{14}H_{11}Cl_2NO_2S$	51.22	51.39	3.38	3.13	21.60	21.78	4.27	4.29	9.77	9.87
2-(3,4-Dichlorophenyl)-ethyl	Phenyl	81	84–85[b]	$C_{15}H_{13}Cl_2NOS$	55.23	55.13	4.02	4.04	21.74	21.71	4.29	4.25	9.83	9.78
3-(3,4-Dichlorophenyl)-propyl	Phenyl	35	64–65[e]	$C_{16}H_{15}Cl_2NOS$	56.46	56.79	4.44	4.66	20.84	20.62	4.12	4.20	9.42	9.15

[a]Prepared by adding 3,4-dichlorobenzyl isothiocyanate to the appropriate phenol. [b]Crystallized from ether – petroleum ether. [c]Petroleum ether – chloroform. [d]Chloroform. [e]Petroleum ether. [f]Benzene. [g]Polymorphic modification, m.p. 108–109°. [h]Calc.: F, 5.76. Found: F, 5.73.

TABLE III

Aryl disubstituted thionocarbamates, RR'NC(S)OR''

R	R'	R''	Yield, %	M.p., °C	Formula	C		H		Cl		N		S	
						Calc.	Found	Calc.	Found	Calc.	Found	Calc.	Found	Calc.	Found
Phenyl	4-Chlorobenzyl	Phenyl	41	138–139[a]	$C_{20}H_{16}ClNOS$	67.87	67.99	4.56	4.59	10.02	10.00	3.96	4.08	9.06	8.92
4-Chlorobenzyl	4-Chlorobenzyl	Phenyl	34	114–115[b]	$C_{21}H_{17}Cl_2NOS$	62.70	62.82	4.26	4.34	17.63	17.67	3.48	3.46	7.97	7.90
4-Chlorobenzyl	4-Chlorobenzyl	β-Naphthyl	46	117–118[b]	$C_{28}H_{19}Cl_2NOS$	66.36	66.56	4.23	4.53	15.68	15.38	3.10	3.15	7.09	6.92
3,4-Dichlorobenzyl	3,4-Dichlorobenzyl	Phenyl	26	120–121[b]	$C_{21}H_{15}Cl_4NOS$	53.51	53.74	3.21	3.15	30.10	30.61	2.97	3.33	6.80	6.93

[a]Crystallized from acetone. [b]Acetone–water.

TABLE IV

Aralkyl aralkylthionocarbamates, RNHC(S)OR'

R	R'	Yield, %	M.p., °C	Formula	C		H		Cl		N		S	
					Calc.	Found	Calc.	Found	Calc.	Found	Calc.	Found	Calc.	Found
Benzyl	2,4-Dichlorobenzyl	84	107–108[a]	$C_{15}H_{13}Cl_2NOS$	55.22	55.16	4.02	4.08	21.74	22.22	4.29	4.14	9.83	9.51
3,4-Dichlorobenzyl	4-Chlorobenzyl	77	73–74[b]	$C_{15}H_{12}Cl_3NOS$	49.93	50.29	3.36	3.24	29.49	29.39	3.88	3.64	8.89	8.77
3,4-Dichlorobenzyl	2,4-Dichlorobenzyl	72	104–105[a]	$C_{15}H_{11}Cl_4NOS$	45.59	45.76	2.81	2.95	35.90	36.17	3.55	3.38	8.11	8.11
3,4-Dichlorobenzyl	3,4-Dichlorobenzyl	80	79–80[b]	$C_{15}H_{11}Cl_4NOS$	45.59	45.49	2.81	2.76	35.90	35.20	3.55	3.45	8.11	7.92

[a]Crystallized from acetone–water. [b]Ethanol–water.

Method B: 4-Methylphenyl 3,4-Dichlorobenzylthionocarbamate

A mixture of 3,4-dichlorobenzyl isothiocyanate (4.36 g, 0.02 mole), *p*-cresol (2.16 g, 0.02 mole), and triethylamine (0.04 g, 0.0004 mole) was heated in a sealed tube at 80° for 4 hours. The reaction mixture was dissolved in ether (100 ml) and the ether solution was washed with 2% sodium hydroxide solution and with water. The residue obtained on evaporation of the ether solution (5.8 g, m.p. 92–96°) was recrystallized from petroleum ether (40 ml) to give the product melting at 115–117°, yield 4.4 g (67.5%). One crystallization from ether – petroleum ether solvent raised the melting point to 118–119°. This reaction was found to be generally applicable to the addition of phenols to aralkyl isothiocyanates. Compounds prepared by this method are included in Table II.

Aralkyl Thionocarbamates

3,4-Dichlorobenzyl 3,4-Dichlorobenzylthionocarbamate

Sodium hydride (0.48 g of a 50% dispersion, 0.01 mole) was added to 3,4-dichlorobenzyl alcohol (1.77 g, 0.01 mole) in benzene (30 ml). The mixture was stirred at room temperature until the evolution of hydrogen ceased, after which it was briefly heated to boiling. The cooled suspension of sodium 3,4-dichlorobenzyloxide was treated with 3,4-dichlorobenzyl isothiocyanate (2.18 g, 0.01 mole) in benzene (10 ml) and the mixture was stirred overnight. The precipitated sodio derivative (4.18 g) was dissolved in acetone and the solution was filtered clear of insoluble impurities (0.34 g). Acidification of the filtrate with aqueous acetic acid precipitated the product (m.p. 103–104°), yield 2.86 g (72.1%). Recrystallization from aqueous acetone raised the melting point to 104–105°.

All of the compounds listed in Table IV were prepared by this procedure.

1,4-Phenylene Di-(3,4-dichlorobenzylthionocarbamate)

A mixture of 3,4-dichlorobenzyl isothiocyanate (2.18 g, 0.01 mole), hydroquinone (1.10 g, 0.01 mole), and triethylamine (0.01 g, 0.0001 mole) was heated in a sealed tube at 144° for 3 hours. The crude product was triturated in ether (100 ml) to give 1.79 g (65.6%) of product (m.p. 165–170°). Recrystallization from aqueous acetone raised the melting point to 170–171°, yield 1.25 g (45.8%). Anal. Calc. for $C_{22}H_{16}Cl_4N_2O_2S_2$: C, 48.38; H, 2.95; Cl, 25.96; N, 5.13; S, 11.74. Found: C, 48.49; H, 3.13; Cl, 25.98; N, 5.27; S, 11.73.

1,4-Phenylene Di-(benzylthionocarbamate)

A mixture of benzyl isothiocyanate (3.83 g, 0.026 mole), hydroquinone (1.41 g, 0.013 mole), and triethylamine (0.023 g, 0.0023 mole) was heated in a sealed tube at 144° for 3 hours. The crude product was extracted with ether, and the residue was recrystallized from aqueous acetone to give crystals melting at 171–172°, yield 0.24 g (4.6%). Recrystallization from acetone raised the melting point to 178–179°. Anal. Calc. for $C_{22}H_{20}N_2O_2S_2$: C, 64.67; H, 4.94; N, 6.86; S, 15.70. Found: C, 64.93; H, 5.07; N, 6.67; S, 15.79.

Aryl Thiolcarbamates

Phenyl chlorothiolformate (b.p. 90–95°/13 mm) was prepared in 18% yield by the method of Rivier (2).

The chlorothiolformate (3.40 g, 0.02 mole) in chloroform (30 ml) was added dropwise to a stirred solution of 3,4-dichlorobenzylamine (4.30 g, 0.04 mole) in chloroform (10 ml) at 25°. The reaction mixture was allowed to stand overnight, and the precipitated 3,4-dichlorobenzylamine hydrochloride (2.87 g, 100%) was recovered by filtration. The residue obtained on evaporation of the filtrate was crystallized from benzene – petroleum ether to give crystals melting at 101–102°, yield 2.65 g (55%).

TABLE V

Aryl N-substituted thiolcarbamates, RNHC(O)SR′

R	R′	Yield, %	M.p., °C	Formula	C		H		Cl		N		S	
					Calc.	Found	Calc.	Found	Calc.	Found	Calc.	Found	Calc.	Found
4-Chlorobenzyl	4-Chlorophenyl	82	192–193[a]	$C_{14}H_{11}Cl_2NOS$	53.85	53.98	3.55	3.68	22.71	22.73	4.49	4.54	10.27	10.02
3,4-Dichlorobenzyl	Phenyl	55	101–102[b]	$C_{14}H_{11}Cl_2NOS$	53.85	53.68	3.55	3.60	22.71	23.07	4.49	4.70	10.27	10.01
3,4-Dichlorobenzyl	4-Chlorophenyl	57	149–150[c]	$C_{14}H_{10}Cl_3NOS$	48.59	48.49	2.91	2.88	30.68	30.92	4.04	4.13	9.25	9.06
3,4-Dichlorophenyl	4-Chlorophenyl	70	209–210[d]	$C_{13}H_8Cl_3NOS$	46.94	47.20	2.42	2.45	31.98	32.23	4.21	4.43	9.64	9.58

[a]Crystallized from ethanol–water. [b]Benzene – petroleum ether. [c]Dioxane – petroleum ether. [d]Dioxane–water.

TABLE VI

Aryl chlorothionoformates, ROC(S)Cl

R	Yield, %	B.p., °C/mm Hg	Formula	C		H		Cl		S	
				Calc.	Found	Calc.	Found	Calc.	Found	Calc.	Found
4-Ethoxyphenyl	90.5	100–104/0.2	$C_9H_9ClO_2S$	49.89	49.67	4.19	4.01	16.36	16.27	14.80	14.48
4-Methylphenyl	92.0	62–65/0.25	C_8H_7ClOS	51.93	51.93	3.78	4.03	19.00	18.45	17.18	16.39
4-*n*-Propylphenyl	74.7	101–102/0.1	$C_{10}H_{11}ClOS$	55.94	56.07	5.16	5.00	16.52	16.62	14.93	14.70
4-Methoxyphenyl	84.8	96/0.4	$C_8H_7ClO_2S$	47.40	47.46	3.48	3.56	17.50	17.40	15.82	15.67
3-Nitrophenyl	54.0	128/0.1[a]	$C_7H_4ClNO_3S$[c]	38.63	39.36	1.85	2.16	16.29	15.90	14.73	14.18
4-Nitrophenyl	44.6	—[b]	$C_7H_4ClNO_3S$[d]	38.63	38.83	1.85	1.91	16.29	16.22	14.71	14.60

[a]M.p. 64–65°. [b]M.p. 59–60°. [c]Calc.: N, 6.44. Found: N, 6.39. [d]Calc.: N, 6.44. Found: N, 6.62.

4-Chlorophenyl chlorothiolformate (b.p. 145–155°/30 mm) was prepared in 67.5% yield from lead 4-chlorophenylmercaptide and phosgene, according to Rivier's method (2). Condensation with the appropriate amine as described above yielded the other thiolcarbamates listed in Table V.

S-*Methyl Phenylxanthate*

The reaction between carbon disulphide and potassium phenolate in ethanol (7) was found to yield only potassium ethylxanthate. Replacement of the ethanol by dimethylformamide yielded the desired potassium phenylxanthate.

Carbon disulphide (6.09 g, 0.08 mole) was added during a 30-minute period to potassium phenolate (10.58 g, 0.08 mole) in dimethylformamide (80 ml) at 20°. Methyl chloride was bubbled through the reaction mixture for 30 minutes at 30°. Water (1500 ml) was added, and the mixture was extracted with ether (5×100 ml). The ether extracts were combined and washed with 5% sodium hydroxide solution, 5% hydrochloric acid, and water. Fractionation of the dried ether solution yielded S-methyl phenylxanthate (b.p. 82–84°/0.11 mm, n_D^{25} 1.62189), yield 6.0 g (41.8%). Anal. Calc. for $C_8H_8OS_2$: C, 52.15; H, 4.38; S, 34.80. Found: C, 52.15; H, 4.45; S, 34.19.

Methyl 3,4-Dichlorobenzyldithiocarbamate

Method A.—3,4-Dichlorobenzylamine (2.58 g, 0.146 mole) was added to S-methyl phenylxanthate (2.7 g, 0.0146 mole) at room temperature. The temperature rose to 42°, and the mixture gradually solidified. Crystallization from chloroform – petroleum ether yielded methyl 3,4-dichlorobenzyldithiocarbamate (m.p. 98–100°), yield 3.37 g (74.1%). Recrystallization from chloroform – petroleum ether gave the analytical sample melting at 100–101°. Anal. Calc. for $C_9H_9Cl_2NS_2$: C, 40.61; H, 3.41; Cl, 26.64; N, 5.26; S, 24.08. Found: C, 41.11; H, 3.44; Cl, 26.07; N, 5.42; S, 24.14.

Method B.—Carbon disulphide (16.75 g, 0.22 mole) was added to a stirred mixture of sodium hydroxide (8.8 g, 0.22 mole) in water (14 ml) and 3,4-dichlorobenzylamine (35.21 g, 0.20 mole) in ether (100 ml) at 0–5°. The mixture was stirred for 1 hour at room temperature, and the sodium 3,4-dichlorobenzyldithiocarbamate (40.7 g, 75%) was recovered by filtration. The sodium salt (13.71 g, 0.05 mole) was added to a solution of methyl iodide (7.10 g, 0.05 mole) in methanol (150 ml) and the mixture was allowed to stand for 1 hour. The solution was concentrated and diluted with water, giving methyl 3,4-dichlorobenzyldithiocarbamate (m.p. 95–100°). Recrystallization from benzene yielded the pure product (9.0 g, 71%), melting point and mixed melting point with the product described above in A was 100–101°.

Methyl 3,4-Dichlorobenzylthionocarbamate

A solution of methyl 3,4-dichlorobenzyldithiocarbamate (1.33 g, 0.005 mole) in methanol (50 ml) was refluxed for 1 hour in the presence of Amberlite IRA-400 resin (25 ml) which had been saturated with phenol. The solution was filtered and evaporated. Crystallization of the residue from chloroform – petroleum ether yielded methyl 3,4-dichlorobenzylthionocarbamate (m.p. 75–76°), yield 0.60 g (48%). Anal. Calc. for $C_9H_9Cl_2NOS$: C, 42.23; H, 3.63; Cl, 28.35; N, 5.60; S, 12.82. Found: C, 42.23; H, 3.90; Cl, 28.60; N, 5.39; S, 12.59.

Ethyl 3,4-Dichlorobenzylthionocarbamate

The procedure is essentially that of Harris and Fischback (1). Methyl chloride was passed through a solution of potassium ethylxanthate (0.20 mole) in ethanol (200 ml) for 1 hour at 25–30°. 3,4-Dichlorobenzylamine (35.2 g, 0.20 mole) was added and the

solution was maintained at 40° for 30 minutes. The solution was evaporated, and the residue was dissolved in chloroform (200 ml). The chloroform solution was extracted with 5% sodium hydroxide solution, 5% hydrochloric acid, and water. The chloroform solution was dried and evaporated to give ethyl 3,4-dichlorobenzylthionocarbamate (m.p. 55–58°), yield 16 g (30.3%). Anal. Calc. for $C_{10}H_{11}Cl_2NOS$: C, 45.46; H, 4.19; Cl, 26.84; N, 5.30; S, 12.14. Found: C, 45.39; H, 4.30; Cl, 27.00; N, 5.70; S, 12.10.

REFERENCES

1. G. H. HARRIS and B. C. FISCHBACK. U.S. Patent No. 2,691,635; Chem. Abstr. **49**, 11696 (1955).
2. H. RIVIER. Bull. soc. chim. France, **1** (4), 733 (1907).
3. H. D. LAW. J. Chem. Soc. **101**, 154 (1912).
4. J. VON BRAUN, M. KUHN, and J. WEISMANTEL. Ann. **449**, 249 (1926).
5. C. WALLING and K. B. WOLFSTIRN. J. Am. Chem. Soc. **69**, 852 (1947).
6. G. SANDULESCO and A. GIRARD. Bull. soc. chim. France, **47** (4), 1300 (1930).
7. P. SACCARDI. Ital. Patent No. 432,082; Chem. Abstr. **43**, 8604 (1949).

ORGANOPHOSPHORUS COMPOUNDS

VIII. O-ALKYL, O′-ARYL PHOSPHOROFLUORIDOTHIOATES AND O-ARYL N-ALKYL PHOSPHORAMIDOFLUORIDOTHIOATES[1, 2]

G. A. OLAH AND A. A. OSWALD[3]

O-Alkyl, O′-aryl phosphorofluoridothioates and O-aryl N-alkyl phosphoramidofluoridothioates were prepared from the corresponding aryl phosphorochlorofluoridothioates and aryl phosphorodifluoridothioates.

In a previous paper (1) the preparation of aryl phosphorochlorofluoridothioates and aryl phosphorodifluoridothioates was described. Using these compounds as starting materials, it was now possible to prepare the previously unknown O-alkyl, O′-aryl phosphorofluoridothioates and O-aryl N-alkyl phosphoramidofluoridothioates.

O-Alkyl, O′-aryl phosphorofluoridothioates have been obtained in good yields by reacting aryl phosphorochlorofluoridothioates with sodium alcoholates, or with alcohols in the presence of NaOH or pyridine.

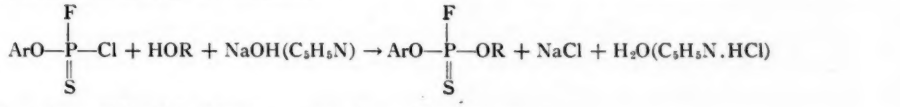

Aryl phosphorodifluoridothioates react in a similar manner:

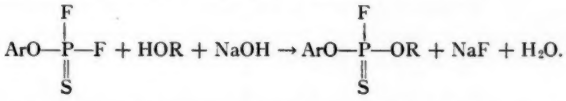

The yields with this method, however, are in general slightly smaller than with aryl phosphorochlorofluoridothioates.

The following O-alkyl, O′-aryl phosphorofluoridothioates were prepared: O-ethyl, O′-phenyl-; O-methyl, O′-*p*-tolyl-; O-ethyl, O′-α-naphthyl-; and O-methyl, O′-*p*-chlorophenyl-phosphorofluoridothioates. Some physical properties and analytical data are shown in Table I.

TABLE I

O-Alkyl, O′-aryl phosphorofluoridothioates

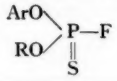

Ar	R	Yield,* %	B.p., °C/mm	n_D^{20}	Fluorine	
					Calculated	Found
Phenyl	Ethyl	77	75–76/3	1.5019	8.62	8.74
p-Tolyl	Methyl	91	79–80/3	1.5069	7.62	7.83
α-Naphthyl	Ethyl	73	124–125/2	1.5730	7.03	7.16
p-Chlorophenyl	Methyl	85	81–82/3	1.5241	7.89	7.89

*Obtained by the reaction of aryl phosphorochlorofluoridothioates with sodium alcoholates.

[1]*Manuscript received May 31, 1960.*
Contribution No. 13 from the Exploratory Research Laboratory, Dow Chemical of Canada, Limited, Sarnia, Ontario, Canada.
[2]*Part VII: J. Org. Chem.* **25**, *603 (1960).*
[3]*Present address: Research Department, Imperial Oil Limited, Sarnia, Ontario, Canada.*

Alkyl esters of phosphoramidofluoridic acid were prepared by Saunders (2), Schrader (3), and Sartori (4) to combine the rapid toxic action and miotic effect of the dialkyl phosphorofluoridates and of the high toxicity of some of the phosphorodiamidofluoridates. The synthesis started from phosphorus oxydichlorofluoride and was carried out without the isolation of the ethyl phosphorofluoridochloridate intermediate according to the following sequence of reactions (5):

$$POCl_2F + C_2H_5OH \rightarrow C_2H_5OPOClF + HCl \xrightarrow{3C_6H_5NH_2} \begin{matrix} C_2H_5O \\ C_6H_5NH \end{matrix}\!\!>\!POF + 2C_6H_5NH_2.HCl.$$

Similar reactions starting from phosphorus thiodichlorofluoride were used for the preparation of the alkyl esters of phosphoramidofluoridothioic acids as described in a previous paper of this series (6). No aryl esters of either phosphoramidofluoridic or phosphoramidofluoridothioic acid were reported.

In this work aryl esters of N-alkyl phosphoramidofluoridothioic acid were prepared by reacting aryl phosphorochlorofluoridothioates with a primary or secondary amine according to the following equation:

$$ArO{-}\overset{\overset{F}{|}}{\underset{\underset{S}{\|}}{P}}{-}Cl + 2HNR_2 \rightarrow ArO{-}\overset{\overset{F}{|}}{\underset{\underset{S}{\|}}{P}}{-}NR_2 + R_2NH.HCl.$$

Aryl phosphorodifluoridothioates react with amines in a similar manner to yield O-aryl N-alkyl phosphoroamidofluoridothioates and amine hydrofluorides:

$$ArO{-}\overset{\overset{F}{|}}{\underset{\underset{S}{\|}}{P}}{-}F + 2HNR_2 \rightarrow ArO{-}\overset{\overset{F}{|}}{\underset{\underset{S}{\|}}{P}}{-}NR_2 + R_2NH.HF.$$

Syntheses starting from aryl phosphorodifluoridothioates required somewhat higher reaction temperatures and gave slightly lower yields.

In the place of the second mole of amine, pyridine (or another organic base) can be used to bind the halogen hydrogen formed in the reaction

$$ArO{-}\overset{\overset{F}{|}}{\underset{\underset{S}{\|}}{P}}{-}Cl + H_2NR + C_5H_5N \rightarrow ArO{-}\overset{\overset{F}{|}}{\underset{\underset{S}{\|}}{P}}{-}NHR + C_5H_5N.HCl.$$

Yields and purity of compounds were equivalent to previous methods.

TABLE II

O-Aryl N-alkyl phosphoramidofluoridothioates

$$ArO{-}\overset{\overset{F}{|}}{\underset{\underset{S}{\|}}{P}}{-}N\begin{matrix}R_1\\R_2\end{matrix}$$

Ar	R_1	R_2	B.p., °C/mm	n_D^{20}	Yield,* %	Fluorine	
						Calculated	Found
Phenyl	Metyhl	Methyl	93–93.5/3	1.5268	92	8.66	8.76
o-Tolyl	Methyl	Methyl	91.5–92/3	1.5251	90	8.14	8.10
o-Tolyl	Methyl	Hydrogen	110–110.5/3	1.5299	92	8.19	8.35
Phenyl	*t*-Butyl	Hydrogen	123–124/2.5	1.5338	75	7.68	7.84

*Obtained by the reaction of aryl phosphorochlorofluoridothioates with amines.

The following O-aryl N-alkyl phosphoramidofluoridothioates were prepared: O-phenyl N,N-dimethyl-; O-*o*-tolyl N,N-dimethyl-; amido-, O-*o*-tolyl N-ethyl-; and O-phenyl N-*t*-butyl-phosphoramidofluoridothioates. The yields and some of the properties of the compounds prepared are shown in Table II.

All derivatives are colorless liquids. They are fairly resistant to hydrolysis. Therefore, they can be prepared also in water media in satisfactory yields.

EXPERIMENTAL

O-Alkyl, O'-Aryl Phosphorofluoridothioates

(A) From Aryl Phosphorochlorofluoridothioates with Alcoholates

Aryl- (phenyl-, *p*-tolyl-, α-naphthyl-, and *p*-chlorophenyl-) phosphorochlorofluoridothioate (0.1 mole) was dissolved in 100 ml of benzene (ether could be also used as an alternate solvent) and placed in a 500-ml three-necked flask equipped with a stirrer, dropping funnel, and thermometer. The other reagent, 0.1 mole of sodium alcoholate (methylate and ethylate), was dissolved in the corresponding alcohol. The sodium alcoholate solution was then added in small portions to the aryl phosphorochlorofluoridate while the reaction mixture was stirred and cooled in an ice bath. Sodium chloride precipitated instantly. After the reaction mixture was allowed to stand for 2 hours, it was washed with three volumes of water, then with 2.5% sodium carbonate solution, and then again with water. The mixture was dried over anhydrous sodium sulphate, and the solvent was removed by distillation at atmospheric pressure and then the remaining product was fractionated *in vacuo*. For yields, physical and analytical data see Table I.

(B) From Aryl Phosphorochlorofluoridothioates with Alcohols

A solution of 0.1 mole of aryl phosphorochlorofluoridothioate in 50 ml of the corresponding alcohol (methanol or ethanol in our experiments) was placed into a 200-ml flask equipped with a mechanical stirrer, dropping funnel, and thermometer. To the alcoholic solution, an aqueous solution of 4.0 g (0.1 mole) of sodium hydroxide (in 15 ml of water) was added dropwise, with effective stirring and ice-water cooling. After the addition, the reaction mixture was allowed to stand overnight at room temperature and then extracted with 150 ml of ether. The ether solution was washed with water, 1% aqueous sodium hydroxide solution, and then again with water. The ether solution was then dried over anhydrous sodium sulphate, the solvent was removed by distillation at atmospheric pressure, and the remaining raw O-alkyl, O'-aryl phosphorofluoridothioate was purified by fractionation *in vacuo*.

In the presence of pyridine.—To a solution of 0.1 mole of aryl phosphorochlorofluoridothioate in 50 ml of the corresponding alcohol, a solution of 0.1 mole of pyridine in 100 ml of ether was added slowly with shaking. After the addition, the reaction mixture was allowed to stand overnight, diluted with 200 ml of water and 100 ml of ether. The ether phase was washed successively with water, 5% aqueous sodium carbonate, and water and then dried over sodium sulphate. The solvent was removed by distillation, and the O-alkyl, O'-aryl phosphorofluoridothioate was obtained by fractionation *in vacuo*.

(C) From Aryl Phosphorodifluoridothioates

Aryl (α-naphthyl-, and *p*-chlorophenyl-) phosphorodifluoridothioate (0.1 mole) was dissolved in 100 ml of benzene and reacted with an alcoholic solution of 0.1 mole of sodium alcoholate (methylate and ethylate) as described under method (*A*).

O-Aryl N-Alkyl Phosphoramidofluoridothioates

(A) From Aryl Phosphorochlorofluoridothioates with Amines

To a solution of 0.1 mole of aryl- (phenyl-, *o*-tolyl-) phosphorochlorofluoridothioate in 100 ml of benzene (or toluene), 0.2 mole of the corresponding alkylamine (methyl, dimethyl, *t*-butyl) in 100 ml of benzene was added with cold water cooling and stirring. The amine hydrochloride precipitated instantly. The reaction mixture was allowed to reach room temperature and to stand overnight. The amine hydrochloride was then removed by filtration and washed with benzene. The combined filtrate was distilled; at first the benzene solvent was removed at atmospheric pressure and then the raw O-aryl N-alkyl phosphoramidofluoridothioate was fractionated *in vacuo*. Yields and physical and analytical data are shown in Table II.

(B) From Aryl Phosphorochlorofluoridothioates with Amines and Pyridine

To a solution of 0.1 mole of aryl phosphorochlorofluoridothioate in 150 ml of benzene, a mixture of 0.1 mole of alkylamine and 0.1 mole of pyridine was added dropwise with stirring. The reaction mixture was warmed to 50° C and kept at that temperature for an hour. Then the pyridine hydrochloride precipitate was removed by filtration and washed with benzene. The combined benzene filtrates were washed with water, dried over anhydrous sodium sulphate and distilled.

(C) From Aryl Phosphorodifluoridothioate

To a benzene solution of 0.1 mole of phenyl phosphorodifluoridothioate, 0.2 mole of alkylamine (dimethyl and *t*-butyl) in 100 ml of benzene was added with stirring. The reaction mixture was heated to 50° C and kept at that temperature for an hour. Then it was worked up as described under method (*A*).

REFERENCES

1. G. A. Olah and A. A. Oswald. J. Org. Chem. **25**, 603 (1960).
2. B. C. Saunders. Some aspects of the chemistry and toxic action of organic compounds containing phosphorus and fluorine. Cambridge at the University Press. 1957. p. 90.
3. G. Schrader. Die Entwicklung neuer Insektizide auf Grundlage organischer Fluor- und Phosphoverbindungen, 2. Aufl., Verlag Chemie GmbH., Weinheim. 1952.
4. M. F. Sartori. Chem. Revs. **48**, 225 (1951).
5. H. G. Cook, J. D. Flett, B. C. Saunders, G. J. Stacey, H. G. Watson, I. G. E. Wilding, and S. J. Woodcock. J. Chem. Soc. 2921 (1949).
6. G. Olah, A. Oswald, and A. Mlinko. Ann. **602**, 123 (1957).

THE DETERMINATION OF THE AREAS OF RESOLVED AND PARTIALLY RESOLVED CHROMATOGRAPHY PEAKS[1]

JOHN C. BARTLET AND D. MORISON SMITH

ABSTRACT

Gas chromatographic peaks were demonstrated to have the form of normal distribution curves. A mathematical treatment has been developed which permits the calculation of the areas of these curves from the statistical parameters, height of the mode (peak height), and standard deviation σ. The standard deviation equals the width of the peak at 0.882 of peak height. Methods given for the evaluation of the mutual effects of overlapping peaks have made it possible to obtain corrected peak heights. The standard deviation of the gas chromatography peak has been found to vary linearly with the retention time, thus permitting the graphical estimation of σ for use with corrected peak heights in the calculation of true areas for overlapping peaks. The method has also been extended to the treatment of skewed, overlapping peaks. The variation of σ with retention time, its constancy, and its relationship to the number of theoretical plates are discussed.

INTRODUCTION

In quantitative gas chromatography using a differential detector, the area under the peak corresponding to a compound is proportional to the amount of that compound present in the gas stream. Area measurements are therefore fundamental.

Various procedures have been proposed for the measurement of peak areas. The integrator built into the recorder is the least laborious, but suffers from obvious disadvantages if there is a base-line drift or if there are overlapping peaks. The triangulation procedure (1) gives a good first approximation. Another procedure which has been widely used is to cut out the peaks or a tracing of the peaks, and to weigh the cut paper. Planimeter tracing has also been used. With all these procedures, precision and accuracy suffer when the peaks are very narrow or if two or more peaks have a moderate overlap.

AREA OF SYMMETRICAL PEAKS

(a) Isolated Peaks

It has been pointed out and developed theoretically (2, 3, 4) that the peaks obtained with a well-designed chromatograph closely approximate a normal or Gaussian distribution curve as shown in Fig. 1. The equation for this type of curve is given by Goulden (5) as

$$Y = \frac{N}{\sigma\sqrt{2\pi}} \cdot e^{-\frac{1}{2}(x/\sigma)^2} \qquad [1]$$

where Y is the height of the curve measured at a distance x from the mean, N is the number of variates, which, for our purposes may be taken as the area, A, and σ is the standard deviation. At the mean or central peak of the curve, $x = 0$, $Y = h$ or peak height, and equation [1] becomes

$$h = \frac{A}{\sigma\sqrt{2\pi}} \qquad [2]$$

or

$$A = h\sigma\sqrt{2\pi} = 2.507h\sigma. \qquad [3]$$

[1]*Manuscript received June 30, 1960.*
Contribution from Food and Drug Directorate, Department of National Health and Welfare, Ottawa, Canada. Presented in part at the Ottawa Meeting of the Chemical Institute of Canada, June 14, 1960.

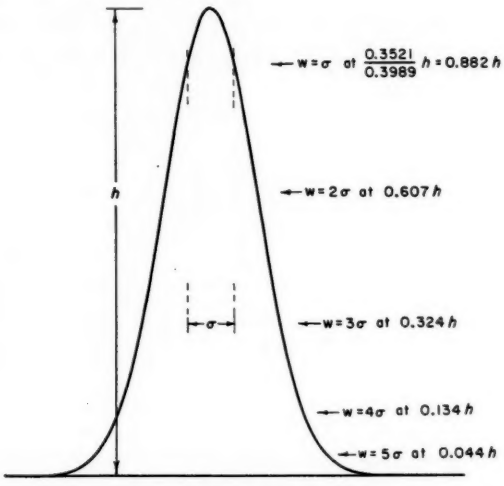

FIG. 1. The normal distribution curve.

For a normal distribution curve, σ may easily be determined, as shown in Fig. 1, by any one of the formulae which have been derived from Sheppard's tables of the Probability Integral (Biometrika Tables) (6). Thus, for an isolated peak, the area may be calculated, without construction, by simply measuring the peak height and the σ derived from the peak width at $0.607h$ or $0.324h$ and substituting in equation [3]. For accuracy, the peak width measurements for σ should be made using a magnifying viewer with reticle such as the Bausch and Lomb spectrum measuring magnifier No. 81-34-97-20.

The conformity of the peaks to the normal distribution curve can be tested by measuring the peak width of an isolated peak at the various heights listed in Fig. 1. The σ obtained should be constant or nearly constant to a peak width of 4σ.

Figure 2 gives a typical chromatogram for which the σ of the various peaks are indicated. Some of these values and others taken from other chromatograms using pure standard substances on the same column have been plotted against retention time in Fig. 3. As may be seen from the figure, the function is linear. In this way, the value for σ may be obtained from the graph for peaks which are insufficiently resolved for accurate measurement. These values of σ can be used directly in equation [3] for resolved peaks.

(b) Unresolved Peaks

If distances along the x axis are measured in terms of σ and the area is taken as 1 (i.e., a standardized normal distribution) then equation [2] becomes

$$h = \frac{1}{\sqrt{2\pi}} \qquad [4]$$

and the ordinate Y becomes Z (5). Then

$$Z = \frac{e^{-\frac{1}{2}(x/\sigma)^2}}{\sqrt{2\pi}}. \qquad [5]$$

Note that $Z = h = 1/\sqrt{2\pi}$ when $x = 0$.

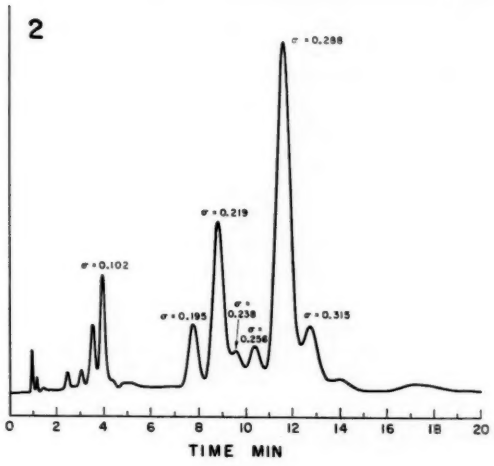

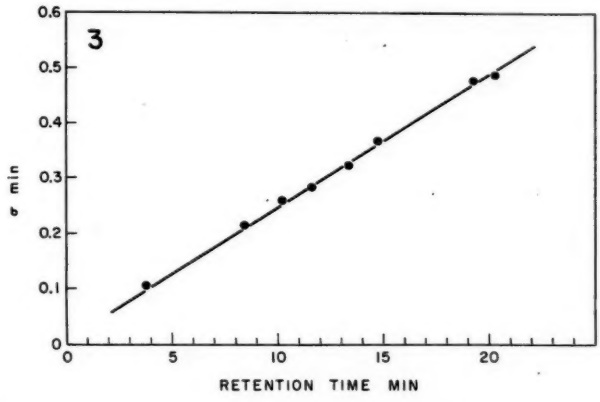

FIG. 2. Gas chromatogram of peppermint oil. Temperature of column, 170°; flow rate, 80 ml/minute of helium; packing, 20% SAIB on Chromosorb W, 2½ meters long.
FIG. 3. Relationship of σ, standard deviation, to retention time, t_r.

The values for Z may be found in Sheppard's table (5) for a standardized normal distribution curve. These values have been converted to percentage of peak height h at a distance x from the mean. Figure 4 gives these percentage corrections at separations, x, measured in units of the σ of the interfering peak.

When there are two incompletely resolved peaks as in Figs. 5 and 6, it is possible to calculate the height of the curve due to one component at the position of the other peak, and thus the contribution of one component to the observed peak height of the other.

For example, let us consider two peaks, a and b, of peak heights h_a and h_b separated by x (measured in units of σ_a and hence called x_a) as shown in Fig. 5. The ordinate Y of the curve of peak a at a distance x_a from the mean is given by substituting h_a for $N/\sigma\sqrt{2\pi}$ in equation [1].

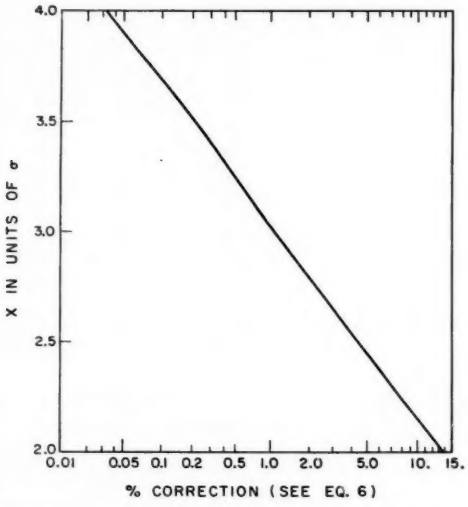

FIG. 4. Peak height corrections for given separations measured in units of the σ of the interfering peak.

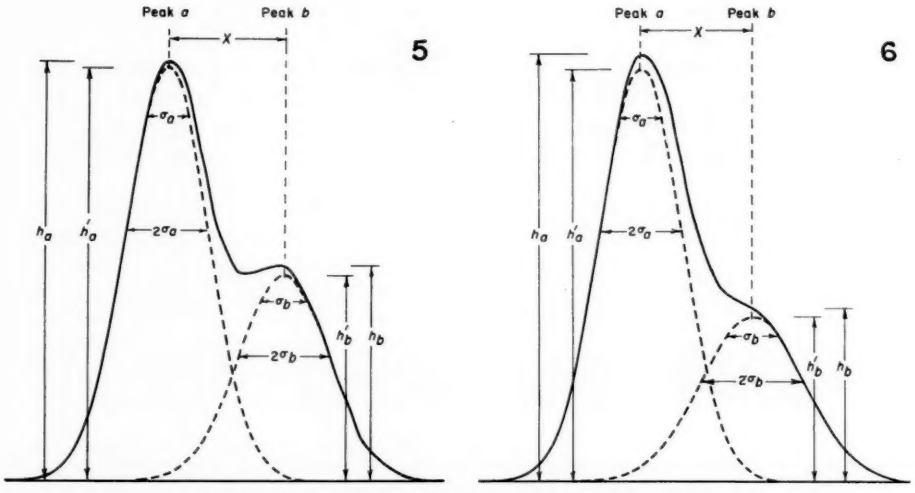

FIG. 5. Symmetrical peak with partially resolved side peak.
FIG. 6. Symmetrical peak with unresolved shoulder.

[6] $$Y = h_a e^{-\frac{1}{2}(x_a/\sigma_a)^2}$$

and the corrected height of peak b, h_b', becomes

[7] $$h_b' = h_b - h_a e^{-\frac{1}{2}(x_a/\sigma_a)^2}$$

and the area, A_b, becomes

[8] $$A_b = h_b' \sigma_b \sqrt{2\pi} = 2.507\, h_b' \sigma_b.$$

This is obviously the first member of a series of iterative approximations, whose later members are usually too small to be considered. However, if both h_a and h_b are large and x is small, it may be necessary to carry through the corrections a second time using h_a' in place of h_a in equation [7] and h_b' in the corresponding correction for h_b.

To simplify the correction for peak height, Fig. 4 or Sheppard's table (6) may be used to obtain the percentage of the height of the interfering peak to be subtracted from the peak under consideration. If the separation is greater than 4σ, the correction is usually negligible even though the valley between the peaks does not return to the base line. In the above example h_a can similarly be corrected for the effect of peak b, using x measured in units of σ_b. Note that if peak b comes after peak a, σ_b will be greater than σ_a as shown in Figs. 5 and 6, x_b will be less than x_a, and the percentage of h_b to be subtracted from h_a will be greater than the percentage correction of h_a on h_b. In Fig. 6 the correction for h_b on h_a is actually larger even though the peak b is smaller.

Figure 5 shows two symmetrical peaks, which, although overlapping, are still well enough separated so that the peak positions can be determined.

Figure 6 shows an extreme case where peak b appears only as a shoulder. The corrections can still be applied provided the retention time of the second compound relative to the first is known from other data. This is necessary so that the distance x can be measured accurately.

Note that although in both Figs. 5 and 6 there is serious overlap, there is still only a relatively small correction on peak height. However, as may be seen from these figures a serious error would be introduced if the σ used in the calculations were taken from the curve. In the case of overlapping peaks the σ to be used must be derived from a graph of the type of Fig. 3 for accurate results.

ASYMMETRICAL PEAKS

A peak may be skewed and still have some of the properties of a normal distribution curve. Skewed peaks which will be considered in detail are of the type shown in Fig. 7

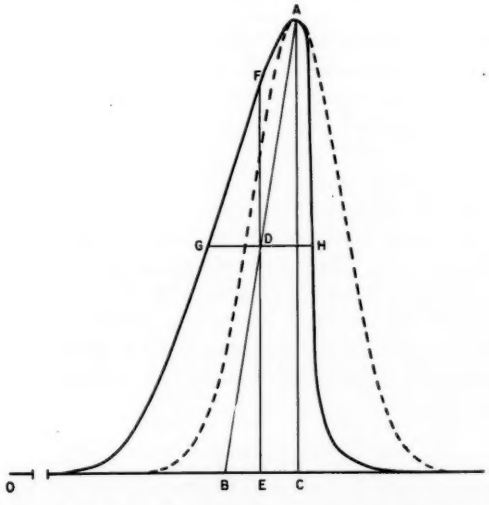

FIG. 7. Comparison of skewed and symmetrical distribution curves.

and have the following properties:

1. The asymmetry is such that the locus of the midpoint of the peak width at all heights is a straight line (AB in Fig. 7).
2. The peak width measured at the various heights listed on Fig. 1 shall yield a constant value for σ.

Skewness has been defined by Pearson (7) as (mean−mode)/σ where the mean is the value which vertically bisects the area and the mode is the position of peak height. Figure 7 shows a skewed curve of the type described, along with a symmetrical normal distribution curve with arbitrary origin at 0. Line AC gives peak height h and line AB is the locus of the midpoint between the ascending and descending portions of the curve. The mode is given by point C. To a first approximation the mean or vertical bisector EDF of the area can be obtained from the half height, GDH, at its intersection, D, of line AB, thus, an approximate skewness, Sk, is given by

$$[9] \qquad Sk = \frac{OE-OC}{\sigma} = \frac{EC}{\sigma} \quad \text{or} \quad \frac{\frac{1}{2}BC}{\sigma}.$$

If the distance BC is less than σ the error of this estimate of the mean is negligible.

The distance BC cannot exceed 1.66σ for any curve which satisfies the conditions of a straight line for the midpoint locus, AB, or a constant value for σ at various points on the curve. Thus, the skewness, Sk, which can be treated, will be -0.83 to $+0.83$ (using the approximate mean derived from the above construction).

(*a*) *Area of isolated asymmetrical peaks.*—As may be seen from Fig. 7, the areas of the symmetrical and the asymmetrical peaks are virtually identical. The area may therefore be calculated from equation [3] where $h = AC$ (Fig. 7).

(*b*) *Area of overlapping asymmetrical peaks.*—If two peaks, only one of which is skewed, overlap, the area of the asymmetrical peak can be calculated using the corrections for the contribution of the symmetrical peak to the peak height of the other as described in the previous section.

The correction for the contribution of an asymmetrical peak to the height of either a symmetrical or skewed peak is more complicated and requires a series of successive approximations. In the remainder of this section, points and lines referred to are taken from Fig. 7. The distance between the peaks is measured in terms of the σ of the asymmetrical peak from the midpoint of the base line (point B) rather than from the mode (point C) to the mode of the second peak. The ordinate, Y, of the curve at the distance x can be calculated in the same way as for a symmetrical peak. The intersection of this height Y with the midpoint locus (line AB) is determined, and a new value for the distance x is measured from this point to the mode of the second peak. The height, Y, is recalculated using the corrected distance, and the entire operation is repeated if necessary.

These corrections, after the successive approximations, are given in terms of percentage of the interfering peak for various values of skewness, Sk, in Table I. The distance x between peaks is given in terms of σ of the interfering peak measured from the midpoint locus intersection with the base line (point B) to the mode of the peak under consideration. The corrections to be applied for symmetrical peaks ($Sk = 0$) have also been plotted on probability paper in Fig. 4.

DISCUSSION

The calculation for area using this method eliminates the subjective errors of construction in the triangulation method or of cutting in the paper weighing method. It is a

TABLE I

Peak height corrections[a] in percentage of peak height of interfering peak

Distance[c] between peaks	Skewness[b]																
	0.83	0.70	0.60	0.50	0.40	0.30	0.20	0.10	0.0	0.10	0.20	0.30	0.40	0.50	0.60	0.70	0.83
	Gently sloping side of curve									Steeply sloping side of curve							
2.0	9.7	10.2	10.4	10.8	11.2	11.7	12.3	12.8	13.5	14.4	15.2	16.3	17.5	19.4	22.2	26.0	Very large
2.1	8.2	8.5	8.8	9.1	9.4	9.7	10.1	10.5	11.0	11.6	12.2	12.9	13.6	14.7	16.2	18.6	21.0
2.2	6.8	7.1	7.3	7.5	7.8	8.0	8.3	8.6	8.9	9.3	9.7	10.1	10.6	11.2	12.0	12.9	14.8
2.3	5.7	5.8	6.0	6.1	6.3	6.5	6.7	6.9	7.1	7.4	7.6	7.9	8.2	8.5	8.9	9.4	10.5
2.4	4.6	4.7	4.9	5.0	5.1	5.2	5.4	5.5	5.6	5.8	5.9	6.1	6.2	6.5	6.7	7.0	7.5
2.5	3.8	3.8	3.9	4.0	4.1	4.2	4.3	4.3	4.4	4.5	4.6	4.7	4.8	4.9	5.0	5.2	5.5
2.6	2.9	3.0	3.1	3.1	3.2	3.2	3.3	3.3	3.4	3.4	3.5	3.6	3.7	3.7	3.8	3.9	4.0
2.7	2.3	2.3	2.4	2.4	2.5	2.5	2.5	2.6	2.6		2.6	2.7	2.8	2.8	2.8	2.9	3.0
2.8	1.8	1.8	1.9	1.9	1.9	1.9	2.0		2.0		2.0	2.1	2.1	2.1	2.2	2.2	2.2
2.9	1.4	1.4	1.4	1.4	1.5				1.5			1.5	1.6	1.6	1.6	1.6	1.6
3.0	1.0	1.0	1.1						1.1						1.1	1.2	1.2
3.1	0.8								0.8								0.8
3.2									0.6								
3.3									0.4								
3.4									0.3								
3.5									0.2								
3.6									0.2								
3.7									0.1								
3.8									0.1								
3.9									0.05								
4.0									0.03								

[a]Unfilled spaces, corrections same as center column.

[b]Skewness, $Sk = \frac{1}{4} BC/\sigma$ (see Fig. 7).

[c]Distance measured in terms of σ from midpoint locus intercept with base line of interfering peak to mode of peak being measured.

reasonably rapid procedure for isolated peaks requiring only the measurement of peak height and the determination of σ, either from the chromatogram itself by direct measurement or from a graph similar to Fig. 3 constructed from such measurements. For overlapping peaks the area determination is much less subjective than by any other method, and can be done quickly after practice.

A probability treatment for gas chromatography has been worked out by Sen (8). The values of the position of the peak (here called t_r) and of σ, the standard deviation, are stated to "completely define the distribution curve or the macroscopic behaviour of the column". Difficulty is frequently encountered in repeating work on two different columns which apparently have been made up identically. The same conditions of flow rate and temperature do not produce the same results due to microscopic differences in packing, etc. With proper manipulation of the adjustable variables, it is possible to reproduce the probability and distribution of successes, that is, curves with the same t_r and σ. This should be aimed at, rather than duplication of flow rate, temperature, etc., since this also corresponds to duplication of the number of theoretical plates, r, for, as pointed out by Schmauch (9),

$$r = \left(\frac{t_r}{\sigma}\right)^2. \qquad [10]$$

Another way of presenting this data is in a plot of σ versus t_r (both in minutes) as given in Fig. 3. By reversing the criteria in the above paragraph, deterioration of the column packing can be detected. Thus, the constancy of the σ versus t_r plot obtained under fixed conditions will indicate that the column is still in its original state.

If a measured value of σ for a given peak falls off the plot of σ versus retention time, two or more compounds have emerged together. Figure 2 gives the plot for a single SAIB column (10) obtained from a large number of chromatograms of peppermint oil. The σ obtained for one peak was invariably well off the curve even though the peak was often reasonably symmetrical. Further investigation showed that two compounds with nearly identical retention volumes were responsible for the wider peak. By a series of successive approximations using equation [3], it was possible to make an estimate of the two areas.

For all calculations in this paper, it has been assumed that the normal distribution curve holds true. Factors affecting the peak shape such as detector volume and sample size have been discussed by Johnson and Stross (11) and others. If both are kept small the curves obtained are sufficiently close to the normal curve for the use of these calculations. The peaks often obtained from highly polar compounds such as water, ammonia, amines, alcohols, etc. are too badly skewed to treat by calculations in this paper.

Using these calculations it is possible to obtain a great deal of information from chromatograms with incompletely resolved peaks. Thus it may be unnecessary to use long columns, a variety of packings, or long elution times to complete a difficult analysis.

SYMBOLS USED

A = area.
h = peak height.
r = number of theoretical plates.
t_r = time between introduction of the sample and the peak emergence.
w = peak width at any specified height.
x = distance from a peak center measured in units of its σ.
Y = the ordinate of the curve at a distance x from peak center.
Z = the special case of Y when $A = 1$.
σ = standard deviation.

ACKNOWLEDGMENTS

The authors wish to thank Mr. J. M. Airth and Dr. Leo Levi, of this Directorate, for valuable discussion and criticism during the development of the method.

REFERENCES

1. A. I. M. KEULEMANS. Gas chromatography. Reinhold Publishing Corp., New York. 1957. p. 32.
2. A. I. M. KEULEMANS. Gas chromatography. Reinhold Publishing Corp., New York. 1957. p. 111.
3. A. KLINKENBERG and F. SJENITZER. Chem. Eng. Sci. **5**, 258 (1956).
4. D. W. GRANT and G. A. VAUGHAN. J. Appl. Chem. **10**, 181 (1960).
5. C. H. GOULDEN. Methods of statistical analysis. 2nd ed. John Wiley and Sons Inc., New York. 1952. p. 30.
6. BIOMETRIKA TABLES FOR STATISTICIANS. Vol. 1. Cambridge University Press, London. 1954. p. 104.
7. K. PEARSON. *In* Methods of statistical analysis. 2nd ed. C. H. Goulden. John Wiley and Sons Inc., New York. 1952. p. 33.
8. B. SEN. Anal. Chim. Acta **22**, 130 (1960).
9. L. J. SCHMAUCH. Anal. Chem. **31**, 225 (1959).
10. D. M. SMITH, J. C. BARTLET, and L. LEVI. Anal. Chem. **32**, 568 (1960).
11. H. W. JOHNSON and F. H. STROSS. Anal. Chem. **31**, 1206 (1959).

SOLVENT EFFECTS AS AN AID IN THE ANALYSIS OF THE PROTON MAGNETIC RESONANCE SPECTRUM OF VINYL BROMIDE[1]

T. SCHAEFER[2] AND W. G. SCHNEIDER

ABSTRACT

By making use of specific solvent effects it has been possible to vary the relative chemical shift between the *geminal* protons of vinyl bromide from about +10 cycles/sec to −4 cycles/sec (at 60 Mc/sec) and to study the resultant changes in the proton resonance spectrum in the limiting region of zero chemical shift. Of particular interest is the growth and displacement of the combination lines, which appear in the resonance signals of the proton bonded to the same carbon atom as the bromine. From the variation of the six possible lines in this region it was confirmed that the *cis* and *trans* proton coupling constants must have the same sign. The intensity distribution of the lines in the *geminal* proton region require the *geminal* coupling constant to be of opposite sign to the other two.

INTRODUCTION

Recent studies of specific solvent interactions (1) have shown that, within limits, it is possible to vary the relative chemical shifts of protons in certain molecules in a continuous and controlled manner by altering the solvent conditions. This provides a very useful aid in arriving at an assignment and analysis of the proton spectrum, as well as a convenient method of studying the pronounced changes of the spectrum in the limit as the relative chemical shift is progressively reduced to zero. Solvent-induced shifts of this kind are generally observed for unsaturated molecules containing a strongly electronegative or electropositive substituent (1). Vinyl bromide, CH_2:CHBr, chosen for the present work, fulfills these conditions. Its proton spectrum is typical of a three-spin system and has been discussed by several authors (2, 3, 4, 5). Depending on the relative proton chemical shifts such spectra may be classed as ABX, ABC, or AB_2 types and are observed in the resonance spectra of many common molecules (2, 4, 5, 6, 7). In general vinyl compounds belong to the type ABC when observed at a measuring frequency of 40 Mc/sec, and usually also at 60 Mc/sec, although a rough analysis is often possible on the basis of an ABX type (8).

Lately it has become a matter of theoretical interest to determine, if not the absolute sign, at least the relative signs of the three coupling constants involved (9, 10, 12). Theory indicates that if the coupling constant is small between protons it may be negative, whereas if it is large it is probably positive (12). The coupling constant between the *geminal* protons in vinyl compounds is small, about 0 to 2 cycles/sec. The *trans* coupling constant is over 10 cycles/sec and often over 15 cycles/sec as compared with about 5 to 10 cycles/sec for the *cis* coupling constant (8). An exact analysis of the proton spectrum involves a numerical solution of the case ABC. This has been done for a number of vinyl compounds by means of a computer (11, 12). In particular, the proton spectrum of vinyl bromide requires the *cis* and *trans* coupling constants to be of the same sign but of opposite sign to the *geminal* coupling constant, the latter being small and presumably negative.

It is the purpose of the present work to present an experimental method for the determination of the relative signs of the *cis* and *trans* coupling constants in vinyl

[1]*Manuscript received June 21, 1960.*
Contribution from the Division of Pure Chemistry, National Research Council, Ottawa, Canada.
Issued as N.R.C. No. 5953.
[2]*Research Associate, summer 1959. Permanent address: Department of Chemistry, University of Manitoba, Winnipeg, Manitoba.*

bromide and to illustrate the appearance and growth of the combination lines as the relative electronic screening of the protons is changed.

EXPERIMENTAL

Measurements of the proton resonance spectra of vinyl bromide in the pure state and at various concentrations in solvents were made at 60 Mc/sec on a Varian n.m.r. spectrometer. The vinyl bromide was distilled before use and the solvents used were acetone, hexane, and benzene. The concentrations in acetone and hexane were 5 mole% but the solutions in benzene were made up approximately by volume. Since vinyl bromide boils below room temperature the pure substance was contained in a sealed tube. The solutions could be measured in an open tube.

RESULTS AND DISCUSSION

(a) Pure Vinyl Bromide

The observed spectrum of pure vinyl bromide is shown in Fig. 1 together with the proton assignment and the spectrum calculated as an *ABC* case. The resultant chemical shifts and spin-coupling constants are compared with those derived by Sheppard (11) and by Karplus, Grant, and Gutowsky (12) in Table I. Chemical shifts have been converted to 60 Mc/sec. It should be noted that Sheppard's parameters apply to a 10% solution in carbon tetrachloride.

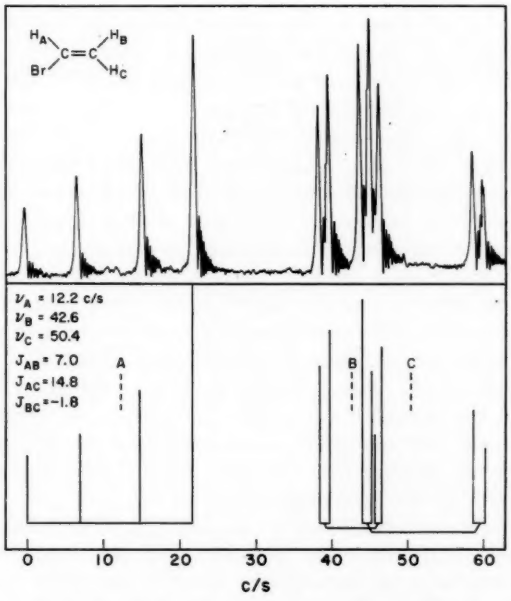

FIG. 1. Observed and calculated proton spectra of vinyl bromide at 60 Mc/sec. Increasing applied field is from left to right.

The opposite signs between J_{BC} and J_{AC} is not obvious from the spectrum at 60 Mc/sec because of the overlap of the two lines at about 45 cycles/sec in the observed spectrum. The relative positions of the lines can be fitted with all coupling constants of the same

TABLE I

Chemical shifts and spin-coupling constants (in cycles/sec) of pure vinyl bromide

	Sheppard,* cycles/sec	Karplus *et al.*, cycles/sec	This paper, cycles/sec
$\nu_C-\nu_B$†	7.3	8.1	8.1
$\nu_C-\nu_A$†	36.2	36.2	38.0
J_{AB}	7.1	6.9	7.0
J_{AC}	15.0	14.3	14.8
J_{BC}	−1.7	−1.8	−1.8

*10% in CCl_4.
†At 60 Mc/sec; notation of Fig. 1.

sign and with slight changes in the values of the parameters. However, at 40 Mc/sec there is no overlap and from the intensity distribution of the lines the other workers deduced the correct sign relationship. It is actually the pair of B lines at high field which decides the matter. In many of the spectra in Fig. 3 it is clear that in this pair the line at low field is much weaker than its neighbor. J_{BC} must be of opposite sign to J_{AC} and J_{AB} if this situation is to be met, together with the right intensities for the other lines arising from transitions of protons B and C.

(b) Relative Signs of J_{AB} and J_{AC}

Considerable labor is involved in the determination of the relative signs of the coupling constants even if a computer is available. It would be of value if there were a way of deciding, before the numerical work is begun, which of the coupling constants have the same sign. An examination of the spectra in Fig. 3 below suggests such a possibility. Note, first, that the most widely separated lines in the A region maintain a constant separation even though $\nu_C-\nu_B$ changes from positive to negative values. Then consider the line separations for the corresponding region for the case XBC given below in Part (*c*) (see also p. 134 of reference 7). One pair of lines (1 and 4 below) is separated by $|J_{AB}+J_{AC}|$ and since coupling constants are independent of chemical shift* this pair of lines should maintain a constant separation as $\nu_C-\nu_B$ is varied. If the line positions (as compared with the line intensities) of the vinyl bromide spectrum approximate sufficiently closely to an XBC spectrum, it follows that the pair of lines maintaining a constant separation in the A region of the observed spectra (X region in the case XBC) must be spaced by $|J_{AB}+J_{AC}|$. Evidently this is the case. In the seven spectra in Figs. 2 and 3 the two outside lines in the A region have a separation of between 21.7 and 22.2 cycles/sec (the variation can be attributed to experimental error and to the fact that we are really dealing with the case ABC). The other lines in the A region vary greatly in position as $\nu_C-\nu_B$ changes.

Hence $|J_{AB}+J_{AC}| \approx 22$ cycles/sec and if J_{AB} and J_{AC} are both less than 22 cycles/sec in magnitude, as seems clear, they must have the same sign. This fact reduces the four possible sign permutations in the three-spin system to two. If, in addition, the change in intensity distribution of the lines in the 40 cycles/sec region with change in $\nu_C-\nu_B$

It is, of course, well known that the chemical shift is directly proportional to the applied magnetic field while the coupling constants are independent of the latter. However, when the relative *electronic shielding of protons in a solute molecule is changed rather drastically by perturbations from solvent molecules, it is not inconceivable that the coupling constants will change somewhat because of a "selective perturbation" of the various bonds in the solute molecule. Experiments along these lines are being made.*

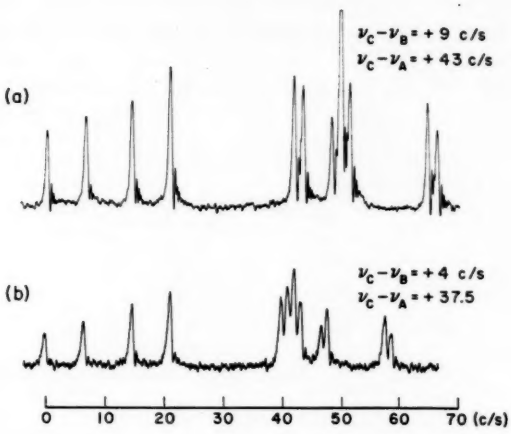

FIG. 2. Proton resonance spectrum of 5 mole% solution of vinyl bromide in (*a*) acetone and (*b*) *n*-hexane.

is taken into account, an a priori sign permutation can be arrived at by inspection of solvent effects on the spectrum.

(c) Combination Lines

The manner in which the relative chemical shifts of the protons in vinyl bromide are altered in different solvents is illustrated by the results shown in Table II. The

TABLE II

Proton chemical shifts of vinyl bromide in various solvents: concentration, 5 mole% (in cycles/sec at 60 Mc/sec, relative to external $CHCl_3$, and corrected for differences in bulk susceptibility)

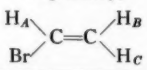

Solvent	Chemical shift (cycles/sec)			
	Proton *A*	Proton *B*	Proton *C*	$\nu_C-\nu_B$
Benzene	114	149	145	−4
n-Hexane	62.5	96	100	+4
Acetone	48	82	91	+9

nature of these solvent effects has been discussed elsewhere (1, 14, 15). Figure 2 shows the proton resonance spectra of vinyl bromide in acetone and hexane solutions and Fig. 3 shows the corresponding spectra for different concentrations of vinyl bromide in benzene. The relative chemical shifts of protons H_B and H_C are roughly indicated. As $\nu_C-\nu_B$ becomes small enough, two extra lines appear in the A region (Fig. 3(*a*)). As $\nu_C-\nu_B$ is further decreased and made negative they approach one another in position, coalesce, and then separate again (Figs. 3(*b*)–3(*e*)). For purposes of discussion it is appropriate to consider this region of the spectrum as the X region of an XBC spectrum. The exact (ABC) calculation in Fig. 1 agrees well with the approximate XBC calculation

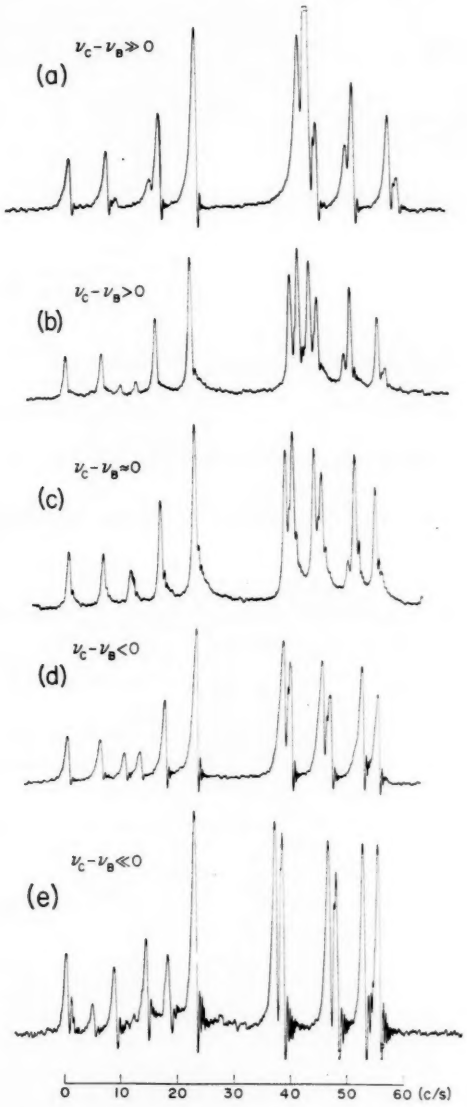

FIG. 3. Proton resonance spectrum of vinyl bromide at various concentrations in benzene. Approximate ratios (by volume) of vinyl bromide to benzene in the solutions are as follows: (*a*) 1:1, (*b*) ~2:3, (*c*) ~1:2, (*d*) ~1:3, (*e*) ~1:20.

in the prediction of the line *positions* in this region of the spectrum. The comparison in Fig. 5 between one of the observed spectra and the spectrum calculated using the parameters indicated is intended to show that the position of the predicted combination lines again agrees well with the *XBC* prediction. There is some disagreement in other

line positions but this only means that the chemical shifts employed in the calculated spectrum are not quite correct: the shift between protons B and C is no doubt not quite zero.

In the present notation the six transitions in the X (or A) region are then written relative to the origin of the lines as:

	Energy	Relative intensity
1.	$-\frac{1}{2}(J_{AB}+J_{AC})$	1
2.	D_+-D_-	$\cos^2(\phi_+-\phi_-)$
3.	$-D_++D_-$	$\cos^2(\phi_+-\phi_-)$
4.	$\frac{1}{2}(J_{AB}+J_{AC})$	1
5.	$-D_+-D_-$	$\sin^2(\phi_+-\phi_-)$
6.	D_++D_-	$\sin^2(\phi_+-\phi_-)$

The positive quantities D_+, D_- and angles ϕ_+, ϕ_- are defined by

$$D_+ \cos 2\phi_+ = \tfrac{1}{2}(\nu_C-\nu_B)+\tfrac{1}{4}(J_{AB}-J_{AC}),$$
$$D_+ \sin 2\phi_+ = \tfrac{1}{2}J_{BC},$$
$$D_- \cos 2\phi_- = \tfrac{1}{2}(\nu_C-\nu_B)-\tfrac{1}{4}(J_{AB}-J_{AC}),$$
$$D_- \sin 2\phi_- = \tfrac{1}{2}J_{BC}.$$

In these expressions $\nu_C-\nu_B$ has the same meaning as in the discussion above, namely, the relative chemical shift between protons C and B in cycles per second.

On this energy level scheme lines 1 and 4 are independent of $\nu_C-\nu_B$ and they are the lines at 0 and about 22 cycles/sec in the observed spectra. The predicted intensities are clearly wrong but they are much more sensitive to the correct wave functions than are the line positions and the main points of the discussion will still be valid.

Figure 4 gives a plot of the energy levels when $\nu_C-\nu_B$ is varied from 10 to 0 cycles/sec with $J_{AB} = 7.0$, $J_{AC} = 14.8$, $J_{BC} = -1.8$ cycles/sec. The plot as $\nu_C-\nu_B$ varies from 0 to -10 cycles/sec is the mirror image of Fig. 4. The combination lines 5 and 6 reach

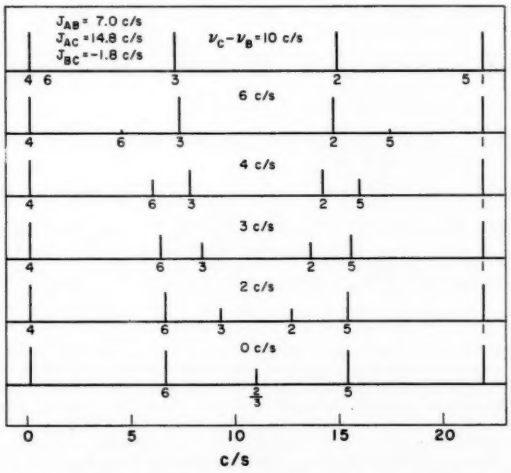

FIG. 4. The X part of an XBC spectrum calculated with the spin-coupling constants given and various values of the relative chemical shift $\nu_C-\nu_B$.

a measurable intensity for the given values of the coupling constants when $\nu_C - \nu_B$ is in the region of 5 cycles/sec. They derive this intensity at the expense of lines 2 and 3 (at about 7 and 15 cycles/sec in Fig. 1). When $\nu_C - \nu_B$ becomes less than 5 cycles/sec, lines 5 and 6 become effectively A lines. When $\nu_C - \nu_B = 0$, lines 2 and 3 coalesce, as is clear from the definitions of D_+ and D_-, and are in effect combination lines. When $\nu_C - \nu_B$ becomes less than zero, lines 2 and 3 separate and recede and eventually become A lines again, while 5 and 6 once more take on the role of combination lines. The sign of J_{BC} does not affect the predicted intensities.*

In the observed spectra this course of events is not followed exactly but is clearly similar. The combination lines arise at about the same value of $\nu_C - \nu_B$ (Fig. 3(a)) and coalesce when $\nu_C - \nu_B \approx 0$ (Fig. 3(c) and Fig. 5). The intensity distribution is, however,

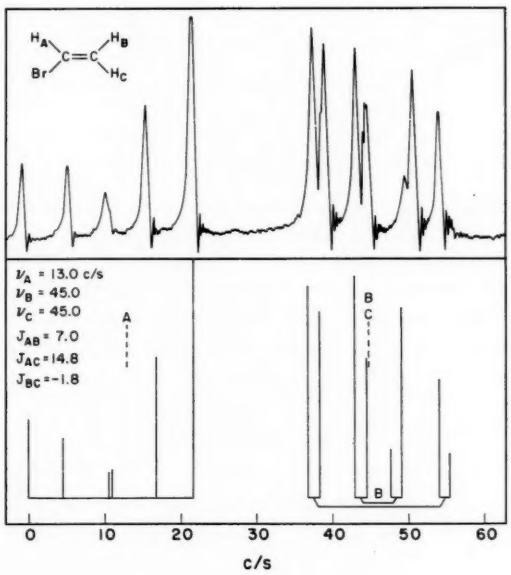

FIG. 5. The observed and calculated spectrum of vinyl bromide diluted in benzene. The spectrum was calculated as an XBC type with $\nu_C - \nu_B = 0$.

not in agreement with the XBC calculation. When $\nu_C - \nu_B$ becomes less than zero the effective combination lines are receding in the direction from which they appeared and have decreased in intensity.† The solvent effects are not large enough to eliminate them entirely.

It should perhaps be noted that it is only when $\frac{1}{2}|J_{BC}| \approx \frac{1}{4}|J_{AB} - J_{AC}|$ that the combination lines have a large predicted intensity. This is immediately clear from the definitions and expressions for the intensities above. If, on the other hand, $|J_{BC}| \gg |J_{AB} - J_{AC}|$ the predicted spectrum would in effect be one of three equally spaced lines when $\nu_C - \nu_B = 0$. These lines would have the intensity ratio 1:2:1 and this could lead to a wrong determination of coupling constants. Such an effect has been discussed and illustrated with actual spectra for p-fluorotoluene (13).

†*In Fig. 3(e) the couplings between C^{13} and H^1 nuclei in the benzene solvent produce a "hump" in the 15–20 cycles/sec region of the spectrum and obscure the true intensity relations of the lines. This effect could be eliminated by using the expensive C_6D_6 as a solvent.*

REFERENCES

1. T. SCHAEFER and W. G. SCHNEIDER. J. Chem. Phys. **32**, 1218, 1224 (1960).
2. W. A. ANDERSON. Phys. Rev. **102**, 151 (1956).
3. M. K. BANERJEE, T. P. DAS, and A. K. SAHA. Proc. Roy. Soc. A, **226**, 490 (1954).
4. H. S. GUTOWSKY, C. H. HOLM, A. SAIKA, and G. A. WILLIAMS. J. Am. Chem. Soc. **79**, 4596 (1957).
5. H. J. BERNSTEIN, J. A. POPLE, and W. G. SCHNEIDER. Can. J. Chem. **35**, 65 (1957).
6. R. E. RICHARDS and T. SCHAEFER. Mol. Phys. **1**, 331 (1958).
7. J. B. LEANE and R. E. RICHARDS. Trans. Faraday Soc. **55**, 707 (1959).
8. J. A. POPLE, W. G. SCHNEIDER, and H. J. BERNSTEIN. High resolution nuclear magnetic resonance. McGraw-Hill Book Co., Inc., New York. 1959. Chap. 2.
9. M. KARPLUS. J. Chem. Phys. **30**, 11 (1959).
10. H. M. MCCONNELL. J. Chem. Phys. **30**, 126 (1959).
11. N. SHEPPARD. Private communication.
12. M. KARPLUS, D. GRANT, and H. S. GUTOWSKY. ONR Report No. 17, University of Illinois. 1959.
13. T. SCHAEFER and W. G. SCHNEIDER. Can. J. Chem. **37**, 2078 (1959).
14. A. D. BUCKINGHAM. Can. J. Chem. **38**, 300 (1960).
15. A. D. BUCKINGHAM, T. SCHAEFER, and W. G. SCHNEIDER. J. Chem. Phys. **32**, 1227 (1960).

SOME FACTORS AFFECTING THE ZONE MOBILITY OF INORGANIC IONS DURING ELECTROMIGRATION IN PAPER[1]

R. A. BAILEY[2,3] AND L. YAFFE

ABSTRACT

A number of factors which affect the zone mobilities of inorganic ions were investigated. The influence of temperature was that expected from its effect on the conductance in free solution. The zone mobility tends to decrease, and the zone size to increase, with increasing migrant concentration. Excess foreign ions in the initial migrant zone can have a similar result. Experiments in the presence of the swelling agent thiourea indicate that swelling has at least a constant and perhaps a negligible influence on the obstructive factor. Finally, variation of the zone mobility with paper type was considered in relation to the ion-exchange capacity. Of the ions studied, only copper showed any correlation. Some observations were made using ion-exchange papers.

INTRODUCTION

The study of the electromigration of ions in moist paper has received considerable attention from the point of view of a separatory technique, but comparatively little has been done to try to understand the interactions between the ions and the porous supporting medium in this process. It is well known that many physical variables affect the zone mobility. However, very little work, aimed at investigating these variables thoroughly, has appeared. This paper will attempt to show quantitatively the effects of some of these variables with regard to inorganic ions.

The following are the factors which can have a direct influence on the zone mobility of an ion in paper.

1. Temperature

Since the conductance in free solution (and hence the mobility) of an ion increases with increasing temperature, a similar effect should be expected for the mobility in paper. This has been found by a few workers (1, 2, 3). Although the mobility values actually obtained may be questionable, the temperature coefficient seems to be similar in free solution and in paper, or about 2% per degree centigrade.

2. Absorbance

As the absorbance (the volume of liquid present per gram of paper) increases, so does the zone mobility. This factor was considered in a previous paper (4).

3. The Nature of the Supporting Medium

The zone mobility varies with the supporting medium, even when two papers are compared at corresponding values of absorbance. Although some effects might result from different fiber structure, this should be small, at least as long as only cellulose papers are considered. Most of the influence is more probably due to specific interactions of the ions with paper itself. This in turn could be different for various papers because of differences in the manufacturing process. In particular, the number of carboxyl groups which are present, and which can take part in ion-exchange reactions with the migrant ions, may differ from paper to paper. The fact that acid-washed paper yields larger

[1]*Manuscript received June 3, 1960.*
Contribution from the Radiochemistry Laboratory, Department of Chemistry, McGill University, Montreal, Que., with financial assistance from the National Research Council of Canada.
[2]*Holder of National Research Council Studentships, 1957–58, 1958–59, and 1959–60.*
[3]*Present address: Department of Chemistry, University College, University of London, London, England.*

values of zone mobility than the same paper without acid washing (3, 5) has been interpreted as implying that exchange processes are important. Exchange presumably takes place more readily between the migrant cation and the metal cation impurity than between the migrant ion and the hydrogen ion which would be on the carboxyl group in the absence of impurities. Examples of the effect of ion-exchange capacity will be shown later.

4. The Concentration and Composition of the Migrant Solution

The concentration of the migrant solution itself can have an effect on the resulting migration, but most studies on this have taken place in complex-forming media. Miller (6), Sato (7), and Strain (8) claimed that if the migrant ion is not adsorbed, the zone mobility is independent of the concentration unless this is greater than that of the background electrolyte solution. When it is greater, the size of the spot increases markedly, and the zone mobility decreases. In cases where small amounts of the migrant are strongly adsorbed by the paper, an increase in migrant concentration may result in an increased over-all mobility because of the more rapid motion of the non-adsorbed part. Such cases usually exhibit trailing. The increase in size of the zone when the migrant concentration exceeds that of the background electrolyte has been noted many times, and has been predicted theoretically by Edward (9).

The actual composition of the migrant solution apart from its concentration may be important also, since interactions between the components may give rise to their anomalous behavior. This may be an effect of ionic strength, or a specific chemical interaction, but the latter need not concern us here.

5. The Background Electrolyte Solution

The ionic strength and viscosity of the background electrolyte solution can affect the mobility of an ion moving in it. This will occur in free solution as well as in paper, as was brought out in a previous communication (4) where the calculation of zone mobilities was discussed. A more important effect of the background solution lies in its ability to form complexes with the migrant ions. If complexing occurs, the mobility observed will depend on the stability of the complex formed, as well as on the mobility of the complexed and non-complexed species present. It can be calculated in principle.

Berbalk and Schier (10) showed that the zone mobility of a weakly dissociated substance such as a weak acid depends on its degree of dissociation b. The zone mobility is given by

$$U_z = b\rho U_F \qquad [1]$$

where ρ is a factor for the slowing of the ions by the paper, and U_F is the actual speed of the ion formed by dissociation. For a weak acid, for example, this could be determined from the limiting conductance of the anion. Equation [1] is equivalent to the statement that the zone mobility is given by the speed of the mobile form and the fraction of time which the migrant spends in that form.

We can extend this to complex-forming systems where a number of mobile species are present in a rapid dynamic equilibrium. In the simplest case, suppose the forms present are M_1 and M_2, and the fraction of the migrant present as M_1 is b_1, and as M_2 is $b_2 = 1-b_1$. If the mobilities in free solution are U_{F_1} and U_{F_2}, respectively, then

$$\begin{aligned} U_z &= \rho[b_1 U_{F_1} + b_2 U_{F_2}] \\ &= \rho[b_1(U_{F_1} - U_{F_2}) + U_{F_2}] \end{aligned} \qquad [2]$$

if we neglect specific adsorption effects. If n species are present,

$$[3] \qquad U_z = \rho\left[\sum_{i=1}^{n} b_i U_{F_i}\right].$$

This takes into account adsorbed and non-ionized forms, since for these $U_F = 0$.

In practice, values of b and the free solution mobility of complex species usually are not known, so that this equation cannot be used to estimate the zone mobility. However, if more were known about ρ, this treatment might provide a means of obtaining information about the stabilities of complexes.

Extraneous factors such as evaporation and flow of background electrolyte solution in the strip can affect the zone mobility very much. Unless such factors are eliminated or corrected for, the zone mobilities obtained have no meaning. The chief factors of this sort which may be encountered are electroosmotic flow of electrolyte solution, flow of electrolyte from the ends toward the center of the strip (due to either evaporation from the strip or initial unsaturation of it), changes in concentration of electrolyte in the strip due to evaporation and non-uniform absorbance. These are problems of experimental technique.

From a very simple model (11) it can be shown that the zone mobility U_z may be given by the expression

$$[4] \qquad U_z = \rho U_F$$

where U_F is the mobility in free solution, and ρ is the obstructive factor which accounts for the tortuous path followed by a particle migrating through a medium such as wet paper. If adsorption effects are neglected, a semiempirical expression can be deduced for the obstructive factor (4, 12). For fibers which do not swell in the presence of the solution, this is

$$[5] \qquad \rho = \alpha\left(\frac{a}{a+v_s}\right) = \alpha\epsilon$$

where a is the absorbance, v_s is the specific volume of the fibers, and ϵ is the void fraction or porosity. Here, α is a constant equal to 0.96. For fibers which do swell,

$$[6] \qquad \rho = \alpha\left(\frac{a-2v_sX}{a+v_s}\right)$$

where X is the fractional increase in volume on swelling. The latter expression would be expected to apply to cellulose papers in aqueous solution, but X is not known.

We may define an apparent obstructive factor

$$[7] \qquad \rho_{app} = \frac{U_z}{U_F}.$$

The term ρ_{app} includes all factors which tend to slow an ion moving through a porous medium—adsorption as well as mechanical obstruction. This gives a means of comparing the hindrance encountered by different ions moving under various conditions.

If r represents an adsorption or hindrance factor,

$$[8] \qquad \rho_{app} = r\rho$$

where ρ is the mechanical obstructive factor calculated from equation [5] or [6]. For a given paper, r may vary with the migrant and the background electrolyte. In effect, r represents the fraction of time during which the ion is free to move.

Attempts have been made to account for adsorption effects by means of the chromatographic R_f factor, which is defined as

$$R_f = \frac{\text{distance moved by zone of substance}}{\text{distance moved by advancing solvent front}}.$$

This was used by Yasunaga and Shimomura (13) and Pucar and Jakovac (14). Since the conditions in paper chromatography and electromigration are not the same, and since the R_f factor is notoriously variable with minor changes in experimental technique, this is not satisfactory. An approach by Maki (15) based on partition chromatography is of interest, but it has not been sufficiently tested. Thus, although there are available a few values of ρ_{app} obtained under conditions such that all of the variables concerned were fixed (4), there is as yet no independent means of obtaining a value for r even if ρ can be calculated.

EXPERIMENTAL

A closed strip technique was used in which the paper was placed between metal plates and kept at a constant temperature. The paper was moistened to the desired absorbance by means of a pipette. Electrodes were placed in direct contact with the paper, and the electrolytic products were prevented from entering the central part of the strip by having suitable buffer solutions at the ends. Normally, no motion of background electrolyte could be detected.

Radioactive migrants were detected by measuring 1-cm broad segments of the strip with a Geiger counter, while inactive migrants were located by suitable chemical means. The migrant concentrations were very low, and small volumes were used. With inactive materials, 10 microliters of 0.001 M solution were used. The concentrations of the radioactive solutions were much lower.

Complete details of the technique and apparatus are given in a previous publication (4).

RESULTS AND DISCUSSION

The variation of zone mobility with temperature in several systems is illustrated in Fig. 1. The effect is that expected from the variation of the conductance. The temperature coefficient over the range 25° C to 39° C is about 2% per degree centigrade in all cases except that of Cu(II) moving in an oxalic acid background electrolyte solution. Here, the copper is present as a negatively charged complex. The increase in zone mobility (expressed as a negative number since the motion is anionic) is only 1.6% per degree centigrade, appreciably less than in the other examples. This would be the expected behavior if the complex were less stable at higher temperatures. There seems to be no change in the interaction of the ions with the paper over this temperature range. In those cases for which U_F could be found, the value of ρ_{app} did not change with temperature. This is shown in Table I.

The effect of migrant concentration was studied for Na^+ in 2.36 M acetic acid. The results are shown in Figs. 2 and 3. The first of these shows that the zone mobility decreases with increasing migrant concentration. This decrease is linear with the square root of the concentration, at least as long as this is greater than the ionic strength of the background electrolyte. In Fig. 3, the size of the zone relative to that given by 'carrier-free' Na^+ also yields a plot which is linear with the square root of the Na^+ concentration in this region.

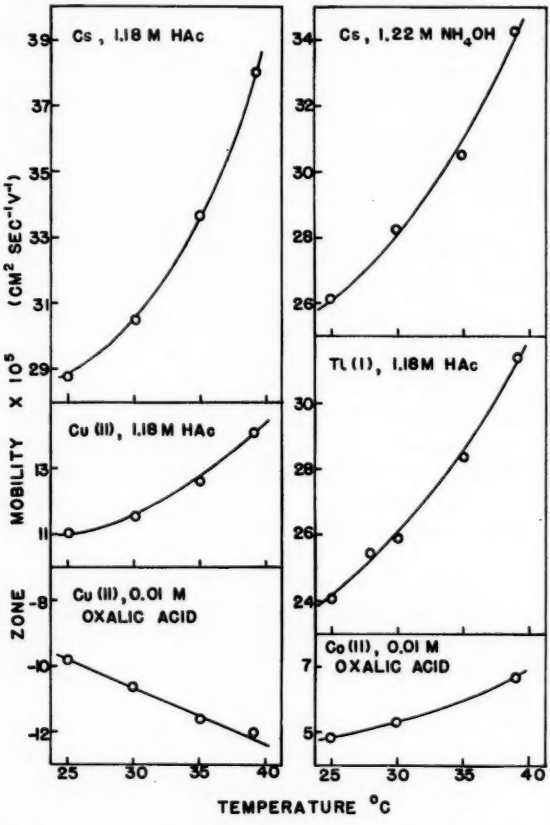

FIG. 1. Zone mobility vs. temperature for several ions in various background electrolytes; absorbance 0.96 ml/g, Whatman No. 52 paper.

TABLE I

Effect of temperature on zone mobility and apparent obstructive factor for Cs^+

Background electrolyte	Temperature, °C	U_z, $cm^2\ v^{-1}\ sec^{-1} \times 10^5$	ρ_{app}
1.18 *M* acetic acid	25	28.8	0.43
	30	30.5	0.42
	35	33.7	0.42
	39	38.0	0.42
1.22 *M* NH_4OH	25	26.1	0.35
	30	28.2	0.35
	35	30.5	0.35
	39	34.3	0.36

Further results on the variation of zone size with migrant concentration are shown in Table II. In both sodium and potassium acetate background solutions, the zone size

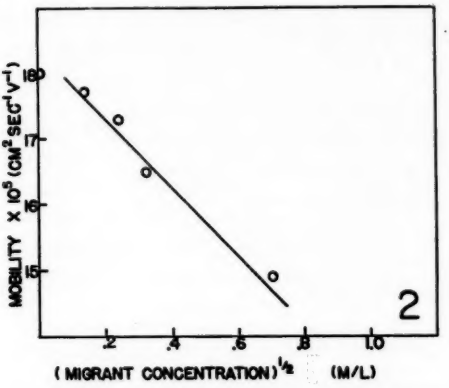

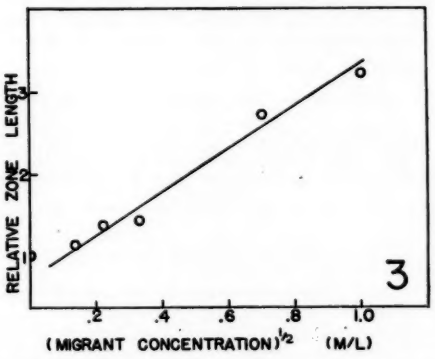

FIG. 2. Zone mobility vs. the square root of the migrant concentration for Na^+ in 2.36 *M* acetic acid; absorbance 0.96 ml/g, Whatman No. 52 paper, 25.0±0.5° C.

FIG. 3. Relative zone length vs. the square root of the migrant concentration for Na^+ in 2.36 *M* acetic acid; absorbance 0.96 ml/g, Whatman No. 52 paper, 25.0±0.5° C.

TABLE II

Variation of size of zone with initial concentration of migrant solution

Background electrolyte solution	Zone length (cm) with initial Na^+ concentration of:		
	0 *M**	0.005 *M*	0.025 *M*
0.005 *M* sodium acetate	4.0	4.0	5.8
0.01 *M* sodium acetate	2.5	2.5	4.5
0.005 *M* potassium acetate	3.5	4.5	8.5
0.01 *M* potassium acetate	2.5	4.0	7.0

NOTE: Migrant is Na^+ in solution as sodium acetate. Absorbance 0.96 ml/g, Whatman No. 52 paper, 25.0±0.5° C.
*'Carrier-free' solution.

becomes quite large when the concentration of the migrant Na^+ is greater than that of the background.

In Table III, the variation of zone mobility and size when the migration of 'carrier-free' Na^+ was carried out in the presence of increasing amounts of HCl in the initial

TABLE III

Effect of excess foreign ions present in the initial migrant solution on the zone mobility and zone size of Na^+

Initial concentration of HCl in migrant solution, moles/liter	U_x of Na^+, $cm^2\ v^{-1}\ sec^{-1} \times 10^5$	Relative zone length*
0	20.7	1
0.001	20.7	1.1
0.012	19.9	1.3
0.12	16.7†	2.0

NOTE: Background electrolyte 1.18 *M* acetic acid, absorbance 0.96 ml/g, Whatman No. 52 paper, 25.0±0.5° C.
*Relative to zone length given by 'carrier-free' Na^+ with no HCl present.
†Zone elongated with trailing.

zone is shown. The behavior can be due only to ionic strength effects here, since the moving zone of sodium is freed rapidly from excess H^+ and Cl^- ions. When the HCl concentration is increased to 0.12 *M*, the zone mobility decreases appreciably, while the zone itself becomes longer. Most of this effect is due to a low concentration tail from the main peak, which does not seem to be influenced very much.

Thiourea is a substance which, in aqueous solution, enhances the swelling of cellulose fibers. Determination of values of ρ_{app} in the presence of thiourea accordingly might give some information about the effect of swelling on a migrating ion. Values of ρ_{app} for Cs^+ and Na^+ in 1.18 *M* acetic acid are compared with those in 1.18 *M* acetic acid in 1 *M* thiourea in Table IV. As is evident, there is no increase in hindrance when

TABLE IV

Variation of the apparent obstructive factor in the presence of the swelling agent thiourea

		1.18 *M* acetic acid		1.18 *M* acetic acid in 1 *M* thiourea	
Ion	Paper (Whatman)	U_x, $cm^2\ v^{-1}\ sec^{-1} \times 10^5$	ρ_{app}	U_x, $cm^2\ v^{-1}\ sec^{-1} \times 10^5$	ρ_{app}
Na^+	52	20.7	0.48	21.4	0.51
	31 double thickness	17.3	0.40	18.8	0.45
	3 MM	19.8	0.46	21.4	0.51
Cs^+	52	28.8	0.43	29.1	0.45
	31 double thickness	24.6	0.35	27.2	0.42
	3 MM	27.5	0.41	30.7	0.47

NOTE: Absorbance 0.96 ml/g, 25.0±0.5° C.

thiourea is present for any of the three papers used. There may even be a slight decrease in those which are not hardened. This may be interpreted as indicating that the swelling is accompanied by an increase in the fractional volume of the fibers now permeable to the ions (16, 17), or to reduced adsorption which counteracts the effects of swelling. However, these results are in agreement with those of Vacik *et al.* (18, 19) which indicate that there is no decrease in void fraction, and hence in ρ, with wet (swollen) paper.

The above authors have studied a number of chromatography papers, and for Whatman No. 52, that used for most of our experiments, they found that ϵ, the porosity or void fraction, of the wet paper was 0.74. The value of ϵ calculated from equation [5] is 0.77

at the appropriate absorbance (2.05 ml/g). Although no value of X is known, any calculation using equation [6] would give a lower value for ρ. A value of X of 0.2, for instance, a reasonable estimate from previous work, would yield a result of 0.68. Values of X determined empirically (4) include adsorption effects as well as swelling. Moreover, the results of these workers indicate that the void fraction of wet paper is greater than that of dry paper, implying that, whatever swelling may occur, it does not decrease the void fraction on a molecular scale, and hence does not contribute to enhanced mechanical hindrance. This is in agreement with the values obtained for ρ_{app} in the presence of thiourea. These data indicate that the mechanical obstructive factor may be calculated reasonably well from equation [5], even for cellulose papers, and the specific effects of adsorption may be taken care of in the hindrance factor r. It remains possible that the fraction of the fibers, permeable to the migrant ions (16, 17), may show some specific nature.

For a given ion and background electrolyte, the zone mobility, and hence also ρ_{app}, may vary with the type of paper used, even if measurements are carried out at the same value of absorbance. Data on this are given in Table V. Of the properties of the

TABLE V

Variation of zone mobility with paper type for several ions

Whatman chromatography paper No.	Exchange capacity, meq/g	U_z, $cm^2\ v^{-1}\ sec^{-1} \times 10^5$				ρ_{app}			
		Cu^{++}	Zn^{++}	Cd^{++}	Na^+	Cu^{++}	Zn^{++}	Cd^{++}	Na^+
7	0.0027	8.4	12.2	11.1	16.5	0.20	0.31	0.30	0.43
52	0.0028	9.0	12.6	11.6	18.1	0.21	0.32	0.32	0.48
42	0.0029	8.2	13.5	11.8	—	0.19	0.34	0.32	—
4	0.0049	9.2	13.5	12.0	—	0.22	0.34	0.33	—
1	0.0056	7.5	10.1	8.5	—	0.18	0.26	0.23	—
20	0.0089	4.9	12.5	11.1	16.9	0.12	0.32	0.30	0.44

NOTE: Background electrolyte 2.36 M acetic acid, absorbance 0.96 ml/g, 25.0±0.5° C.

paper which may influence the mobility of an ion, adsorption by ion-exchange processes seems to be one of the most probable (15, 20). The values of the exchange capacity included in the table were determined by the method of Ultee (21); this is claimed to give a measure of the carboxyl content, and hence the ion-exchange capacity, of the paper. As is evident, the effects on ρ_{app} are very specific. There is no correlation between ρ_{app} and the exchange capacity except in the case of Cu(II). With this ion, ρ_{app} decreases roughly linearly as the exchange capacity increases (Fig. 4). Copper is more hindered than the other ions considered (ρ_{app} is smaller), indicating that more interaction is taking place. It appears that copper undergoes a different type of reaction with the paper and, although this seems to take place with the ion exchange sites, it may not be an ion-exchange process.

Jakovac and Lederer (22) have proposed from electromigration studies that copper, like a few other ions, forms complexes with cellulose. However, evidence indicates that these form with the hydroxyl groups on adjacent carbon atoms, rather than with carboxyl groups which are the chief ion-exchange sites.

Copper is also more hindered than zinc in Reeve Angel 934AH glass fiber filter paper. The zone mobilities and apparent obstructive factors of these ions in acetic acid are given in Table VI; the calculated obstructive factor is 0.86. This is considerably larger

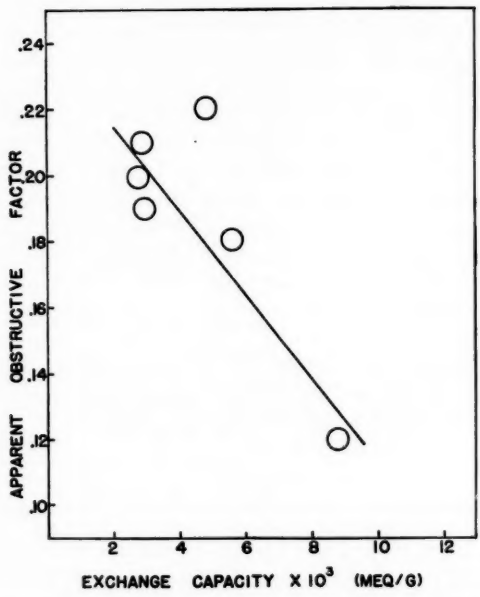

FIG. 4. Apparent obstructive factor vs. exchange capacity of the paper for Cu^{++}; background electrolyte 2.36 *M* acetic acid, absorbance 0.96 ml/g, 25.0±0.5° C.

TABLE VI

Zone mobilities of Cu^{++} and Zn^{++} in Reeve Angel 934AH glass fiber paper in acetic acid background electrolyte

Ion	Concentration of acetic acid, moles/liter	U_s, $cm^2\ v^{-1}\ sec^{-1} \times 10^5$	ρ_{app}
Zn^{++}	0.01	ca. 34	ca. 0.6
	0.12	34.0	0.66
	0.59	31.2	0.64
	2.36	25.9	0.66
	5.89	19.0	0.66
Cu^{++}	0.01	ca. 22	ca. 0.4
	0.12	23.0	0.42
	0.59	21.4	0.40
	2.36	17.1	0.43
	5.89	11.8	0.38

NOTE: Absorbance 3.96 ml/g, 25±0.5° C.

than any value of ρ_{app} for these ions, and indicates a good deal of adsorption. However, in cellulose acetate paper,* zinc and copper have similar mobilities. Although accurate measurements could not be made because of electroosmosis and difficulties in establishing a known, uniform absorbance, ρ_{app} was fairly close to the calculated value of ρ for copper, zinc, and sodium in acetic acid background electrolyte.

**'Oxoid electrophoresis strips' manufactured by Courtaulds Limited for Oxo Limited.*

Further experiments were carried out in paper loaded with Amberlite ion-exchange resins, and with cellulose ion-exchange papers. In Reeve Angel SA-2 papers which have strong cation exchange properties, cobalt, zinc, copper, and cesium all had very low mobilities in acetic acid. The mobilities in Reeve Angel WA-2 paper, a weakly acid exchanger, were higher under similar conditions, implying weaker adsorption. This is reasonable, since the carboxyl groups of this material are not strongly ionized in an acid solution. The bivalent ions showed similar behavior in Whatman P20 cellulose phosphate paper, and in Whatman CM50 carboxymethyl cellulose paper (strong and weak cation exchangers, respectively), but the univalent ions were comparatively faster. In the former, the zone mobility of Na^+ was about 10×10^{-5} cm^2 v^{-1} sec^{-1} in 2.36 *M* acetic acid at an absorbance of 0.98 ml/g. All mobilities in these materials were much lower than in ordinary papers, but this cannot be attributed completely to ion-exchange adsorption. In Whatman DE 20 diethylaminoethyl cellulose paper, an anion exchanger, the zone mobility of Na^+ was only 8.3×10^{-5}, and that of Zn^{++} and Cu^{++} about 3.7×10^{-5} and 1×10^{-5} cm^2 v^{-1} sec^{-1}, respectively, under similar conditions. These figures are not too significant because of factors such as electroosmosis, but they do show that even in this material copper is more hindered than zinc.

In anion-exchange resin loaded paper (Reeve Angel SB-2) the zone mobilities of cations are still much lower than in ordinary paper, although they are larger than in the cation-exchange papers. Jakubovic *et al.* (23) have reported some ionic mobilities in ion-exchange resins which indicate that bivalent ions in particular are hindered a great deal.

Most of the above work in ion-exchange papers, and in cellulose acetate, is only qualitative. Flow of background electrolyte is often different in these materials from that in ordinary paper; in some cases this was clearly evident from the visible distribution of liquid in the strip after electromigration. This was especially marked with cellulose acetate. Although in this instance the flow was measured with H_2O_2, uncertainties in corrections obtained from such measurements, and the non-uniform absorbance which was set up, make the figures obtained for U_s have little quantitative value. They do indicate, however, that this material offers less hindrance by non-mechanical effects (adsorption) than do the other materials studied. The zones, especially of sodium, were very sharp.

Ion-exchange papers may prove useful for separations, although the higher obstruction which they in general seem to possess is a disadvantage. A few preliminary experiments with cobalt and zinc in Reeve Angel SA-2, WA-2, and SB-2 papers showed that separations were possible in suitable complexing agents, but ordinary papers gave as good or better results.

REFERENCES

1. M. Maki. Japan Analyst, **3**, 311 (1954).
2. S. Yasunaga and O. Shimomura. J. Pharm. Soc. Japan, **74**, 62 (1954).
3. S. Achiwa. J. Electrochem. Soc. Japan, **25**, 266 (1957).
4. R. A. Bailey and L. Yaffe. Can. J. Chem. **37**, 1527 (1959).
5. S. Achiwa. J. Electrochem. Soc. Japan, **25**, 131 (1957).
6. J. Miller, W. F. Pickering, and F. L. Ward. Anal. Chim. Acta, **14**, 538 (1956).
7. T. R. Sato, W. P. Norris, and H. H. Strain. Anal. Chem. **27**, 521 (1955).
8. H. H. Strain. Anal. Chem. **24**, 356 (1952).
9. J. T. Edward. Chem. & Ind. (London), 276 (1958).
10. H. Berbalk and O. Schier. Monatsh. Chem. **88**, 1095 (1957).
11. H. G. Kunkel and A. Tiselius. J. Gen. Physiol. **35**, 89 (1951).
12. R. Crawford and J. T. Edward. Anal. Chem. **29**, 1543 (1957).

13. S. YASUNAGA and O. SHIMOMURA. J. Pharm. Soc. Japan, **74**, 321 (1954).
14. Z. PUCAR and Z. JAKOVAC. J. Chromatog. **2**, 320 (1959).
15. M. MAKI. Japan Analyst, **5**, 26 (1956).
16. J. J. BIKERMAN. J. Phys. Chem. **46**, 724 (1942).
17. D. A. I. GORING and S. G. MASON. Can. J. Research, B, **28**, 307 (1950).
18. J. VACIK and J. CABICAR. Collection Czechoslov. Chem. Communs. **25**, 404 (1960).
19. J. VACIK, O. GRUBNER, and J. DVORAK. Collection Czechoslov. Chem. Communs. **25**, 625 (1960).
20. M. MAKI. Japan Analyst, **5**, 23 (1956).
21. A. J. ULTEE and J. HARTEL. Anal. Chem. **27**, 557 (1955).
22. Z. JAKOVAC and M. LEDERER. J. Chromatog. **2**, 658 (1959).
23. A. O. JAKUBOVIC, G. J. HILLS, and J. A. KITCHENER. Trans. Faraday Soc. **55**, 1570 (1959).

LA RÉACTION DE REFORMATSKY APPLIQUÉE À L'OXO-2 CYCLOHEXANE-PROPIONITRILE ET À DES CÉTO-NITRILES ANALOGUES[1]

F. BRUDERLEIN,[2] HÉLÈNE BRUDERLEIN,[3] H. FAVRE, R. LAPIERRE[3] ET Y. LEFEBVRE[4]

RÉSUMÉ

L'action du bromo-acétate d'éthyle et du zinc sur l'oxo-2 cyclohexane-propionitrile, le diméthyl-4,4 oxo-2 cyclohexane-propionitrile et l'oxo-2 cyclohexane-acétonitrile est discutée; en plus de l'hydroxy-ester-nitrile attendu, on obtient divers composés: lactones-esters et acides carboxyliques. Les acides méthylène-2 cyclohexane-propionique, diméthyl-4,4 méthylène-2 cyclohexane-propionique et méthylène-2 cyclohexane-acétique sont décrits.

Pour des fins de synthèse dans le domaine des terpènes nous avons examiné les produits résultant de l'action du bromo-acétate d'éthyle et du zinc sur quelques céto-nitriles: oxo-2 cyclohexane-propionitrile (I) (1), diméthyl-4,4 oxo-2 cyclohexane-propionitrile (II) et oxo-2 cyclohexane-acétonitrile (III) (2). Baumgarten et Eifert (3) ont rapporté que la réaction de Reformatsky appliquée à l'acétyl-4 valéronitrile conduisait au composé normalement attendu, l'ester éthylique de l'acide cyano-6 hydroxy-3 diméthyl-3,4 hexanoïque, avec un rendement de 35%.

Nous attribuons la constitution II au produit de monocyanoéthylation de la diméthyl-3,3 cyclohexanone selon la méthode de Stork (1), parce que l'hydrolyse de ce céto-nitrile conduit à l'acide cétonique IV, p.f. 61–62°, que l'on obtient également par hydrolyse du composé V, issu de la cyanoéthylation de l'ester éthylique de l'acide diméthyl-4,4 oxo-2 cyclohexane-carboxylique.[5] La constitution du composé V est établie par le fait que ce céto-ester ne donne plus de réaction colorée avec le chlorure ferrique alcoolique: il n'est donc plus énolisable (voir (6)).

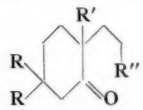

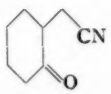

III

I	R = R' = H	R'' = CN	
II	R = CH_3	R' = H	R'' = CN
IV	R = CH_3	R' = H	R'' = COOH
V	R = CH_3	R' = COOEt	R'' = CN

La réaction de Reformatsky, à partir des cétones cyanoéthylées I et II, conduit à trois types de composés facilement séparables les uns des autres: 1) les hydroxy-ester-nitriles VI et VII; malgré plusieurs tours de distillation ils n'ont pu être obtenus tout à fait purs, mais leurs spectres infrarouges montrent bien leurs bandes nitrile, hydroxyle et ester; 2) les lactone-esters IX et X, caractérisées par une bande unique dans la région carbonyle du spectre infrarouge (1730 cm^{-1}, ester et δ-lactone); 3) des acides carboxyliques:

[1]*Manuscrit reçu le 6 juillet 1960.*
Contribution du Département de Chimie de l'Université de Montréal, Montréal, Qué. Ce mémoire a été présenté en partie au Congrès de l'Institut de Chimie du Canada, Vancouver, 3–5 juin 1957; il est tiré en partie de la thèse de doctorat de Y.L. et du mémoire de maîtrise de F.B.
[2]*Boursier du Conseil National de Recherches du Canada, 1957–1960.*
[3]*Madame Bruderlein et R. Lapierre ont reçu une bourse de l'Office de la Recherche Scientifique de la Province de Québec, 1956–1959.*
[4]*Boursier du Conseil National de Recherches du Canada 1953–1957. Adresse actuelle: Ayerst, McKenna & Harrison Ltd., Montréal, Qué.*
[5]*Pour la synthèse de ce céto-ester, voir (4, 5).*

(*a*) dans la série diméthylée l'acide est solide, de formule $C_{13}H_{22}O_5$, p.f. 144.5–145.5°; nous lui attribuons la constitution XIII bien supportée par un spectre infrarouge; il se décompose par chauffage en acide diméthyl-4,4 méthylène-2 cyclohexane-propionique (XV), dont la constitution est discutée plus loin.

(*b*) dans la série non méthylée les acides par chauffage se décomposent soit en acide méthylène-2 cyclohexane-propionique (XIV) dont la constitution est prouvée plus loin, soit en (éthoxycarbonyl-méthyl)-8*a* oxo-2 perhydro-chromanne (IX), identique à celui obtenu plus haut en 2); comme ces acides sont des huiles qui résistent à toute tentative de cristallisation leur nature exacte n'a pu être déterminée. La fraction acide qui se décarboxyle en acide à double liaison semicyclique pourrait renfermer soit le diacide hydroxylé XI par analogie avec la série diméthylée, soit un diacide déshydraté (du type XVII avec double liaison sur le cycle), soit encore l'acide VIII; tous ces composés sont susceptibles d'engendrer par chauffage une double liaison semicyclique (7, 8, 9, 10, 11). L'acide qui engendre la lactone IX serait l'ester XII. Ces fractions acides sont certainement des mélanges des isomères cis et trans.

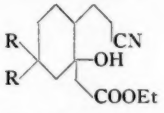

VI R = H
VII R = CH_3

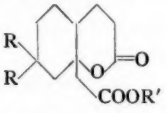

VIII R = H R′ = H
IX R = H R′ = C_2H_5
X R = CH_3 R′ = C_2H_5

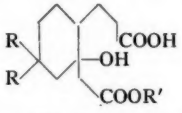

XI R = R′ = H
XII R = H R′ = C_2H_5
XIII R = CH_3 R′ = H

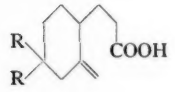

XIV R = H
XV R = CH_3

XVI

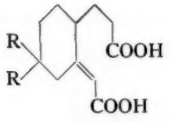

XVII R = H
XVIII R = CH_3

Les deux acides à insaturation semicyclique XIV et XV ont dans leurs spectres infrarouges les bandes caractéristiques, 1645 et 890 cm^{-1}, de la double liaison méthylénique, comme Stauffacher et Schinz (11) l'ont mentionné pour l'acide diméthyl-6,6 méthylène-2 cyclohexane-propionique. La formaldéhyde formée, selon le mode opératoire de Seidel, Schinz et Ruzicka (12), indique une teneur de 87% en liaison méthylénique chez l'acide XIV; cet acide fut obtenu également, avec un rendement global de 7–10%, en faisant réagir le méthylène-triphényl-phosphorane (13)[6] sur l'oxo-2 cyclohexane-propionitrile (I) et en saponifiant le nitrile méthylénique XVI brut.

L'hydrolyse (hydroxyde de potassium–méthanol) des lactone-esters IX et X conduit à des diacides que nous formulons comme XVII et XVIII rsepectivement, après examen de leurs spectres ultraviolets caractéristiques d'acides cyclohexylidène-acétiques (15) (XVII: λ_{max} 220.5 mμ, log ϵ = 4.11; XVIII: λ_{max} 221.5 mμ, log ϵ = 4.10) et de leurs spectres infrarouges montrant deux sortes de groupes carbonyles.

La saponification de l'hydroxy-ester-nitrile XI conduit à un acide brut, p.f. 124–137°, qui, traité par de l'acide chlorhydrique conduit à un carboxyméthyl-8*a* oxo-2 perhydro-chromanne (VIII), p.f. 150°; cette constitution est établie par spectroscopie infrarouge et par titrage alcalimétrique. Cet acide se décarboxyle difficilement par

[6]*Pour cette nomenclature, voir (14).*

chauffage en acide méthylène-2 cyclohexane-propionique (XIV) (rendement de 20%) et en divers autres composés que nous n'avons pas étudiés plus à fond. La pyrolyse de l'acide brut, p.f. 124–127°, mène à l'acide XIV avec un rendement voisin de 60%; il se forme également dans cette réaction des traces de γ-lactones et de δ-lactones, décelées par spectroscopie infrarouge.

À partir de l'oxo-2 cyclohexane-acétonitrile (III) la réaction de Reformatsky donne trois composés également: l'hydroxy-ester-nitrile XIX, dont le spectre infrarouge est typique pour ces groupes fonctionnels; l'ester lactonique XX, dont le spectre infrarouge présente les deux bandes caractéristiques de la γ-lactone et de l'ester; et une fraction acide, probablement XXI, qui donne XX par chauffage. L'hydrolyse de l'hydroxy-ester-nitrile XIX donne un mélange d'acides (diacide hydroxylé correspondant à XXI et acides non saturés XXII, selon le spectre infrarouge et le titrage alcalimétrique) qui se décarboxylent pour donner l'acide méthylène-2 cyclohexane-acétique (XXIII); cet acide a été caractérisé par son sel de benzyl-iso-thio-uronium; il est identique à celui que l'on obtient à partir du nitrile XXIV (préparé par la réaction de Wittig (13) au départ du céto-nitrile III). L'ozonolyse de cet acide XXIII confirme sa structure; le spectre infrarouge présente les bandes (1645 et 892 cm^{-1}) caractéristiques de la double liaison semi-cyclique.

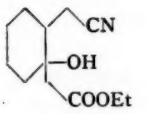

XIX

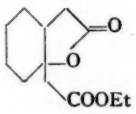

XX

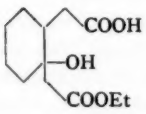

XXI

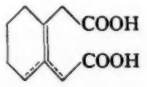

XXII

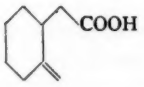

XXIII

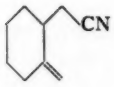

XXIV

La façon dont les divers produits de réaction se forment doit être soulignée. Une fois la condensation terminée et le composé zincique décomposé par de l'acide sulfurique on ne retrouve dans la phase organique, lors des extractions usuelles, que l'hydroxy-ester-nitrile. L'ester-lactone et la fraction acide se séparent peu à peu de la phase aqueuse acide sous forme d'une huile rouge; il faut donc admettre que ces derniers composés, solubles dans les solvants organiques, n'existent pas comme tels au moment de la décomposition du composé zincique, sans quoi on les retrouverait dans la phase organique à côté de l'hydroxy-ester-nitrile; nous formulons un composé intermédiaire basique formé dans le milieu anhydre requis par la condensation, puis retenu dans les eaux acides sous forme de sel, s'hydrolysant enfin petit à petit en lactone-ester et en acides carboxyliques; ce composé basique est une imino-O-lactone du type:[7]

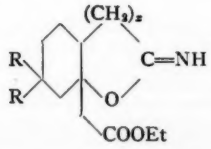

R = H ou CH_3

x = 1 ou 2

[7]*Les sels des imino-éthers s'hydrolysent en esters en milieu aqueux lorsque le catalyseur est un acide minéral fort (16, 17, 18, 19).*

PARTIE EXPÉRIMENTALE[8]

1. Diméthyl-4,4 oxo-2 cyclohexane-propionitrile (II)

1.1. La diméthyl-3,3 cyclohexanone est préparée d'après la méthode de Frank et Hall (20), selon le mode opératoire décrit en (21) pour la préparation de l'homocamphre.

1.2. Selon la technique de Cohen et Witkop (22) on prépare avec un rendement de 93.5% la N-(diméthyl-5,5 cyclohexényl-1) pyrrolidine, à partir de diméthyl-3,3 cyclohexanone et de pyrrolidine. C'est un liquide incolore, p. é. 125° sous 18 mm, brunissant très rapidement. Calculé pour $C_{12}H_{21}N$: C, 80.38; H, 11.81; N, 7.81%. Trouvé: C, 80.47; H, 11.55; N, 7.97%. Cette ène–amine est cyanoéthylée selon la technique décrite en (22). On obtient avec un rendement de 73% le *diméthyl-4,4 oxo-2 cyclohexane-propionitrile* qui, purifié par distillation, présente les constantes: p. é. 97–98° sous 0.55 mm, $n_D^{29} = 1.4640$. Calculé pour $C_{11}H_{17}NO$: C, 73.70; H, 9.56; N, 7.81%. Trouvé: C, 73.94; H, 9.47; N, 7.92%. Spectre infrarouge: —CN, 2250 cm^{-1}; =C=O, 1700 cm^{-1}. Dinitro-2,4 phénylhydrazone: aiguilles orangé, p.f. 148.5–149.5° (CH_3OH–$CHCl_3$). Calculé pour $C_{17}H_{21}N_5O_4$: C, 56.81; H, 5.89; N, 19.49%. Trouvé: C, 56.90; H, 5.93; N, 19.46%.

1.3. Le céto-nitrile précédent (1 g) est chauffé à reflux avec 625 mg d'hydroxyde de potassium dans 6.25 ml d'eau pendant 20 heures. Après refroidissement, on extrait par de l'éther pour éliminer les composés neutres, refroidit la solution aqueuse alcaline à 5°, ajoute lentement de l'acide chlorhydrique concentré refroidi à 5° jusqu'au virage bleu du rouge congo. On extrait l'acide libéré par de l'éther; on lave deux fois la solution éthérée avec de l'eau, sèche sur sulfate de sodium et distille l'éther; le résidu est recristallisé dans un mélange d'éther et d'éther de pétrole (p. é. 40–60°): on obtient 1 g d'acide diméthyl-4,4 oxo-2 cyclohexane propionique (IV), p.f. 61–62°, ne donnant pas de dépression avec l'acide préparé en 2.

2. Acide diméthyl-4,4 oxo-2 cyclohexane-propionique (IV)

On ajoute à 58 g de diméthyl-4,4 oxo-2 cyclohexane-carboxylate d'éthyle, dans 77 g de *tert*-butanol, 2 ml de Triton B (solution aqueuse d'hydroxyde de benzyl-triméthyl-ammonium à 40%), puis, goutte à goutte, en maintenant la température à 25°, 20 g d'acrylo-nitrile. Il y a précipitation abondante; on fait passer le précipité en solution par adjonction de 40 ml de benzène anhydre. Après 4 heures d'agitation le catalyseur est neutralisé par de l'acide chlorhydrique; la solution benzénique est lavée à neutralité. On distille le solvant et recristallise le résidu dans un mélange d'éther et d'éther de pétrole: 73 g (98% de rendement) d'éthoxycarbonyl-7 diméthyl-4,4 oxo-2 cyclohexane-propionitrile, p.f. 63°. Calculé pour $C_{14}H_{21}NO$: N, 5.57%. Trouvé: N, 5.62%. On hydrolyse le tout en chauffant à reflux avec 82.5 g d'hydroxyde de potassium dans 825 ml d'eau. Après 24 heures de chauffage on isole comme plus haut en 1.3, 55 g d'acide diméthyl-4,4 oxo-2 cyclohexane-propionique brut, p.f. 59°. On en prépare l'ester éthylique (méthode ordinaire à l'alcool éthylique et l'acide sulfurique) que l'on saponifie (méthode habituelle par KOH) et obtient ainsi l'acide plus pur, p.f. 62°; P.M. calculé 198.27; trouvé 197.3. Calculé pour $C_{11}H_{18}O_3$: C, 66.64; H, 9.15%. Trouvé: C, 66.43%; H, 9.05%.

[8]*Les points de fusion (p.f.) ont été déterminés en tubes capillaires, le thermomètre étant étalonné avec des substances de point de fusion connu (Bureau des Standards de Washington). Les spectres infrarouges ont été déterminés à l'aide d'un spectromètre Perkin–Elmer, modèle 21, optique* NaCl; *les liquides étaient sous forme de film, les solides en suspension dans le nujol; seules les bandes servant à l'identification des composés sont indiquées: les valeurs en* cm^{-1} *correspondent aux maxima d'absorption, sauf celles qui correspondent aux groupes* —OH *des acides carboxyliques et qui montrent la région entière de l'absorption. Les spectres ultraviolets ont été déterminés au moyen d'un spectromètre Beckman DK1, dans l'éthanol 95%. Les poids moléculaires (P.M.) des acides ont été déterminés par titrages alcalimétriques. Les analyses sont de Geller Laboratoires, Hackensack, N.J., et de W. Manser, Herrliberg, Suisse.*

Dinitro-2,4 phénylhydrazone de l'ester méthylique.—En traitant l'acide oxo-2 cyclohexane-propionique par une quantité équimoléculaire de dinitro-2,4 phénylhydrazine dans 20 fois son poids de méthanol contenant 4% d'acide chlorhydrique concentré on obtient la dinitro-2,4 phénylhydrazone de l'ester méthylique correspondant, aiguilles jaunes (MeOH), p.f. 110–111°. Calculé pour $C_{18}H_{24}N_4O_6$: C, 55.09; H, 6.16%. Trouvé: C, 55.15; H, 6.07%.

3. Action du bromo-acétate d'éthyle sur l'oxo-2 cyclohexane-propionitrile en présence de zinc

3.1. Dans un ballon rond à deux tubulures, surmonté d'un refrigérant et d'une ampoule à robinet, on introduit 33.3 g (0.510 mole) de zinc en fine grenaille, préalablement lavé avec de l'acide chlorhydrique à 5% et à l'eau et séché sous 12 mm à 100° en présence d'un petit cristal d'iode. On fait couler dans le ballon 40 ml du mélange: 70 g (0.463 mole) d'oxo-2 cyclohexane-propionitrile, 92.7 g (0.555 mole) de bromo-acétate d'éthyle, 140 ml de benzène et 93 ml de toluène anhydres. On amorce la réaction en chauffant légèrement et on fait couler, goutte à goutte, le reste du mélange, de façon à maintenir une douce ébullition. À la fin de l'addition on reprend le chauffage et maintient l'ébullition à reflux durant 2 heures 30 minutes. On abandonne ensuite la solution à 25° pendant 12 heures. On projette alors le tout sur 800 g de glace concassée et on ajoute 750 ml d'acide sulfurique 2 *N*. On obtient deux phases limpides que l'on agite vivement, sépare par décantation et examine séparément.

3.2. Examen de la phase organique.—Elle est lavée successivement par des solutions d'acide sulfurique à 5%, de carbonate de sodium à 10% et par de l'eau jusqu'à neutralité. Après séchage sur sulfate de sodium, on élimine les solvants par distillation et rectifie le résidu sous vide; fraction I: p. é. 96–149° sous 0.6 mm, 7 g, formée principalement par le céto-nitrile non entré en réaction; fraction II: p. é. 149–152° sous 0.6 mm, 21.9 g, constituée essentiellement de l'*ester éthylique de l'acide (cyano-2 éthyl)-2 hydroxy-1 cyclohexane-acétique* (VI), p. é. 128–130° sous 0.15 mm, $n_D^{23} = 1.4782$, après redistillation. Calculé pour $C_{13}H_{21}NO_3$: C, 65.24; H, 8.85; N, 5.85%. Trouvé: C, 65.92; H, 8.96; N, 5.04%. Spectre infrarouge: —OH (—COOH), 3400–2400 cm^{-1}; —OH (alcool), 3500 cm^{-1}; —CN, 2552 cm^{-1}; =CO ester, 1730 cm^{-1}.

3.3. Examen de la phase aqueuse.—Elle laisse déposer peu à peu une huile rouge, qui, après 8 heures, est extraite par de l'éther. La solution éthérée est lavée avec une solution d'hydroxyde de sodium à 10%, ce qui permet d'en extraire une fraction acide. Ce qui reste dans l'éther est isolé, après séchage de la solution et évaporation du solvant, et rectifié par distillation: l'*(éthoxycarbonyl-méthyl)-8a oxo-2 perhydro-chromanne* (IX) est un liquide incolore, p. é. 138° sous 0.4 mm, $n_D^{27} = 1.4842$. Calculé pour $C_{13}H_{20}O_4$: C, 64.97; H, 8.39. Trouvé: C, 64.82; H, 8.26%. Spectre infrarouge: =CO ester et δ-lactone, 1730 cm^{-1}.

La fraction acide est isolée en acidifiant les eaux alcalines et en extrayant l'huile formée par de l'éther. L'huile obtenue après distillation de l'éther ne cristallise pas. Par chauffage à 165°, sous vide de 0.1 mm, cette fraction acide se décompose en acide *méthylène-2 cyclohexane-propionique* (XIV) (voir plus loin en 5.2).

3.4. Au cours de certaines réactions de Reformatsky la fraction acide ne se décarboxyle pas en acide méthylène-2 cyclohexane-propionique, mais conduit à la lactone ester IX mentionnée en 3.3, p. é. 135° sous 0.3 mm, $n_D^{26} = 1.4842$ (identité prouvée par spectres infrarouges). Le spectre infrarouge de cette fraction acide montre une bande à 3520 cm^{-1} (—OH, alcool), une région d'absorption prononcée de 3400 à 2500 cm^{-1} (—OH, acide carboxylique), une bande large dans la région du groupe carbonyle, maximum à 1730 cm^{-1}, provenant des groupes —COOH et COOEt.

4. Carboxyméthyl-8a oxo-2 perhydro-chromanne (VIII)

On chauffe à l'ébullition à reflux durant 24 heures 5 g d'ester éthylique de l'acide (cyano-2 éthyl)-2 hydroxy-1 cyclohexane-acétique avec 5 g d'hydroxyde de potassium dans 50 ml d'eau. Après refroidissement on extrait par de l'éther pour éliminer les parties neutres; on acidifie par de l'acide chlorhydrique concentré la solution alcaline et on extrait les acides précipités par de l'éther; la solution éthérée est lavée à l'eau, séchée sur du sulfate de sodium et évaporée. Le résidu (4.18 g, 90%) se solidifie lentement. Après quatre cristallisations dans le mélange acétone–éther de pétrole le point de fusion s'étend de 124° à 137°. Le composé ainsi obtenu (14.2 g) est chauffé, 2 heures durant, sous un séparateur d'eau, dans 350 ml de benzène contenant 2 ml d'acide chlorhydrique concentré. Après distillation du benzène on recueille 14.0 g d'acide, p.f. brut 144–146°, montant à 150° après cristallisation dans le mélange acétone–éther de pétrole. P.M. trouvé 210.7; calculé 212.25. Calculé pour $C_{11}H_{16}O_4$: C, 62.25; H, 7.60%. Trouvé: C, 62.16; H, 7.68%. Spectre infrarouge: —OH (COOH), 3400–2400 cm^{-1}; bande forte à 1700 cm^{-1} (=C=O, acide) avec fort épaulement à 1730 cm^{-1} (δ-lactone).

5. Acide méthylène-2 cyclohexane-propionique (XIV)

5.1. Première méthode.—À une solution 14.3 g (0.170 mole) de phényl-lithium dans 150 ml d'éther on ajoute 61 g (0.170 mole) de bromure de méthyl-triphényl-phosphonium) puis on agite 1 heure à reflux sous atmosphère d'azote; à la solution rouge-brique refroidie à 0°, on ajoute goutte à goutte 25.7 g (0.170 mole) d'oxo-2 cyclohexane-acétonitrile; on chauffe à reflux pendant 3 heures, puis centrifuge et lave le précipité à l'éther. Les solutions éthérées réunies sont lavées à l'eau, séchées sur sulfate de sodium. Le résidu de la distillation de l'éther est distillé plusieurs fois pour fournir une fraction, p. é. 110–112° sous 0.5 mm, présentant des bandes à 2250 cm^{-1} (—CN) et 890 cm^{-1} (double liaison semicyclique), donc riche en méthylène-2 cyclohexane-propionitrile. Ce nitrile (3 g) est hydrolysé par chauffage avec 3 g d'hydroxyde de sodium dans 50 ml d'eau, pendant 24 heures. On isole à la manière habituelle 2.1 g d'acide; l'acide méthylène-2 cyclohexane-propionique pur présente les constantes suivantes: p. é. 108° sous 0.7 mm, $n_D^{25} = 1.4810$. Calculé pour $C_{10}H_{16}O_2$: C, 71.39; H, 9.59%. Trouvé: C, 71.29; H, 9.59%. Spectre infrarouge: OH (—COOH), 3400–2400 cm^{-1}; =CO acide, 1715 cm^{-1}; insaturation semi-cyclique, 1650 et 890 cm^{-1}.

5.2. Deuxième méthode.—En la chauffant à 165° sous vide de 0.1 mm, dans un ballon de Claisen, la fraction acide décrite plus haut en 3.3 se décarboxyle pour donner l'acide méthylène-2 cyclohexane-propionique, p. é. 107–109° sous 0.7 mm, $n_D^{21} = 1.4838$.

5.3. Troisième méthode.—En le chauffant à 165° sous 0.1 mm dans un ballon de Claisen le carboxyméthyl-8*a* oxo-2 perhydro-chromanne brut décrit en 4, p.f. 124–137°, se décarboxyle pour donner l'acide méthylène-2 cyclohexane-propionique qui distille; acide purifié par distillation, p. é. 104–114° sous 1.0 mm, $n_D^{23.5} = 1.4840$. Rendement de l'opération: 61%. Le spectre infrarouge montre des épaulements, sur la bande à 1715 cm^{-1} vers 1735 (δ-lactone) et 1770 (γ-lactone). En pyrolysant le carboxyméthyl-8*a* oxo-2 perhydro-chromanne, p.f. 150° (décrit en 4), on obtient à côté de l'acide méthylène-2 cyclohexane-propionique, p. é. 102° sous 0.4 mm, $n_D^{25} = 1.4842$ (25%), une fraction huileuse importante, p. é. 185°, dont le spectre infrarouge montre des bandes à 1740 et 1770 cm^{-1} indiquant une forte teneur en δ- et γ-lactones.

5.4. Sel de benzyl-iso-thio-uronium.—Aiguilles (MeOH), p.f. 145–145.5°. Calculé pour $C_{18}H_{26}N_2O_2S$: C, 64.64; H, 7.84%. Trouvé: C, 64.73; H, 7.90%.

5.5. Ozonolyse.—En suivant fidèlement la technique et les proportions indiquées par

Stauffacher et Schinz (11) 250 mg d'acide méthylène-2 cyclohexane-propionique ont donné 130 mg du dérivé formaldéhyde-dimédon (soit une teneur de 87% en liaison méthylénique) et 40 mg d'acide oxo-2 cyclohexane-propionique, p.f. 62.5°, ne donnant pas de dépression de point fusion en mélange avec l'acide authentique, p.f. 64° (23).

6. Acide carboxyméthylène-2 cyclohexane-propionique (XVII)

On chauffe sur un bain-marie, durant 2 heures 1 g d'(éthoxycarbonyl-méthyl)-8*a* oxo-2 perhydro-chromanne (IX), 1 g d'hydroxyde de potassium dans 20 ml de méthanol. On distille le méthanol et projette le résidu sur 50 g de glace. On acidifie la solution par de l'acide chlorhydrique concentré, jusqu'au virage bleu du rouge congo. L'acide carboxyméthylène-2 cyclohexane-propionique qui précipite (918 mg) est cristallisé dans l'eau, p.f. 161–162°. P.M. trouvé 211.8; calculé 212.24. Spectre ultraviolet: λ_{max} 220.5 mμ, log ϵ = 4.11. Spectre infrarouge: —OH (—COOH) 3400–2400 cm^{-1}; 1714 cm^{-1}, =CO acide non conjugué; 1690 cm^{-1}, =CO acide conjugué; 1623 cm^{-1}, double liaison conjuguée. Calculé pour $C_{11}H_{16}O_4$: C, 62.25; H, 7.60%. Trouvé: C, 62.11; H, 7.59%.

7. Action du bromo-acétate d'éthyle sur le diméthyl-4,4 oxo-2 cyclohexane-propionitrile en présence de zinc

En procédant comme plus haut en 3, on ajoute à 18.3 g de zinc un mélange de 44.4 g de diméthyl-4,4 oxo-2 cyclohexane-propionitrile, 51.8 g de bromo-acétate d'éthyle, 100 ml de benzène et 66 ml de toluène anhydres. On recueille (*a*) dans la phase organique 17 g de céto-nitrile de départ, p. é. 104–118°, et 4.8 g d'un mélange riche en ester éthylique de l'*acide (cyano-2 éthyl)-2 hydroxy-1 diméthyl-5,5 cyclohexane-acétique* (VII), p. é. 140–150° sous 0.45 mm. Calculé pour $C_{15}H_{25}NO_3$: C, 67.38; H, 9.43; N, 5.24%. Trouvé: C, 68.70; H, 9.16; N, 4.05%. Spectre infrarouge: —OH, 3505 cm^{-1}; —CN, 2268 cm^{-1}; =CO ester non conjugué, 1729 cm^{-1}; on décèle également une bande faible à 1717 cm^{-1}. (*b*) Dans la phase aqueuse acide (séparation en composés acide et neutre comme en 3.3) on recueille: l'*acide carboxyméthyl-2 hydroxy-2 diméthyl-4,4 cyclohexane-propionique* (XIII), 8.5 g, p.f. 144.5–145.5°. Anal. Calculé pour $C_{13}H_{22}O_5$: C, 60.45; H, 8.58%. Trouvé: C, 60.55; H, 8.58%. Spectre infrarouge: —OH (—COOH), 3400–2400 cm^{-1}; —OH (hydroxyle), 3505 cm^{-1}; =CO acide, 1700 cm^{-1} et l'*(éthoxycarbonyl-méthyl)-8a diméthyl-7,7 oxo-2 perhydro-chromanne* (X), qui après redistillation présente les constantes suivantes: p. é. 137° sous 0.3 mm; n_D^{22} = 1.4847. Calculé pour $C_{15}H_{24}O_4$: C, 67.14; H, 9.01%. Trouvé: C, 66.91; H, 8.90%. Spectre infrarouge: =CO ester et δ-lactone, 1731 cm^{-1}.

8. Acide diméthyl-4,4 méthylène-2 cyclohexane-propionique (XV)

L'acide carboxyméthyl-2 hydroxy-2 diméthyl-4,4 cyclohexane-propionique (XIII) (8.5 g) est chauffé dans un ballon de Claisen jusqu'à 165° à pression atmosphérique, puis à 0.6 mm jusqu'à 220°. Le vide varie de 0.6 à 2.7 mm, puis revient à 2 mm. En même temps un liquide incolore distille, p. é. 117–124° (3 g ou 48% de rendement); l'acide diméthyl-4,4 méthylène-2 cyclohexane-propionique redistillé présente les constantes: p. é. 102–103° sous 0.2 mm, n_D^{25} = 1.4755. Calculé pour $C_{12}H_{20}O_2$: C, 73.43; H, 10.27%. Trouvé: C, 73.35; H, 10.23%. Spectre infrarouge OH (acide) 3400–2400 cm^{-1}; =CO acide, 1706 cm^{-1}; double liaison semicyclique, 1647 et 894 cm^{-1}.

9. Acide carboxyméthylène-2 diméthyl-4,4 cyclohexane-propionique (XVIII)

Comme décrit en 6, la saponification de 11 g d'(éthoxycarbonyl-méthyl)-8*a* diméthyl-7,7 oxo-2 perhydro-chromanne (X) conduit à 9.2 g d'acide carboxyméthylène-2 diméthyl-4,4 cyclohexane-propionique. Le point de fusion brut 136–138° passe à 135–140° par

cristallisation dans un mélange d'acétone et d'éther de pétrole et à 137–140° par cristallisation dans l'eau. P.M. trouvé 246.2; calculé 240.30. Spectre ultraviolet: λ_{max} 221.5 mμ, log ϵ = 4.10. Spectre infrarouge: —OH (—COOH) 3400–2400 cm^{-1}; =CO acide conjugué, 1678 cm^{-1}; =CO acide non conjugué, 1707 cm^{-1}; double liaison conjuguée, 1629 cm^{-1}. Calculé pour $C_{13}H_{20}O_4$: C, 64.98; H, 8.39%. Trouvé: C, 64.91; H, 8.42%.

10. Action du bromo-acétate d'éthyle sur l'oxo-2 cyclohexane-acétonitrile en présence de zinc

Selon la technique décrite en 3, on ajoute à 37.3 g de zinc un mélange de 71 g d'oxo-2 cyclohexane-acétonitrile, 104 g de bromo-acétate d'éthyle, 150 ml de benzène et 100 ml de toluène anhydres. On examine immédiatement la phase organique et au bout de 24 heures la phase aqueuse.

(*A*) La phase organique contient 23 g d'*ester éthylique de l'acide cyanométhyl-2 hydroxy-1 cyclohexane-acétique* (XIX) qui après distillation présente les constantes: p. é. 128° sous 0.3 mm, n_D^{24} = 1.4788. Calculé pour $C_{12}H_{19}NO_3$: C, 63.97; H, 8.50; N, 6.22%. Trouvé: C, 63.98; H, 8.47; N, 6.06%. Spectre infrarouge: —OH, 3500 cm^{-1}; —CN, 2260 cm^{-1}; =CO 1720 cm^{-1}.

(*B*) La phase aqueuse abandonne: (*a*) 54.5 g d'*(éthoxy-carbonyl-méthyl)-7a oxo-2 oxa-1 perhydro-indène* (XX), p. é. 132° sous 0.5 mm, n_D^{22} = 1.4788. Calculé pour $C_{12}H_{18}O_4$: C, 63.70; H, 8.02%. Trouvé: C, 63.65; H, 7.94%. Spectre infrarouge: =CO (γ-lactone) 1780 cm^{-1}; =CO (ester) 1735 cm^{-1}. (*b*) 2.2 g d'acide qui par distillation donne 1.2 g d'un composé dont le spectre infrarouge est superposable à celui de l'(éthoxycarbonyl-méthyl)-*7a* oxo-2 oxa-1 perhydro-indène (XX).

11. Acide mthyélène-2 cyclohexane-acétique (XXIII)

11.1. Première méthode.—Selon le mode opératoire décrit en 5.1, on ajoute 15.4 g d'oxo-2 cyclohexane-acétonitrile dans 120 ml d'éther anhydre à une solution éthérée préparée à partir de 40.0 g de bromure de méthyl-triphényl-phosphonium, 2.4 g de lithium et 27 g de bromobenzène dans 106 ml d'éther. On chauffe à reflux, en atmosphère d'azote, pendant 3 heures. On obtient après extraction et distillation 2.2 g (15) d'un liquide incolore, jaunissant très rapidement, p. é. 95–105° sous 25 mm. Bande —CN à 2254 cm^{-1} et bandes à 1645 et 892 cm^{-1} (double liaison semicyclique) dans le spectre infrarouge. On hydrolyse immédiatement ce nitrile: 3 g sont chauffés à reflux durant 24 heures avec 3.8 g d'hydroxyde de potassium dans 10 ml d'eau. L'acide méthylène-2 cyclohexane-acétique, extrait à la manière habituelle, est un liquide, p. é. 139° sous 11 mm, n_D^{25} = 1.4814. P.M. trouvé 156.9; calculé 154.21. Calculé pour $C_9H_{14}O_2$: C, 70.10; H, 9.15%. Trouvé: C, 70.13; H, 9.16%. Spectre infrarouge: —OH (—COOH) 3400–2400 cm^{-1}; =CO acide, 1700 cm^{-1}; double liaison semicyclique, 1646 et 892 cm^{-1}.

11.2. Deuxième méthode.—Selon le mode opératoire décrit plus haut en 4, 20.8 g d'ester éthylique de l'acide cyanométhyl-2 hydroxy-1 cyclohexane-acétique (XIX) sont saponifiées par 20.8 g d'hydroxyde de potassium dans 200 ml d'eau. On obtient 17 g d'acides, cristallisant en partie dans le nitrométhane, p.f. 153.5–154.5°. P.M. trouvé: 208.8. Calculé pour l'acide hydroxy-1 cyclohexane diacétique-1,2, 216.24, et pour l'acide déshydraté correspondant XXII, 198.22. La littérature (24) donne pour un mélange des acides XXII isomères un point de fusion de 164–166°. En chauffant 125 g de l'acide, p.f. 153.5–154.5°, à 250° sous pression atmosphérique, puis sous 11 mm dans un ballon de Claisen, on recueille un distillat de 204 mg, p. é. 125–139°, n_D^{24} = 1.4795. On reprend cet acide par de l'éther; on lave la solution avec une solution aqueuse $NaHCO_3$ 10% refroidie à 5°; on libère l'acide méthylène-2 cyclohexane-acétique par HCl 10% (température 5°) que l'on isole à la manière habituelle par de l'éther. Le spectre infrarouge de cet acide est superposable à celui obtenu par la première méthode.

11.3. Sel de benzyl-iso-thio-uronium.—Après trois cristallisations dans l'acétone, aiguilles p.f. 159–160° (première méthode), 158–158.5° (deuxième méthode); pas de dépression en mélange. Calculé pour $C_{17}H_{24}N_2O_2S$: C, 63.72; H, 7.55; N, 8.74%. Trouvé: C, 63.71; H, 7.54; N, 8.69%.

11.4. Ozonolyse.—Selon le mode opératoire mis en œuvre en 5.5, 254 mg d'acide méthylène-2 cyclohexane-acétique donnent 150 mg de dérivé formaldéhyde-dimédon, p.f. 189–190°, soit un rendement de 34.2% correspondant à une teneur de 102.6% en insaturation semicyclique.

REMERCIEMENTS

Nous remercions le Conseil National de Recherches du Canada de son aide financière (subvention de recherches (H.F.) et bourses d'études (F.B. et Y.L.)), ainsi que l'Office de Recherches Scientifiques de la Province de Québec pour des bourses d'études à H.B. et R.L. Nous remercions aussi M. le Professeur C. Sandorfy de son aide dans l'étude des spectres infrarouges.

BIBLIOGRAPHIE

1. G. Stork, R. Terrell et J. Szmuszkovicz. J. Am. Chem. Soc. **76**, 2029 (1954).
2. B. Belleau. Can. J. Chem. **35**, 651 (1957).
3. H. E. Baumgarten et R. L. Eifert. J. Org. Chem. **18**, 1177 (1935).
4. R. Adams, S. Loewe, C. W. Theobald et C. M. Smith. J. Am. Chem. Soc. **64**, 2653 (1942).
5. A. Brenner et H. Schinz. Helv. Chim. Acta, **35**, 1333 (1952).
6. D. Stauffacher et H. Schinz. Helv. Chim. Acta, **37**, 1223 (1954).
7. N. A. Abraham et M. Vilkas. Compt. rend. **248**, 2880 (1959).
8. O. Wallach. Ann. **360**, 26 (1908).
9. B. Willhalm, U. Steiner et H. Schinz. Helv. Chim. Acta, **41**, 1359 (1958).
10. H. Favre et H. Schinz. Helv. Chim. Acta, **41**, 1368 (1958).
11. D. Stauffacher et H. Schinz. Helv. Chim. Acta, **37**, 1227 (1954).
12. C. F. Seidel, H. Schinz et L. Ruzicka. Helv. Chim. Acta, **32**, 1739 (1949).
13. G. Wittig et U. Schollkopf. Chem. Ber. **87**, 1318 (1954).
14. J. Levisalles. Bull. soc. chim. France, [5], 1021 (1958).
15. A. T. Nielsen. J. Org. Chem. **22**, 1539 (1957).
16. J. Stieglitz. Am. Chem. J. **39**, 29, 166, 402 (1908).
17. I. H. Derby. Am. Chem. J. **39**, 437 (1908).
18. W. McCracken. Am. Chem. J. **39**, 586 (1908).
19. H. I. Schlesinger. Am. Chem. J. **39**, 719 (1908).
20. R. L. Frank et H. K. Hall. J. Am. Chem. Soc. **72**, 1645 (1950).
21. H. Favre, B. Marinier et J. C. Richer. Can. J. Chem. **34**, 1329 (1956).
22. L. A. Cohen et B. Witkop. J. Am. Chem. Soc. **77**, 6595 (1955).
23. R. D. Haworth et C. R. Mavin. J. Chem. Soc. 1012 (1933).
24. C.-K. Chuang et C.-M. Ma. Ber. B, **68**, 871 (1935).

SELECTIVE ENZYMOLYSIS OF POLY-β-D-GLUCANS, AND THE STRUCTURE OF THE POLYMERS[1]

F. W. PARRISH,[2] A. S. PERLIN, AND E. T. REESE[3]

ABSTRACT

The soluble poly-β-D-glucan from oats has been subjected to degradation by two different types of enzymes. "Cellulase" converts the polysaccharide to a trisaccharide, 4-*O*-β-D-laminaribiosyl-D-glucose, and two tetrasaccharides, 3′-*O*-β-D-cellobiosyl-D-cellobiose and 4′-*O*-β-D-laminaribiosyl-D-cellobiose.* Degradation by the second enzyme, "laminarinase", produces a trisaccharide, 3-*O*-β-D-cellobiosyl-D-glucose, and a tetrasaccharide, 3-*O*-β-D-cellotriosyl-D-glucose.† These products, which account for 75–85% of the polymer in each experiment, have been characterized by chemical methods. The data show that the glucan is composed almost entirely of two types of structural sequences: one is a tetrameric unit in which a single β-(1 → 3) linkage alternates with two β-(1 → 4) linkages, and the other, a pentameric unit in which a single β-(1 → 3) linkage alternates with three consecutive β-(1 → 4) linkages.

The soluble poly-β-D-glucan from barley has been shown by enzymolysis with the "cellulase" to be closely related in detailed structure to the oat polymer.

Steric aspects of the enzymic degradations are discussed.

The grains of oats and barley contain water-soluble polysaccharides which are composed of β-D-glucopyranosyl units (1, 2, 3, 4, 5). In barley, the polyglucan appears to be closely associated with the malting process, during which there occurs a large increase in the proportion of the water-soluble polymer. Results from several investigations (6, 7, 8, 9) have shown that these polysaccharides are linear and that the monomeric units are joined by either (1 → 3) or (1 → 4) β-D-glycosidic linkages. An examination by Peat, Whelan, and Roberts (9) of the products formed by partial acid hydrolysis of oat glucan, has demonstrated clearly that both types of linkage occur together in the same chain, and that a major proportion of the polymer may be represented by a tetrameric repeating unit (I) in which two (1 → 4) linkages and a (1 → 3) linkage alternate. Lichenin, a poly-β-D-glucan from Iceland moss, was found also by this approach to be constituted in a closely similar fashion (9).

In the current study, the β-D-glucans from oats and barley have been degraded selectively with two different enzymic preparations, a "cellulase" and a "laminarinase". From the identity of the products formed detailed information about the structure of the polysaccharides has been obtained. The basic type of formula (I) advanced by Peat, Whelan, and Roberts has been confirmed for the oat glucan, and shown to apply also for barley glucan, and additional data about the constitution of these polymers provided.

$$G_p1 \rightarrow 3\ G_p1 \rightarrow 4\ G_p1 \rightarrow 4\ G_p$$

I

[1]*Manuscript received June 27, 1960.*

Contribution from the National Research Council of Canada, Prairie Regional Laboratory, Saskatoon, Saskatchewan, and the Microbiology Laboratory, Quartermaster Research and Engineering Center, Natick, Massachusetts.

Issued as N.R.C. No. 5975.

[2]*National Research Council of Canada Postdoctorate Fellow, 1959–1960.*

[3]*Microbiology Laboratory, Quartermaster Research and Engineering Center, Natick, Massachusetts.*

**For the sake of brevity, trivial names are used where possible in describing the oligosaccharides reported in this paper. More formal descriptions of the trisaccharide and two tetrasaccharides, respectively, are: O-β-D-glucopyranosyl-(1 → 3)-O-β-D-glucopyranosyl-(1 → 4)-D-glucose; O-β-D-glucopyranosyl-(1 → 4)-O-β-D-glucopyranosyl-(1 → 3)-O-β-D-glucopyranosyl-(1 → 4)-D-glucose; and O-β-D-glucopyranosyl-(1 → 3)-O-β-D-glucopyranosyl-(1 → 4)-O-β-D-glucopyranosyl-(1 → 4)-D-glucose.*

†*O-β-D-Glucopyranosyl-(1 → 4)-O-β-D-glucopyranosyl-(1 → 3)-D-glucose and O-β-D-glucopyranosyl-(1 → 4)-O-β-D-glucopyranosyl-(1 → 4)-O-β-D-glucopyranosyl-(1 → 3)-D-glucose, respectively.*

Enzymic Degradation by Cellulase

The glucans were found to be hydrolyzed rapidly and extensively by a cellulase isolated from *Streptomyces* sp. QM B814. This enzyme preparation hydrolyzes cellulose in high yield to cellobiose and cellotriose (10). Under conditions expected to minimize transglycosylation side-reactions, the products formed from both glucans were mainly one tri- and two tetra-saccharides, and only minor or trace proportions of higher oligosaccharides, disaccharides, and glucose were detected. The products (Table I) were isolated by preparative paper chromatography.

TABLE I

Yields of products from enzymolysis of poly-β-D-glucans*

Fraction	Cellulase				Laminarinase	
	Barley glucan		Oat glucan		Oat glucan	
Trisaccharide	628	(2.7)	638	(2.5)	520	(2.3)
Tetrasaccharides	303		337		302	
Disaccharide	68		75		61	
Glucose	9		8		81	
Unidentified†	93		67		—	

*Milligrams of crude product/1.0 g polyanhydroglucose. Figures in parentheses are moles trisaccharide : moles tetrasaccharide.
†Components remaining close to the origin on paper chromatograms.

The major product obtained from each glucan (yield, about 60%) was an amorphous trisaccharide, which was purified by conversion to a crystalline acetate. The physical constants of the derived acetate corresponded to those reported for 4-*O*-β-D-laminaribiosyl-D-glucose undecaacetate (9), and the free trisaccharide was found to possess this structure (II)* in the following way. On treatment with lead tetraacetate in the presence of potassium acetate the compound produced formic acid at the same rate as cellotriose (11), and consumed 4 moles of oxidant, consistent with the formulation of a

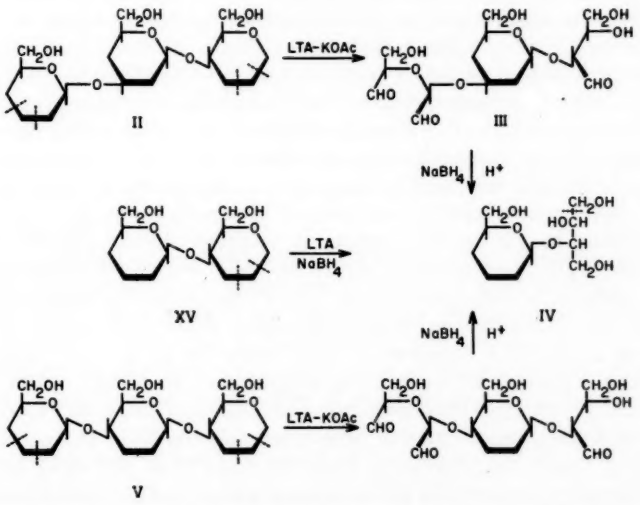

**All hexopyranosyl units represented by these formulae possess the D-gluco-configuration.*

4-substituted reducing end-unit, and the production of III. The oxidation product was reduced with sodium borohydride (12), and selectively hydrolyzed with acid under the conditions recommended by Smith and co-workers (13), yielding 2-*O*-β-D-glucopyranosyl-D-erythritol (IV) (14). Hence the central unit of the original trisaccharide was attached to the reducing end-unit by a β-(1 → 4) linkage. The validity of this degradation procedure was checked with cellotriose (V), which also yielded IV since the central unit in this trisaccharide is resistant to lead tetraacetate oxidation under the conditions used (11). In the absence of potassium acetate, a relatively slow uptake of about 1.7 moles of lead tetraacetate was observed with II, characteristic of a 4-substituted D-glucose (14), and reduction of the product afforded 2-*O*-β-D-laminaribiosyl-D-erythritol (VI). Presence of the β-(1 → 3) linkage in II was confirmed by partial hydrolysis, which afforded laminaribiose, characterized as the octaacetate.

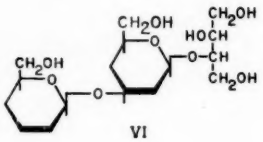

VI

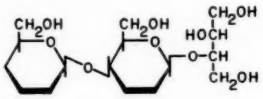

VII

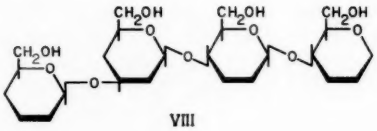

VIII

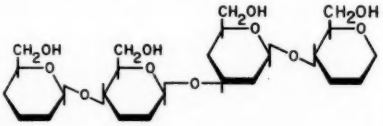

IX

The amorphous tetrasaccharide fraction obtained from the oat and barley glucans accounted for about 30% of the original polysaccharides. Oxidation of each fraction with lead tetraacetate – potassium acetate, followed by reduction of the oxidized tetramer with sodium borohydride and selective acid hydrolysis (13), yielded two products in a ratio of approximately 3 to 2. The major product was 2-*O*-β-D-cellobiosyl-D-erythritol (VII) and the other, 2-*O*-β-D-laminaribiosyl-D-erythritol (VI). Isolation of these two triitols showed that the tetrasaccharide fractions contained two components (not separable by paper chromatography), one containing a central β-(1 → 4) linkage and the other a central β-(1 → 3) linkage, and both having a β-(1 → 4) linkage adjacent to the reducing end-unit. One of these components was isolated by fractional crystallization,* and when degraded according to the reaction sequence described above afforded VII. Also, on reduction followed by partial acid hydrolysis, the crystalline tetrasaccharide gave laminaribiose, cellobiose, and trisaccharide (II). These properties therefore characterized the compound as 4′-*O*-β-D-laminaribiosyl-D-cellobiose (VIII). The second tetrasaccharide component was amorphous. However, it was shown to be 3′-*O*-β-D-cellobiosyl-D-cellobiose (IX), since it yielded VI on selective degradation (as above), and after reduction followed by partial hydrolysis it afforded cellobiose, laminaribiose, and trisaccharide (X).

A detailed structure for the major proportion (about 85%) of the oat and barley β-D-glucans may clearly be formulated from the identity of the three oligosaccharides obtained by enzymolysis. Since the molar ratio of trisaccharide to tetrasaccharide formed

**Two modifications of this tetrasaccharide were obtained, the α-anomer and a dihydrate of the β-anomer.*

is about 2.5 to 1, and since (on the average) about seven glucose units are linked by $(1 \rightarrow 4)$ bonds and three by $(1 \rightarrow 3)$ bonds, a structural relationship between polymer and products may be depicted as in Fig. 1.* According to this scheme, the polymers

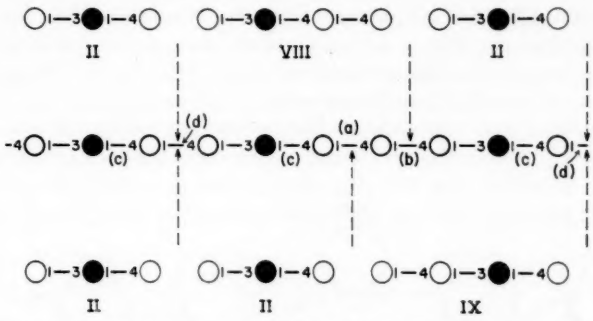

FIG. 1. Structural relationship between oat and barley poly-β-D-glucan (central row of circles) and oligosaccharides produced by the action of "cellulase". All circles represent β-D-glucopyranosyl units; those units which are bonded glycosidically through positions-1 and -3 are in black, for contrast.

contain two types of repeating units represented by (*a*) a tetrameric unit (I, page 2094) in which a single β-$(1 \rightarrow 3)$ linkage alternates with two consecutive β-$(1 \rightarrow 4)$ linkages (9), and (*b*) a pentameric unit in which a single β-$(1 \rightarrow 3)$ linkage alternates with three consecutive β-$(1 \rightarrow 4)$ linkages. The $(1 \rightarrow 3)$ bonds occur solely in isolated positions, but there can be few, if any, isolated $(1 \rightarrow 4)$ bonds in the molecule.† Rather, the $(1 \rightarrow 4)$ linkages are found most frequently in pairs and less often as a sequence of three, but the available evidence suggests that there are never more than three $(1 \rightarrow 4)$ linkages in consecutive order along the polymer chain.

Formation by the cellulase of the two tetrasaccharides VIII and IX appears to involve cleavage of bond (*b*) or (*a*), respectively (Fig. 1), 2 moles of trisaccharide II being formed in either instance. Since more of VIII than IX is produced, bond (*a*) is the more easily cleaved although the difference is rather small (ratio of 3.5 to 2). However, it may be noted that bond (*c*) is *not* cleaved by the enzyme, although it is also of the β-$(1 \rightarrow 4)$ type usually associated with cellulase action. As noted elsewhere (15), the D-glucosyl unit to the left of bond (*c*) is substituted at position-3, rather than at position-4, making for a "$(\rightarrow 3)$-β-$(1 \rightarrow 4)$" relationship. By contrast, linkages (*a*), (*b*), and (*d*), which possess a "$(\rightarrow 4)$-β-$(1 \rightarrow 4)$" arrangement, all are cleaved by the cellulase.

Enzymic Degradation by Laminarinase

A second type of enzyme, classified as a "laminarinase" by Reese and Mandels (16) since it shows high specificity for laminarin, was also found capable of rapidly degrading the β-D-glucans. This glycosidase is an endo-enzyme produced by *Rhizopus arrhizus* QM 1032. Acting on laminarin, it yields laminaribiose and laminaritriose as the dominant products (16). With the oat polymer, a tri- and tetra-saccharide were detected in the hydrolyzate together with a small proportion of laminaribiose. The major product, which

*For simplicity, the ratio of tri- to tetra-saccharide in Fig. 1 is 2 to 1. However, closer agreement is obtained with the ratio found experimentally by considering a larger repeating structure (e.g., one containing 20–25 units). The molecular weight of the polysaccharides was not estimated, but the low yield of formic acid produced during periodate oxidation of the materials (experimental section) indicated a D.P. value of not less than 50–100 units.

†Oligosaccharides having D.P. greater than 4, which were formed in low yield (Table I), were not examined and may represent minor structural sequences not accommodated by Fig. 1.

accounted for about 50% of the glucan, was an amorphous trisaccharide, characterized as the derived acetate. This trisaccharide was shown to be 3-*O*-β-D-cellobiosyl-D-glucose (X)* by the following reactions. It rapidly consumed 1 mole of lead tetraacetate per mole and yielded an equivalent of pentose showing that the reducing end-unit was substituted at position-3 (14). In agreement with this assignment the compound migrated on an electrophoretogram (18) at a rate close to that of laminaribiose. The oxidized trisaccharide was reduced to the corresponding glycitol (XI, not isolated) which was treated in turn with 2 moles of lead tetraacetate, followed by a second reduction. This degradation procedure had been used earlier to convert a 3-linked hexose disaccharide to a 2-*O*-glycosyl-glyceritol (19). Accordingly, the final product obtained was 2-*O*-β-D-cellobiosyl-glyceritol (XII).

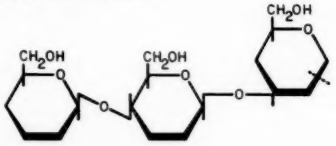

X

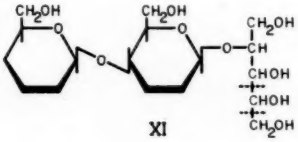

XI

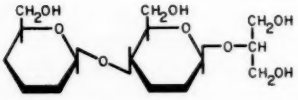

XII

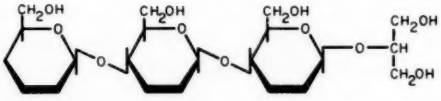

XIII

The tetrasaccharide, which accounted for 30% of the polymer, was crystalline. Its behavior on oxidation with lead tetraacetate and ionophoresis paralleled that of the trisaccharide (X) (above), showing that this compound also possesses a 3-substituted reducing end-unit. By selectively degrading the reducing end-unit to a 2-substituted glyceritol unit (as for X to XI), 2-*O*-β-D-cellotriosyl-glyceritol (XIII) was obtained. Accordingly, the tetrasaccharide produced by laminarinase action is 3-*O*-β-D-cellotriosyl-D-glucose (XIV, Fig. 2).

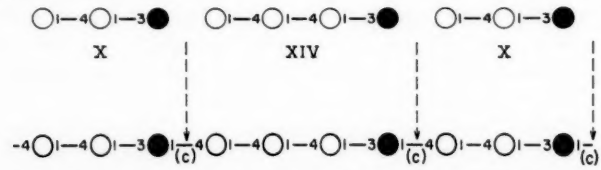

FIG. 2. Structural relationship between oat poly-β-D-glucan (lower row of circles) and oligosaccharides produced by the action of "laminarinase". All circles represent β-D-glucopyranosyl units; those units which are bonded glycosidically through positions-1 and -3 are in black, for contrast.

Together, the tri- and tetra-saccharide account for about 80% of the original oat β-D-glucan and are produced in a molar ratio of about 2.3 to 1. As shown in Fig. 2, formation of these products can readily be accommodated by the polymeric structure

*Two sets of physical constants have been reported for the undecaacetate of this compound: m.p. 110° C, $[\alpha]_D$ −8° (9) and m.p. 183° C, $[\alpha]_D$ −22° (17). (The acetate obtained in the current study has the same properties as recorded in reference 9.) Consequently, a confirmation of the structure of X appeared necessary, and is reported herein.

already depicted in Fig. 1.* With laminarinase, cleavage was specific for linkage (*c*), i.e., one adjacent to a β-D-glucosyl unit *substituted at position-3*, rather than the β-(1 → 3) bond itself (15). Hence, in contrast to the action of cellulase, only one tetrasaccharide was obtained. These results, therefore, fully complement those obtained by enzymolysis of the β-D-glucans with cellulase, and show clearly that the major proportion of the polysaccharides is constituted as depicted in Figs. 1 and 2. It is possible that the glucans comprise a mixture of molecules, some of which contain only the tetrameric repeating unit and others only the pentameric unit. However, formation of the two tetrasaccharides by the "cellulase" is accommodated most readily by assuming that both types of repeating units occur interspersed within the same molecule. Of possible significance in this connection is the fact that fractional precipitation of barley glucan yielded several fractions, each of which was hydrolyzed to the same degree by cellulase and gave the same mixture of products.

EXPERIMENTAL

Paper chromatography was carried out with ethyl acetate:pyridine:water (10:4:3) as solvent (20); for preparative chromatography Whatman 3MM paper was used. Spray reagents used were aniline oxalate (21) and ammoniacal silver nitrate (22). R_G represents the rate of travel of a compound on a chromatogram relative to the rate for glucose.

Paper electrophoresis (18) was carried out using borate buffer (pH 9.2 (23)) at 10 volts per centimeter.

Copper-reducing power was measured by the method of Nelson (24).

Solutions were evaporated at 40–50° C, and optical rotations were measured at approximately 25° C. Melting points are corrected.

Oat flour was milled from Fortune oats grown at the University of Saskatchewan, and barley flour from husky six-rowed barley grown in the Saskatoon area.

Isolation of Polyglucans

A combination of the procedures described by Morris (2) and by Meredith, Watts, and Anderson (5) was used. Oat or barley flour (3 kg), previously heat-inactivated with boiling 80% ethanol, was extracted with water (24 liters) for 3 hours in the presence of papain (6 g). The digest was centrifuged and ammonium sulphate (2200 g) was added to the supernatant solution causing flocculation of the polyglucan. The latter was collected, washed with 50% ethanol until sulphate-free, then with acetone, and air-dried. The barley glucan (19.0 g) was a white powder, $[\alpha]_D^{22}$ −13.1° (*c*, 0.9, H_2O). Found: anhydroglucose (copper-reducing power after hydrolysis), 89.0%; N, 0.37%; ash, 0.81%; moisture, 12.4%. The oat glucan (26.0 g) was a white fibrous material, $[\alpha]_D^{27}$ −8.3° (*c*, 0.9, H_2O). Found: anhydroglucose, 86.9%; N, 0.36%; ash, 0.17%; moisture, 10.2%.

Periodate Oxidation of Polyglucans

By oxidation of the polyglucans with 2 molar equivalents of sodium metaperiodate at 20° C in the dark, the following results were obtained:

Periodate consumed by barley glucan (moles/mole (hours)): 0.72 (20), 0.73 (45), 0.79 (95), 0.81 (141). Formic acid production (moles/mole) at 20 and 141 hours was 0.005 and 0.055, respectively, giving a corrected value of about 0.75 mole periodate consumed per anhydroglucose unit at 141 hours.

Closely similar data were obtained with the oat glucan. Periodate consumption (moles/

*See footnote, p. 2097.

mole (hours)): 0.65 (23), 0.76 (47), 0.77 (102), 0.80 (143). At 47 hours the yield of formic acid was 0.016 mole/mole.

Degradation of Barley Glucan Fractions with Cellulase

Ethanol was added dropwise to a vigorously stirred barley glucan solution (500 mg, 22.5 ml). Precipitates obtained (weights in parentheses) between zero and 17% ethanol (115 mg), 17–23% (276 mg), 23–31% (57 mg), 31–47% (21 mg), and 47–64% (5 mg) were collected and dried. The first four fractions (18 mg) were incubated in water (1.7 ml) at 48° C and pH 6 with cellulase (6 mg). No difference was observed between fractions in rate of hydrolysis (copper-reducing power). In addition, when the reducing power became constant (at glucose equivalent of 25%, 2 hours), paper chromatographic examination of the digests showed the presence in each of two main products, corresponding to a tri- and tetra-saccharide, respectively (R_G 0.45 and 0.22). Of the three minor products detected, two were indistinguishable from glucose and cellobiose, and the third had R_G 0.10.

Further experiments with the unfractionated glucan showed that the glucan:cellulase ratio could be increased to 8:1 with little effect on the degree of hydrolysis attained and the type of products formed.

Degradation of Oat and Barley Glucans with Cellulase

Oat or barley glucan (1.0 g) in water (100 ml) was incubated at 48° C with cellulase (0.12 g) for 5 hours. The enzyme was then inactivated by heating the digest for 10 minutes on the boiling-water bath, the digest was filtered, concentrated, and the syrup obtained was chromatographed on Whatman 3 MM paper sheets. After elution from the papers with water, the sugars were purified by use of mixed-bed ion-exchange resins. Yields of individual sugars are given in Table I.

Products from the Cellulase Degradation of Barley Glucan

*4-O-β-*D*-Laminaribiosyl-*D*-glucose* (II)

The trisaccharide fraction was chromatographically homogeneous containing neither laminaritriose nor cellotriose, $[\alpha]_D$ +11.6° (*c*, 1.3, H_2O). Partial hydrolysis of the material yielded cellobiose, laminaribiose, and glucose (paper chromatogram). On treatment with lead tetraacetate the rate of uptake of oxidant was closely similar to that of cellotriose and cellobiose (11, 14), and in the presence of potassium acetate the lead tetraacetate oxidation characteristics were those of a hexopyranosyl trisaccharide possessing a 4-linked reducing end-unit (11).

*4-O-β-*D*-Laminaribiosyl-β-*D*-glucose Undecaacetate*

A portion (53 mg) of II was heated at 100° C for 2 hours with acetic anhydride containing anhydrous sodium acetate. After evaporation of the acetic anhydride the product was isolated by extraction into chloroform and crystallized from ethanol (weight, 75 mg), m.p. 120–122° C and $[\alpha]_D$ −20.0° (*c*, 1.5, $CHCl_3$) (lit. (9) m.p. 121–123° C and $[\alpha]_D$ −22.2°). Calculated for $C_{40}H_{54}O_{27}$: C, 49.69%; H, 5.63%; acetyl, 48.98%. Found: C, 49.55%; H, 5.70%; acetyl, 49.10%.

Deacetylation of the material in the mother liquors, followed by paper chromatography, indicated the presence of II only.

Degradation of II *to 2-O-β-*D*-Glucopyranosyl-*D*-erythritol*

The amorphous material (149 mg) in water (1 ml) was taken up in acetic acid (9 ml) and treated with a solution of lead tetraacetate (660 mg, 5 molar proportions) and potassium acetate (400 mg) in acetic acid (27 ml). After 11 hours the excess tetravalent

lead was reduced with a 10% solution of oxalic acid in acetic acid (0.2 ml), and the solution was treated with excess Amberlite IR-120 and concentrated. By repeated addition of ethanol and toluene to the residue, and evaporation, the last traces of acetic acid were removed. The final residue was dissolved in water (5 ml) and added slowly to a solution of sodium borohydride (150 mg) in ice water (5 ml). After 16 hours, sodium ions were removed with Amberlite IR-120 and borate as the volatile methyl ester, and the reduced product was treated with 0.1 *N* sulphuric acid at room temperature for 16 hours (13). The hydrolyzate was neutralized with Dowex-1 resin and concentrated, and was found by paper chromatographic examination to contain two main components indistinguishable from 2-*O*-β-D-glucosyl-D-erythritol and glycerol. This mixture (105 mg) was fractionated on a column of coconut charcoal (25) (5 g) by gradient elution with aqueous ethanol up to a concentration of 20% ethanol, affording 2-*O*-β-D-glucopyranosyl-D-erythritol (40 mg), m.p. 191–194° C and $[\alpha]_D$ −15.2° (*c*, 1.3, H_2O). The X-ray diffraction pattern of the compound was indistinguishable from that of an authentic sample (14). Calculated for $C_{10}H_{20}O_9$: C, 42.25%; H, 7.09%. Found: C, 42.42%; H, 7.39%.

Degradation of II *to Laminaribiose*

A portion (800 mg) of II was hydrolyzed with 0.33 *N* sulphuric acid (30 ml) for 1 hour at 100° C, the hydrolyzate was neutralized, concentrated, and fractionated on a cellulose column using butanol saturated with water as solvent. Laminaribiose (117 mg) was isolated and characterized by conversion to the β-octaacetate, m.p. 163–165° C and $[\alpha]_D$ −26.2° (*c*, 2, $CHCl_3$), which gave an X-ray powder diagram indistinguishable from that of an authentic specimen. Calculated for $C_{28}H_{38}O_{19}$: C, 49.56%; H, 5.65%. Found: C, 49.38%; H, 5.78%.

2-O-β-D-Laminaribiosyl-D-erythritol (VI)

4-*O*-β-D-Laminaribiosyl-D-glucose (II) (200 mg) in water (0.5 ml) was taken up in acetic acid (30 ml) and oxidized with lead tetraacetate (320 mg). After 5 hours excess tetravalent lead was reduced and divalent lead precipitated by addition of excess 10% oxalic acid in acetic acid. The product was reduced with sodium borohydride and crystallized from methanol–ethanol, m.p. 164–166° C and $[\alpha]_D$ −23.8° (*c*, 1.5, H_2O). Calculated for $C_{16}H_{30}O_{14}$: C, 43.05%; H, 6.77%. Found: C, 42.84%; H, 7.08%.

2-O-β-D-Cellobiosyl-D-erythritol (VII) *and 2-O-β-D-Laminaribiosyl-D-erythritol* (VI) *from the Tetrasaccharide Fraction*

The tetrasaccharide fraction appeared to be chromatographically homgeneous, $[\alpha]_D$ +9° (*c*, 3.1, H_2O). The copper-reducing power ratio before and after acid hydrolysis was 1:3.9 (requires 4.0).

A portion (229 mg) of the material was oxidized in 90% acetic acid with lead tetraacetate (916 mg, 6 molar proportions) in the presence of potassium acetate (440 mg) for 11.5 hours. By the procedure described above, the oxidation product was recovered, reduced with sodium borohydride, and partially hydrolyzed. Paper chromatographic examination of the hydrolyzate showed the presence of two triitol components which, after separation by preparative paper chromatography, were found to be:

(*a*) *2-O-β-D-Laminaribiosyl-D-erythritol* (VI) (29 mg).—Crystallized from methanol–ethanol, it had a melting point of 171–173° C and gave an X-ray powder diagram indistinguishable from that of the authentic material.

(*b*) *2-O-β-D-Cellobiosyl-D-erythritol* (VII) (65 mg)—which, after crystallization from aqueous methanol, had a melting point of 209–211° C, $[\alpha]_D$ −8.3° (*c*, 1.2, H_2O), and gave an X-ray powder diagram indistinguishable from that of a specimen prepared from

cellotriose* (27). Calculated for $C_{16}H_{30}O_{14}$: C, 43.05%; H, 6.77%. Found: C, 42.86%; H, 6.84%.

Isolation of these two products showed that the original fraction contained two tetrasaccharide components. The ratio of the triitols, estimated by the anthrone method (26) after elution of the products from paper chromatograms, was 1.8 to 1.

*4′-O-β-*D*-Laminaribiosyl-α-*D*-cellobiose* (VIII)

The tetrasaccharide fraction (243 mg) afforded crystalline material (120 mg) from solution in aqueous methanol, m.p. 221–224° C (decomp.), $[\alpha]_D$ +12.9° (2 minutes) → +10.6 (45 minutes, constant) (*c*, 3.6, H_2O). Calculated for $C_{24}H_{42}O_{21}$: C, 43.24%; H, 6.35%. Found: C, 43.16%; H, 6.67%.

Degraded by the procedure described in the previous section, the crystalline tetrasaccharide afforded 2-*O*-β-D-cellobiosyl-D-erythritol (VII), but no laminaribiosyl-erythritol. Reduction of the tetrasaccharide with sodium borohydride, followed by partial acid hydrolysis with 0.33 *N* sulphuric acid at 100° C for 1 hour, yielded glucose, laminaribiose, cellobiose, and 4-*O*-β-D-laminaribiosyl-D-glucose (II) (paper chromatographic and electrophoretic evidence).

*3′-O-β-*D*-Cellobiosyl-*D*-cellobiose* (IX)

After separation of the crystalline tetrasaccharide (VIII) a second crop of impure VIII was precipitated by addition of ethanol to the mother liquor. Concentration of the supernatant solution afforded an amorphous product (80 mg), $[\alpha]_D$ +19.8° (*c*, 1.6, 90% CH_3COOH). On oxidation with lead tetraacetate – potassium acetate followed by reduction and partial hydrolysis, this material was found chromatographically to account for the production of 2-*O*-β-D-laminaribiosyl-D-erythritol (VI) from the tetrasaccharide fraction; a minor proportion of the cellobiosyl-erythritol (VII) was also detected. The material was reduced with sodium borohydride, then hydrolyzed with hot 0.33 *N* sulphuric acid for 1 hour, yielding glucose, laminaribiose, cellobiose, and 3-*O*-β-D-cellobiosyl-D-glucose (X) (paper chromatographic and electrophoretic evidence).

Products from the Cellulase Degradation of Oat Glucan

*4-O-β-*D*-Laminaribiosyl-*D*-glucose* (II)

This product, which was chromatographically homogeneous, was characterized by conversion to the β-undecaacetate (540 mg from 310 mg of free sugar), m.p. 120–122° C and $[\alpha]_D$ −22.7° (*c*, 1.5, $CHCl_3$). Calculated for $C_{40}H_{54}O_{27}$: C, 49.69%; H, 5.63%; acetyl, 48.98%. Found: C, 49.77%; H, 5.55%; acetyl, 48.73%.

Tetrasaccharide Fraction

The amorphous product afforded crystalline material from aqueous methanol, m.p. 223–227° C (decomp.), indistinguishable from VIII by comparison of X-ray diffraction powder diagrams. Calculated for $C_{24}H_{42}O_{21}$: C, 43.24%; H, 6.35%. Found: C, 43.04%; H, 6.38%.

In one experiment, a second crystalline modification of this tetrasaccharide was obtained and found to be a dihydrate of the β-anomer, m.p. 180–181° C and $[\alpha]_D$ +7° (2 minutes) → +10° (constant) (*c*, 2, H_2O). Calculated for $C_{24}H_{42}O_{21}.2H_2O$: C, 41.02%; H, 6.60%. Found: C, 41.05%; H, 6.76%. By seeding, the higher-melting α-form (m.p. 221–223° C) of the tetrasaccharide obtained from barley glucan (above) was converted to this lower-melting modification.

By the degradative procedure described above the original, amorphous, tetrasaccharide

**2-O-β-D-Cellobiosyl-D-erythritol was prepared from cellotriose by oxidation with 1.8 molar proportions of lead tetraacetate followed by reduction with sodium borohydride, as in the conversion of cellobiose to 2-O-β-D-glucopyranosyl-D-erythritol (14).*

fraction was shown (chromatographically) to yield both cellobiosyl-erythritol and laminaribiosyl-erythritol in a ratio of 1.7 to 1 (anthrone method (26)).

Enzymic Degradation of Oat Glucan with Laminarinase

Oat glucan (9.3 mg) in water (1.5 ml) was incubated at 40° C with laminarinase (1, 2 or 3 mg). At the two highest levels of enzyme concentration the copper-reducing power was virtually constant in 2 to 3 hours, when the apparent conversion to glucose was about 25%. A substantially slower reaction was observed at the substrate:enzyme ratio of 9:1. Examined by paper chromatography, all three digests were found to contain two major components which corresponded to a tri- and tetra-saccharide, respectively (R_G 0.47 and 0.22). Minor components detected were glucose, laminaribiose, and material having R_G 0.04.

Oat glucan (1.5 g) in water (100 ml) was incubated with laminarinase (0.25 g) for 2.5 hours. The digest was heated on the boiling-water bath for 7 minutes, filtered, and concentrated. The sugar mixture was fractionated by preparative paper chromatography; individual components were eluted and purified with mixed ion-exchange resins. Yields of the products are given in Table I.

3-O-β-D-Cellobiosyl-D-glucose (X)

The amorphous trisaccharide fraction was chromatographically and electrophoretically homogeneous, $[\alpha]_D$ +12.1° (*c*, 1.7, H_2O). On oxidation with lead tetraacetate in 97% acetic acid an uptake of 0.8 mole of oxidant per mole was found in 15–30 minutes and, in 90% acetic acid and in the presence of potassium acetate, the consumption of lead tetraacetate was 2.9 moles per mole. In both oxidations, approximately 1 mole of pentose (estimated colorimetrically (28)) was produced per mole of trisaccharide, the over-all data being consistent with presence of a 3-linked reducing end D-glucose unit.

Acetylation of the material (225 mg) with hot acetic anhydride – sodium acetate yielded a β-undecaacetate (340 mg), m.p. 104–105° C and $[\alpha]_D$ −9.7° (*c*, 1.6, $CHCl_3$). Calculated for $C_{40}H_{54}O_{27}$: C, 49.69%; H, 5.63%; acetyl, 48.98%. Found: C, 49.42%; H, 5.69%; acetyl, 49.37%.

2-O-β-D-Cellobiosyl-glyceritol (XII)

Trisaccharide X (264 mg) in water (1.5 ml) was taken up in acetic acid (50 ml) and treated with lead tetraacetate (232 mg, 1 molecular proportion) for 2 hours. Excess oxalic acid was added to precipitate the divalent lead, and the filtrate was concentrated. The residue in water (2 ml) was neutralized with sodium bicarbonate and the solution added dropwise to ice-cold sodium borohydride solution (264 mg, 12 ml). After 16 hours the reaction mixture was worked up, affording a solid product (227 mg), which was treated in 97% acetic acid (24 ml) with lead tetraacetate (424 mg, 2 molar proportions) for 16 hours. A second reduction with sodium borohydride followed, and the final product was crystallized from aqueous ethanol, m.p. 138–141° C and $[\alpha]_D$ −15.6° (*c*, 2.5, H_2O). The compound gave an X-ray diffraction pattern indistinguishable from that of an authentic sample* (27). Calculated for $C_{15}H_{28}O_{13}$: C, 43.27%; H, 6.78%. Found: C, 43.00%; H, 6.83%.

3-O-β-D-Cellotriosyl-α-D-glucose (XIV)

The tetrasaccharide fraction readily crystallized from solution in hot aqueous ethanol, m.p. 241–245° C (decomp.) and $[\alpha]_D$ +11.4° (5 minutes) → +8.4° (3 hours, constant)

**Prepared from 2-O-β-D-cellobiosyl-D-erythritol* (VII) *by oxidation with 1 molar proportion of lead tetraacetate followed by reduction with sodium borohydride, as in the degradation of 2-O-β-D-glucopyranosyl-D-erythritol to 2-O-β-D-glucopyranosyl-glyceritol (14).*

(*c*, 2.7, H_2O). Calculated for $C_{24}H_{42}O_{21}$: C, 43.24%; H, 6.35%. Found: C, 43.19%; H, 6.37%.

Treated in 97% acetic acid with 3 molar proportions of lead tetraacetate, the tetrasaccharide (20 mg) consumed 0.91, 0.96, and 0.99 mole of oxidant/mole at 5, 15, and 30 minutes, respectively, and yielded 1.0 mole of pentose/mole. Hydrolysis of the oxidation product with 0.33 *N* sulphuric acid at 100° C for 1 hour yielded arabinose, glucose, cellobiose, and cellotriose as well as two pentose-containing oligosaccharides (detected chromatographically).

*2-O-β-*D*-Cellotriosyl-glyceritol* (XIII)

Tetrasaccharide XIV (157 mg) was degraded as described above for the conversion of X to XI. The procedure involved, successively, oxidation with 1 molar proportion of lead tetraacetate, reduction with sodium borohydride, oxidation with 2 molar proportions of lead tetraacetate, and reduction with sodium borohydride. The final product was crystallized from aqueous ethanol (weight, 122 mg), m.p. 234–237° C; the X-ray powder diagram was indistinguishable from that of 2-*O*-β-D-cellotriosyl-glyceritol* (27), $[\alpha]_D$ −12.4° (*c*, 1.4, H_2O). Calculated for $C_{21}H_{38}O_{18}$: C, 43.60%; H, 6.62%. Found: C, 43.16%; H, 6.87% (hygroscopic material).

ACKNOWLEDGMENTS

The authors gratefully acknowledge the technical assistance of Mr. J. W. L. C. Christ. Barley flour was kindly provided by Mr. R. Teed, University of Saskatchewan, and a sample of Fortune oats by Dr. D. Knott, University of Saskatchewan. Microanalyses were performed by M. Mazurek, and X-ray diffraction patterns prepared by Miss Inez Gaffney.

REFERENCES

1. C. O'Sullivan. J. Chem. Soc. **41**, 24 (1882).
2. D. L. Morris. J. Biol. Chem. **142**, 881 (1942).
3. I. A. Preece and K. G. Mackenzie. J. Inst. Brewing, **58**, 353 (1952).
4. I. A. Preece and R. Hobkirk. J. Inst. Brewing, **59**, 385 (1953).
5. W. O. S. Meredith, T. A. Watts, and J. A. Anderson. Can. J. Chem. **31**, 653 (1953).
6. K. Gilles, W. O. S. Meredith, and F. Smith. Cereal Chem. **29**, 314 (1952).
7. G. O. Aspinall and R. G. J. Telfer. J. Chem. Soc. 3519 (1954).
8. R. A. Aitken, B. P. Eddy, M. Ingram, and C. Weurman. Biochem. J. **64**, 63 (1956).
9. S. Peat, W. J. Whelan, and J. G. Roberts. J. Chem. Soc. 3916 (1957).
10. E. T. Reese, E. Smakula, and A. S. Perlin. Arch. Biochem. Biophys. **85**, 171 (1959).
11. A. S. Perlin and A. R. Lansdown. Can. J. Chem. **34**, 451 (1956).
12. M. L. Wolfrom and H. B. Wood. J. Am. Chem. Soc. **73**, 2933 (1951).
13. I. J. Goldstein, G. W. Hay, B. A. Lewis, and F. Smith. American Chemical Society, 135th Meeting, Abstracts, 3D (1959).
14. A. J. Charlson and A. S. Perlin. Can. J. Chem. **34**, 1200 (1956).
15. F. W. Parrish and A. S. Perlin. Nature. In press.
16. E. T. Reese and M. Mandels. Can. J. Microbiol. **5**, 173 (1959).
17. H. Ono and M. Dazai. Nature, **183**, 1055 (1959).
18. A. B. Foster. J. Chem. Soc. 982 (1953).
19. A. J. Charlson, P. A. J. Gorin, and A. S. Perlin. Can. J. Chem. **35**, 365 (1957).
20. M. A. Jermyn and F. A. Isherwood. Biochem. J. **44**, 402 (1949).
21. R. H. Horrocks. Nature, **164**, 444 (1949).
22. S. M. Partridge. Nature, **158**, 270 (1946).
23. J. L. Frahn and J. A. Mills. Australian J. Chem. **12**, 65 (1959).
24. N. Nelson. J. Biol. Chem. **158**, 375 (1944).
25. F. W. Barth and T. E. Timell. Can. J. Chem. **36**, 1321 (1958).
26. D. L. Morris. Science, **107**, 254 (1948).
27. P. A. J. Gorin and A. S. Perlin. Unpublished results.
28. W. R. Fernell and H. K. King. Analyst, **78**, 80 (1953).

**Prepared from cellotetraose by a sequence of reactions involving two oxidations with lead tetraacetate and two reductions with sodium borohydride, the procedure being the same as used in degrading cellobiose* (XV) *to 2-O-β-*D*-glucopyranosyl-glyceritol (14), and cellotriose to 2-O-β-*D*-cellobiosyl-glyceritol (see above).*

STRUCTURE OF BRIDGMAN'S BLACK CARBON DISULPHIDE[1]

E. WHALLEY

ABSTRACT

The infrared spectrum of black carbon disulphide dispersed in a potassium bromide disk has been examined. The blackness and the infrared spectrum are consistent with its being a linear polymer, $-(C{=}S.S)_n$.

1. INTRODUCTION

Bridgman (1) found that carbon disulphide transformed slowly to a black solid at pressures of about 45 kilobars and temperatures over 175° C. When heated to about 200° C at normal pressure it decomposed to carbon and sulphur. It was denser than either graphite or sulphur, and it gave a broad, diffuse X-ray diffraction pattern. He suggested that the structure might be similar to that of silicon dioxide, i.e. a three-dimensional network of carbon and sulphur atoms linked by single bonds. It is difficult to see how a substance with this structure would be black. The blackness of black carbon disulphide demands a highly polarizable system, probably a conjugated one. The simplest that can be envisaged is a linear structure with the unit

repeated indefinitely. The group

is a strong chromophore (2, 3) and thiophene is an aromatic compound, so it seems very likely that the C—S—C group can conjugate with the C=S group. It is difficult to imagine any other structure which is conjugated and in which the atoms are not formally charged.

In order to test this structure, we have investigated the infrared spectrum of black carbon disulphide.

2. EXPERIMENTS AND RESULTS

A small amount of black carbon disulphide was made by subjecting carbon disulphide to a pressure of about 55 kilobars at 185° C in a simple squeezer (4). About 0.1 to 0.2 mg were incorporated into a disk with 400 mg of potassium bromide; more than this amount in the disk caused too much scattering. The spectra were recorded with a Perkin–Elmer Model 21 double-beam infrared spectrophotometer with a sodium chloride prism and with a Beckman IR-4 double-beam spectrophotometer with a cesium bromide prism. Many of the absorption bands observed were very weak and so a 10-times scale expansion was used, and the transmission of a disk containing the sample was divided

[1]*Manuscript received July 8, 1960.*
Contribution from the Division of Applied Chemistry, National Research Council, Ottawa, Canada.
Issued as N.R.C. No. 5946.

point by point by the transmission of a disk containing only potassium bromide. Calibration was conveniently done on the 10-times scale by using incompletely compensated atmosphere bands. The spectrum is shown in Fig. 1. A strong band of variable relative

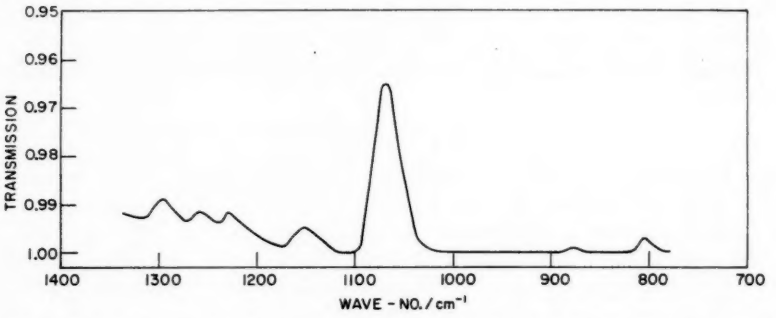

FIG. 1. Infrared spectrum of black carbon disulphide dispersed in a potassium bromide disk.

intensity was always present at $1502\pm\sim5$ cm^{-1}. It could be removed by prolonged evacuation and gentle warming either before or after making the potassium bromide pellet, and it is attributed to unchanged carbon disulphide. The small shift from the vapor frequency, which is 1522 cm^{-1}, indicates that the carbon disulphide is not very strongly attached to the black carbon disulphide. The difficulty of removing it is therefore probably due to slow diffusion through the black carbon disulphide. The other bands were of constant relative intensity, and are listed in Table I.

TABLE I

Infrared bands of black carbon disulphide

Frequency cm^{-1}	Rough relative intensity	Assignment
$1286\pm\sim5$	w	O—H bending, end group?
$1250\pm\sim5$	w	C—O stretching, end group, and bands due to imperfections in the chain?
$1220\pm\sim5$	w	
$1144\pm\sim5$	w	
$1063\pm\sim5$	vs	C═S stretching
$870\pm\sim10$	vw	C—S stretching
$806\pm\sim5$	m	

In order to avoid confusion with graphite, the spectrum of graphite was recorded in a similar manner; no bands were observed. The spectrum is discussed in another publication.

3. DISCUSSION

If black carbon disulphide has the structure suggested here then it should show a C═S stretching band. It is well established that compounds that contain the group

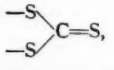

such as the trithiocarbonates (5, 6, 7), have a strong infrared band near 1060 cm^{-1}

which is due to the C=S stretching vibration. The strong band in the spectrum of black carbon disulphide at 1063 cm^{-1} is very strong evidence for the presence of this group, in agreement with our expectation. The decrease of frequency of the C=S stretching vibration from its value of about 1220 cm^{-1} in compounds (7) with the group

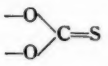

is consistent with a decrease of force constant due to conjugation with the singly bonded sulphur atoms.

If the chain of black carbon disulphide is mainly planar, as it probably is in order to facilitate conjugation, the repeating unit is

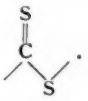

In an isolated chain, the only infrared-active vibrations are those that are in phase in each repeating unit, and so the factor group of the line group that describes the symmetry of the chain is appropriate for analyzing the spectrum. There are two parallel reflection planes, one through the S=C group and one through the singly bonded S atom, both perpendicular to the plane of the chain, and a reflection plane in the plane of the chain. There are, of course, twofold axes at the junctions of the planes. The corresponding point group is therefore C_{2v}. There are three atoms in the repeating unit and so there are $(3\times3-4) = 5$ fundamental vibrations that are potentially active. These can be described approximately as a C=S stretching vibration of species a_1, two C—S stretching vibrations of species a_1 and b_1, an S—C=S in-plane bending vibration of species b_1, and an S—C=S out-of-plane bending vibration of species b_2. All are active in infrared absorption.

It is likely that the medium band at 806 cm^{-1} is due to one of the C—S stretching vibrations, and perhaps the very weak band at 870 cm^{-1} is due to the other. There is almost no published information about similar vibrations in simple molecules. The only relevant spectra the author knows of is that of ethylene trithiocarbonate

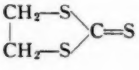

which was deposited with the Chemical Society by Haszeldine and Kidd (5). There is a moderate band at about 870 cm^{-1} which may correspond to the C—S stretching vibration. The stretching frequency of an unconjugated C—S bond is usually between 700 and 600 cm^{-1} according to Bellamy (8), but conjugation with C=S will probably increase the force constant and so increase the frequency. Our assignment of the 806-cm^{-1} and perhaps the 870-cm^{-1} band to the C—S vibrations seems therefore to be reasonable. The bending vibrations are probably of lower frequency, and are probably weak. They are not observed.

The remaining bands, which are all very weak, cannot be certainly assigned, but plausible guesses can be made. Although it is possible that the chains end in free radicals, as presumably sometimes occurs with the sheets of graphite, it is also possible that

chemically saturated end groups are present. A possible complete structure is

$$HO\left(\begin{matrix} S \\ \| \\ C-S \end{matrix}\right)_n H,$$

the end groups being derived from a molecule of water, in a similar manner to the polyaldehydes (9). The 1286-cm^{-1} band is perhaps an OH deformation and one of the bands at somewhat lower frequency (1144 cm^{-1}?) is perhaps a C—O stretching vibration. No OH stretching band was observed, though this is not surprising in view of the greater scattering in this region and the presence of adsorbed water. Some of the other bands could be due to imperfections in the chain such as a —C—S— group the wrong way round, but because there are few published spectra of model simple compounds detailed speculation is fruitless.

The author is indebted to Mr. A. Lavergne for help with the high-pressure experiments and to Mr. R. Ironside for taking the infrared spectra.

REFERENCES

1. P. W. Bridgman. Proc. Am. Acad. Arts Sci. **74**, 399 (1941).
2. J. E. Purvis, H. O. Jones, and H. S. Tasker. J. Chem. Soc. **97**, 2287 (1910).
3. E. A. Challenger, E. A. Mason, E. C. Holdsworth, and R. Emmett. J. Chem. Soc. 292 (1953).
4. D. T. Griggs and G. C. Kennedy. Am. J. Sci. **254**, 722 (1956).
5. R. N. Haszeldine and J. M. Kidd. J. Chem. Soc. 3871 (1955).
6. W. I. Jones, W. Kynaston, and J. L. Hales. J. Chem. Soc. 614 (1957).
7. R. Mecke, R. Mecke, and A. Lüttringhaus. Z. Naturforsch. B, **10**, 367 (1955).
8. L. J. Bellamy. The infra-red spectra of complex molecules. 2nd ed. Methuen & Co., Ltd., London. 1958. p. 353.
9. A. Novak and E. Whalley. Trans. Faraday Soc. **55**, 1490 (1959); Can. J. Chem. **37**, 1710, 1718, 1722 (1959).

IONIZATION OF ORGANIC COMPOUNDS IN ACID

I. ALIPHATIC KETONES[1]

H. J. CAMPBELL[2] AND J. T. EDWARD

ABSTRACT

The changes in the ultraviolet absorption spectra of aliphatic ketones in aqueous sulphuric acid have been followed as the acid strength is increased from 0 to 98%. With increase in strength up to 65% the weak peak at about 270 mμ is shifted to shorter wavelengths by a medium effect. However, with further increase in acid strength the peak disappears altogether because of protonation of the carbonyl group. The pK_{BH^+} values of several ketones have been calculated from the spectrophotometric results to be about −7. The pK_{BH^+} values of cyclic ketones vary systematically with ring size. The significance of the present work to recent studies on the rate of enolization of acetone is discussed.

INTRODUCTION

In absolute sulphuric acid, aliphatic and aromatic ketones (B) are essentially completely protonated to form the conjugate acid (BH^+) (1). The extent of protonation of the ketone in a less concentrated acid solution may be determined by the ultraviolet absorption at a given wavelength, according to the equation

$$[1] \qquad [B]/[BH^+] = (\epsilon_{BH^+}-\epsilon)/(\epsilon-\epsilon_B)$$

where ϵ_B, ϵ_{BH^+}, and ϵ are the molecular extinction coefficients of the unprotonated ketone, the protonated ketone, and the ketone in the test solution, and the quantities in brackets represent concentrations (2, 3). From the variation of $[B]/[BH^+]$ with the acidity function H_0 (4, 5) of the acid solvent, the protonation constant (pK_{BH^+}) of BH^+, defined by

$$[2] \qquad pK_{BH^+} = H_0 - \log [B]/[BH^+],$$

may be determined. For acetophenone Hammett (2) found a pK_{BH^+} of −6.03, recalculated as −6.15 by use of a corrected acidity function scale (5). This value was confirmed recently by Stewart and Yates (6).

By analogy with the behavior of other aliphatic and aromatic oxygen bases, e.g. benzoic acid ($pK_{BH^+} = -7.38$) and acetic acid ($pK_{BH^+} = -6.2$ (5)), the pK_{BH^+} values of aliphatic ketones would also be expected to be about −6. This view finds support in measurements of the relative basicities of various ketones from their effect on the rate of the acid-catalyzed etherification of benzhydrol in refluxing benzene (7), which indicated cyclopentanone, cyclohexanone, and diethyl ketone to have about the same basicity as *p*-methylacetophenone ($pK_{BH^+} = -5.47$ (6)). Furthermore, Lemaire and Lucas (8) observed no measurable protonation of acetone, acetophenone, and benzophenone by small concentrations of perchloric acid in acetic acid, and concluded that these compounds must have pK_{BH^+} values below −4.5. On the other hand, Nagakura, Minegishi, and Stanfield (9) recently reported a spectrophotometric determination of a pK_{BH^+} of −1.58 for acetone. This unexpectedly high basicity has prompted our reinvestigation by spectrophotometry of the ionization of acetone and other aliphatic ketones. We have found that protonation of the ketones occurs only in much more concentrated acids than those investigated by Nagakura *et al.*, and that in fact most aliphatic ketones have pK_{BH^+} values of about −7.

[1]*Manuscript received in original form March 28, 1960, and, as revised, August 2, 1960. Contribution from the Department of Chemistry, McGill University, Montreal 2, Que.*
[2]*Holder of C.I.L. Scholarship, 1959–60.*

EXPERIMENTAL

Materials

Chemically pure acetone and methyl ethyl ketone were purified by treatment with potassium permanganate according to Vogel (10), followed by fractionation through a 25×1 cm vacuum-jacketed column packed with glass helices, the middle fraction being taken. Cyclobutanone (Aldrich Chemical Co.) was distilled, and the middle fraction, b.p. 98–99° C at 759 mm, was used. Methyl isopropyl ketone, methyl *t*-butyl ketone, cyclopentanone, cyclohexanone, cycloheptanone (Aldrich), and cyclooctanone (Aldrich) were purified via their semicarbazones (11), which were recrystallized to constant melting point and then decomposed with 10% sulphuric acid. The ketones were removed by steam distillation, dried over magnesium sulphate, and then distilled as above.

The acid solutions were obtained by dilution of Nichols C.P. Reagent sulphuric acid (95.5–96.5%) and Baker and Adamson Reagent perchloric acid (70–72%), and the concentrations determined by titration with standard alkali. Sulphuric acid (98%) was prepared by adding 30% fuming sulphuric acid (Baker and Adamson Reagent) to 96% sulphuric acid. The corresponding H_0 values were read from large scale plots of H_0 against acid concentration, constructed from the data of Paul and Long (5).

Apparatus

Most measurements were made with a Beckmann Model DU spectrophotometer using quartz cells of 1 cm light path. The cell compartment was maintained at 25±0.1° C by thermospacers. With this instrument measurements could be taken down to a wavelength of about 220 mμ. For a few measurements down to wavelengths of about 185 mμ, a Unicam SP 500 spectrophotometer was used. There was no temperature control in the cell compartment of this instrument; the temperatures of the solutions in these cases were about 22±3° C.

Procedure

Solutions were made up by weighing the ketone (10–20 mg) directly into a 10-ml volumetric flask containing about 2 ml of the acid solution to be used as solvent, and swirling to mix the solution. In this manner weighing errors due to evaporation of the ketone were reduced. The solutions were made up to volume, mixed, and their extinction coefficients at various wavelengths measured. A solvent blank of acid of the same concentration as that containing the ketone was used.

RESULTS AND DISCUSSION

A selection of curves for the absorption above 220 mμ of acetone (Figs. 1A and 1B) and of cyclohexanone (Figs. 1C and 1D) in various strengths of sulphuric acid is shown. The family of curves over this range of wavelengths for methyl ethyl ketone in 0 to 65.3% acid resembled that of acetone; those for the other ketones resembled more that of cyclohexanone. The positions of the long wavelength peaks in water and in 65.3% sulphuric acid are given in Table I. The spectra of solutions of acetone in 0–66.6% perchloric acid varied with acid concentration in a fashion similar to that shown in Fig. 1A for solutions in sulphuric acid.

Extent of Condensation Reactions in Strong Acid Solution

Acetone in 96% sulphuric acid, when in fairly high concentration, is converted to mesityl oxide, phorone, and other compounds having strong ultraviolet absorption (9). However, it is believed that following the experimental procedure given above such condensation reactions are almost negligible, because of the great dilution almost

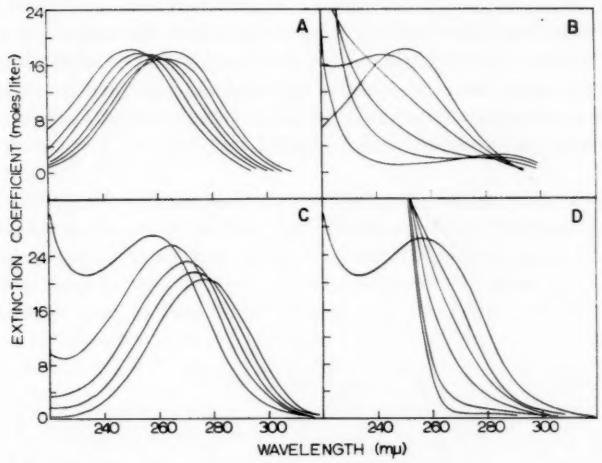

FIG. 1. Ultraviolet absorption curves of ketones in sulphuric acid solutions.
(A) Acetone in dilute acid: 0, 24.0, 41.7, 50.7, 58.8, and 65.3% H_2SO_4 reading from right to left, respectively.
(B) Acetone in concentrated acid: 65.3, 74.1, 80.0, 84.7, 89.2, and 98.2% H_2SO_4 respectively.
(C) Cyclohexanone in dilute acid: 0, 32.2, 44.9, 57.2, and 65.3% H_2SO_4 respectively.
(D) Cyclohexanone in concentrated acid: 65.3, 72.2, 76.3, 81.3, 87.0, and 98.6% H_2SO_4 respectively.

TABLE I

Wavelengths (in mμ) of peaks for $n \rightarrow \pi^*$ transitions of ketones in different media

Ketone	In inert solvent	In water	In 65.3% H_2SO_4
Acetone	277[a]	266	250
Methyl ethyl ketone	278[b]	268	254
Methyl isopropyl ketone	285[b]	275	259
Methyl *t*-butyl ketone	288[c]	278	262
Cyclobutanone	280[d]	274	255
Cyclopentanone	300,[c] 299,[d] 295[b]	281	261
Cyclohexanone	285,[d] 288[b]	277	262
Cycloheptanone	281[e]	278	259
Cyclooctanone	290[c]	277	(<260)[f]

[a]In cyclohexane, ref. 21. [b]In ethylene dichloride, ref. 22. [c]In cyclohexane. [d]In hexane, ref. 11. [e]In hexane, ref. 23. [f]Submerged by edge of much more intense peak at ca. 185 mμ due to $\pi \rightarrow \pi^*$ transition.

instantaneously achieved by the ketone in the acid solutions. (The importance of the dilution effect has been emphasized by Grace and Symons (12).) Thus, when a solution of acetone in 98% sulphuric acid was diluted to give an acid concentration of 50%, the spectrum was practically identical with that of a solution prepared directly from 50% acid; the latter preparation would almost certainly be free from condensation products. However, it seems likely that the small peak found at about 280 mμ for solutions of acetone, methyl ethyl ketone, and cyclooctanone in the stronger acid solutions (see Fig. 1B for acetone) comes from condensation products. Mesityl oxide in concentrated sulphuric acid has λ_{max} at 284 mμ (9); the condensation to mesityl oxide of 0.03% of the acetone dissolved in 98.2% sulphuric acid would suffice to give the molecular extinction coefficient observed by us (Fig. 1B) at 284 mμ. This portion of the spectrum, further-

more, was found to have an optical density which increased very slowly with time; however, the portion from 220–260 mμ, which furnished the values of the extinction coefficient for the calculations mentioned below, did not change with time.

While we may conclude that the spectra obtained in the present instance are substantially those of the ketones themselves and not of condensation products, the reverse has been true for the spectra previously reported for aliphatic ketones in concentrated acid solution (13).

Gillespie, Hughes, and Ingold (14), in cryoscopic studies of very dilute solutions of acetone in absolute sulphuric acid, assumed that no destruction of the ketone was taking place, although the condensation of two molecules of acetone to form one molecule of mesityl oxide and one molecule of water would have led to no change in the cryoscopic behavior of the solution. However, the present work shows their assumption to have been justified.

Effect of Acid Strength on the $n \rightarrow \pi^*$ Transition of Ketones

The weak, long wavelength absorption of aliphatic ketones is ascribed to the excitation of an electron from a non-bonding (n) orbital of the oxygen to an antibonding (π^*) orbital of the carbonyl group (15). The absorption peak is shifted to shorter wavelengths (a "blue shift") with increasing polarity of the solvent, because of the preferential stabilization of the ground state of the carbonyl group by dipole–dipole interactions or by hydrogen-bonding with a solvent molecule (16, 17, 18, 19, 20). This effect accounts for the different wavelengths of the absorption peaks of the ketones in hydrocarbon or other inert solvents and in water (Table I).

It has long been known that the 265 mμ peak of acetone in water undergoes a further blue shift to 261 mμ in 5 *M* aqueous calcium chloride (24); we have found the peak also at 261 mμ in 15 *M* lithium bromide. In these concentrations of electrolyte a fair proportion of the water is bound in the primary or secondary hydration shells of the cations (25). The polarization of these water molecules, induced by the charge of the cation, should increase the strengths of the hydrogen bonds to the carbonyl oxygen (26). The progressive blue shifts produced by increasing hydronium ion concentration in going from 0 to 65.3% sulphuric acid (Table I and Figs. 1A and 1C) and from 0 to 66.6% perchloric acid are also best explained by a progressive increase in the strength of the hydrogen-bonding of solvent molecules to ketone. In dilute aqueous solution the hydronium ion exists as the relatively stable ion $H^+.4H_2O$ (I) (27, 28). However, in 65.3% sulphuric acid only 3 moles of water are present for each mole of acid, so that it is possible that in this strength of acid the ketone molecules are for the most part associated directly with hydronium ions as pictured in (II).

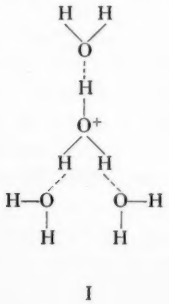

I

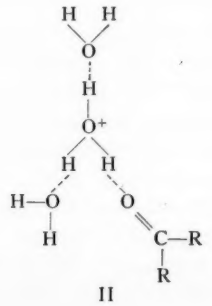

II

Nagakura, Minegishi, and Stanfield (9) have interpreted the blue shifts of acetone with increasing acid concentration as due to protonation of the ketone. However, their arguments for this interpretation are unsound for the following reasons:

1. They claim that a simple equilibrium between two species of molecules is shown by the presence of an isobestic point in the family of absorption curves. However, only the curves for acetone (Fig. 1A) and methyl ethyl ketone show an approximation to an isobestic point (cf. Fig. 1C).

2. They point out that the pK_B ($= -pK_{BH^+}$) values for acetone calculated from extinction coefficients at various wavelengths, and on both sides of the isobestic point, are approximately constant, varying from 1.39 to 1.72. However, they restricted their attention to solutions having $H_0 = -2.32$ or more. Over this limited range of acidities the absorption of acetone and methyl ethyl ketone (but *not* of the other ketones) does indeed change with H_0 according to equations 1 and 2. However, this correspondence of experimental results with those expected for a $pK_{BH^+} = -1.58$ for acetone is limited to the region above $H_0 = -2.3$, and is not found if one takes account of the absorption in more acidic solutions of $H_0 = -3$ to -5.

It seems more reasonable to associate protonation of the ketone with the disappearance of the long wavelength peak (16) as the sulphuric acid concentration is increased from 65% to 98% (Figs. 1B and 1D), a region of acid concentrations not investigated by Nagakura *et al.* This explanation is confirmed by the fact that in this region of acid concentrations the changes in absorption *for all ketones* follow approximately the changes in acidity function according to equations 1 and 2. This is shown in Figs. 2A and 2B

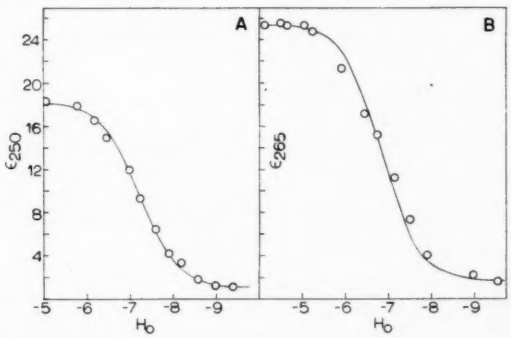

FIG. 2. (A) Ionization of acetone in H_2SO_4. Theoretical curve for equations 1 and 2, with $pK_{BH^+} = -7.2$. (B) Ionization of cyclohexanone in H_2SO_4. Theoretical curve for $pK_{BH^+} = -6.8$.

for acetone and cyclohexanone, in which the molecular absorption coefficients at 250 mμ and 265 mμ, respectively, have been plotted against the values of the acidity function of the solutions. The experimental values fit reasonably well with the theoretical curve calculated from equations 1 and 2, using the values of ϵ_B and ϵ_{BH^+} recorded in Table II. Plots of ϵ at other wavelengths against H_0 indicated slightly different pK_{BH^+} values. Those for acetone (wavelengths given) were: -7.4 (245 mμ), -7.3 (248 mμ), -7.1 (252 mμ), -7.0 (255 mμ). However, the fit of the experimental points to the theoretical curve was less satisfactory than that found taking ϵ at 250 mμ. It was assumed that these deviations were caused by the medium effect (2), and the wavelength chosen (λ, Table II) was that which afforded the best fit of experimental points to the theoretical curve. However

TABLE II

Basicities of ketones

Ketone	λ (mμ)	ϵ_B	ϵ_{BH^+}	$-pK_{BH^+}$
Acetone	250	18.2	1.2	7.2
Methyl ethyl ketone	250	21.8	0.9	7.2
Methyl isopropyl ketone	260	34.0	3.2	7.1
Methyl *t*-butyl ketone	265	36.5	1.8	7.1
Cyclobutanone	260	33.0	3.0	9.5
Cyclopentanone	260	24.8	1.8	7.5
Cyclohexanone	265	25.4	1.8	6.8
Cycloheptanone	265	32.3	3.8	6.6
Cyclooctanone	270	24.5	6.4	6.2

it seems likely that because of the uncertainty in allowing for the medium effect the precision of the pK_{BH^+} values cannot be better than about ±0.2 unit. These values, listed in Table II, were all obtained by this graphical method. Graphical analysis of the absorption results by the slightly different method of Davis and Geissman (29) gave substantially the same pK_{BH^+} values.

It is apparent that unstrained cyclic and acyclic ketones all have pK_{BH^+} values of about −7. Contrary to the evidence of Pratt and Matsuda (7), the basicities of cyclopentanone and cyclohexanone differ considerably from that of *p*-methylacetophenone; however, it is not to be expected that exactly the same order of basicities will be shown in aqueous acids and in benzene.

In the series acetone, methyl ethyl ketone, methyl isopropyl ketone, and methyl *t*-butyl ketone, it is probable that the tendency for basicity to be increased by the inductive effect of an increasing number of alkyl groups on the α-carbon atom is offset by the effect of these groups in restricting the stabilization of the protonated ketone by solvation (30). The increase in basicity with ring size on going from cyclobutanone to cyclooctanone agrees with recent findings that the strengths of hydrogen bonds between these ketones and methanol or chloroform increase in the same order (31). These changes in basicity parallel changes in the infrared stretching frequency of the carbonyl group, as shown in Fig. 3. A similar change has been noted in both basicity and infrared frequency

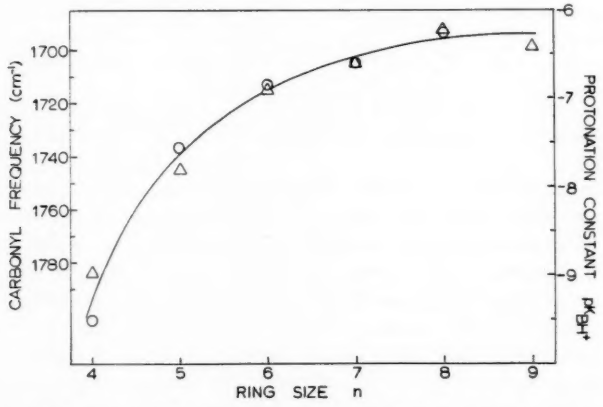

FIG. 3. Change of infrared stretching frequency (△) and pK_{BH^+} (○) with number of carbon atoms (*n*) in cyclic ketones.

of the carbonyl group of benzlactams with increasing ring size (32), while Stewart and Yates (6) have shown a linear relationship between the basicity and carbonyl frequency of *meta*- and *para*-substituted acetophenones.

The simple aliphatic ketones of Table II are much weaker bases than enolized β-diketones such as 5,5-dimethylcyclohexane-1,3-dione (pK_{BH^+} −0.8) and acetylacetone (pK_{BH^+} −3.7) (33); this is to be expected because of the resonance stabilization of the protonated forms of the latter compounds (e.g., V).

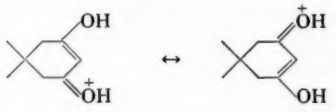

Va ↔ Vb

Effect of Acid on the $\pi \rightarrow \pi^*$ Transition of Aliphatic Ketones

Besides the $n \rightarrow \pi^*$ transition, ketones show a more intense absorption at shorter wavelengths due to a $\pi \rightarrow \pi^*$ transition. In the case of α,β-unsaturated ketones the change from an inert solvent to a hydrogen-bonding (17, 24, 34) or protonating solvent (9) causes a red shift in this peak, but acetone shows a blue shift on changing the solvent from isooctane (λ_{max} 187.6 mμ (34)) to water (34, 35). It has been claimed that this differing behavior is to be expected for two-center (36) and four-center (9) $\pi \rightarrow \pi^*$ transitions. However, the $\pi \rightarrow \pi^*$ peak for cyclohexanone showed a red shift on protonation (Table III). Unfortunately, with the spectrophotometers available it was not

TABLE III

Molecular extinction coefficients at 190 mμ of ketones in various solvents

Ketone	Solvent			
	Cyclohexane	Water	65% H_2SO_4	96% H_2SO_4
Acetone	1060[a]	148	34	340
Cyclohexanone	440	800	1540	2520[b]
Cyclooctanone	2900	1360	2400	3610

[a]At 194 mμ. [b]$\lambda_{max} \simeq 192$ mμ (flat peak); $\epsilon_{max} = 2520$.

possible to measure the absorption at low enough wavelengths to define this peak for the protonated forms of acetone and cyclooctanone. However, it seems likely, from the change in extinction coefficient at 190 mμ (Table III) that it undergoes a red shift on protonation in these cases also. The results in Table III indicate that the spectra of the non-protonated ketones vary with the solvent in an irregular fashion.

The Basicity and Rate of Enolization of Acetone

The enolization of ketones is known to involve the participation of one or more water molecules in addition to the protonated ketone molecule in the rate-determining step (37). However, Archer and Bell (38) recently showed that if a pK_{BH^+} of −1.58 were accepted for acetone, then its rate of enolization in 1–8 *M* hydrochloric acid is approximately proportional to the fraction of the compound protonated. According to the Hammett–Zucker hypothesis (39, 40), this would indicate that the reaction does *not*

involve a water molecule in rate-determining step, and hence the results were interpreted as a disproof of the hypothesis. However, it seems likely that Archer and Bell's correlation is fortuitous because of the limited range of acid concentrations investigated by them. In fact, accepting a pK_{BH^+} of -7.2, a better correlation of their enolization rates with changing acidity is obtained by plotting $\log k_\psi + H_0$, where k_ψ is the experimental first-order rate constant based on the concentration of acetone, against $\log a_{H_2O}$, where a_{H_2O} is the activity of the water in the various concentrations of hydrochloric acid. The points fit closely to a straight line of slope 3.7. Bunnett (41) has recently shown that such a relation is more general than the Hammett–Zucker relations, and that the slope of the curve defines a hydration parameter w for the reaction, which is related to the number of water molecules in the transition state of the rate-determining step.

ACKNOWLEDGMENTS

We are grateful to the National Research Council for generous financial help.

REFERENCES

1. R. J. Gillespie and J. A. Leisten. Quart. Revs. (London), **8**, 40 (1954).
2. L. A. Flexser, L. P. Hammett, and A. Dingwall. J. Am. Chem. Soc. **57**, 2103 (1935).
3. L. A. Flexser and L. P. Hammett. J. Am. Chem. Soc. **60**, 885 (1938).
4. L. P. Hammett. Physical organic chemistry. McGraw-Hill, New York. 1940. p. 262.
5. M. A. Paul and F. A. Long. Chem. Revs. **57**, 1 (1957).
6. R. Stewart and K. Yates. J. Am. Chem. Soc. **80**, 6355 (1958).
7. E. F. Pratt and K. Matsuda. J. Am. Chem. Soc. **75**, 3739 (1953).
8. H. Lemaire and H. J. Lucas. J. Am. Chem. Soc. **73**, 5198 (1951).
9. S. Nagakura, A. Minegishi, and K. Stanfield. J. Am. Chem. Soc. **79**, 1033 (1957).
10. A. I. Vogel. Practical organic chemistry. Longmans, Green & Co., London. 1956. p. 171.
11. S. W. Benson and G. B. Kistiakowsky. J. Am. Chem. Soc. **64**, 80 (1942).
12. J. A. Grace and M. C. R. Symons. J. Chem. Soc. 958 (1959).
13. L. C. Anderson and C. M. Gooding. J. Am. Chem. Soc. **57**, 999 (1935).
14. R. J. Gillespie, E. D. Hughes, and C. K. Ingold. J. Chem. Soc. 2473 (1950).
15. H. L. McMurry and R. S. Mulliken. Proc. Natl. Acad. Sci. **26**, 312 (1940). H. L. McMurry. J. Chem. Phys. **9**, 231, 241 (1941).
16. M. Kasha. Discussions Faraday Soc. **9**, 14 (1950).
17. H. McConnell. J. Chem. Phys. **20**, 700 (1952).
18. N. S. Bayliss and E. G. McRae. J. Phys. Chem. **58**, 1002 (1954).
19. G. J. Brealey and M. Kasha. J. Am. Chem. Soc. **77**, 4462 (1955).
20. G. C. Pimentel. J. Am. Chem. Soc. **79**, 3323 (1957).
21. T. M. Lowry and R. E. Lishmund. J. Chem. Soc. 1313 (1935).
22. M. F. Hawthorne and W. D. Emmons. J. Am. Chem. Soc. **80**, 6399 (1958).
23. A. Castille and E. Ruppol. Bull. soc. chim. biol. **10**, 623 (1928).
24. G. Scheibe. Ber. **58**, 588 (1925).
25. J. O'M. Bockris. Quart. Revs. (London), **3**, 173 (1949).
26. C. A. Coulson. Research (London), **10**, 149 (1957).
27. E. Wicke, M. Eigen, and T. Ackermann. Z. physik. Chem. **1**, 340 (1954).
28. K. N. Bascombe and R. P. Bell. Discussions Faraday Soc. **24**, 158 (1957).
29. C. T. Davis and T. A. Geissman. J. Am. Chem. Soc. **76**, 3507 (1954).
30. H. C. Brown, D. H. McDaniel, and O. Häfliger. *In* Determination of organic structures by physical methods. *Edited by* E. A. Braude and F. C. Nachod. Academic Press, New York. 1955. p. 567.
31. M. Tamres and S. Searles. J. Am. Chem. Soc. **81**, 2100 (1959).
32. R. Huisgen, I. Ugi, H. Brade, and E. Rauenbusch. Ann. **586**, 30 (1954).
33. B. Eistert, E. Merkel, and W. Reiss. Chem. Ber. **87**, 1513 (1954).
34. E. M. Kosower. J. Am. Chem. Soc. **80**, 3261 (1958).
35. H. Ley and B. Arends. Z. physik. Chem. B, **12**, 132 (1931).
36. L. Goodman. Footnote (44) in ref. 34.
37. C. G. Swain, A. J. DiMilo, and J. P. Cordner. J. Am. Chem. Soc. **80**, 5983 (1958).
38. G. Archer and R. P. Bell. J. Chem. Soc. 3228 (1959).
39. L. Zucker and L. P. Hammett. J. Am. Chem. Soc. **61**, 2791 (1939).
40. F. A. Long and M. A. Paul. Chem. Revs. **57**, 935 (1947).
41. J. F. Bunnett. J. Am. Chem. Soc. **82**, 500 (1960).

THE USE OF THE HELLMANN–FEYNMAN THEOREM TO CALCULATE MOLECULAR ENERGIES[1]

RICHARD F. W. BADER

ABSTRACT

The Hellmann–Feynman theorem has been employed to calculate the repulsion between two helium atoms and the molecular energies of H_2 and H_3. The method of molecular orbitals was used to determine the necessary expressions for the electron densities. The screening constants of the atomic orbitals comprising the molecular orbitals were treated as functions of the internuclear separation according to an empirical expression which duplicates very closely the "best" values for these parameters as determined by the variational method. The results of the calculations indicate that the present method is capable of yielding estimates of molecular energies which are comparable to those obtained by the more elaborate and time-consuming variational methods.

I. THE ELECTROSTATIC METHOD OF CALCULATING MOLECULAR ENERGIES

The Hellmann–Feynman theorem states that the x-component of the force acting on the αth nucleus, considered as occupying some fixed position in a molecule, is

$$F_{\alpha x} = \frac{\partial}{\partial x_\alpha}\left(\sum_{\beta(\neq\alpha)} \frac{Z_\alpha Z_\beta e^2}{r_{\alpha\beta}}\right) - \int \rho \mathfrak{E}_{\alpha x}\, d\mathbf{r} \qquad [1]$$

where Z_α is the nuclear charge of nucleus α, $r_{\alpha\beta}$ an internuclear separation, ρ is the electron density at the point (x, y, z), and $\mathfrak{E}_{\alpha x}$ is the electric field produced by the αth nucleus in the x-direction at the position of the ith electron (1). Equation [1] states that the force $F_{\alpha x}$ acting on a nucleus in any system of nuclei and electrons is simply the sum of the classical electrostatic forces due to the other nuclei and to the electron charge distribution. Thus, once the electronic charge density $\rho(x, y, z)$ has been determined by the methods of quantum mechanics, the forces acting on the nuclei are interpretable entirely in terms of classical electrostatics. The wave function for a molecule containing n electrons is a function of $3n$ space co-ordinates. However, due to the equivalence of all the electrons in a molecule, the electron density at any point is a three-dimensional quantity of physical significance. Because of this the formulation given by equation [1] of the forces which bind a molecule together is conceptually simpler than the more usual discussion in terms of the energies involved.

Hurley, in a series of papers (2, 3, 4, 5), has given a reformulation of the Hellmann–Feynman theorem together with a very thorough comparison of the electrostatic method of calculating molecular energies with the more usual method employing the Ritz variational procedure. Hurley has shown that if the exact wave function is used in equation [1] then the forces acting on the nucleus as calculated by the electrostatic method will agree precisely with those calculated from the results obtained by the variational procedure. However, when an approximation is made to the wave function, either in terms of molecular orbitals or Heitler–London functions, the two methods will not necessarily agree. Hurley has examined this question and has shown that when all of the variable parameters in the wave function, excluding the scale factor (the orbital exponent in hydrogen-like atomic orbitals), are determined by the variational procedure, the electrostatic and the conventional methods will lead to identical results. Variation of the scale factor as well insures that the results will be consistent with the virial theorem.

[1]*Manuscript received July 5, 1960.*
Contribution from the Department of Chemistry, University of Ottawa, Ottawa, Ontario.

Can. J. Chem. Vol. 38 (1960)

Although not always thought of as such, the internuclear distance is a variable parameter in a valence bond or molecular orbital wave function. Thus to insure agreement between the electrostatic and the variational methods it is necessary to employ so-called floating wave functions. These are wave functions which allow for the possibility of the electron charge detaching itself from the nucleus and taking up an optimum position along the internuclear axis, thus in effect making the internuclear separation a parameter to be varied in terms of the *electronic* co-ordinates.

There is no reason a priori to prefer the variational method to the electrostatic method in the calculation of molecular energies. One is forced to employ approximate wave functions in both methods and the ultimate test is the agreement with experiment. Thus there is no need to employ floating wave functions in electrostatic calculations in order to insure that the results of such a calculation will agree with those obtained from the conventional method.* In fact it is well known that a wave function based on the molecular orbital approximation leads to incorrect results at large internuclear distances when this wave function is employed in a variational type of calculation. If this same simple molecular orbital formulation is used to approximate the electron density for use in equation [1] this difficulty does not arise as the function leads to the correct expression for the electron density at infinite internuclear separation. Thus to employ a floating wave function in an electrostatic calculation would but reintroduce the errors of the conventional method when molecular orbitals were employed.

Hurley (2) has employed the simple molecular orbital approximation in the electrostatic calculations for the hydrogen molecule and for the repulsion between two helium atoms. The agreement of these calculations with the experimental results was fair. The great merit of the electrostatic calculations lies in their great simplicity and the ease with which they may be carried out. It would be of great value, therefore, if they could be improved to the point where the accuracy of their results would justify their application to systems which at present are too complicated by the conventional methods. Such calculations would also be very useful for rapid estimates of the properties of transition-state molecules with reference to absolute rate theory and isotope effects.

It is the purpose of the present investigation to show that an improvement may be obtained in the calculation of molecular energies by the electrostatic method by employing molecular orbitals in which certain of the parameters are adjusted empirically so as to give a wave function which approximates very closely the one obtained by a variational calculation. The great beauty of the variational method whereby parameters may be varied to minimize the energy is of course not found in the electrostatic method. Instead some means must be devised to adjust the parameters in the wave function empirically. The most suitable parameters to vary in a simple molecular orbital function are the orbital exponents or screening constants. This is the procedure that has been adopted in the present calculations.

The expression for the electron density to be substituted into equation [1] was determined by the methods of molecular orbitals. The molecular orbitals were taken as linear combinations of Slater atomic orbitals. The screening constant $Z(R)$ in the atomic orbitals is treated as a parameter, a function of the internuclear separation, R. The empirical rule used to govern the variation of $Z(R)$ with R is

$$[2] \qquad Z(R) = Z_s - \Delta Z e^{-R}$$

**Shull and Ebbing (19) have in fact shown that much of the previously published numerical work involving floating wave functions is in error, and that very little improvement in energy results from allowing the orbitals to float.*

where R is expressed in atomic units (a.u.). Z_s is the value of the screening constant for the separated atoms (when R equals infinity) and $\Delta Z = Z_s - Z_u$, Z_u being the screening constant for the united atom (when R equals zero). It is well known from variational calculations that the value of $Z(R)$ varies in a smooth fashion from the value for the separated atoms to that for the united atom. Equation [2] reproduces the values obtained for $Z(R)$ by the variational method in a very striking fashion. The merits of this function have been previously discussed by Musulin (6).

II. AN ELECTROSTATIC CALCULATION OF THE ENERGY OF THE HYDROGEN MOLECULE

The hydrogen molecule correlates with the ^1S state of the helium atom. Thus for this calculation $Z_s = 1$, $Z_u = 2$, and the expression for $Z(R)$ becomes

$$Z(R) = 1+\epsilon^{-R}.$$

If we let the atomic orbital centered on nucleus α be represented by ϕ_α and that on nucleus β by ϕ_β then the electron density for the hydrogen molecule, as given by the molecular orbital theory, is

[3] $$\rho = (1+s)^{-1}(\phi_\alpha^2+\phi_\beta^2+2\phi_\alpha\phi_\beta)$$

where s is the overlap integral between ϕ_α and ϕ_β. When this expression for the electron density is substituted into equation [1] the following expression is obtained for the force in atomic units acting on nucleus α in the line of the nuclei which is taken as the x-axis,

[4] $$F_{\alpha x} = \frac{1}{R^2} - (1-s)^{-1}[\langle\phi_\beta\phi_\beta|\cos\theta_{\alpha i}/r_{\alpha i}^2\rangle+2\langle\phi_\alpha\phi_\beta|\cos\theta_{\alpha i}/r_{\alpha i}^2\rangle],$$

where $\theta_{\alpha i}$ and $r_{\alpha i}$ are the polar co-ordinates of the ith electron with origin at nucleus α. All of the integrals occurring in equation [4] have been evaluated analytically by Coulson (7). Equation [4] together with equation [3] allows one to calculate the force acting on nucleus α for any value of R. The results of the calculation are shown in Fig. 1

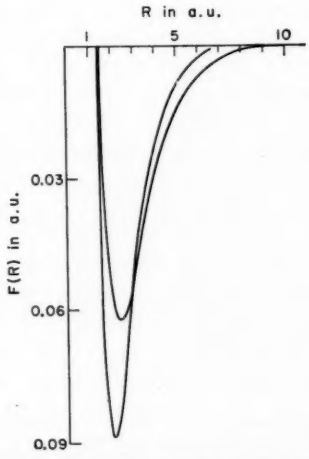

FIG. 1. Experimental (lowest curve at 2 a.u.) and calculated force curves for H_2.

together with the experimental curve obtained from the derivative of the Morse potential for the hydrogen molecule. It is seen that the force predicted by equation [4] is too large at large distances and not quite large enough at shorter distances. The agreement, however, is very good and represents a substantial improvement over the earlier electrostatic calculations and over the variational method. The energy of the hydrogen molecule as obtained from an integration of the calculated curve together with the equilibrium internuclear distance is compared in Table I with the experimental values and with those obtained by other methods as indicated.

TABLE I

	Present calc.	Hurley (2)	Simple M.O. (8)	Expt. (9)
Binding energy (in a.u.)	0.158	0.136	0.098	0.174
R_e (in a.u.)	1.56	1.8	1.6	1.4

III. AN ELECTROSTATIC CALCULATION OF THE REPULSION BETWEEN TWO HELIUM ATOMS

The approach of two normal helium atoms results in the molecular state $(\sigma_g 1s)^2\ (\sigma_u 1s)^2\ {}^1\Sigma_g^+$. For very small internuclear separations this state will correlate with the $1s\sigma^2 2p\sigma^2\ {}^1\Sigma_g^+$ state, which in the limit of the united atom reverts to the $1s^2 2p^2$ electronic configuration of the beryllium atom. However, the splitting of a beryllium atom with a $1s^2 2s^2$ electronic configuration will also give rise to a ${}^1\Sigma_g^+$ molecular state, which for small internuclear separations must lie lower than the state resulting from the $1s^2 2p^2$ configuration (9). This second ${}^1\Sigma_g^+$ state correlates with two separated helium atoms in ${}^3S$ states and thus for large internuclear separations it must possess a higher energy than the state resulting from the configuration $(\sigma_g 1s)^2\ (\sigma_u 1s)^2$. It is evident from these considerations that for large separations the molecular orbitals of the He_2 system are best considered as $\sigma_g 1s$ and $\sigma_u 1s$ while for very close approach of the two nuclei the system is more faithfully represented by an electronic configuration of the form $(\sigma_g 1s)^2\ (\sigma_g 2s)^2$.

Buckingham (20) and Wu (10) have pointed out that all of the quantum mechanical calculations performed so far for the He_2 system have used an upper molecular orbital of σ_u character. This, they feel, explains why all such calculations have been in serious error for small values of R. Much better results should be obtained if instead one employed an orbital with more $\sigma_g 2s$ character for small internuclear separations.

We have employed two wave functions in the electrostatic calculations for the He_2 system. The first is similar to that employed by Huzinaga (11) in the best variational treatment so far performed for He_2. It is derived from the electronic configuration $(\sigma_g 1s)^2\ (\sigma_u 1s)^2$. The second was used in calculations for very small values of R and thus employed the $\sigma_g 2s$ orbital in place of the $\sigma_u 1s$ orbital.

In this case it is necessary to employ two screening constants, one for the σ_g orbital and one for the σ_u orbital. The value of Z_s for the σ_g orbital is 1.70, the value of the screening constant for the helium atom. The screening constant for the united atom is taken equal to 4.00, the nuclear charge for the beryllium atom.* The expression for the screening constant for the σ_g orbital, $Z(R)_g$ is

$$Z(R)_g = 1.70 + 2.30e^{-R}.$$

**The presence of the second electron in the orbital is not taken into account in determining the screening constant for the united atom. Thus Z_u in the case of H_2 was taken as 2.00, not as 1.70, and for the helium atoms, Z_u is given a value of 4.00, not 3.70. This procedure is followed simply because the values so obtained for the energies are in better agreement with the experimental ones and $Z(R)$ is in any event an empirical parameter.*

The screening constant for the σ_u orbital goes to the same limit for infinite internuclear separation as it does for the σ_g orbital, i.e., 1.70. However, the united atom limit for the σ_u orbital is a $2p$ atomic orbital of a beryllium atom, screened by two $1s$ electrons. Thus $Z_u = 2.30/2$. (The result is divided by 2, the principal quantum number, as required by the Slater recipe.) The screening constant for the σ_u orbital, $Z(R)_u$, is

$$Z(R)_u = 1.70 - 0.55e^{-R}.$$

There are thus two atomic orbital functions necessary for each helium atom. They are of the form

$$\phi_{\alpha g} = (Z(R)_g^3/\pi)^{1/2} \exp(-Z(R)_g r_\alpha),$$

$$\phi_{\alpha u} = (Z(R)_u^3/\pi)^{1/2} \exp(-Z(R)_u r_\alpha).$$

The wave function for a system of two helium atoms is

$$\Psi = (4!)^{-1/2} \sum (-1)^p P \sigma_g(1)\sigma_g(2)\sigma_u(3)\sigma_u(4)\alpha(1)\beta(2)\alpha(3)\beta(4)$$

where σ_g and σ_u are the orthonormal molecular orbitals

$$\sigma_g = (2+2s_g)^{-1/2}(\phi_{\alpha g} + \phi_{\beta g}); \qquad \sigma_u = (2-2s_u)^{-1/2}(\phi_{\alpha u} - \phi_{\beta u})$$

and s_g and s_u are the appropriate overlap integrals. The electron density resulting from this wave function is

$$\rho = (1+s_g)^{-1}(\phi_{\alpha g}^2 + \phi_{\beta g}^2 + 2\phi_{\alpha g}\phi_{\beta g}) + (1-s_u)^{-1}(\phi_{\alpha u}^2 + \phi_{\beta u}^2 - 2\phi_{\alpha u}\phi_{\beta u})$$

and thus the force exerted on nucleus α along the line of approach of the two atoms is

$$[5] \qquad F_{\alpha z}(R) = \frac{4}{R^2} - 2(1+s_g)^{-1}[\langle \phi_{\beta g}\phi_{\beta g} | \cos\theta_{\alpha i}/r_{\alpha i}^2\rangle + 2\langle \phi_{\alpha g}\phi_{\beta g} | \cos\theta_{\alpha i}/r_{\alpha i}^2\rangle]$$

$$-2(1-s_u)^{-1}[\langle \phi_{\beta u}\phi_{\beta u} | \cos\theta_{\alpha i}/r_{\alpha i}^2\rangle - 2\langle \phi_{\alpha u}\phi_{\beta u} | \cos\theta_{\alpha i}/r_{\alpha i}^2\rangle]$$

where the symbols have the same significance as previously. Again, as in the case of the hydrogen molecule, only one- and two-center one-electron integrals arise which are easily evaluated. The results of the calculation are shown in Fig. 2 together with the best variational calculation that has so far been performed (11) and the experimental results of Amdur and Harkness (12). The electrostatic calculations in this case almost duplicate the variational treatment. It is evident that the repulsion predicted by the electrostatic and the variational calculations at small values of R is far too extreme. This is to be expected of a wave function with σ_u character in the light of the opening discussion on the He_2 system. If we assume that for small values of R we are justified in excluding all σ_u character and instead employ a wave function resulting from the electronic configuration $(\sigma_g 1s)^2\,(\sigma_g 2s)^2$, then a separate electrostatic calculation may be performed. From this we may hope to determine whether or not the contribution from the $\sigma_g 2s$ orbital does improve the calculation to a point where it gives results of the right order of magnitude and at the same time gain some idea of where the transition from $\sigma_u 1s$ to $\sigma_g 2s$ character occurs. Both of these features would be of value in a more refined variational treatment which took account of the $\sigma_g 2s$ contribution.

We begin by assigning the four electrons to two orthogonal molecular orbitals

$$\Psi = (4!)^{-1/2} \sum (-1)^p P \sigma_g(1)\sigma_g(2)\sigma_{g0}(3)\sigma_{g0}(4)\alpha(1)\beta(2)\alpha(3)\beta(4)$$

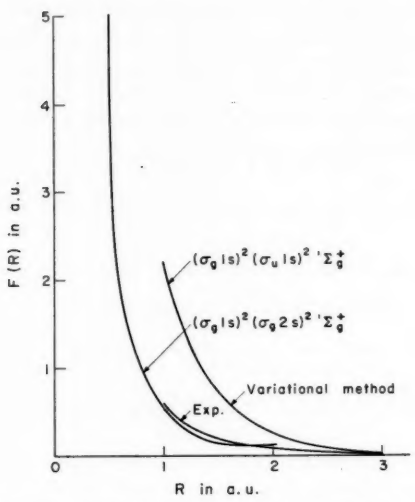

FIG. 2. Force curves for He_2. The curve of the results obtained by the variational method (3 a.u.→1 a.u.) is identical with that obtained by the indicated electrostatic method to the accuracy of this plot.

where σ_g is identical with the corresponding orbital employed above and σ_{g0} is given by

$$\sigma_{g0} = (\sigma_{g'} - s_{gg'}\sigma_g)(1-s_{gg'}^2)^{-1/2}.$$

The $\sigma_{g'}$ molecular orbital is composed of atomic $2s$ orbitals and is of the form

$$\sigma_{g'} = (2+2s_{g'})^{-1/2}(X_\alpha + X_\beta)$$

where

$$X_\alpha = (Z_{g'}^5/3\pi)r_\alpha \exp(-Z_{g'}r_\alpha).$$

The electron density for the system is then found to be

$$\rho = (\sigma_g^2 + \sigma_{g'}^2 - 2s_{gg'}\sigma_{g'}\sigma_g)(1-s_{gg'}^2)^{-1}.$$

The expression for the force on nucleus α is obtained in the same manner as previously, but due to the lack of orthogonality between the σ_g and $\sigma_{g'}$ orbitals is too cumbersome to be set down here. Since the Slater method of assigning screening constants does not differentiate between orbitals of the same principal quantum number, i.e., the $2s$ and $2p$ of the united atom beryllium, we have employed the same value for $Z_{g'}$ as was employed for Z_u.

The results of the calculations are given in Fig. 2. Obviously the answer to improving the calculations for He_2 does depend upon the inclusion of the $\sigma_g 2s$ orbital. The electrostatic calculations now predict a repulsion which is actually slightly less than that obtained experimentally for small values of R. It is only for values of R less than 3 a.u. that the function with σ_u character diverges seriously. Any contribution from this function must be small in the region of 1 a.u. A calculated point has been included for 0.5 a.u., a region which is not covered by experiment. The force of repulsion is seen to rise very steeply in this region to a value of 5.02 a.u.

IV. AN ELECTROSTATIC CALCULATION OF THE ENERGY OF THE H_3 MOLECULE

The electronic energy of a system of three hydrogen atoms has been the subject of many theoretical investigations. The most recent of these calculations was carried out by Boys and Shavitt (13), who employed the method of molecular orbitals with the superposition of configurations. This very extensive variational calculation demanded the use of an electronic computer. It is of interest to compare with their results those which can be obtained by an electrostatic calculation, a calculation which is easily carried out using a desk computer.

The three hydrogen atoms are arranged in a linear symmetric fashion as shown:

$$\underset{\alpha}{\cdot}\xleftarrow{R}\underset{\beta}{\cdot}\underset{\gamma}{\cdot}$$

The two internuclear distances $R_{\alpha\beta}$ and $R_{\beta\gamma}$ are maintained equal to each other ($= R$) and varied from infinity to the equilibrium value R_e. For any value of R the force exerted on nucleus α is equal and opposite to the force exerted on nucleus γ. There is no net force acting on nucleus β in the linear symmetrical configuration. The energy of H_3 in this configuration can thus be obtained by the integration of the force acting on nucleus α as the three atoms are brought together in the symmetric fashion from infinity to the equilibrium separation R_e.

The correlation diagram for the approach of three hydrogen atoms (the system at all times possessing $D_{\infty h}$ symmetry) is shown in Fig. 3. Two molecular orbitals will be

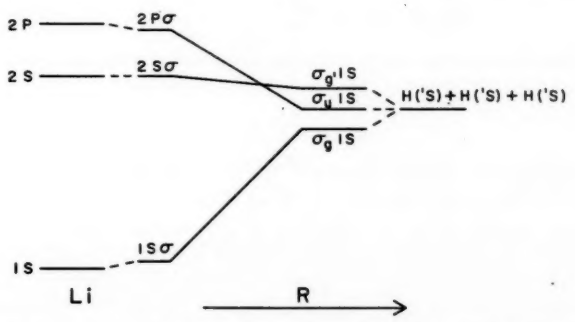

FIG. 3. Correlation diagram for H_3 in the $D_{\infty h}$ nuclear configuration.

occupied in the ground electronic configuration, a σ_g and a σ_u orbital. The value of Z_s for all three of the molecular orbitals will be unity and Z_u will equal 3.00 and 0.65 for the σ_g and σ_u orbitals, respectively. The screening constants for the two occupied orbitals are therefore,

$$Z(R)_g = 1+2e^{-R} \qquad \text{and} \qquad Z(R)_u + 1 - 0.35e^{-R}.$$

The forms of the three molecular orbitals which result from the linear combinations of the hydrogen $1s$ atomic orbitals are

$$\sigma_g = N_g(\phi_{\alpha g}+\lambda\phi_{\beta g}+\phi_{\gamma g})$$

$$\sigma_u = N_u(\phi_{\alpha u}-\phi_{\gamma u})$$

$$\sigma_{g'} = N_g'(\phi_{\alpha g}'-\lambda'\phi_{\beta g}'+\phi_{\gamma g}')$$

where the N_i are normalizing factors and the ϕ's are again normalized atomic orbitals of the Slater type. The ground state wave function for linear symmetric H_3 is

$$\Psi = (3!)^{-1/2}\sum (-1)^p P\sigma_g(1)\sigma_g(2)\sigma_u(3)\alpha(1)\beta(2)\alpha(3)$$

and this results in an electron density

$$\rho = 2[2+2S^g_{\alpha\gamma}+2\lambda(S^g_{\alpha\beta}+S^g_{\beta\gamma})]^{-1}[\phi_{\alpha g}{}^2+\lambda^2\phi_{\beta g}{}^2+\phi_{\gamma g}{}^2+2\lambda\phi_{\alpha g}\phi_{\beta g} + 2\lambda\phi_{\beta g}\phi_{\gamma g}+2\phi_{\alpha g}\phi_{\gamma g}]+[2-2S^u_{\alpha\gamma}]^{-1}[\phi_{\alpha u}{}^2+\phi_{\gamma u}{}^2-2\phi_{\alpha u}\phi_{\gamma u}].$$

The five necessary atomic orbitals will be of the forms

$$\phi_{\alpha g} = (Z(R)_g{}^3/\pi)^{1/2}\exp(-Z(R)_g r_\alpha) \qquad \text{for the } \sigma_g \text{ orbital,}$$

$$\phi_{\alpha u} = (Z(R)_u{}^3/\pi)^{1/2}\exp(-Z(\mathrm{R})_u r_\alpha) \qquad \text{for the } \sigma_u \text{ orbital.}$$

The application of the Hellmann–Feynman theorem gives the following expression for the force acting on nucleus α along the line of centers

$$\begin{aligned} F_{\alpha x}(R) = \frac{1.25}{R^2} &- 2N_g^2\{\langle\phi_{\beta g}\phi_{\beta g}|\cos\theta_{\alpha i}/r^2_{\alpha i}\rangle+\langle\phi_{\gamma g}\phi_{\gamma g}|\cos\theta_{\alpha i}/r^2_{\alpha i}\rangle \\ &+ 2\lambda\langle\phi_{\alpha g}\phi_{\beta g}|\cos\theta_{\alpha i}/r^2_{\alpha i}\rangle+2\lambda\langle\phi_{\beta g}\phi_{\gamma g}|\cos\theta_{\alpha i}/r^2_{\alpha i}\rangle \\ &+ 2\langle\phi_{\alpha g}\phi_{\gamma g}|\cos\theta_{\alpha i}/r^2_{\alpha i}\rangle\} - N_u^2\{\langle\phi_{\gamma u}\phi_{\gamma u}|\cos\theta_{\alpha i}/r^2_{\alpha i}\rangle \\ &- 2\langle\phi_{\alpha u}\phi_{\gamma u}|\cos\theta_{\alpha i}/r^2_{\alpha i}\rangle\}. \end{aligned}$$

All but one of the integrals occurring in equation [6] are similar to the ones previously encountered. The one new integral is

$$\langle\phi_\beta\phi_\gamma|\cos\theta_{\alpha i}/r^2_{\alpha i}\rangle.$$

This is a three-center one-electron integral and it possesses no analytical solution. The integral represents the interaction of an ideal dipole centered on nucleus α with the charge distribution arising from the overlap of the atomic orbitals on nuclei β and γ. The value of this integral can be approximated by a transformation to known integrals of the type $\langle\phi_\beta\phi_\beta|\cos\theta_{\alpha i}/r^2_{\alpha i}\rangle$ using an expansion first suggested by Mulliken (14) and later commented on and discussed by Rüdenberg (15) and Csavinszky (16). Both ϕ_β and ϕ_γ are expanded in terms of an orthonormal set of hydrogenic wave functions centered on the opposite atom, i.e.,

$$\phi_\beta = \sum_j s_{\beta\gamma(j)}\phi_{\gamma(j)} \qquad \text{and} \qquad \phi_\gamma = \sum_i s_{\gamma\beta(i)}\phi_{\beta(i)}$$

where the coefficients of the expansion, $s_{\beta\gamma(j)}$, are the corresponding overlap integrals

$$\langle\phi_\beta|\phi_{\gamma(j)}\rangle.$$

With this expansion $\phi_\beta\phi_\gamma$ becomes

$$\phi_\beta\phi_\gamma = 1/2s_{\beta\gamma(1)}(\phi_\beta\phi_{\beta(1)}+\phi_\gamma\phi_{\gamma(1)})+1/2s_{\beta\gamma(2)}(\phi_\beta\phi_{\beta(2)}+\phi_\gamma\phi_{\gamma(2)})+\ldots\ .$$

Rüdenberg has pointed out that this expansion is best for small values of R. Under these conditions the coefficients $s_{\beta\gamma(j)}$, $j \neq 1$ become vanishingly small because of their near orthogonality. As a guide to the approximation we have employed the same

expansion to approximate the known integral $\langle\phi_\alpha\phi_\beta|\cos\theta_\alpha/r_{\alpha i}^2\rangle$. Out to 4 a.u. the major portion is contributed by the leading term as is to be expected. Beyond 4 a.u. the contributions from terms of larger j values became increasingly important and made the approximation prohibitive. Instead, it was found that the known integral was very well approximated by the values of

$$R^{-1/2}S_{\alpha\beta}\langle\phi_\beta\phi_\beta|\cos\theta_{\alpha i}/r_{\alpha i}^2\rangle.$$

For values of $R > 4$ a.u. this same form was used to approximate the three-center integral as well.

The value which is to be given to the parameter λ, which occurs in the expression for the σ_g orbital, is yet to be determined. In variational calculations the energy is minimized with respect to λ and its optimum value is thus determined. The parameter λ possesses no optimum value in an electrostatic calculation, the force exerted on nucleus α by the electrons in the σ_g orbital increasing to a limiting value of $2\langle\phi_\beta\phi_\beta|\cos\theta_\alpha/r_\alpha^2\rangle$ as the value of λ is increased. However, a lower limit can be given to λ even in the electrostatic calculations. For large values of R, λ must approach the value $\sqrt{2}$ if the wave function is to give the correct electron density for large separations. Walsh and Matsen (17) have carried out a variational calculation for H_3 using the wave function employed in this investigation and have found the optimum value for λ to be 1.5 when the effective nuclear charges were simultaneously varied. It is to be expected that λ will have a value greater than $\sqrt{2}$ as charge is forced onto the central atom from the two neighboring atoms as the internuclear separation is decreased.*

TABLE II

	Present calc.		Simple M.O. (17)	M.O. with C.I. (13)	Expt. (13)
	$\lambda = \sqrt{2}$	$\lambda = 1.5$			
Binding energy (in a.u.)	0.1307	0.1482	0.0733	0.1278	0.1625
R_e (in a.u.)	1.66	1.61	1.82	1.779	—

The energy of H_3 has been determined for λ equal to $\sqrt{2}$ and to 1.5, that is, the lower limiting value and a higher one, consistent with that found from a variational calculation. The results of the calculations are given in Table II. The electrostatic calculation with $\lambda = \sqrt{2}$ (equivalent to treating λ as a constant in a variational calculation) is seen to far surpass the simple molecular orbital approach and to match the more elegant calculation of Boys and Shavitt which included the contributions from configurational interaction. When the value of λ is increased to 1.5, only a 9% error remains in the calculated energy, and of course this is a more realistic value of λ than is $\sqrt{2}$. The values of the frequencies for the symmetrical stretch ω_1 and the bending vibration ω_2 of the H_3 molecule are easily determined from the results of the electrostatic calculation. The value of the frequency for the antisymmetric stretching vibration cannot, unfortunately, be determined in these calculations unless some additional assumptions are made. The frequencies obtained, together with those determined by Boys and Shavitt (13) and by Weston (18) are given in Table III. The values reported by Weston were obtained by an application of Sato's method for determining potential energy surfaces, in this

**The parameter λ was not treated as a function of R in the electrostatic calculations. A variation of λ from 1.5 at $R = 2$ to $\lambda = \sqrt{2}$ at $R = \infty$ would not significantly change the result since the variation is slight and since the major change brought about by a change in λ is in the region of $R = 2$.*

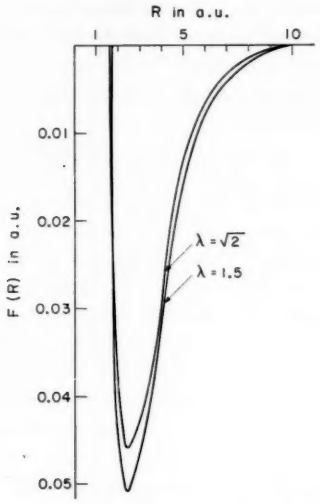

FIG. 4. Force curves for H_3 for two values of the parameter λ.

TABLE III

	Present calc.		Boys and Shavitt (13)	Weston (18)
	$\lambda = \sqrt{2}$	$\lambda = 1.5$		
ω_1 (cm^{-1})	2066	2093	1945	2108
ω_2 (cm^{-1})	1292	1307	952	877

case applied to the H + H_2 reaction. The values for ω_1 are seen to be in fair agreement with the other calculations, while a higher value is predicted for the bending vibration.

V. DISCUSSION

The results of the present calculations indicate that the electrostatic method, when complemented with the empirical expression [2] for determining the screening constant, is capable of giving very reliable estimates of binding energies and force constants. Furthermore, these results may be obtained with relative ease and in a short period of time. This method should be of value in the calculation of the properties of transition states where calculations capable of giving reliable results would be of great help.

It should be pointed out that the use of equation [2] need not necessarily be considered an empirical correction. Since it reproduces the "best" wave functions as determined by the variational procedure to such a remarkable degree, it can be argued that its use is simply to provide the electrostatic method with the best possible wave function obtainable from the variational method.

REFERENCES

1. J. O. HIRSCHFELDER, C. F. CURTISS, and R. B. BIRD. Molecular theory of gases and liquids. John Wiley & Sons, Inc., New York. 1954. p. 934.
2. A. C. HURLEY. Proc. Roy. Soc. A, **226**, 170 (1954).
3. A. C. HURLEY. Proc. Roy. Soc. A, **226**, 179 (1954).
4. A. C. HURLEY. Proc. Roy. Soc. A, **226**, 193 (1954).

5. A. C. HURLEY. Proc. Roy. Soc. A, **235**, 224 (1956).
6. B. MUSULIN. J. Chem. Phys. **25**, 801 (1956).
7. C. A. COULSON. Proc. Cambridge Phil. Soc. **38**, 210 (1942).
8. H. HELLMANN. Einführung in die Quantum-chemie. Leipzig. 1937.
9. G. HERZBERG. Molecular spectra and molecular structure I. Spectra of diatomic molecules. Van Nostrand, New York. 1950.
10. TA-YOU WU. J. Chem. Phys. **28**, 986 (1958).
11. S. HUZINAGA. Progr. Theoret. Phys. (Kyoto), **18**, 139 (1957).
12. I. AMDUR and A. L. HARKNESS. J. Chem. Phys. **22**, 664 (1954).
13. S. F. BOYS and I. SHAVITT. Tech. Rept. WIS-AF-13, Ser. 3, AF 33 (616)-3414, March, 1959.
14. R. S. MULLIKEN. J. chim. phys. **46**, 500 (1949).
15. K. RÜDENBERG. J. Chem. Phys. **19**, 1433 (1951).
16. P. CSAVINSKY. J. Chem. Phys. **28**, 996 (1958).
17. J. M. WALSH and F. A. MATSEN. J. Chem. Phys. **19**, 526 (1951).
18. R. E. WESTON. J. Chem. Phys. **31**, 892 (1959).
19. H. SHULL and D. D. EBBING. J. Chem. Phys. **28**, 866 (1958).
20. R. A. BUCKINGHAM. Trans. Faraday Soc. **54**, 453 (1958).

THE REACTIONS OF PERFLUOROETHYL RADICALS WITH HYDROGEN AND METHANE[1]

S. J. W. PRICE[2] AND K. O. KUTSCHKE

ABSTRACT

The reactions of C_2F_5 radicals, produced by the photolysis of $(C_2F_5)_2CO$, with methane and hydrogen have been studied. Assuming zero activation energy for $2C_2F_5 \rightarrow C_4F_{10}$ the activation energies for $C_2F_5 + CH_4 \rightarrow C_2F_5H + CH_3$ and $C_2F_5 + H_2 \rightarrow C_2F_5H + H$ are 10.6 kcal/mole and 11.9 kcal/mole respectively. The present results have been correlated with data on the reactions of CF_3, C_3F_7, and CH_3 radicals with H_2, D_2, CH_4, and C_2H_6. Taking $E_{\text{recombination}} \approx 0$ in all cases and assuming the frequency factor for the recombination reaction varies little from radical to radical, the order of ease of hydrogen abstraction from a given substrate is $CF_3 > C_2F_5 > C_3F_7 > CH_3$. Similarly the ease of hydrogen abstraction from a substrate by a given fluorinated radical is $C_2H_6 > H_2 > CH_4 > D_2$. A calculation based on very limited data indicates the reaction $CH_3 + C_2F_5COC_2F_5 \rightarrow CH_3COC_2F_5 + C_2F_5$ may occur with an activation energy of approximately 7 kcal/mole.

INTRODUCTION

The availability of CF_3 and n-C_3F_7 radicals from the photolysis of the appropriate ketone (1, 2) has led to the study of the reactions of these radicals with simple hydrocarbons, hydrogen, and deuterium (3, 4, 5, 6). Recently C_2F_5 radicals have been obtained by the photolysis of $(C_2F_5)_2CO$ (7). In the present work the reactions of this radical with hydrogen and with methane have been studied.

As was the case in the study of n-C_3F_7 radical reactions the condensable product could not be separated quantitatively from the ketone by low-temperature distillation. A combination of gas phase adsorption chromatography and mass spectrometry has been used in an attempt to obtain complete analysis of the reaction products.

EXPERIMENTAL

Apparatus

The photolysis apparatus was similar to that employed in similar investigations in this laboratory (2, 5). The quartz reaction cell (optical path 10 cm, 190 cc) was mounted inside a hot box which could be controlled to $\pm 0.1°$ C. It was fully illuminated by a parallel beam of light in the 3130 Å region obtained via a standard set of filters (8) from a Hanovia S500 lamp operated on a regulated supply. The cell was connected to the vacuum system through a mercury cutoff mounted immediately below the hot box. The volume of the connecting tubing and a small Dewar sealed to the top of the reaction cell, both of which were outside the irradiated region, was approximately 20 cc thus giving a total volume of 210 cc for the reaction system.

Materials

The perfluorodiethyl ketone used in this work was supplied by Merck and Company of Canada. The ketone contained significant quantities of benzene and some unidentified bromine compound. These impurities were removed in the later stages of the work by a method described previously (7). Phillips Research Grade methane was used without further purification. Hydrogen was purified by passage through a palladium thimble.

[1]*Manuscript received July 20, 1960.*
Contribution from the Division of Pure Chemistry, National Research Council, Ottawa, Canada.
Issued as N.R.C. No. 5965.
[2]*National Research Council Postdoctorate Fellow 1958–59. Present address: Chemistry Department, Essex College, Assumption University, Windsor, Ontario.*

C_2F_5H for calibration of the mass spectrometer and the chromatographic columns was prepared by photolysis of $(C_2F_5)_2CO$ (80 mm) with hydrogen (160 mm) at 250° C and low light intensity (approximately 0.8×10^{12} quanta/cc sec). The mass spectrum of C_2F_5H is given in Table I.

TABLE I

Mass spectrum of C_2F_5H*

Mass No.	Relative height	Probable positive ion
31	8.33	CF
32	2.68	CFH
44	3.80	C_2FH
50	2.88	CF_2
51	100.00	CF_2H
69	27.60	CF_3
100	2.16	C_2F_4
101	47.0	C_2F_4H
119	1.53	C_2F_5

*The isotope peaks are not recorded.

Procedure

Perfluorodiethyl ketone was admitted to the reaction zone and to connecting tubing of the mixing volume, and its pressure read on a mercury manometer. The ketone was condensed in a side arm of the mixing chamber which then was isolated from the measuring volume. Hydrogen or methane was admitted and measured in a similar manner. The ketone was warmed and transferred back to the measuring volume by means of a Toepler pump. After they were mixed 10 times by expansion into the Toepler pump the mixed gases were compressed to their original volume. The reaction zone was isolated by raising the mercury in the cutoff below the hot box and the experiment was started by removing a stop from the light beam. The experiments were allowed to proceed to 2.5% to 10% decomposition of the ketone, most experiments being in the region of 5% decomposition.

Analysis

(*i*) $(C_2F_5)_2CO + CH_4$

The products of the photolysis were passed through two traps at −120° C to remove the bulk of the ketone and then through a trap at −210° C to remove the remaining condensable materials. Carbon monoxide and methane were transferred to a copper oxide furnace at 300° C. After 2 hours, during which time the gases in the copper oxide furnace were mixed several times, the mixture in the furnace was condensed at −196° C and the methane pumped off. The CO_2 was measured in a gas burette.

Since C_4F_{10} and the ketone cannot be separated readily by low-temperature distillation, the entire mixture of condensable products was transferred to a gas chromatographic apparatus where it was analyzed using a 3-ft alumina column (4 mm I.D.) maintained at 25° C. Hydrogen was used as a carrier gas at a flow rate of approximately 60 cc per minute. Exact retention volumes or appearance times cannot be given as these varied considerably with the moisture content of the alumina and the age of the column. As far as could be ascertained the ketone is completely absorbed on the column. Because of this the columns have a useful life of approximately 15 analyses. During this time the sensitivity based on peak height increases by as much as a factor of two.

The elution times similarly decrease. However, for a given column at a fixed temperature and flow rate, the relative elution times remain constant as does the sensitivity based on peak area (this latter point was checked by running a standard C_4F_{10} sample immediately after each analysis). In all cases the products appeared in the order C_2H_6, C_4F_{10}, a peak initially unidentified which was later shown to be C_2F_5Br, and a peak consisting of a mixture of C_2F_5H and $C_2F_5CH_3$. Under the stated conditions the appearance time of C_4F_{10} varied from column to column and with column age over the approximate range 10 minutes to 30 minutes. When the appearance time for C_4F_{10} was about 10 minutes the following approximate appearance times were observed: C_2H_6, 1 minute; C_2F_5Br, 17 minutes; $C_2F_5H + C_2F_5CH_3$, 35 minutes.

The mass spectrum of accumulated C_2F_5Br peaks is shown in Table II.

TABLE II

Mass spectrum of C_2F_5Br

Mass No.	Relative peak height	Probable positive ion
31	20.0	CF
50	10.7	CF_2
69	44.9	CF_3
79	5.9	Br
81	6.1	Br
91	1.1	CBr
93	1.1	CBr
100	4.9	C_2F_4
110	2.0	CFBr
112	2.0	CFBr
119	100	C_2F_5
129	30.6	CF_2Br
131	30.0	CF_2Br
141	.05	C_2F_2Br
143	.05	C_2F_2Br
160	.17	C_2F_3Br
162	.17	C_2F_3Br
179	13.9	C_2F_4Br
181	13.5	C_2F_4Br
198	17.7	C_2F_5Br
200	19.0	C_2F_5Br

The mixture of C_2F_5H and $C_2F_5CH_3$ was collected as it was eluted from the column, its volume measured in a gas burette, and the mixture analyzed on a mass spectrometer using the mass 51 (CF_2H) and mass 101 (C_2F_4H) peaks for C_2F_5H and the mass 65 (CF_2CH_3) peak for $C_2F_5CH_3$. The mass spectrometer was calibrated using C_2F_5H. Hence C_2F_5H was determined directly and the $C_2F_5CH_3$ calculated by difference. In each case the relative sensitivity to C_2F_5H (based on mass 51) and $C_2F_5CH_3$ (based on mass 65) was 0.63:1.00. During the course of the work a new element was installed in the mass spectrometer. This changed the sensitivity to CH_4 (using mass 15) from approximately 7 cm peak height per micron to 24 cm peak height per micron but had no apparent effect on the relative sensitivity of C_2F_5H to $C_2F_5CH_3$ (as based on masses 51 and 65). The mass spectrum of $C_2F_5CH_3$ obtained by subtracting the C_2F_5H spectrum from that of a mixture of the compounds is given in Table III. Virtually the same $C_2F_5CH_3$ spectrum is obtained using any of the analyses carried out in the course of the work.

(*ii*) $(C_2F_5)_2CO + H_2$

The condensable products were trapped out as described in Section (*i*). Carbon monoxide and hydrogen were oxidized to carbon dioxide and water in a copper oxide furnace

TABLE III

Mass spectrum of $C_2F_5CH_3$ obtained by subtracting the C_2F_5H spectrum from the spectrum of a mixture of these compounds

Mass No.	Relative height	Probable positive ion
15	1.7	CH_3
31	1.9	CF
44	12.0	CFCH
45	15.5	$CFCH_2$
50	0.2	CF_2
64	5.6	CF_2CH_2
65	100.0	CF_2CH_3
69	13.0	CF_3
115	5.2	$C_2F_4CH_3$
119	10.0	C_2F_5
134	3.2	$C_2F_5CH_3$

and the CO_2 was estimated by transferring it to a gas burette. Several degassings of the water–CO_2 mixture were carried out to obtain as complete a separation as possible. During removal of CO_2 the CO_2–water mixture was kept at $-90°$ C. Since $C_2F_5CH_3$ is not formed in this photolysis complete analysis of the condensable products was carried out using the gas chromatographic system described in Section (*i*).

RESULTS

The observed products of the photolyses may be accounted for qualitatively by the following mechanisms:

(*a*) *Photolysis in the presence of methane.*—

$$C_2F_5COC_2F_5 + h\nu \rightarrow 2C_2F_5 + CO,$$

$$C_2F_5 + CH_4 \rightarrow C_2F_5H + CH_3, \quad [1]$$

$$2C_2F_5 \rightarrow C_4F_{10}, \quad [2]$$

$$C_2F_5 + CH_3 \rightarrow C_2F_5CH_3, \quad [4]$$

$$2CH_3 \rightarrow C_2H_6. \quad [5]$$

For the unpurified ketone two additional reactions are required:

$$C_2F_5 + \text{impurity} \rightarrow C_2F_5H + \text{radical}, \quad [6]$$

$$C_2F_5 + \text{impurity} \rightarrow C_2F_5Br + \text{radical}. \quad [7]$$

The impurities shown in equations [6] and [7] are not necessarily the same. The exact nature of the contaminants was not established; however, mass spectrometric analyses and infrared experiments suggest benzene as one possible impurity in which case the "radical" in equation [6] would be the phenyl radical, which would presumably either dimerize or abstract from methane regenerating benzene. The impurity containing bromine may possibly be present as bromobenzene in which case the radical in equation [7] would also be the phenyl radical. When impure ketone was used, the material balance was always low, i.e., less product was found than is compatible with the production of $2C_2F_5$ per CO. This fact also suggests an unsaturated impurity.

(*b*) *Photolysis in the presence of hydrogen.*—

$$C_2F_5COC_2F_5 + h\nu \rightarrow 2C_2F_5 + CO,$$

$$C_2F_5 + H_2 \rightarrow C_2F_5H + H, \quad [3]$$

$$H + C_2F_5 \rightarrow C_2F_5H, \quad [4]$$

plus reactions [2], [6], and [7]. It has been assumed that [10] is of negligible importance under the experimental conditions used (5).

$$H + H + M \rightarrow H_2 + M. \qquad [10]$$

If this reaction did contribute appreciably then all values reported for $k_3/k_2^{\frac{1}{2}}$ should be increased by a factor lying between one and two.

The results of the photolyses in the presence of methane are given in Table IV and those for the photolyses in the presence of hydrogen in Table V. Except as noted the

TABLE IV

The reaction of C_2F_5 radicals with methane

Temp., °C	Length of run, 10^3 sec	Ketone 10^{-6} mole/cc†	CH_4 10^{-6} mole/cc†	CO	C_2F_5H	C_4F_{10}	C_2H_6	$C_2F_5CH_3$	C_2F_5Br
				10^{-6} mole					
272	59.16	1.50	1.37	10.8	23.8	4.62	0.10	4.60	0.70
255	18.60	1.30	1.18	18.6	15.4	13.5	—	3.40	0.83
255	16.74	1.24	1.18	15.2	11.9	9.98	0.23	3.16	1.50
240*	11.46	1.36	1.73	8.20	8.05	6.40	0.047	1.78	0.00
235	14.70	1.21	1.74	13.0	10.0	8.50	0.28	2.80	0.86
229	18.96	1.34	1.28	20.8	10.0	15.8	0.17	3.70	1.45
211	19.44	1.45	1.76	18.8	9.35	14.5	0.16	2.95	0.89
212	22.38	1.37	3.24	20.0	18.44	12.9	0.38	5.76	0.83
212	18.00	1.49	0.795	—	4.45	15.0	0.05	1.25	1.37
212	71.64	1.45	1.29	13.8	12.2	10.4	0.25	2.20	0.80
212	40.08	1.45	1.32	21.7	11.5	17.5	0.10	3.00	1.13
210	16.50	1.30	2.15	14.8	8.42	10.7	0.32	2.80	0.76
191	18.54	1.23	2.02	16.9	6.00	13.1	0.29	2.10	1.67
184*	14.22	1.46	2.16	11.1	3.86	9.65	0.065	1.40	0.00
184*	68.52	1.46	1.35	11.9	5.68	10.33	0.055	1.53	0.00
160	18.00	1.49	2.32	18.0	3.85	12.40	0.31	1.17	1.24
159	17.64	1.88	1.82	18.7	3.60	14.3	0.11	1.30	0.94
150	22.02	1.33	2.90	24.0	4.95	17.0	0.33	1.55	—

*Runs with pure $C_2F_5COC_2F_5$. †Volume of reaction zone 190 cc.

TABLE V

The reaction of C_2F_5 radicals with hydrogen

Temp., °C	Length of run, 10^3 sec	Ketone 10^{-6} mole/cc†	H_2 10^{-6} mole/cc†	C_2F_5H	C_2F_5Br	C_4F_{10}	CO
				10^{-6} mole			
237	12.60	1.20	1.22	20.8	1.12	1.57	13.6
212	12.60	1.30	1.39	16.5	1.36	2.62	13.2
193*	12.12	1.48	1.08	10.3	0.00	4.89	10.2
193	12.72	1.35	1.38	13.2	1.73	4.38	13.8
174*	12.18	1.32	0.40	3.00	0.00	8.37	9.80
174	13.20	1.30	0.49	4.54	1.74	8.93	13.1
174	13.26	1.35	1.35	9.70	1.46	6.35	13.4
174*	11.94	1.38	1.45	10.3	0.00	6.45	10.9
174	13.20	1.25	4.28	18.8	1.35	2.83	13.9
154	13.50	1.49	1.44	6.70	1.63	9.73	14.5
138*	9.42	1.58	2.25	3.58	0.00	5.82	7.57
137	13.02	1.15	1.70	4.11	0.92	7.00	11.50

*Runs with pure ketone. †Volume of reaction zone 190 cc.

experiments were done using the slightly impure ketone. Since it had been found previously that the photolysis of the impure ketone gave C_2F_5H as a product (unpublished results of work carried out in connection with reference 7), a correction for this was made as follows.

$$R_{C_2F_5H} = k_6[C_2F_5][\text{impurity}]+k_1[C_2F_5][CH_4]$$

$$R_{C_2F_5H}/R^{\frac{1}{2}}_{C_4F_{10}} = (k_6/k_2^{\frac{1}{2}})([\text{impurity}]/[\text{ketone}])[\text{ketone}]+(k_1/k_2^{\frac{1}{2}})[CH_4].$$

From experiments in the absence of CH_4

$$(k_6/k_2^{\frac{1}{2}})([\text{impurity}]/[\text{ketone}]) = \text{antilog}\ (\bar{3}.987+461/T)$$

(second-order rate constants are expressed in $(\text{mole/cm}^3)^{-1}\ \text{sec}^{-1}$). Hence values of $k_1/k_2^{\frac{1}{2}}$ could be calculated. As may be seen from Fig. 1, the ratios $k_1/k_2^{\frac{1}{2}}$ obtained in this manner are in excellent agreement with those calculated from data taken with the purified ketone. A similar correction was applied to the data from the hydrogen – impure ketone system; good agreement was also achieved with data obtained when purified ketone was used. In the hydrogen system

$$\tfrac{1}{2}R_{C_2F_5H}/R^{\frac{1}{2}}_{C_4F_{10}} = \tfrac{1}{2}(k_6/k_2^{\frac{1}{2}})([\text{impurity}]/[\text{ketone}])[\text{ketone}]+(k_3/k_2^{\frac{1}{2}})[H_2].$$

With a ketone concentration of approximately 1.45×10^{-6} mole/cc, varying the methane concentration from 0.80×10^{-6} to 3.24×10^{-6} mole/cc had no apparent effect on $k_1/k_2^{\frac{1}{2}}$ ($t = 212°$ C). Similarly with a ketone concentration of approximately 1.3×10^{-6} mole/cc, a variation in the hydrogen concentration from 0.40×10^{-6} to 4.28×10^{-6} mole/cc did not alter the value of $k_1/k_3^{\frac{1}{2}}$ ($t = 174°$ C).

DISCUSSION

The following values have been obtained from Fig. 1:

$$E_1-\tfrac{1}{2}E_2 = 10.62\ \text{kcal/mole}; \qquad A_1/A_2^{\frac{1}{2}} = 4.17\times10^4\ (\text{mole/cm}^3)^{-\frac{1}{2}}\ \text{sec}^{-\frac{1}{2}};$$

$$E_3-\tfrac{1}{2}E_2 = 11.90\ \text{kcal/mole}; \qquad A_3/A_2^{\frac{1}{2}} = 5.25\times10^5\ (\text{mole/cm}^3)^{-\frac{1}{2}}\ \text{sec}^{-\frac{1}{2}}.$$

By analogy with other simple radicals the activation energy for the recombination of two C_2F_5 radicals may be expected to be very small (9, 10, 11, 12, 13). Therefore the observed activation energies should be approximately those for the hydrogen abstraction reactions.

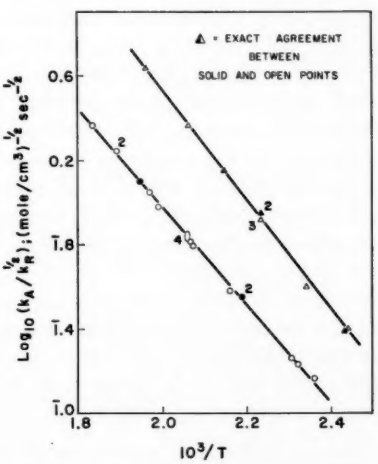

FIG. 1. Arrhenius plots for the reactions of C_2F_5 radicals with methane (○) and with hydrogen (△). Solid points refer to runs using the purified ketone. Subscripts refer to number of experiments averaged to obtain a point; the maximum and minimum values of each set lie within the point.

TABLE VI

Summary of data on reactions $R + R^1H \rightarrow RH + R^1$

R =	CH_3			C_3F_7			C_2F_5			CF_3		
R^1H	E	log A	k	E	log A	k	E	log A	k	E	log A	k
C_2H_6	10.4	4.45*	.276	9.20	5.24‖	6.41	—	—	—	7.50	4.97‡	22.8
H_2	10.0	4.65†	.675	12.3	5.64**	0.96	11.9	5.74‡‡	1.82	8.80	4.92††	7.94
CH_4	13.0	4.41‡	.014	9.5	3.99††	0.41	10.6	4.62‡‡	0.55	10.3	4.99‡	1.74
D_2	12.2	4.71§	.068	13.8	5.78**	.107	—	—	—	9.70	4.77††	1.25

NOTE: In each case $E = E_1 - \frac{1}{2}E_2$, $\log A = A_1/(A_2)^{\frac{1}{2}}$, and $k = k_1/k_2^{\frac{1}{2}}$ where the subscript 1 refers to the abstraction reaction and the subscript 2 to the reaction $R + R \rightarrow R_2$. Units: E kcal/mole; A_1, A_2, k_1, and k_2 (moles $cm^{-3})^{-1}$ sec^{-1}; all k's refer to 200° C.

*Reference 14. These values actually refer to $CD_3 + C_2H_6$; however, the limited data available indicates that rates of abstraction by CH_3 and CD_3 do not differ greatly. †Reference 15. ‡Reference 3. §Reference 16. ‖Reference 4. **Reference 5. ††Reference 6. ‡‡Present work.

In Table VI the present results are compared with those obtained with similar radicals and substrates. As indicated in the footnotes of Table VI, the tabulated E values are $E_{\text{abstraction}} - \frac{1}{2}E_{\text{recombination}}$; however, in the ensuing discussion it will be assumed that $E_{\text{recombination}}$ is effectively zero in each case. The further assumption will be made that $A_{\text{recombination}}$ is approximately the same for the four radicals considered. This has been borne out by experiment for CH_3 and CF_3 (9, 10, 11); it might not be true for C_2F_5 and C_3F_7 recombinations but will serve as a basis for discussion, any errors thus introduced being remedied easily when experimental values become available. As may be seen from Table VI there is no consistent trend in either activation energies or frequency factors. However, there is a marked and in fact almost unique pattern in the values of k calculated at 200° C. In many of these investigations the exact slope of the Arrhenius curve is somewhat doubtful. Since the A factors are calculated using the experimental E, compensation between A and E must occur if E is incorrectly calculated. However, provided k values are calculated from these A and E values within or close to the experimental temperature range, much less relative error is to be expected in these than in A or E separately. Using k as a measure of the relative radical reactivity with respect to hydrogen abstraction, the following sequence is observed for all four substrates: $CF_3 > C_2F_5 > C_3F_7 > CH_3$. Although this order is obtained from k's at 200° C the convergence of values with temperature is so small that it apparently should hold over all readily accessible temperatures, except in the case of C_3F_7 and C_2F_5, which would apparently replace each other in the reactivity series below approximately 70° C. Similarly, for all three fluorinated radicals the ease of hydrogen abstraction from a given substrate is observed to be $C_2H_6 > H_2 > CH_4 > D_2$. It is assumed that the abstraction by C_2F_5 from C_2H_6 and from D_2 would follow this pattern although at present this is not known.

Although the data are extremely limited another point may be considered. In the photolysis of azomethane in the presence of hexafluoro-acetone, Pritchard and Steacie (17) found that the over-all reaction $CH_3 + CF_3COCF_3 \rightarrow CH_3COCF_3 + CF_3$ had an activation energy of approximately 6 kcal/mole. In the three runs with pure $C_2F_5COC_2F_5$ in the presence of methane the following material balance was expected:

$$(C_4F_{10} + \tfrac{1}{2}C_2F_5H + \tfrac{1}{2}C_2F_5CH_3)/CO = 1, \qquad \text{(i)}$$

$$(2C_2H_6 + C_2F_5CH_3)/C_2F_5H = 1. \qquad \text{(ii)}$$

However, it was observed that (i) exceeded unity and (ii) was much less than unity. The total radical balance

$$(C_4F_{10} + C_2F_5CH_3 + C_2H_6)/CO = 1 \qquad \text{(iii)}$$

was obeyed experimentally (1.002 ± 0.001). This suggests that [9] occurs. The reaction merely exchanges free radicals so that (iii) should be obeyed whereas (i) and (ii) should not.

$$CH_3 + C_2F_5COC_2F_5 \rightarrow C_2F_5 + CH_3COC_2F_5 \qquad [9]$$

The reaction might proceed via an addition complex but the lifetime of the complex must be sufficiently small that it will not scavenge free radicals to form an ether.

Considering reactions [9], [2], and [4]

$$(R_{C_4F_{10}} \cdot R_{\text{exchange}})/R_{C_2F_5CH_3} = \{(k_2^{\frac{1}{2}}k_9)/k_4\}[C_2F_5COC_2F_5]$$

and assuming k_2 and k_4 to be temperature independent, the value of E_9 is found to be 7 ± 1 kcal/mole where, noting that the result is based on only three experiments, the limits of error are rather arbitrary. In principle it would also be possible to use reactions [9] and [5] to calculate this quantity. However, the quantities of C_2H_6 are very small and the accuracy of their analysis is questionable. Therefore any calculations employing ethane yields would be of very doubtful value.

In the photolyses with H_2 it was expected that $(\frac{1}{2}C_2F_5H + C_4F_{10})/CO = 1$. This was indeed the case when purified ketone was used. Thus the analogue with H of reaction [9],

$$H + C_2F_5COC_2F_5 \rightarrow C_2F_5CHO + C_2F_5,$$

does not occur.

Consideration of reactions [2], [4], and [5] indicates that

$$R_{C_2F_5CH_3}/(R_{C_4F_{10}}R_{C_2H_6})^{\frac{1}{2}} = k_4/(k_2k_5)^{\frac{1}{2}},$$

which should be a constant equal to about 2.5 if $E_2 = E_4 = E_5 = 0$ and if the collision theory cross-sections are related by $\sigma_4 = (\sigma_2\sigma_5)^{\frac{1}{2}}$. The data for all the experiments, except that at the highest temperature, give values of the left side of this expression in the range 2 ± 1. A slight trend toward larger values at the higher temperatures was noted, but the lack of good precision in the ethane analysis, leading to considerable scatter, prevents the drawing of a definite conclusion in this regard.

ACKNOWLEDGMENTS

The authors wish to express their thanks to Mrs. R. H. Riem for the mass spectrometric analyses and to Dr. R. N. Jones for infrared experiments on the impure ketone. We also wish to thank Dr. E. W. R. Steacie for many stimulating discussions during the course of this work.

REFERENCES

1. P. B. Ayscough and E. W. R. Steacie. Proc. Roy. Soc. A, **234**, 476 (1956).
2. G. H. Miller, G. O. Pritchard, and E. W. R. Steacie. Z. physik. Chem. **15**, 262 (1958).
3. E. W. R. Steacie. J. Chem. Soc. 3991 (1956).
4. G. Giacometti and E. W. R. Steacie. Can. J. Chem. **36**, 1493 (1958).
5. G. H. Miller and E. W. R. Steacie. J. Am. Chem. Soc. **80**, 6486 (1958).
6. G. O. Pritchard, H. O. Pritchard, and A. F. Trotman-Dickenson. Trans. Faraday Soc. **52**, 849 (1956).

7. G. GIACOMETTI, H. OKABE, S. J. W. PRICE, and E. W. R. STEACIE. Can. J. Chem. **38**, 104 (1960).
8. P. B. AYSCOUGH, J. C. POLANYI, and E. W. R. STEACIE. Can. J. Chem. **33**, 743 (1955).
9. G. B. KISTIAKOWSKY and E. K. ROBERTS. J. Chem. Phys. **21**, 1637 (1953).
10. A. SHEPP. J. Chem. Phys. **24**, 939 (1956).
11. P. B. AYSCOUGH. J. Chem. Phys. **24**, 944 (1956).
12. A. SHEPP and K. O. KUTSCHKE. J. Chem. Phys. **26**, 1020 (1957).
13. S. G. WHITEWAY and C. R. MASSON. J. Chem. Phys. **25**, 233 (1956).
14. A. F. TROTMAN-DICKENSON, J. R. BIRCHARD, and E. W. R. STEACIE. J. Chem. Phys. **19**, 163 (1951).
15. E. WHITTLE and E. W. R. STEACIE. J. Chem. Phys. **21**, 993 (1953).
16. S. DAVIDSON and M. BURTON. J. Am. Chem. Soc. **74**, 498 (1952). *See also* M. H. J. WIJNEN and E. W. R. STEACIE. Discussions Faraday Soc. **14**, 118 (1953).
17. G. O. PRITCHARD and E. W. R. STEACIE. Can. J. Chem. **35**, 1216 (1957).

ÉTARD REACTION

III. NATURE OF THE COMPLEX[1]

OWEN H. WHEELER

ABSTRACT

Magnetic susceptibility measurements have shown that the chromium atoms in the toluene – chromyl chloride complex are tetravalent. The structure of the complex and the reaction mechanism are discussed. Spectroscopic evidence has been found of the initial formation of a π-complex. The products of reaction of chromyl chloride and ethylbenzene, isopropylbenzene, tetralin, and indane have been determined.

An insoluble dark-brown complex is formed as an intermediate in the Étard oxidation of toluenes with chromyl chloride (1, 2, 3), and although a number of structures have been suggested for the complex (3) no positive evidence has been published concerning its structure.

The analysis of the complex formed with toluene agrees with the empirical formula $C_7H_8.2CrO_2Cl_2$. The complexes are generally sparingly soluble in organic solvents and are decomposed by water to give benzaldehydes and to liberate chromium in a valence state of +4 or +5 (1). The chromium atoms in the complex must thus have some valency from four to the six of the original chromyl chloride.

Hartford and Darrin (3) have suggested structures involving hydrogen bonding between two hydrogen atoms of the methyl group of toluene and two chlorine or oxygen atoms of two molecules of chromyl chloride. Structure I, proposed by Rhode (4), also involves Cr^{VI} but with the rather improbable co-ordination number of 5.

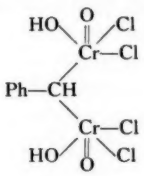

I

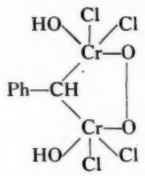

II

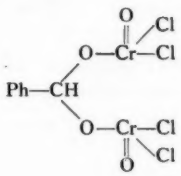

III

Two structures (II and III) can be envisaged for pentavalent chromium. However, the former (II) again has a co-ordination number of 5. In structure III the Cr^{V} has a co-ordination number of 4, and, although the molecule lacks two hydrogen atoms, the formula could be accommodated by the analysis. Étard (5) and later Westheimer (6) proposed structure IV involving tetravalent and tetraco-ordinate chromium.

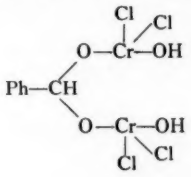

IV

[1]*Manuscript received in original form October 13, 1959, and, as revised, May 30, 1960.*
Contribution from the Departments of Chemistry of Dalhousie University, Halifax, N.S., and the College of Agriculture and Mechanic Arts, University of Puerto Rico, Mayaguez, Puerto Rico. Presented in part at the VII Congreso Latinoamericano de Química, in Mexico City, March 1959. Part II: Can. J. Chem. **36**, *667 (1958).*

In order to determine the valency state of the chromium atoms the magnetic susceptibility (7) of the toluene complex was measured and it gave a value of 3.16 Bohr magnetons per chromium atom. This value (Table I) can only correspond to two unshared electrons

TABLE I

Magnetic susceptibilities of chromium*

	n†	μ_{calc}‡	μ_{obs}§
Cr^{VI}	0	0	0
Cr^{V}	1	1.73	1.7–1.8
Cr^{IV}	2	2.83	2.8–3.1
Cr^{III}	3	3.87	3.85–3.9

*Values for covalent atoms, from ref. 8. †Number of unshared electrons. ‡Magnetic moment calculated from $\mu = \sqrt{\{n(n+2)\}}$. §Magnetic moments observed in covalent bond complexes of Cr and other atoms with the same number of unshared electrons.

per atom. The fact that the value is a little higher than that usually found is probably due to the approximations involved in determining the susceptibility of a solid, or to interaction between the two chromium atoms in the same molecule. The chromium atoms must thus be tetravalent and the complex must have structure IV.

The infrared spectrum of the complex, either as a Nujol mull or as a potassium bromide disk, was rather ill-defined but showed evidence of the presence of a hydroxyl group (maxima at 2.35, 9.3, and 9.7 μ, which may be due to OH stretching and deformation vibrations).

It might be expected that the third hydrogen atom of toluene would be displaced, but the product of the Étard reaction is always a benzaldehyde and not a benzoic acid. The fact that the reaction terminates after displacing two hydrogen atoms probably has its origin in the low solubility of the complex formed with two molecules of chromyl chloride, although a more important factor is probably a steric one. The commonest stereochemical configuration of co-ordination number four is the square planar (dsp^2) form (8), and with two such planes joined to a carbon atom, together with the benzene ring in IV, the third hydrogen atom will be completely hindered to displacement by the bulky chromyl chloride molecule. In the alternative tetrahedral (d^3s) form of the complex the molecule would be even more crowded. It may be noted that ortho-substituted toluenes with large substituents, such as an iodo-atom or nitro-group, give much lower yields of benzaldehydes than their para isomers (1) and this is no doubt largely due to steric hindrance.

The structure IV is in accord with the reactions of the complex, since hydrolysis of the chromium–oxygen bonds will give benzaldehyde (initially as its hydrate). The loss of half the chlorine as hydrogen chloride on heating the complex (3) is also easily explained since a structure with tetravalent chromium atoms such as V could be readily formed.

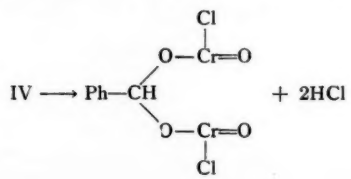

V

As has been already suggested (1) the first stage in the reaction of chromyl chloride and a toluene will be the formation of a π-complex, the chromyl chloride acting as a Lewis acid and the aromatic ring as the corresponding base. The formation of such a π-complex accounts for the initial exothermic reaction observed (1, 3) and spectroscopic evidence for this complex has now been obtained (Fig. 1). A solution of chromyl chloride in carbon tetrachloride has maxima at 290 and 415 mμ (curve II), while a solution of toluene has no significant absorption above 270 mμ (curve I). On mixture of the two solutions, the intensity near 290 mμ increases while the intensity at 415 mμ decreases (curve III). This is consistent with the reaction of the chromyl chloride (decrease in intensity of visible band) with the toluene to form a π-complex with a maximum near 300 mμ. When the mixture is allowed to stand, a precipitate forms and the intensity of both bands decreases, although the greatest decrease is observed at 300 mμ (curve IV) since the π-complex is transformed into the insoluble reaction complex.

The oxidation of a methyl group to an aldehyde is not the only reaction which can take place between an aromatic compound and chromyl chloride. In a previous publication (2) it was shown that the methylene groups in 9,10-dihydroanthracene, phenanthrene, and fluorenene could be oxidized to quinones and that 9-methylanthracene was oxidized to anthraquinone. The products of the oxidation of ethylbenzene have been found to be acetophenone (oxidation of methylene group) and phenylacetaldehyde (oxidation of terminal methyl group) in about equal quantities. It has been reported (12) that benzaldehyde is also formed but this could not be detected in the infrared spectrum of the products. Isopropylbenzene similarly afforded acetophenone (displacement of a methyl group, cf. 9-methylanthracene) and α-phenyl propionaldehyde (oxidation of terminal methyl group) again in about equal amounts (cf. 13). Under the same conditions tert-butylbenzene was unaffected. It has also been found that the oxidation of tetralin gave about equal amounts of α- and β-tetralone. The formation of two products again illustrates the high reactivity of chromyl chloride since the chromic oxide oxidation of tetralin gives only α-tetralone (14). Indane similarly gave apparently a mixture of α- and β-indanone, although the yield was very low and a large amount of polymer was formed.

EXPERIMENTAL

Toluene Complex

Toluene (2.5 g, 0.027 mole) in carbon tetrachloride (20 ml) was treated dropwise with stirring with chromyl chloride (9) (7.75 g, 0.05 mole) in carbon tetrachloride (30 ml) during 1/2 hour, stirred for a further 2 hours, and allowed to stand at room temperature overnight. The suspension was filtered and the precipitate washed with carbon tetrachloride until the washings were colorless, and then dried in a vacuum (9.3 g). Analysis: found, Cl = 34.5, 34.8%; calc. for C_7H_8 $(Cr\ O_2Cl_2)_2$, Cl = 35.16%.

Reaction of benzene (3.9 g) in a like manner gave an oily precipitate (0.20 g) which fumed in air.

Similarly reaction of *tert*-butylbenzene (5.0 g) gave a dark-black precipitate (0.8 g) which decomposed on standing.

Magnetic Measurements

The magnetic susceptibility (χ) was determined by the method of Gouy (7). $X = (a+b\ \delta w)/W$ (10), where $a = k.v$ (k = volume susceptibility of air, v = volume of specimen) and $b = 2\ gv/AH^2$ (A = cross-sectional area and H = field strength). The

susceptibility (diamagnetic) of air is very small and the formula can be reduced to $X = b\ \delta w/W$. For two specimens occupying the same volume, this becomes

$$\chi_1/\chi_2 = \delta w_1 . W_2/\delta w_2 . W_1.$$

Ferrous ammonium sulphate ($\chi = 9500\times10^{-6}/(T+1)$ (11)) was used to calibrate the apparatus. The molecular susceptibility ($\chi_M = \chi \times$ mol. wt.) was corrected for the diamagnetic susceptibility of the other atoms using the values of Pascal (7) and the corrected value was halved to obtain the atomic susceptibility (χ_A) of each chromium atom. The atomic magnetic moment (μ_A) was then calculated using the Langevin formula,

$$\mu_A = \sqrt{(3\,RT\,\chi_A/N)}.$$

Spectroscopic Measurements

The ultraviolet and visible spectra (Fig. 1) were determined in stoppered Corex cells using carbon tetrachloride as solvent. Chromyl chloride had two maxima, at 290 mμ ($\epsilon = 3600$) and 415 mμ ($\epsilon = 2900$).

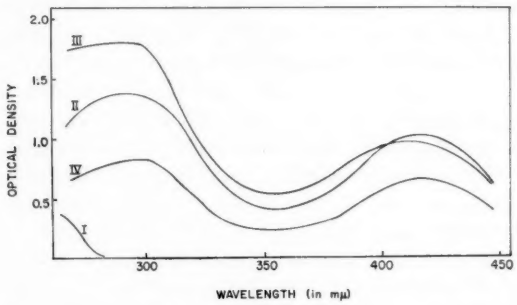

FIG. 1. Spectra of complex. (I) Toluene (1.3×10^{-3} *M*) in CCl_4. (II) CrO_2Cl_2 (4×10^{-4} *M*) in CCl_4. (III) Toluene (1.3×10^{-3} *M*) + CrO_2Cl_2 (4×10^{-4} *M*). (IV) Same after 24 hours.

The infrared spectrum of the toluene complex was determined in a Nujol mull and as a potassium bromide disk.

The principal maxima and their most probable assignments (values in microns and relative intensities in parenthesis) are:

Nujol mull	2.35 (m)	6.26 (m)	6.58 (m)	—	6.85 (s)
KBr disk	—	6.25 (s)	6.54 (s)	6.68 (m)	—
Assignment	OH?	Benzene	Benzene	Benzene	Nujol
Nujol mull	7.26 (s)	8.49 (w)	9.33 (w)	9.74 (w)	
KBr disk	—	8.47 (m)	9.29 (m)	9.74 (m)	
Assignment	Nujol	Mono-sub. benzene	OH?	OH?	

Reactions with Aromatic Hydrocarbons

(Ultraviolet spectra determined in ethanol solution and infrared spectra in carbon tetrachloride.)

Ethylbenzene

Ethylbenzene (21 g) in carbon tetrachloride (100 ml) was treated dropwise with stirring and cooling to 20–25° with chromyl chloride (60 g) in carbon tetrachloride (100 ml) during 1 hour, stirred for 2 hours more, and allowed to stand at room temperature overnight. The reaction mixture was decomposed by being poured into excess aqueous sodium

bisulphite solution and the organic phase separated and dried. After removal of the solvent, the residue was distilled to give a product (10.5 g), b.p. 76–80° at 100 mm, with infrared maxima at 5.85 and 5.97 μ (acetophenone and benzaldehyde have bands at 5.97 and 5.75 μ, respectively). Ultraviolet absorption λ_{max} 242 mμ, ϵ = 7500 corresponding to 59% acetophenone (242 mμ, ϵ = 12,700). A small sample gave a precipitate with 2,4-dinitrophenylhydrazone sulphate solution, which was separated by chromatography on a long column of alumina and elution with benzene, into two fractions; one melting point 247° (from ethyl acetate) (mixed melting point with acetophenone derivative 246–247°) and a second melting point 108–110° (mixed melting point with phenyl acetaldehyde derivative 110–111°).

Isopropylbenzene

Isopropylbenzene (16 g) in carbon tetrachloride (40 ml) was treated dropwise with chromyl chloride (43 g) in carbon tetrachloride (50 ml) over 1 hour at 20–25°. The mixture was stirred for 2 hours, allowed to stand overnight, and worked up as usual, giving a fraction (5.5 g), b.p. 80–85° at 100 mm, having infrared bands at 5.85 and 5.98 μ. Ultraviolet absorption λ_{max} 242 mμ, ϵ = 5850 corresponding to 46% acetophenone. A small sample gave a mixture of 2,4-dinitrophenylhydrazones, separated by chromatography on alumina and elution with benzene into a fraction, m.p. 246° (from ethyl acetate) (no depression on admixture with authentic derivative of acetophenone), and another, m.p. 227–233° (mixed melting point with derivative of α-phenylpropionaldehyde (m.p. 238°) 235–237°).

tert-Butylbenzene

Reaction of *tert*-butylbenzene (20 g) in the same manner gave recovered material (18.5 g), b.p. 168–170°, which showed a very weak carbonyl infrared band, but gave no precipitate with 2,4-dinitrophenylhydrazine reagent.

Tetralin

Freshly distilled tetralin (10 g) in carbon tetrachloride (50 ml) was treated with chromyl chloride (25 g) in carbon tetrachloride (50 ml) at 0° during 2 hours and stirred at 0° for a further 5 hours. Decomposition of the complex in the usual manner gave unchanged tetralin (2 g) and a mixture of α- and β-tetralones (5.6 g), b.p. 112–124° at 10 mm, which had infrared bands at 5.85 and 5.97 μ (authentic α-tetralone had a band at 5.98 μ), and ultraviolet absorption of λ_{max} 242 mμ, ϵ = 5300 (α-tetralone showed λ_{max} 248 mμ, ϵ = 11,400). A small sample gave a 2,4-dinitrophenylhydrazone, m.p. 200–215°, separated as above, into a fraction, m.p. 272° (from ethyl acetate) (mixed melting point with the derivative of α-tetralone 270–271°) and another melting point, 250° (mixed melting point with the derivative of β-tetralone 251–252°).

The main portion (5.2 g) was shaken with an excess of 10% aqueous sodium bisulphite and allowed to stand overnight. The precipitate was filtered, washed with ether, and decomposed with acid, giving β-tetralone (2.5 g), b.p. 123° at 10 mm, 2,4-dinitrophenylhydrazone, melting point and mixed melting point 251°. The ether washings yielded α-tetralone (2.3 g), b.p. 120° at 10 mm, 2,4-dinitrophenylhydrazone melting point and mixed melting point 271°.

Indane

Indane (5.5 g) (prepared by Clemmensen reduction of α-indanone) in carbon tetrachloride (50 ml) was reacted, as above with chromyl chloride (17.0 g) in carbon tetrachloride (50 ml) giving a mixture of α- and β-indanones (0.8 g), b.p. 130–132° at 25 mm,

having infrared maxima at 5.73 and 5.86 μ (α-indanone showed a band at 5.86 μ) and ultraviolet absorption λ_{max} 245 mμ, ϵ = 4100. The amount of product was insufficient to identify it completely. (α-Indanone showed λ_{max} 250 mμ, ϵ = 10,800.)

ACKNOWLEDGMENTS

The author is grateful to Dr. D. A. Ryan, Dalhousie University, for the loan of the Gouy balance and Dr. J. L. Mateos, University of Mexico, for determining the infrared spectra of the toluene complex.

REFERENCES

1. O. H. WHEELER. Can. J. Chem. **36**, 667 (1958).
2. O. H. WHEELER. Can. J. Chem. **36**, 949 (1958).
3. W. H. HARTFORD and M. DARRIN. Chem. Revs. **58**, 1 (1958).
4. G. ROHDE. Sammlung chemische und chemisch-technischer Vortrage. Vol. VI. F. Enke, Stuttgart. 1901. p. 241–302.
5. A. ÉTARD. Ann. chim. et phys. [5] **22**, 218 (1881).
6. F. H. WESTHEIMER. Chem. Revs. **45**, 419 (1949).
7. P. W. SELWOOD. Magnetochemistry. Interscience Publishers, Inc., New York. 1956.
8. R. S. NYHOLM. Quart. Revs. (London), **7**, 377 (1953).
9. H. H. SISLER. Inorganic syntheses. Vol. 2. McGraw-Hill Book Company, New York. 1946. p. 205.
10. F. G. BADDAR, O. M. M. HITAL, and S. SUDGEN. J. Chem. Soc. 132 (1949).
11. L. C. JACKSON. Phil. Trans. Roy. Soc. London, A, **224**, 1 (1923).
12. W. VON MILLER and G. ROHDE. Ber. **23**, 1070 (1890).
13. W. VON MILLER and G. ROHDE. Ber. **23**, 1356 (1890).
14. I. N. NAZAROV and M. S. BURMISTROVA. Zhur. Obshcheĭ Khim. **20**, 1304 (1950).

THE SOLID–LIQUID EQUILIBRIUM BETWEEN ANHYDROUS MAGNESIUM CHLORIDE AND N,N-DIMETHYLFORMAMIDE[1]

DENYS COOK

ABSTRACT

The solid–liquid equilibrium between anhydrous magnesium chloride and N,N-dimethylformamide has been investigated between −58° and +97° C, and up to 25 mole% in magnesium chloride by the techniques of thermal analysis. The following compounds and their melting points have been noted: $MgCl_2.12DMF$, 8.7°; $MgCl_2.6DMF$, 35.0° (incongruent); $MgCl_2.5DMF$, 51.0°; $MgCl_2.4DMF$, 69.0° C. Infrared examination of some of the compounds suggests that co-ordination is through the carbonyl group.

INTRODUCTION

Anhydrous magnesium chloride is known to form complexes with a variety of molecules such as H_2O (1), NH_3 (2), etc. These are usually of the form $Mg6X.Cl_2$ where the cation is octahedrally surrounded by six equivalent donor molecules. These can be thermally degraded and lose some or all of the donor molecules. The thermodynamic properties of this process for the hexahydrate (1) and diammonate (2) have been known for some time.

Because of an interest in the remarkable solvent properties of N,N-dimethylformamide (DMF) it was decided to investigate the solid–liquid equilibrium of the $MgCl_2$–DMF system. It was hoped that specific information concerning the possible formation of an octahedral complex of DMF around Mg^{++} would result. This was of interest since the DMF molecule is a good deal larger than either H_2O or NH_3 mentioned previously, and steric factors could easily play a part in the equilibrium. It was also hoped to ascertain the site of the donor center in DMF.

EXPERIMENTAL

To establish the phase boundaries, the method of thermal analysis of cooling curves of mixtures of $MgCl_2$ and DMF was employed (3). A pyrex cooling cell was constructed, provided with an efficient, magnetically operated stirring system, and a thin-walled tube to accommodate a copper–constantan thermocouple. A Brown strip-chart recorder traced the temperature–time cooling curves.

A weighed amount of $MgCl_2$ was placed in the cell and the proper amount of DMF was added. These operations were performed in a dry box. This mixture was outgassed and then heated to dissolve the $MgCl_2$. A cooling curve was started when all the $MgCl_2$ was in solution. A jacket, which could be evacuated, was placed round the cell, and the appropriate refrigerant surrounded this. The melting point was always easily discernible, particularly as with many mixtures supercooling, occasionally up to 10° C, was observed. The eutectic points, however, were much more elusive and few were recorded with any confidence.

Originally, mixtures were made up by adding further DMF to a known mixture, but some irreproducibility seemed to be introduced by this technique, so subsequently mixtures were freshly and individually prepared.

Between three and five cooling curves were recorded for each mixture and the average

[1]*Manuscript received July 27, 1960.*
Contribution No. 33 from the Exploratory Research Laboratory, Dow Chemical of Canada, Limited, Sarnia, Ontario.

melting point taken. Temperatures could be read to about 0.5° C but points were reproducible to probably 1–2° C.

RESULTS

The results obtained are shown in Table I and are plotted in Fig. 1. Table II shows the melting points of compounds as determined by the dystectic points of the curves.

TABLE I
Melting points of mixtures

Mole% $MgCl_2$	M.p., °C	Mole% $MgCl_2$	M.p., °C
0.0	−58.0	14.65	40.0
4.2	−21.5	15.95	50.0
5.93	+ 2.3	16.79	50.5
7.70	8.7	17.37	56.0
9.15	5.2	18.50	66.0
10.08	4.7	20.68	67.5
11.12	17.0	21.22	78.0
12.02	29.5	22.52	79.5
13.54	33.0	23.85	96.5
14.07	35.0	24.47	89.7

TABLE II
Melting points of compounds

Compound	Mole% $MgCl_2$	M.p., °C	Remarks
$MgCl_2$.12DMF	7.70	8.7	
$MgCl_2$.6DMF	14.28	35.0	Incongruent
$MgCl_2$.5DMF	16.33	51.0	
$MgCl_2$.4DMF	20.00	69.0	

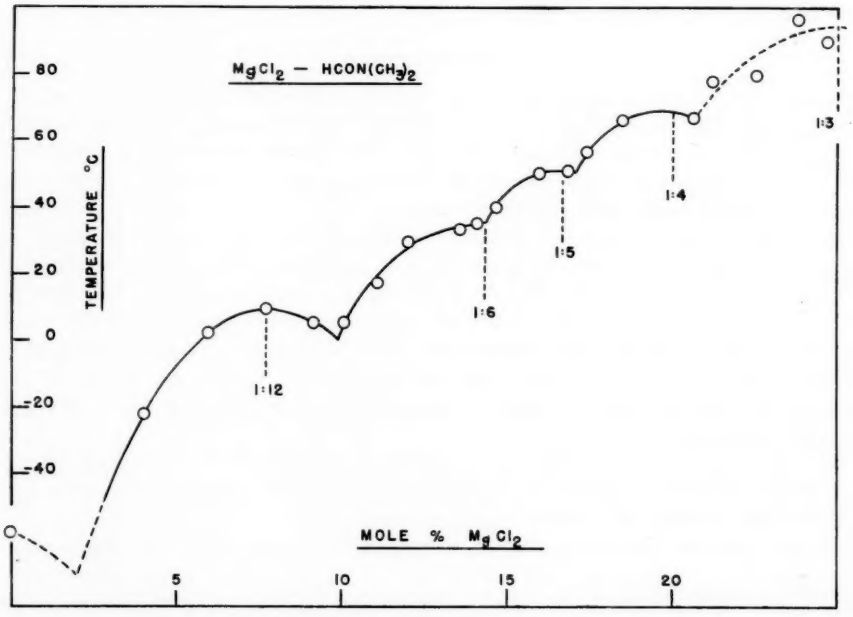

FIG. 1.

DISCUSSION

The appearance of a compound albeit of incongruent melting point at a molecular ratio of 1:6, i.e. $MgCl_2.6DMF$, indicates that even a relatively large molecule like DMF can co-ordinate, probably octahedrally, round the Mg^{++}. (A powder X-ray diffraction pattern of the 1:6 compound showed marked differences from those of anhydrous $MgCl_2$ or the hexahydrate.) The compounds with fewer DMF molecules are probably derived from this compound by successive loss of a DMF molecule from the co-ordination shell at higher temperatures. A 1:3 compound has been tentatively shown in Fig. 1. It probably exists but, in this temperature region, the reproducibility of the melting points was growing worse. There is a strong possibility that thermal decomposition may be a factor at these elevated temperatures.

For all these mixtures, in the crystallization period, especially if supercooling occurred, the first crystals observed were nearly transparent and had a cubic structure. Furthermore, when a mixture of approximately 14.28 mole% $MgCl_2$ was made up, heated to dissolve all the $MgCl_2$, and then cooled slowly, a mass of poorly shaped crystals grew. But by leaving them in a place exposed to weak sunlight, after a few days, a portion of a beautiful cubic crystal grew on top of the other crystals, with an edge of about 6 mm. This cubic structure could be consistent with octahedral co-ordination around the Mg^{++} ion.

Infrared examination of the 4:1 and 3:1 complexes showed a spectrum very similar to that of DMF except that its carbonyl frequency was displaced to lower frequencies by about 46 cm^{-1}. This phenomenon is well known to occur when there is an interaction with the carbonyl oxygen, as in hydrogen bond formation, or Lewis acid–base interaction (4). It is concluded, therefore, that the carbonyl group is the donor group in DMF in this case. Very similar results have been obtained recently for the DMF_2:$TiCl_4$ complex, in which the carbonyl frequency was some 30 cm^{-1} lower than in DMF (5).

The 1:12 compound was rather unexpected, although a compound of the same constitution is observed in the $MgCl_2$–H_2O system. On freezing the $MgCl_2.12DMF$ compound, a mass of small white crystals appeared with no supercooling so observation of their shape was difficult. Their appearance was different enough from the $MgCl_2.6DMF$, or lower compounds, to infer a difference in lattice type. While conjecture on the structure is quite speculative, it seems most unlikely that this could be a Mg^{++} with 12 DMF molecules co-ordinated around it. What is more likely is a six co-ordinated Mg^{++} with six further DMF molecules not interacting with the cation but incorporated in the lattice. Since this compound melted at 9° C it was not possible to take the infrared spectrum to see if two carbonyl bands were present due to two environmentally different DMF molecules.

Finally, a rough estimate of the stability of the 1:6 compound can be deduced from the following evidence. Treatment of a solution of $MgCl_2$ in DMF with NH_3 gave a slow-forming white precipitate, which settled very slowly. By contrast, a solution of $MgCl_2$ in water which is, in effect, $Mg(6H_2O)^{++}$, $2Cl^-$, when treated with NH_3 gave an immediate, copious white precipitate of $MgCl_2.6NH_3$, identified by its infrared spectrum. This is a rough indication that the stability of the $MgCl_2.6DMF$ is intermediate between $MgCl_2.6NH_3$ and $MgCl_2.6H_2O$.

ACKNOWLEDGMENT

The author is indebted to Miss C. D. Anderson for preparing the infrared spectra.

REFERENCES

1. C. H. SHOMATE and E. H. HUFFMAN. J. Am. Chem. Soc. **65**, 1625 (1943).
2. W. BILTZ and G. F. HÜTTIG. Z. anorg. u. allgem. Chem. **119**, 115 (1921).
3. D. COOK, Y. LUPIEN, and W. G. SCHNEIDER. Can. J. Chem. **34**, 957 (1956).
4. D. COOK. Can. J. Chem. **37**, 48 (1959).
5. J. ARCHAMBAULT and R. RIVEST. Can. J. Chem. **36**, 1461 (1958).

SEARCH FOR INDEPENDENT FORMATION OF Cs^{134m} IN FISSION[1]

A. P. Baerg,[2] R. M. Bartholomew, and R. H. Betts

ABSTRACT

The independent yield of Cs^{134m} in thermal neutron fission of U^{235} is less than 1.7×10^{-6} of the mass 134 chain yield and that of Cs^{136} was found to be $(0.94\pm0.04)\times10^{-3}$ of the mass 136 chain yield. The half-life for Cs^{134m} was measured as 2.91 ± 0.01 hours.

INTRODUCTION

The principal mode of formation of the shielded nuclide Cs^{134} in neutron-irradiated uranium is generally thought to be by neutron capture in Cs^{133}. This latter nuclide is a fission product of high yield which builds up in the uranium during a long irradiation. However, recent unpublished work (1) involving highly irradiated uranium dioxide has shown that, in some cases at least, the amount of Cs^{134} is apparently considerably larger than that expected from the 30-barn (2) neutron capture cross section of Cs^{133}. One explanation suggested to account for this anomaly was that the independent fission yield of Cs^{134} may be unexpectedly large; a value of about $7\times10^{-3}\%$ would account for the "excess" Cs^{134} found.

Although it would be very difficult in a short irradiation to detect independent formation of the order of $7\times10^{-3}\%$ yield for 2.2-year Cs^{134} in the presence of other fission product cesium isotopes, it would be readily observable as the high-spin Cs^{134m} isomer (3 hours half-life), if this were formed in amounts comparable with that of the 2.2-year ground state. Judging from the limited information available on isomer ratios of independently formed fission products (3, 4) this is not an unlikely situation. This paper reports on the results of a search which was made for Cs^{134m} formed directly in thermal neutron fission of U^{235}.

EXPERIMENTAL

The method consisted of extracting carrier-free fission product cesium from a sample of uranium which had been irradiated for a short time only to avoid production of Cs^{134m} through neutron capture in fission-produced Cs^{133}. Samples of the carrier-free material were counted in a 4π beta proportional counter to determine the Cs^{134m} relative to Cs^{136} and Cs^{137}. The counting efficiency for the low-energy electrons from the isomeric transition in Cs^{134m} was determined in separate experiments by a coincidence counting method, using Cs^{134m} produced by neutron capture in Cs^{133}.

Irradiation and Purification

Approximately 1 g samples of natural uranium, as UO_2, were sealed in quartz capsules and irradiated in a self-serve position of the Chalk River, NRX reactor. The neutron flux was about $10^{13}/cm^2$ sec and the irradiations were limited to 3 hours. The purification of the cesium, requiring about 3 hours, was delayed 12 hours to permit 32-minute Cs^{138} and 9-minute Cs^{139} to decay to negligible levels.

The irradiated UO_2 was dissolved in a solution 9 *N* in hydrochloric and 3 *N* in nitric

[1]*Manuscript received July 13, 1960.*
Contribution from the Chemistry and Metallurgy Division, Research Chemistry Branch, Atomic Energy of Canada Limited, Chalk River, Ontario.
Issued as A.E.C.L. No. 1099.
[2]*Present address: National Research Council, Ottawa, Ontario.*

acid. This solution was evaporated and the residue taken up in 10 ml of 1 *M* sodium citrate buffer solution adjusted to pH 6 with nitric acid. The cesium was extracted, carrier-free, from this solution with an amyl acetate solution 0.05 *M* in sodium tetraphenyl boron (5). After scrubbing with water the cesium was backwashed with 3 *N* hydrochloric acid and the latter scrubbed with pure amyl acetate. This acid solution was again evaporated and the extraction procedure repeated three times.

It was found that carrier-free silver is also extracted very efficiently in this procedure and so an ion-exchange purification step was introduced. The cesium, in 0.1 *N* hydrochloric acid, was adsorbed on a 200–400 mesh Dowex-50 (8% cross-linked) cation resin column, 10 cm long and 3 mm in diameter. The column was washed, first with 3 ml of 0.1 *N* hydrochloric acid which removed all the silver.* This was followed by about 24 ml of 0.5 *N* hydrochloric acid and finally the cesium was collected in about 2 ml of this eluant. This cesium fraction was further purified by two more extractions with sodium tetraphenyl boron and another cation resin column elution. An additional check on the purity was made in each experiment by adding cesium carrier to a portion of the sample and precipitating cesium silicotungstate (6). These several samples always showed identical decay characteristics and gamma-ray spectra.

Samples of Cs^{134m} for determination of counting efficiency were prepared by irradiation of approximately 1 mg of "spec-pure" CsCl, sealed in a quartz ampoule. The irradiated cesium was purified by several elutions from a cation resin column (see above). Purity checks were made by precipitation of a portion of the cesium with silicotungstic acid and comparison of the decay characteristics.

Counting

Samples of the fission product cesium were prepared for 4π beta counting by evaporating aliquots onto VYNS films. These films were rendered conducting by evaporated gold (10 $\mu g/cm^2$) (7). The dried sources were covered with a similar film. Frequent counts were taken during the first day after the purification, accumulating a minimum of 10^6 counts in each measurement. Subsequently the decay was followed over a period of about 2 months to determine the relative amounts of Cs^{136} and Cs^{137}.

The 4π beta proportional counter-efficiency for the detection of Cs^{134m} was determined by a coincidence technique, using about 1 μg samples of irradiated Cs^{133} mounted in the same way as the fission product samples. Coincidence counting equipment similar to that described by Campion (8) was used. In Fig. 1 is given the decay scheme for Cs^{134m}

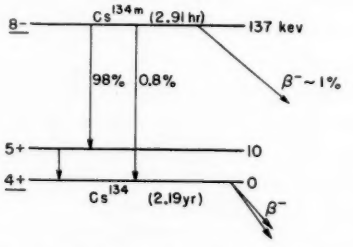

FIG. 1. Disintegration scheme of Cs^{134m}.

**The silver was found by gamma-energy analysis and half-life measurements to be of very high purity. Decay of the Ag^{111}, observed over a period of 60 days, yielded a half-life of 7.45±0.01 days. The purification described appears to be an excellent one for both carrier-free silver as well as for cesium.*

(9) showing 98% of the transitions going to the 10.5-kev level. The transitions from this level are essentially 100% converted in the *L* shell (10) giving rise to 4.5- to 6.2-kev electrons. The detection efficiency for these electrons was determined by counting in coincidence with the 127-kev gamma rays from those transitions to the 10.5-kev level which are not themselves converted. Provided these low-energy electrons are detected with good efficiency, it is reasonable to assume nearly 100% efficiency for the other conversion electrons which are of much higher energy.

Treatment of Data

The total disintegration rate of the fission product cesium samples at any time, t, following the irradiation is given by

$$[1] \qquad Cs_{total} = Cs_0^{137}e^{-\lambda_7 t} + Cs_0^{136}e^{-\lambda_6 t} + Cs_0^{134m}e^{-\lambda_4 t}$$

where the subscripts 0 denote initial disintegration rates and λ_7, λ_6, and λ_4 are the respective disintegration constants. No contribution from Cs^{138} and Cs^{139} is indicated in the equation because the purification was delayed long enough to allow these to decay. Since the irradiations were of short duration no significant amount of Cs^{134} would have been formed by neutron capture in fission-produced Cs^{133}. The contribution to the observed counting rate is also negligible from Cs^{135}, due to its long half-life (2×10^6 years).

In the long-term counting data there is no contribution from Cs^{134m} and equation [1] may be rearranged to

$$[2] \qquad Cs_{total}e^{\lambda_7 t} = Cs_0^{136}e^{(\lambda_7-\lambda_6)t} + Cs_0^{137}$$

so that if the total observed count, multiplied by $e^{\lambda_7 t}$, is plotted versus $e^{(\lambda_7-\lambda_6)t}$, a straight line should result having a slope equal to Cs_0^{136} and a zero intercept equal to Cs_0^{137}.

Having determined Cs_0^{136} and Cs_0^{137}, the initial counting rate of Cs^{134m} may be determined by rearrangement of equation [1] as follows,

$$[3] \qquad (Cs_{total} - Cs_0^{137}e^{-\lambda_7 t})e^{\lambda_6 t} = Cs_0^{136} + Cs_0^{134m}e^{(\lambda_6-\lambda_4)t},$$

and plotting the term on the left versus $e^{(\lambda_6-\lambda_4)t}$. The slope of the straight line then represents Cs_0^{134m} and the zero intercept represents Cs_0^{136}.

RESULTS AND DISCUSSION

Two measurements on the Cs^{134m} yield were made, treating in each case first the long-term counting data according to equation [2] to determine the Cs^{136} and Cs^{137} content of the samples. This treatment of the data is illustrated in Fig. 2. The values of Cs_0^{136} and Cs_0^{137} thus obtained were then used in equation [3] and the short-term counting data plotted as shown in Fig. 3. The errors indicate the standard deviation of the observed count. It is evident from this figure that the contribution of Cs^{134m} to the observed counting rate is very small indeed and that at best an upper limit may be set for the yield of this isomer. This limit is estimated to be $<1.3\times10^{-5}$%. The parameters used in arriving at this value are given in Table I. The results of the counting data are summarized in Table II, together with the estimated limits. These limits will, however, depend on various factors including the Cs^{134m} counting efficiency, the accuracy of the Cs^{136} and Cs^{137} determinations, and the half-life values used in the calculations.

The detection efficiency of the 4π beta counter for the conversion electrons from the 10.5-kev transition in Cs^{134m} was found, in three separate experiments, to be (86 ± 2)%. In view of this fairly high efficiency the conversion electrons from the 127-kev transition

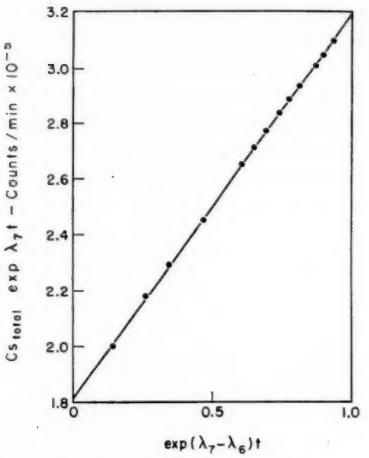

FIG. 2. Long-term decay of fission product cesium.

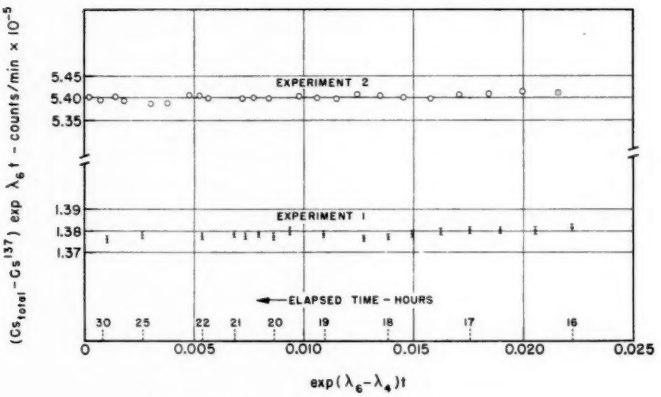

FIG. 3. Short-term decay of fission product cesium.

TABLE I

Values of parameters used to estimate the yield of Cs^{134m}

Irradiation time	3 hours
Half-life of Cs^{136}	12.9 days (11)
Half-life of Cs^{137}	30.0 years (12)
Correction to Cs^{137} activity	0.909 (12)
Half-life of Cs^{134m}	2.91 hours
Counting efficiency of Cs^{134m}	0.974

were assumed to be detected with 100% efficiency. These transitions are 86.9% converted in the K and L shells. The conversion coefficient for the 137-kev transition is not known. It constitutes only 0.8% of all transitions and was assumed not detected. The 1% abundant beta transition was taken to be detected with 100% efficiency. These considerations then lead to an over-all counting efficiency of 97.4% for the Cs^{134m}.

TABLE II

Experimental data and results

Experiment	Cs_0^{137}, counts/min	Cs_0^{136}, counts/min	Cs_0^{134m}, counts/min	Fission yield ratios	
				Cs^{136}/Cs^{137}	Cs^{134m}/Cs^{136}
1	1.81×10^5	1.38×10^5	$<0.2\times10^5$	0.99×10^{-3}	$<2\times10^{-3}$
2	7.12×10^5	5.40×10^5	$<0.9\times10^5$	0.98×10^{-3}	$<2.2\times10^{-3}$

Fission yields*

	% Yield	Fraction of mass chain
Cs^{136}	$(6.1\pm0.24)\times10^{-3}$	$(0.94\pm0.04)\times10^{-3}$
Cs^{134m}	$<1.3\times10^{-5}$	$<1.7\times10^{-6}$

*Taking the cumulative yields of Cs^{137}, mass 136, and mass 134 to be 6.15%, 6.44%, and 8.03% respectively (13).

The counting efficiency for Cs^{136} and Cs^{137} was taken to be 100%. This is believed not to be in error by more than 4% and it is expected that these nuclides were counted with equal efficiency within 1%. In the two measurements a value of 0.76 was obtained for the counting ratio Cs_0^{136}/Cs_0^{137}, with an estimated error of 4%. After a correction factor of 0.909 is applied to the counting rate of Cs^{137} for Ba^{137m} (12), the yield of Cs^{136} becomes $(0.94\pm.04)\times10^{-3}$ as the fraction of the mass 136 chain yield. This value agrees favorably with that of 1×10^{-3} given by Grummitt and Milton (14).

The decay of Cs^{134m}, obtained from the irradiated and purified Cs^{133}, was followed over at least eight half-lives in each of the three counting efficiency measurements. These data yielded a half-life of 2.91 ± 0.01 hours, the value that was used in the calculation. It is somewhat lower than the accepted one of 3.2 hours (9).

The largest error in estimating the Cs^{134m} arises from errors in the value of the term Cs_0^{136} and in the half-life of Cs^{136}. Neither of these is believed to be greater than 5%. It is estimated that even a 10% error in either Cs_0^{136} or its half-life would not change the present results for the Cs^{134m}/Cs^{136} yield ratio by more than a factor of two.

The upper limit for the yield of Cs^{134m} relative to the mass 134 cumulative yield becomes $<1.7\times10^{-6}$ taking the yields of masses 134, 136, and 137 as given in Table II. Extrapolation of existing correlations (14) for independent fission yields suggests a value for Cs^{134} of the order of 5×10^{-6}. The present results then do not indicate any unusual behavior in the independent formation of Cs^{134m} in fission.

REFERENCES

1. R. C. Hawkings. A.E.C.L. Rept. PR-CM-17. March, 1959.
2. D. J. Hughes and R. B. Schwartz. U.S. Atomic Energy Rept. BNL 325.
3. Sylvia Mae Bailey. U.S. Atomic Energy Rept. UCRL-8710. Unpublished.
4. R. A. Sharp and A. C. Pappas. J. Inorg. & Nuclear Chem. **10**, 173 (1959).
5. T. Prach, C. Auerbach, and H. L. Finston. Brookhaven Natl. Lab. Unpublished.
6. Rosalie M. Bartholomew and A. P. Baerg. Can. J. Chem. **34**, 201 (1956).
7. B. D. Pate and L. Yaffe. Can. J. Chem. **33**, 15 (1955).
8. P. J. Campion. Intern. J. Appl. Radiation and Isotopes, **4**, 232 (1959).
9. D. Strominger, J. M. Hollander, and G. T. Seaborg. Revs. Modern Phys. **30**, No. 2, Part 2 (1958).
10. A. N. Sunyar, J. W. Mihelich, and M. Goldhaber. Phys. Rev. **95**, 570 (1954).
11. J. L. Olsen and G. D. O'Kelley. Phys. Rev. **95**, 1539 (1954).
12. F. Brown, G. R. Hall, and A. J. Walter. J. Inorg. & Nuclear Chem. **1**, 241 (1955).
13. J. A. Petruska, H. G. Thode, and R. H. Tomlinson. Can. J. Phys. **33**, 693 (1955).
14. W. E. Grummitt and Gwen M. Milton. J. Inorg. & Nuclear Chem. **5**, 93 (1957).

TRYPTAMINES, CARBOLINES, AND RELATED COMPOUNDS

PART VIII. δ-CARBOLINE[1,2]

R. A. Abramovitch, K. A. H. Adams, and A. D. Notation

ABSTRACT

The first unambiguous synthesis of δ-carboline has been achieved starting with 3-amino-2-phenylpyridine. This was converted to the azide which was thermally cyclized to δ-carboline. The carboline gave a *py*-*N*-methiodide which was converted to the anhydronium base. The pK_a of the anhydronium base was determined and its significance is discussed. The anhydronium base formed a methiodide which, on dry distillation, gave *ind*-*N*-methyl-δ-carboline. The spectral properties of the various derivatives of δ-carboline were examined and the bond structures of the anhydronium base and the methiodides are discussed.

Whereas the chemistry of α-, β-, and γ-carboline has been well studied and a number of unambiguous methods are available for the synthesis of these ring systems practically nothing is known concerning δ-carboline (I). There has appeared only one reference to the synthesis of the parent compound and that to the Graebe–Ullmann cyclization of 1-β-pyridylbenztriazole by Späth and Eiter (1), who obtained a mixture of β-carboline and what was tentatively identified as δ-carboline (since it was not identical with either α-, β-, or γ-carboline) in unspecified low yield. *N*-3-Pyridylaniline was also obtained in this reaction. Subsequently, Eiter (2) was unable to obtain any of the supposed δ-carboline by carrying out this reaction on a larger scale. A similar cyclization of 4-methyl-1-β-pyridylbenztriazole gave 5-methyl-β-carboline as the main product together with a small amount of a compound for which the structure 5-methyl-δ-carboline was suggested (3). Gulland, Robinson, Scott, and Thornley (4) were unable to degrade 3,4-methylenedioxyquindoline to δ-carboline. However, oxidation of this compound with nitric acid gave 7-nitro-δ-carboline-2-carboxylic acid in low yield.

Apart from the fact that it is the only member of the carboline family whose chemistry has not been studied to any degree δ-carboline is interesting from a number of other points of view. It is present in the ring system of the alkaloid cryptolepine (5), which is noteworthy from a biogenetic point of view (6). Also, the relative basicities of α-, β-, and γ-carboline anhydronium bases have been measured by Gray (7), who proposed an explanation for the observed order of base strengths (β- > γ- > α-) and suggested, on the basis of considerations outlined below, that the δ-carboline anhydronium base should have a dissociation constant almost as high as that of the β-isomer. It was of interest to try and test this prediction experimentally.

Smith and Boyer (8) attempted to cyclize 2-*o*-azidophenylpyridine to δ-carboline but obtained instead 2-*o*-aminophenylpyridine.* When 2-*o*-nitrophenylpyridine was heated with ferrous oxalate, cyclization took place preferentially at the pyridine nitrogen atom to give pyrid[1,2-*b*]indazole (9). The Pschorr-type cyclization of 2-amino-*N*-methyl-*N*-3′-pyridylaniline gave a relatively good yield of *ind*-*N*-methyl-δ-carboline (II) (together with some *ind*-*N*-methyl-β-carboline) (10*a*) but attempted *N*-demethylation using a variety of procedures failed (10*b*).

δ-Carboline has now been synthesized unambiguously from 3-amino-2-phenylpyridine

[1]*Manuscript received June 6, 1960.*
Contribution from the Department of Chemistry, University of Saskatchewan, Saskatoon, Saskatchewan. Presented at the 43rd Annual Meeting of the Chemical Institute of Canada in Ottawa, June 1960.
[2]*Part VII: Can. J. Chem.* **38**, *2273 (1960).*
**Our results in this reaction differ from those of Smith and Boyer and will be reported in a subsequent paper.*

(V). The amine was obtained from 2-phenyl-3-picoline (III), which was oxidized to the carboxylic acid (IV) (11); this was transformed into the amine (V) via the acid chloride and the Curtius reaction. It could also be obtained directly by the action of phenyllithium on 3-aminopyridine (12). It was diazotized and converted to 3-azido-2-phenylpyridine (VI), which on being heated in decalin, gave variable yields of δ-carboline (I).

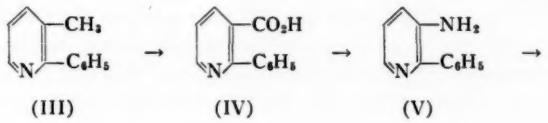

(III) (IV) (V)

(VI) (I)

The base formed a yellow methiodide (VII) readily but resisted all attempts at *ind-N*-methylation. Treatment of the methiodide with alkali gave the orange anhydronium base (VIII); this gave a yellow methiodide (IX) identical with that obtained from *ind-N*-methyl-δ-carboline (II), thus establishing conclusively the structure which had been assigned (10*a*) to (II), as well as the fact that methylation of the anhydronium base occurs at the *ind-N*-atom. Finally, dry distillation of the methiodide (IX) gave *ind-N*-methyl-δ-carboline (II) identical with the sample obtained from the Pschorr reaction (10*a*).

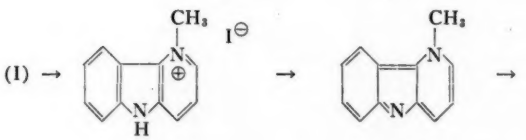

(VII) (VIII)

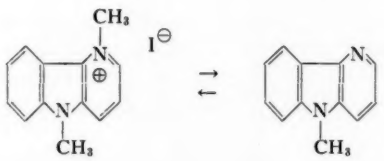

(IX) (II)

Ultraviolet Absorption Spectra and pK_a

Gray (7) obtained the following values for the pK_a's of the carboline anhydronium bases: α-, 7.75; β-, 11.11; and γ-, 10.54. The greater basicity of the β-derivative was ascribed to a lower stabilization energy of the β-carboline anhydronium base indicated from a consideration of the relative contributions made by quinonoid canonical forms. The low basic strength of the α- as compared with the γ-derivative was interpreted on

the basis of two complementary factors: (*a*) a much increased stability of the α-anhydronium base as a result of the juxtaposition of the oppositely charged centers; and (*b*) a reduced stability of the α-carboline salt owing to the inductive effect of the indole nitrogen attached to the same carbon as the positively charged pyridine nitrogen. Support for point (*a*) comes from the fact that pyrid[1,2-*b*]indazole, in which the charged centers are even closer together, is very reluctant to form a methiodide at all (9). A consideration of the basicities of the pyridonimines led Gray to suggest that there is some slight evidence that the aromatic charge-separated forms more nearly represent the properties of all three anhydronium bases. Additional support for this suggestion comes from the high dipole moment of sempervirine (13). Paoloni and Marini-Bettòlo (14) have argued that it is unnecessary to write a formula bearing separated charges for the β-carboline anhydronium base as suggested by Schwarz (15), and have carried out calculations using the LCAO method on 1-methyl-7-azaindole and on 7-methyl-7H-pyrrolo[2,3-*b*]pyridine, the results of which they say support their contention. It was hoped that the determination of the pK_a and spectral properties of the δ-carboline anhydronium base would shed some light on this problem and also verify or disprove Gray's suggestion concerning its base strength.

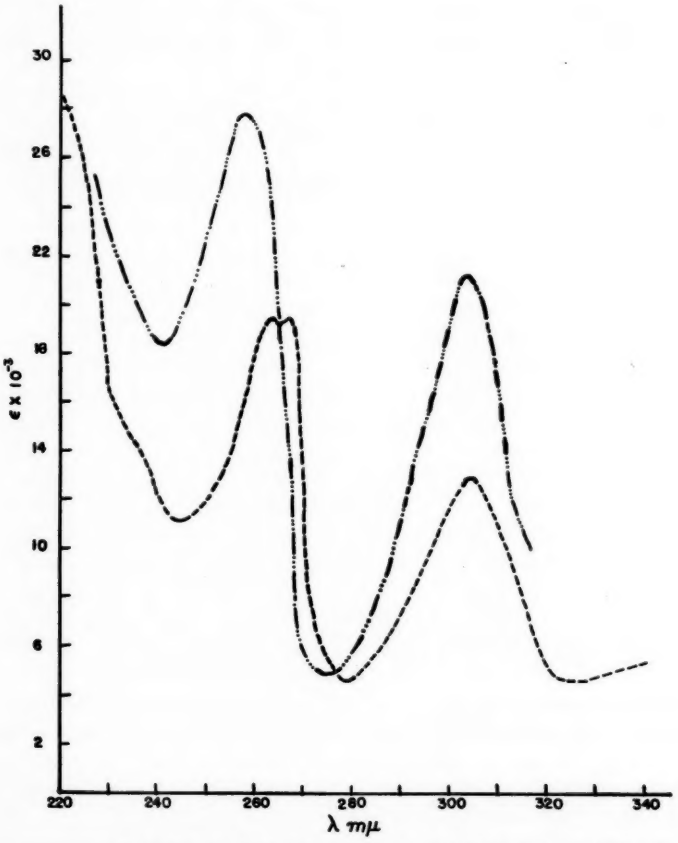

FIG. 1. —·—·— δ-Carboline in 95% ethanol. – – – *ind*-*N*-Methyl-δ-carboline in 95% ethanol.

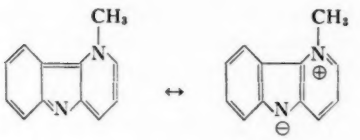

A A′

The pK_a's of the anhydronium bases prepared from the methosalts of α-, β-, and δ-carboline were determined both spectroscopically and by potentiometric titration of the methiodides in 60% ethanol with 0.1 *N* sodium hydroxide, the pH at half neutralization being taken as the pK_a value, no correction for the ionic strength being applied. The average values of several determinations are given in Table I.

TABLE I

Anhydronium base	*py*-*N*-Methyl-α-carboline	*py*-*N*-Methyl-β-carboline*	*py*-*N*-Methyl-δ-carboline
pK_a	7.55	10.88	10.77

*Methiodide kindly supplied by Dr. I. D. Spenser, McMaster University, Hamilton, Ontario.

The values for the α- and β-bases are somewhat lower than those reported by Gray (7) but, as suggested by him, *py*-*N*-methyl-δ-carboline anhydro-base is almost as strong a base as its β-isomer. This result would seem to favor the quinonoid structure A as being an important contributor to the structure of the base, resulting in its having a lower stabilization energy as compared with its salt in which the benzenoid structure is preserved.* The infrared spectrum of *py*-*N*-methyl-δ-carboline anhydronium base afforded some slight tentative *negative* evidence in support of this suggestion. In the infrared spectra of two compounds, pyrid[1,2-*b*]indazole (9) and anthranil (16) in which the grouping $C_6H_4N^{\ominus}$ is known to make a strong, if not predominant contribution, bands have been observed at 1650 and 1642 cm^{-1}, respectively, which have been tentatively assumed to be characteristic of such a grouping. No such band was observed for the δ-carboline anhydronium base. A medium band at 1619 cm^{-1} might be ascribed to a highly conjugated C=N as would be present in A, or alternatively to an aromatic ring vibration as is present in A′. *py*-*N*-Methyl-α-carboline anhydronium base exhibits a band at 1630 cm^{-1} which is intermediate between the above values as might be expected from the suggested structure for this compound in which the benzenoid structure remains unchanged and in which the dipolar structure makes an important contribution. The evidence seems to indicate a mesomeric structure A ↔ A′ for the δ-anhydronium base with the quinonoid structure A making perhaps the weightier contribution to the ground state.

The analysis values of *py*-*N*-methyl-δ-carboline anhydronium base were unsatisfactory, but this seems to be characteristic of this type of compound (17). Its anhydro-base character was confirmed by its ultraviolet absorption spectrum (Fig. 2) compared with that of *py*-*N*-methyl-δ-carbolinium iodide; the bands for the anhydro-base exhibited the usual bathochromic shifts. The colors of the methiodides and anhydronium bases and of their solutions are of interest. Thus, both *py*-*N*-methyl-β- and -δ-carbolinium iodide are yellow in the solid state whereas the unmethylated bases are colorless and

**That disruption of the benzenoid structure is an important factor in the destabilization of the bases is shown by the recent work of Adler and Albert on the ionization constants of the diazaindenes (21) where this factor is not present and the order of base strengths is 1,5 > 1,6 > 1,4 > 1,7.*

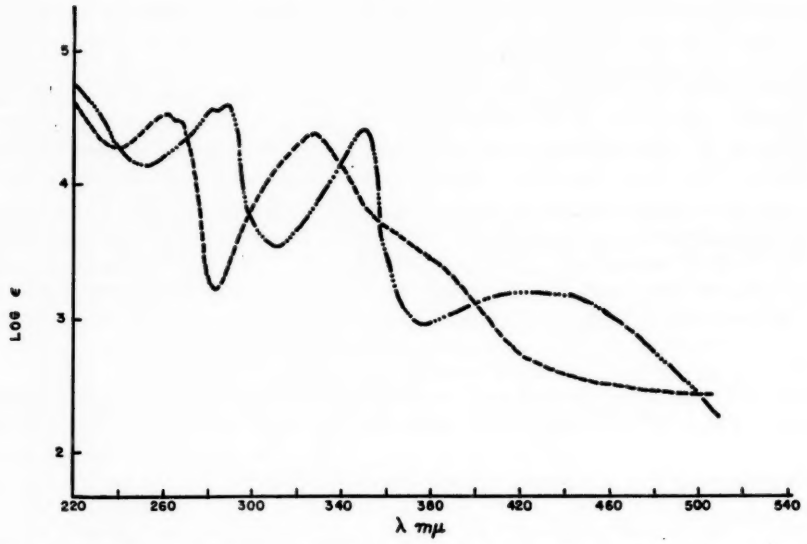

FIG. 2. *py-N*-Methyl-δ-carbolinium iodide. – – – In acidified 95% ethanol. —···— In alkaline 95% ethanol.

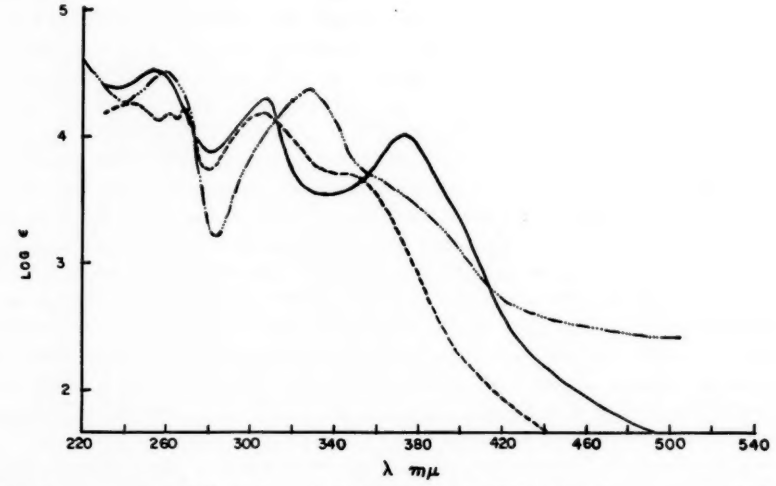

FIG. 3. – – – *py-N*-Methyl-α-carbolinium iodide (in 95% ethanol). ——— *py-N*-Methyl-β-carbolinium iodide (in 95% ethanol). —···— *py-N*-Methyl-δ-carbolinium iodide (in 95% ethanol).

the α-methiodide is cream-colored (see Fig. 3). The anhydronium bases are all orange-colored and give yellow solutions in hydroxylic solvents. The ultraviolet spectra of *py-N*-methyl-δ-carbolinium iodide and of its anhydronium base in 95% ethanol are identical, indicating the ease with which the anhydronium base reverts to the more stable salt structure (compare the case of the β-carboline anhydro-base (18, and references

cited therein)). On the other hand, solutions of *py-N*-methyl-δ-carboline anhydronium base in non-polar solvents such as ether are darker in color than those in hydroxylic solvents and this is reflected in the ultraviolet absorption spectrum of an ethereal solution of this compound when the bands at 282, 289, 350, and 422 mμ (in alkaline 95% ethanol) are shifted to 289, doublet at 295 and 300, 362 and 464 mμ (in ether) respectively. This contrasts with the behavior of the β-carboline anhydro-base whose spectrum in alkaline ethanol is reported to be the same as that in ether solution despite the fact that the latter solution is darker than the former (18). For the δ-carboline anhydro-base the deepening of the yellow color on passing from aqueous ethanolic alkali to ether solution is undoubtedly due to the fact that the color is due to an $n \rightarrow \pi$ transition and that in aqueous ethanolic alkali the unshared electrons of the nitrogen atoms are stabilized in the ground state by hydrogen bonding. As regards the bands in the 282–350 mμ region the bathochromic shift is in the *opposite* direction to that expected for *K*-bands (19) which arise from $\pi \rightarrow \pi$ transitions. Such a blue shift on passing from a non-polar to a polar solvent might indicate an appreciable instantaneous change in polarity from the ground state to the excited state causing the solvating molecules of a polar solvent to be more disoriented than those of a non-polar one during such a transition. If this conclusion is valid it could be taken as providing some tenuous support for the suggestion that structure A is the more important of the two structures contributing to the resonance hybrid. Some comment may also be made concerning the yellow color of the δ-carboline methiodide as compared with the unmethylated base and the α-carboline methiodide. It seems likely that a structure such as (VII′) is contributing to the structure of the ground

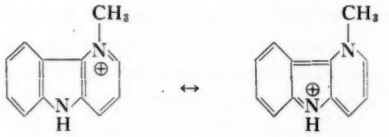

VII VII′

state of the δ-carboline methiodide, the introduction of a positive charge on the *py-N*-atom producing a strong perturbation of the π-electron cloud. Similar comments will apply to the β-carboline methiodide. Due to the closeness of the two nitrogen atoms the perturbation in the α-carboline methiodide case is not as great (this is reflected in the lower pK_a of this compound).

In connection with the ultraviolet absorption spectra of the δ-carbolines it is of interest to note that Eiter and Nezval (3) claimed to have prepared 5-methyl-δ-carboline (no analysis given) and reported that this compound had two bands at 351 and 288 mμ in the ultraviolet. δ-Carboline itself has two bands at 303 and 258 mμ (Fig. 1); furthermore, the shape of the absorption curve given by Eiter and Nezval is quite different from that of δ-carboline reported here, but resembles that of 5-methyl-β-carboline (3). Horner compared the ultraviolet spectra of α- and β-carboline and found them to be similar (20). Both, however, are substantially different from the spectrum of δ-carboline. It seems unlikely therefore, that the compound isolated in very low yield by Eiter and Nezval was really 5-methyl-δ-carboline.

EXPERIMENTAL

Melting points are uncorrected. Infrared spectra were measured with a Perkin–Elmer

Model 21 spectrometer using sodium chloride optics. Ultraviolet absorption spectra were recorded on a Beckman DK2 spectrophotometer.

3-Amino-2-phenylpyridine

2-Phenylpyridine-3-carboxylic acid (11) (0.5 g) was kept at room temperature with thionyl chloride (3.5 ml) for ½ hour. The excess thionyl chloride was removed under vacuum, the residue dissolved in dry acetone, and the solvent evaporated leaving the acid chloride behind as a powder. This was dissolved in dry acetone (9 ml) and sodium azide (0.5 g) in water (1 ml) was stirred into the solution, the temperature being maintained below 20°. After 15 minutes, water (14 ml) was added and the mixture basified with 2 *N* sodium hydroxide. The mixture was heated on a steam bath for 3 hours, cooled, and extracted with ether. The combined extracts were dried (Na_2SO_4) and evaporated to give crude 3-amino-2-phenylpyridine (0.4 g; 92% yield) which was distilled under vacuum and had a boiling point of 119–121°/0.35 mm. The distillate solidified on cooling, and was recrystallized from benzene – light petroleum (b.p. 40–60°) to give colorless crystals, m.p. 62–64°, whose infrared spectrum was identical with that of a sample prepared from 3-aminopyridine and phenyllithium (12). The picrate, m.p. 204–206° (from ethanol), was identical (mixed melting point) with that of the specimen prepared by the 3-aminopyridine method (12).

δ-Carboline

3-Amino-2-phenylpyridine (1.0 g) was dissolved in concentrated hydrochloric acid (2.6 ml) and water (1 ml). A solution of sodium nitrite (0.41 g) in water (1 ml) was added with stirring and cooling on ice to the above solution at such a rate that the temperature remained below 3°. The excess nitrous acid was destroyed by the addition of urea and then a solution of sodium azide (0.45 g) in water (1.5 ml) was added below 3°. At the completion of this addition the solution gave a negative alkaline β-naphthol coupling test. The reaction mixture was allowed to stand at 0° for 1 hour, the solution was then made alkaline with cold sodium hydroxide solution (temperature kept below 5° at all times) and the aqueous solution was then extracted with ether repeatedly. Acidification of the aqueous layer caused the precipitation of 3-hydroxy-2-phenylpyridine (0.3 g; 33% yield), m.p. 206–207°, undepressed on admixture with an authentic specimen (12). The dried (Na_2SO_4) ether extract was evaporated to give the crude azide (0.67 g) as a reddish oil which could not be purified but was used as such in the next stage. Infrared spectrum (liquid film): 2120 (s) (azide), 1580 (m), 1285 (s) (broad), 1185 (m), 802 (m), 735 (s), 695 cm^{-1} (s).

The crude 3-azido-2-phenylpyridine (0.67 g) was dissolved in redistilled decalin (70 ml) and heated at 155–170° for 3 hours. Nitrogen was evolved smoothly at this temperature. On cooling of the reaction mixture, some crystals of δ-carboline separated. The whole mixture was extracted with dilute hydrochloric acid, the acid extracts made alkaline, and the solution extracted with ether. The dried (Na_2SO_4) ether extract was evaporated to give *δ-carboline* (0.44 g), which was recrystallized from benzene to give colorless needles, m.p. 216°. Calc. for $C_{11}H_8N_2$: C, 78.55; H, 4.79. Found: C, 78.15; H, 4.72. The *monopicrate* was recrystallized from ethanol and had a melting point of 277–279°. Calc. for $C_{11}H_8N_2$, $C_6H_3O_7N_3$: C, 51.39; H, 2.79. Found: C, 51.69; H, 2.78. The yields of δ-carboline obtained in several runs varied appreciably, the one reported above being the highest obtained. In some runs, some 3-amino-2-phenylpyridine, formed undoubtedly by hydrogen abstractions from the solvent, was isolated.

py-N-Methyl-δ-carbolinium Iodide (VII)

δ-Carboline (110 mg) in 95% ethanol (1 ml) was treated with an excess of methyl iodide (2 ml) and the solution kept overnight at room temperature. The precipitate (200 mg) was filtrated and recrystallized from methanol to give the *methiodide* as light yellow needles, m.p. 250–252°. Calc. for $C_{12}H_{11}N_2I$: C, 46.47; H, 3.57. Found: C, 46.27; H, 3.70. λ_{max} 262, 328 mμ; λ_{infl} 266, 348 mμ; log ε 4.53, 4.50, 4.35, 3.70 (in 95% ethanol).

py-N-Methyl-δ-carboline Anhydronium Base (VIII)

The above methiodide (50 mg) was dissolved in hot water (2 ml) and the solution treated with a warm 20% aqueous solution of sodium hydroxide (4 ml). The yellow precipitate (22.6 mg) which separated from the cooled suspension was filtered off and washed with a little cold water. The combined filtrates were extracted repeatedly with ether, the extracts dried (Na_2SO_4), and the ether evaporated to yield a further small quantity of base. The combined solids were recrystallized from anhydrous benzene to give the *anhydronium base* as orange-yellow plates which became almost black at ca. 200° and melted at 204–205°. The microanalytical values were unsatisfactory as is common for such substances (17). Calc. for $C_{12}H_{10}N_2$: C, 79.09; H, 5.53. Found (average of two determinations): C, 71.33; H, 6.00. Infrared spectrum (KBr disk) (main peaks only): 1619 (m), 1588 (m), 1335 (s), 797 (m), and 718 cm^{-1} (ms). λ_{max} 282, 290, 350, 422 mμ; log ε 4.56, 4.60, 4.38, 3.20 (in alkaline 95% ethanol).

ind-N-Methyl-δ-carboline py-N-Methiodide (IX)

A benzene solution of *py-N*-methyl-δ-carboline anhydronium base was treated with an excess of methyl iodide to give an immediate precipitate of the *methiodide* which was recrystallized from 95% ethanol and formed light yellow needles, m.p. 270.5–271.5°, identical with the authentic specimen obtained by treating *ind-N*-methyl-δ-carboline (10*a*) in 95% ethanol with methyl iodide and allowing the solution to stand at room temperature overnight. The melting points of the two specimens were undepressed on admixture and their infrared spectra were identical. Calc. for $C_{13}H_{13}N_2I$: C, 48.14; H, 4.01. Found: C, 48.08; H, 4.12.

ind-N-Methyl-δ-carboline (II)

The anhydro-base methiodide (IX) (13.7 mg) was heated at 300–310°/0.15 mm in a microsublimation apparatus. The methiodide decomposed smoothly and practically no residue was left. The condensate was washed off with ether and the ether evaporated to give the demethylated product (6.3 mg; 82% yield) as a colorless oil which crystallized on standing to a colorless solid, m.p. 77.5–78.5°, undepressed on admixture with an authentic specimen (10*a*). The two samples had identical infrared spectra.

pK_a *Determinations*

The titrimetric determinations were carried out by dissolving the methiodides (ca. 26 mg) in carbon-dioxide-free 60% aqueous ethanol (6 ml) and titrating with 0.998 *N* sodium hydroxide. The pH measurements were carried out with a Leeds–Northrup pH meter equipped with micro pH electrodes; the solution being titrated was stirred by means of a magnetic stirrer. The *py-N*-methyl-δ-carboline anhydronium base was similarly titrated with 0.989 *N* sulphuric acid.

The spectrophotometric determinations were carried out by measuring the extinction coefficients of acid, alkaline, and buffered (pH 10.61) solutions of the methiodides at two or more wavelengths.

ACKNOWLEDGMENTS

The authors are indebted to Drs. L. Vining and J. E. Newell for the use of recording ultraviolet spectrophotometers. This work was carried out during the tenure (by (K. A. H. A.) of a Canadian Kodak Fellowship and (by A. D. N.) of the Thorvaldson Scholarship. Financial support from the National Research Council is gratefully acknowledged.

REFERENCES

1. E. SPÄTH and K. EITER. Ber. **73**, 719 (1940).
2. K. EITER. Monatsh. **79**, 17 (1948).
3. K. EITER and A. NEZVAL. Monatsh. **81**, 404 (1950).
4. J. M. GULLAND, R. ROBINSON, J. SCOTT, and S. THORNLEY. J. Chem. Soc. 2924 (1929).
5. E. GELLÉRT, RAYMOND-HAMET, and E. SCHLITTLER. Helv. Chim. Acta, **34**, 642 (1951).
6. R. ROBINSON. Structural relations of natural products. Oxford University Press. 1955. p. 105.
7. A. P. GRAY. J. Am. Chem. Soc. **77**, 5930 (1955).
8. P. A. S. SMITH and J. H. BOYER. J. Am. Chem. Soc. **73**, 2626 (1951).
9. R. A. ABRAMOVITCH. Chem. & Ind. **422** (1957).
10. R. A. ABRAMOVITCH. (*a*) Can. J. Chem. Submitted. (*b*) Unpublished observations.
11. R. A. ABRAMOVITCH, A. D. NOTATION, and GIAM CHOO SENG. Tetrahedron Letters, **8**, 1 (1959).
12. R. A. ABRAMOVITCH and A. D. NOTATION. Can. J. Chem. **38**, 1445 (1960).
13. B. WITKOP. J. Am. Chem. Soc. **75**, 3361 (1953).
14. L. PAOLONI and G. B. MARINI-BETTÒLO. Nature, **179**, 41 (1957).
15. H. SCHWARZ. Experientia, **6**, 330 (1950).
16. R. A. ABRAMOVITCH. Proc. Chem. Soc. 8 (1957).
17. H. SCHWARZ and E. SCHLITTLER. Helv. Chim. Acta, **34**, 629 (1951).
18. I. D. SPENSER. J. Chem. Soc. 3659 (1956).
19. A. E. GILLAM and E. S. STERN. An introduction to electronic absorption spectroscopy in organic chemistry. Edward Arnold & Co., London. 1957. p. 303.
20. L. HORNER. Ann. **540**, 73 (1939).
21. T. K. ADLER and A. ALBERT. J. Chem. Soc. 1794 (1960).

THE PHOTOLYSIS OF DEUTERATED ACETONE AND OF DEUTERATED ACETONE–HYDROGEN MIXTURES[1]

J. F. HENDERSON[2] AND E. W. R. STEACIE

ABSTRACT

The photolyses of acetone, acetone-d_6, and acetone-d_6 – hydrogen mixtures were investigated at 471° K. The rates of formation of methane, ethane, and carbon monoxide and the ratio $R_{methane}/R^{\frac{1}{2}}_{ethane}$ were independent of the fractional amount of acetone which photolyzed, as measured by 100[CO]/[A]$_0$, which was varied from <1% to 18%. When the acetone-d_6 – hydrogen mixtures were photolyzed, $R_{CD_4}/R^{\frac{1}{2}}_{C_2D_6}[A]_0$, $R_{CD_3H}/R^{\frac{1}{2}}_{C_2D_6}[H_2]_0$, and $R_{CD_3H}/R_{CD_4}[A]_0/[H_2]_0$ were observed to be functions of $[A]_0$ and $[H_2]_0$. It is postulated that some of the CD_4 and CD_3H was formed by a reaction between methyl radicals and an excited molecule which contained both C—D and C—H bonds.

INTRODUCTION

The results of many investigations indicate that, during the photolysis of acetone and acetone–hydrogen mixtures, methane and ethane are formed by the following reactions (1, 2, 3, 4, 5):

$$CD_3 + CD_3 \rightarrow C_2D_6, \qquad (a)$$

$$CD_3 + CD_3COCD_3 \rightarrow CD_4 + CD_2COCD_3, \qquad (b)$$

$$CD_3 + H_2 \rightarrow CD_3H + H. \qquad (c)$$

Hence

(i) $$R_{CD_4}/R^{\frac{1}{2}}_{C_2D_6}[A] = k_b/k_a^{\frac{1}{2}},$$

(ii) $$R_{CD_3H}/R^{\frac{1}{2}}_{C_2D_6}[H_2] = k_c/k_a^{\frac{1}{2}},$$

(iii) $$R_{CD_3H}/R_{CD_4}[A]/[H_2] = k_c/k_b.$$

It has been suggested by Long that, in addition to these reactions, methane is formed by reaction between methyl radicals and the ethane formed by step (*a*), and that this reaction is important even when the amount of acetone decomposed is small, e.g. <5% (6). Kutschke and Steacie have summarized evidence which indicates that reaction between methyl radicals and the product ethane is negligible under these conditions (7).

If Long's suggestion were correct, the rate constants calculated by equations (i), (ii), and (iii) would be functions of the length of photolysis. However, in none of the many investigations which have been made has this question been subjected to a detailed experimental test. Consequently, experiments have been carried out here to determine whether these rate constants vary with the extent of decomposition of the acetone.

[1]*Manuscript received July 20, 1960.*
Contribution from the Division of Pure Chemistry, National Research Council, Ottawa, Canada.
Issued as N.R.C. No. 5976.
[2]*National Research Council Postdoctorate Fellow 1957–59. Present address: Polymer Corporation Limited, Sarnia, Ontario.*

EXPERIMENTAL

The apparatus and methods of analysis were similar to those described elsewhere (2). The cracking pattern for CD_3H suggested by McNesby and Gordon was used when determining the isotopic composition of the methane fractions mass spectrometrically (4).

The reaction cell, which was 10 cm in length and 5 cm in diameter (195 cc volume), was filled with a nearly parallel beam of light from B.T.H. ME/D 250-w mercury lamp. The light was filtered either by a Corning filter 9863 in combination with a solution of potassium chromate (filter A) or a Corning filter 7910 (filter B) (8). The light intensity was varied either by neutral density filters or wire gauzes and both gave similar results. In some experiments the light absorption was measured by a photocell placed at the rear of the cell.

Reagent grade acetone (Merck), deuterated acetone (Merck of Canada; 98.2% acetone-d_6 and 1.8% acetone-d_5), and the hydrogen were purified by methods described earlier (2). Perfluoro-*n*-butane (Minnesota Mining and Manufacturing Co.) was outgassed at −160° C.

In a few experiments, the methyl ethyl ketone produced during the photolysis of acetone was analyzed by gas chromatography on a 30-ft column consisting of 30% dinonyl phthalate on firebrick held at 94° C.

The temperature of the reaction cell was controlled by a Fenwal 560 temperature regulator, and the experiments were done at 471±0.5° K.

RESULTS

Deuterated acetone was photolyzed at pressures of 50 mm and 100 mm Hg, and the results are shown in Table I. The extent of the decomposition of the acetone, measured by 100 $[CO]/[A]_0$, was varied over a considerable range, and $R_{CD_4}/R^{\frac{1}{2}}_{C_2D_6}[A]_0$, R_M/R_E, and $(R_M+2R_E)/R_{CO}$ were independent of the conversion except at the very low conversions. It is interesting to note that at a given light intensity the rates of formation of methane, ethane, and carbon monoxide were independent of the length of photolysis. The light absorption, measured in a few experiments, was also independent of time for conversions up to 18%.

To determine more about the decrease in $R_{CD_4}/R^{\frac{1}{2}}_{C_2D_6}[A]_0$ at very low conversions, light acetone at 100 mm Hg was photolyzed, and the results are shown in Fig. 1. When

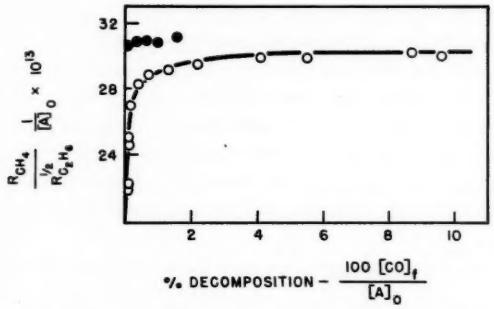

FIG. 1. Variation of $R_{CH_4}/R^{\frac{1}{2}}_{C_2H_6}[A]_0$ with percentage of decomposition of acetone.
○ Analysis by distillation. ● Mass spectrometric analysis.

TABLE I

The photolysis of deuterated acetone

Run	Time, seconds	Molecules/cc sec $\times 10^{-12}$ CO	Methane	Ethane	R_{CD_3H}/R_{CD_4}	$R_{C_2D_5H}/R_{C_2D_6}$	$(R_M/R_E^{\frac{1}{2}})(1/[A]_0)\times 10^{13}$	$(R_{CD_4}/R_{C_2D_6}^{\frac{1}{2}})(1/[A]_0)\times 10^{13}$	R_M/R_E	$100[CO]/[A]_0$
					Filter A					
					(Mean conc. *d*-acetone 1.07×10^{18} molecules/cc)					
32	3600	3.13	1.08	2.17	.0198	.0157	6.87	6.77	.498	1.05
33	5400	2.89	1.02	1.95	.0189	.0163	6.89	6.81	.523	1.47
27	7200	3.31	1.14	2.27	.0203	.0156	7.05	6.99	.502	2.23
31	9000	3.55	1.17	2.46	.0196	.0159	6.96	6.91	.476	2.99
26	10800	3.80	1.22	2.66	.0200	.0158	7.06	6.99	.459	3.87
30	12600	3.21	1.09	2.17	.0195	.0157	6.93	6.85	.502	3.77
25	14400	3.81	1.27	2.68	.0202	.0160	7.23	7.13	.474	5.13
29	16200	3.67	1.20	2.54	.0203		7.06		.472	5.56
28	19800	3.16	1.11	2.15	.0205	.0155	7.07	7.00	.516	5.84
24	21600	3.66	1.20	2.54	.0198	.0140	6.97	6.92	.472	7.31
					(Mean conc. *d*-acetone 2.16×10^{18} molecules/cc)					
3	1800	7.69	3.21	4.76			6.81		.674	.641
5	1800	6.76	2.95	4.12			6.82		.716	.572
6	1800	7.03	3.04	4.17			6.80		.729	.578
21	3600	6.18	2.79	3.68	.0206		6.74		.758	1.04
22	7200	6.10	2.82	3.60	.0201	.0169	6.79	6.73	.783	2.02
24	9000	6.41	2.99	3.74	.0310	.0163	6.95	6.87	.799	2.62
20	10800	5.97	2.78	3.57		.0172	6.90		.779	3.03
					(Mean conc. *d*-acetone 2.16×10^{18} molecules/cc)					
12	12600	7.07	3.20	4.28		.0166	6.97		.748	4.01
19	14400	6.05	2.85	3.60	.0196	.0169	6.99	6.90	.792	4.05
18	18000	6.66	2.97	3.97	.0198	.0153	6.97	6.89	.748	5.61
17	21600	5.84	2.68	3.40	.0206	.0150	6.87	6.78	.788	5.95
					Filter B					
					(Mean conc. *d*-acetone 1.48×10^{18} molecules/cc)					
63	1920	10.6	2.84	8.07	.0216	.0141	6.75	6.66	.460	2.84
					(Mean conc. *d*-acetone 2.13×10^{18} molecules/cc)					
85	300	9.53	3.28	6.74			5.93		.487	.134
82	300	9.43	3.15	6.77			5.98		.465	.139
83	450	9.92	3.62	6.74			6.54		.537	.210
81	600	10.5	3.73	7.21			6.51		.517	.295
75	600	13.4	4.19	9.77	.0237	.0157	6.23	6.14	.429	.375
65	1320	14.6	4.68	10.3	.0212	.0154	6.84	6.73	.454	.898
78	1800	10.9	4.06	7.31	.0241		6.98		.555	.916
76	3600	8.60	3.47	5.46	.0216	.0148	6.97	6.90	.636	1.45
51	3600	16.2	4.94	11.7	.0247	.0174	6.83	6.77	.422	2.74
53	7200	15.9	4.93	11.7	.0213	.0174	6.76	6.79	.421	5.37
					(Mean conc. *d*-acetone 2.13×10^{18} molecules/cc)					
69	9000	13.9	4.53	9.67	.0209	.0170	6.84	6.76	.468	5.86
52	10800	18.2	5.31	13.4	.0213	.0152	6.81	6.72	.396	9.21
68	19800	13.3	4.42	9.09	.0208	.0155	6.87	6.81	.486	12.3
56	18000	15.3	4.79	10.9	.0205	.0151	6.81	6.77	.439	13.0
55	21600	17.7	5.21	12.7	.0209	.0149	6.83	6.73	.410	17.8

the mixtures of methane, ethane, and carbon monoxide were analyzed by distillation, $R_{CH_4}/R_{C_2H_6}^{\frac{1}{2}}[A]_0$ decreased rapidly at low conversions, but this was not observed when these mixtures were analyzed by mass spectrometric analyses. It is concluded that a small but constant amount of methane was being occluded in the solid nitrogen trap

used to separate methane and carbon monoxide from ethane by distillation, and at low conversions this was appreciable relative to the total yields of methane and ethane. The amount of methane occluded varied with the temperature of the solid nitrogen. Recently similar observations were made elsewhere (9).

A few experiments were done in which the methyl ethyl ketone produced during the photolysis of acetone was determined, and the results (Table II) agree with those of Mandelcorn and Steacie (10).

TABLE II

The formation of methyl ethyl ketone during the photolysis of acetone

Run	Time, seconds	Molecules/cc sec $\times 10^{-12}$ CO	Methane	Ethane	MEK	$\frac{R_M + R_{MEK} + 2R_E}{2R_{CO}}$	$\frac{R_{CH_4}}{R_{C_2H_6}^{\frac{1}{2}}}$	$\frac{1}{[A]_0}$	$\frac{100[CO]}{[A]_0}$
		(Conc. acetone 2.13×10^{18} molecules/cc)							
108	1320	14.3	12.4	4.03	7.17	0.93		29.0	.886
106	4500	11.3	10.8	2.95	6.14	0.98		29.5	2.38
105	10800	10.8	10.6	2.79	5.33	0.96		29.8	5.48
103	14400	12.9	12.1	3.54	5.83	0.94		30.2	8.70

Mixtures of deuterated acetone and hydrogen at pressures of 100 mm Hg and 50 mm Hg, respectively, were photolyzed, and the results are shown in Table III. The two

TABLE III

The photolysis of deuterated acetone in the presence of hydrogen

Run	Time, seconds	Molecules/cc sec $\times 10^{-12}$ CO	Methane	Ethane	$\frac{R_{CD_3H}}{R_{CD_4}}$	$\frac{R_{C_2D_5H}}{R_{C_2D_6}}$	$\frac{(R_{CD_4}/R_{C_2D_6}^{\frac{1}{2}})}{(1/[A]_0) \times 10^{13}}$	$\frac{(R_{CD_3H}/R_{C_2D_6}^{\frac{1}{2}})}{(1/[H_2]_0) \times 10^{13}}$ Method I	Method II	$\frac{R_M}{R_E}$	$\frac{100[CO]}{[A]_0}$
						Filter A					
		(Mean conc. *d*-acetone 2.15×10^{18} molecules/cc; mean conc. hydrogen 1.02×10^{18} molecules/cc)									
40	1800	4.54	4.88	1.64	1.63	.0186	6.78	23.3	23.4	2.98	.390
39	3600	4.62	5.12	1.54	1.66	.0132	7.28	26.3	25.3	3.32	.770
38	5400	4.69	5.23	1.43	1.72	.0214	7.55	27.8	26.4	3.66	1.18
35	7200	4.89	5.28	1.65	1.82	.0192	7.15	26.4	25.8	3.20	1.76
45	9000	5.45	5.85	1.82	1.68	.0223	7.60	28.2	26.7	3.21	2.27
42	10800	4.99	5.50	1.73	1.72	.0237	7.23	26.3	25.5	3.18	2.51
43	14400	4.31	4.79	1.36	1.68	.0226	7.22	26.3	25.4	3.52	2.89
46	16200	4.66	5.03	1.56	1.73	.0263	6.97	25.7	25.1	3.22	3.52
44	18000	4.62	5.10	1.48	1.72	.0278	7.29	26.5	25.5	3.45	3.87
41	19800	4.64	5.06	1.50	1.70	.0274	7.23	26.1	25.2	3.37	4.27
37	21600	4.85	5.02	1.54	1.71	.0267	7.06	25.0	24.7	3.26	4.87
						Filter B					
61	3600	17.2	12.7	8.81	1.66	.0195	7.56	27.7	26.1	1.44	2.87
49	7200	17.3	12.8	8.73	1.68	.0222	7.57	28.1	26.6	1.47	5.76
60	11040	15.8	11.9	7.91	1.69	.0235	6.75	27.3	27.5	1.50	8.09
57	14460	14.7	11.7	7.12		.0247		28.8		1.64	9.86
50	14400	18.8	13.9	10.0	1.71	.0267	7.66	28.9	27.3	1.39	12.6
59	21660	16.5	12.7	8.57	1.66	.0300	7.70	28.4	26.6	1.48	16.6

procedures called methods I and II for calculating $R_{CD_3H}/R^{\frac{1}{2}}_{C_2D_6}[H_2]_0$ are the same as those used by Whittle and Steacie (2). The formation of CD_3H was determined either by using results obtained when deuterated acetone was photolyzed alone (method I) or by mass spectrometric analyses of the methane fractions (method II). The CD_3H arising from the small amount of acetone-d_5 present in the deuterated acetone was evaluated by equation (iv) and subtracted from the total CD_3H formed

$$\text{(iv)} \qquad R_{CD_3H}/R^{\frac{1}{2}}_{C_2D_6} = 0.014[A]_0 \times 10^{-12}(\text{molecules/cc})^{\frac{1}{2}}\ \text{sec}^{-\frac{1}{2}}.$$

No CD_2H_2 could be detected.

The values of $R_{CD_4}/R^{\frac{1}{2}}_{C_2D_6}[A]_0$, $R_{CD_3H}/R^{\frac{1}{2}}_{C_2D_6}[H_2]_0$, R_{CD_3H}/R_{CD_4}, R_M/R_E, and $(2R_E+R_M)/R_{CO}$ were independent of the fraction of the acetone that was photolyzed, and again the rates of formation of methane, ethane, and carbon monoxide were independent of conversion. The addition of hydrogen to deuterated acetone caused the ratio $R_{C_2D_5H}/R_{C_2D_6}$ to increase very slightly.

In both the presence and absence of hydrogen the formation of methane and ethane during the photolysis of deuterated acetone was linear in the carbon monoxide produced (Fig. 2).

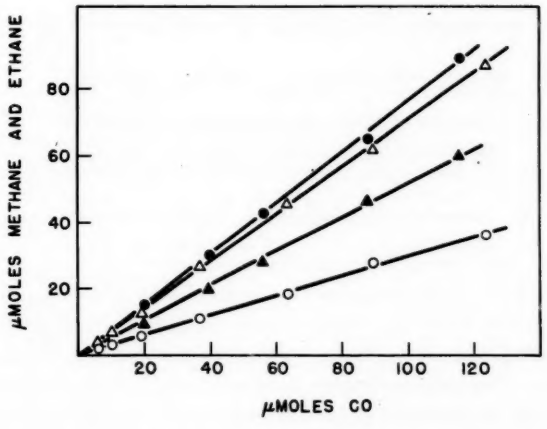

FIG. 2. Variation of the yields of methane and ethane with carbon monoxide.
○ CD_4 from 100 mm Hg *d*-acetone. △ C_2D_6 from 100 mm Hg *d*-acetone.
● Methane from 100 mm Hg *d*-acetone and 50 mm Hg hydrogen.
▲ Ethane from 100 mm Hg *d*-acetone and 50 mm Hg hydrogen.

It is interesting to note that in the presence of hydrogen $R_{CD_4}/R^{\frac{1}{2}}_{C_2D_6}[A]_0$ and $R_{CD_3H}/R^{\frac{1}{2}}_{C_2D_6}[H_2]_0$ but not R_{CD_3H}/R_{CD_4} depended on the light intensity. Experiments were made to investigate this effect in more detail, and the results are shown in Figs. 3 and 4. At zero light intensity, differences between the results calculated by methods I and II became very small.

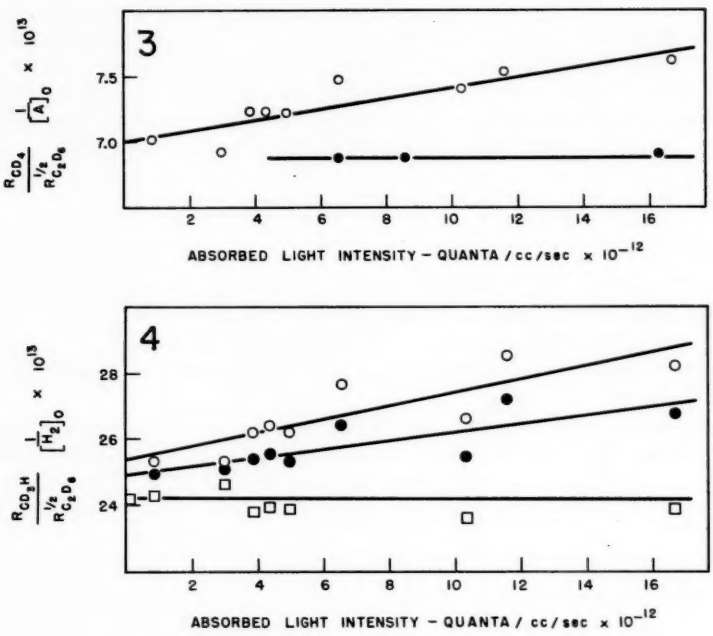

FIG. 3. Variation of $R_{CD_4}/R^{\frac{1}{2}}_{C_2D_6}[A]_0$ with light intensity.
● 100 mm Hg *d*-acetone.
○ 100 mm Hg *d*-acetone and 50 mm Hg hydrogen.

FIG. 4. Variation of $R_{CD_3H}/R^{\frac{1}{2}}_{C_2D_6}[H_2]_0$ with light intensity.
○ Method I. ● Method II.
□ $(R_{CD_3H}/R_{CD_4})\,([A]_0/[H_2]_0)\times 6.83\times 10^{-13}$.

Some experiments were carried out to determine the variations, if any, of $(R_{CD_4}/R^{\frac{1}{2}}_{C_2D_6})(1/[A]_0)$, $R_{CD_3H}/R^{\frac{1}{2}}_{C_2D_6}[H_2]_0$, and $(R_{CD_3H}/R_{CD_4})\,([A]_0/[H_2]_0)$ with the pressures of deuterated acetone and hydrogen. The results, shown in Figs. 5, 6, and 7, are rather surprising. Although the photolysis of deuterated acetone alone was not affected by the addition of perfluoro-*n*-butane, both $R_{CD_4}/R^{\frac{1}{2}}_{C_2D_6}[A]_0$ and $R_{CD_3H}/R^{\frac{1}{2}}_{C_2D_6}[H_2]_0$ were decreased when this substance was added to the deuterated acetone–hydrogen mixtures.

In one experiment, following the photolysis of deuterated acetone alone, about 50 mm Hg of hydrogen was added to the system, and it was shown that this had no effect on the analyses of the methane and ethane.

DISCUSSION

The object of this investigation, as mentioned earlier, was to determine the importance of the reaction between methyl radicals and the ethane produced during the photolysis of acetone or acetone–hydrogen mixtures.

If this reaction were important, then, $R_{CD_4}/R^{\frac{1}{2}}_{C_2D_6}[A]_0$, $R_{CD_3H}/R^{\frac{1}{2}}_{C_2D_6}[H_2]_0$, R_M/R_E, and

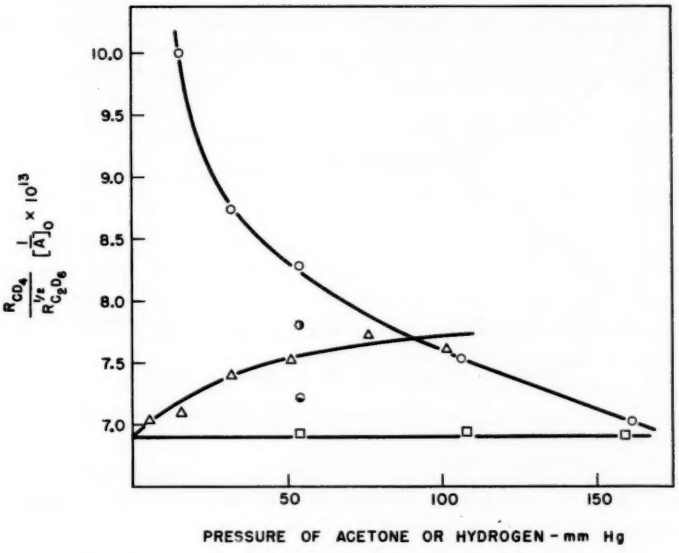

FIG. 5. Variation of $R_{CD_4}/R^{\frac{1}{2}}_{C_2D_6}[A]_0$ with *d*-acetone, hydrogen, and perfluoro-*n*-butane pressure.

○ 50 mm Hg hydrogen, *d*-acetone pressure varied.
△ 100 mm Hg *d*-acetone, hydrogen pressure varied.
□ 100 mm Hg *d*-acetone, perfluoro-*n*-butane pressure varied.
◑ 50 mm Hg *d*-acetone, 50 mm Hg hydrogen, and 50 mm Hg perfluoro-*n*-butane.
◒ 50 mm Hg *d*-acetone, 50 mm Hg hydrogen, and 150 mm Hg perfluoro-*n*-butane.

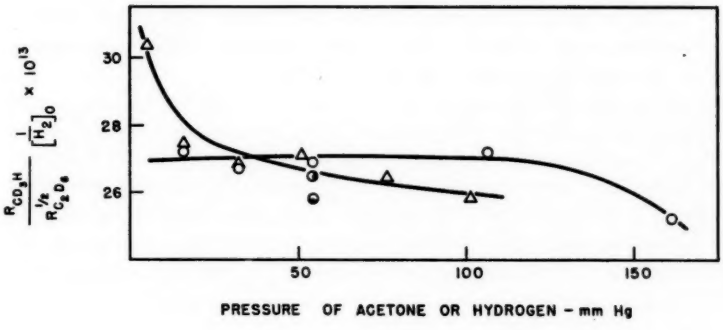

FIG. 6. Variation of $R_{CD_3H}/R^{\frac{1}{2}}_{C_2D_6}[H_2]_0$ with *d*-acetone, hydrogen, and perfluoro-*n*-butane pressure.

○ 50 mm Hg hydrogen, *d*-acetone pressure varied.
△ 100 mm Hg *d*-acetone, hydrogen pressure varied.
◑ 50 mm Hg *d*-acetone, 50 mm Hg hydrogen, and 50 mm Hg perfluoro-*n*-butane.
◒ 50 mm Hg *d*-acetone, 50 mm Hg hydrogen, and 150 mm Hg perfluoro-*n*-butane.

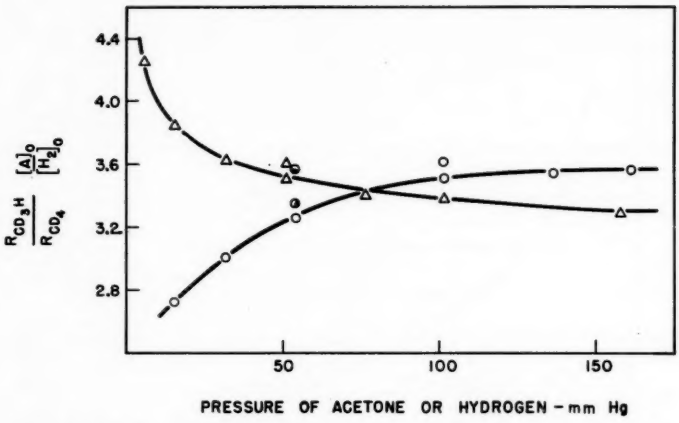

FIG. 7. Variation of R_{CD_3H}/R_{CD_4} $[A]_0/[H_2]_0$ with *d*-acetone, hydrogen, and perfluoro-*n*-butane pressure.
○ 50 mm Hg hydrogen, *d*-acetone pressure varied.
△ 100 mm Hg *d*-acetone, hydrogen pressure varied.
◑ 50 mm Hg *d*-acetone, 50 mm Hg hydrogen and 50 mm Hg perfluoro-*n*-butane.
◒ 50 mm Hg *d*-acetone, 50 mm Hg hydrogen, and 150 mm Hg perfluoro-*n*-butane.

R_{CD_3H}/R_{CD_4} in all probability would have been functions of the length of photolysis, but this was not observed. Furthermore, in the presence of hydrogen, a larger yield of C_2D_5H than was found would be expected due to the reaction of C_2D_5 radicals with hydrogen. Finally, the linear relations between both the methane and ethane and the carbon monoxide produced (Fig. 2) would not have been observed.

Both these observations and the evidence already summarized (7) make it apparent that this reaction of methyl radicals with the ethane, though possible under certain conditions, is negligible when the decomposition of the acetone is small.

It is difficult to discuss the observed independence of the absorbed light intensity and of the rates of formation of methane, ethane, and carbon monoxide with time as the length of photolysis was increased. Very many reactions become possible at the larger conversions due to the accumulation of products.

It is apparent that the results observed during the photolysis of the deuterated acetone–hydrogen mixtures are not predicted by reactions (*a*), (*b*), and (*c*) alone. The fact that the ratio (R_{CD_3H}/R_{CD_4}) $([A]_0/[H_2]_0)$ varies with $[H_2]_0$ and $[A]_0$ but is independent of conversion suggests that the anomalous behavior cannot be ascribed entirely to the production of ethane by a reaction other than (*a*) or by the consumption of ethane by radical attack. Consequently, it is postulated that appreciable amounts of methane were formed by reactions in addition to (*b*) and (*c*), and equations (i) and (ii) should be rewritten as follows:

$$(v) \qquad (R_{CD_4}/R_{C_2D_6}^{\frac{1}{2}})_{meas} = (k_b/k_a^{\frac{1}{2}})[A]_0 + (R_{CD_4}/R_{C_2D_6}^{\frac{1}{2}})_{excess},$$

$$(vi) \qquad (R_{CD_3H}/R_{C_2D_6}^{\frac{1}{2}})_{meas} = (k_c/k_a^{\frac{1}{2}})[H_2]_0 + (R_{CD_3H}/R_{C_2D_6}^{\frac{1}{2}})_{excess}.$$

Although neither $(R_{CD_4}/R_{C_2D_6}^{\frac{1}{2}})_{excess}$ nor $(R_{CD_3H}/R_{C_2D_6}^{\frac{1}{2}})_{excess}$ could be estimated with high

precision, they were found to be approximately equal in all the experiments and tended to zero at zero light intensity, zero hydrogen pressure, and infinite acetone pressure.

To account for these observations it is proposed that the excess methane was produced by reaction of methyl radicals with an activated molecule X* which was formed by a reaction involving hydrogen atoms, and this contained both C—H and C—D bonds.

$$CD_3 + X^* \rightarrow CD_4 + R \qquad (d)$$

$$\rightarrow CD_3H + R' \qquad (e)$$

$$X^* + M \rightarrow X + M \qquad (f)$$

If the reactivities of both hydrogen atoms and methyl radicals toward acetone are similar, some hydrogen atoms would be available for combination with methyl and acetonyl radicals to form CD_3H^* and $CD_3COCD_2H^*$. Very little quantitative information is available for the reaction between hydrogen atoms and acetone, but it can be shown that hydrogen atoms are about 10 times more reactive toward ethane at 471° K than are methyl radicals (11, 12). If CD_3H^* is unlikely because of the rapidity of

$$H + CD_3COCD_3 \rightarrow HD + CD_2COCD_3$$

then the formation of $CD_3COCD_2H^*$ must be rejected for a similar reason. On the other hand, if CD_3H^* and $CD_3COCD_2H^*$ are formed, it is likely that they would be partially stabilized very rapidly though it is possible that many collisions (10^6) may be required before they are deactivated to their ground vibrational states (13).

If X* represents an excited molecule of CD_3H, reaction (*d*) would give rise to CD_2H radicals, and some would undoubtedly combine with CD_3 radicals to form C_2D_5H. It was observed, however, that although $(R_{CD_4}/R^{\frac{1}{2}}_{C_2D_6})_{excess}$ was independent of the conversion and increased with increasing light intensity, the small yield of C_2D_5H increased with increasing conversion and decreased with increasing light intensity. Furthermore, due to reaction (*f*) the addition of a third body to the reaction mixture would cause the ratio $(R_{CD_3H}/R^{\frac{1}{2}}_{C_2D_6})_{excess}/(R_{CD_4}/R^{\frac{1}{2}}_{C_2D_6})_{excess}$ to increase and this was not observed.

On the other hand, if X* represents an excited molecule of $CD_3COCD_2H^*$ the observed kinetics are predicted. However, more direct evidence is required before it will be possible to identify the excited molecule X* with any degree of certainty.

The formation of some such excited molecule during the photolysis of acetone–hydrogen mixtures will account for the observations made here. It also suggests an explanation for the differing values obtained here, and earlier (1, 2), by methods I and II for the rate constant for the reaction of methyl radicals with hydrogen. Such an explanation could also account for the lowering of the apparent value of the activation energy of the reaction of methyl radicals with acetone as observed by Whittle and Steacie (2) for the two systems, acetone-d_6 – hydrogen and acetone–deuterium. It is possible that for the same reason the activation energies reported for the reaction of methyl radicals with hydrogen are slightly low, for example, by about 1 kcal/mole.

ACKNOWLEDGMENTS

We wish to thank Drs. K. O. Kutschke and K. J. Laidler for their interest in this work, Mrs. R. H. Riem for the mass spectrometric analyses, and Mr. R. Pilon for the gas chromatographic analyses.

REFERENCES

1. T. G. MAJURY and E. W. R. STEACIE. Can. J. Chem. **30**, 800 (1952).
2. E. WHITTLE and E. W. R. STEACIE. J. Chem. Phys. **21**, 993 (1953).
3. J. R. MCNESBY, A. S. GORDON, and S. R. SMITH. J. Am. Chem. Soc. **78**, 1287 (1956).
4. J. R. MCNESBY and A. S. GORDON. J. Am. Chem. Soc. **76**, 1416 (1954).
5. E. W. R. STEACIE. Atomic and free radical reactions. Reinhold Publishing Corp., New York. 1954.
6. L. H. LONG. J. Phys. Chem. **61**, 821 (1957).
7. K. O. KUTSCHKE and E. W. R. STEACIE. J. Phys. Chem. **62**, 866 (1958).
8. M. KASHA. J. Opt. Soc. Am. **38**, 929 (1948).
9. J. HEICKLEN and W. A. NOYES, JR. J. Am. Chem. Soc. **81**, 3858 (1959).
10. L. MANDELCORN and E. W. R. STEACIE. Can. J. Chem. **32**, 79 (1954).
11. M. R. BERLIE and D. J. LE ROY. Discussions Faraday Soc. No. 14, **50** (1953).
12. J. R. MCNESBY and A. S. GORDON. J. Am. Chem. Soc. **77**, 4719 (1955).
13. B. H. MAHON. J. Phys. Chem. **62**, 100 (1958).

SOME DEUTERIUM KINETIC ISOTOPE EFFECTS

IV. β-DEUTERIUM EFFECTS IN WATER SOLVOLYSIS OF ETHYL, ISOPROPYL, AND *tert*-BUTYL COMPOUNDS[1]

K. T. LEFFEK,[2] J. A. LLEWELLYN,[2] AND R. E. ROBERTSON

ABSTRACT

The secondary β-deuterium isotope effects have been measured in the water solvolytic reaction of alkyl halides and sulphonates for primary, secondary, and tertiary species. In every case the kinetic isotope effect was greater than unity ($k_H/k_D > 1$). This isotope effect may be associated with varying degrees of hyperconjugation or altered non-bonding intramolecular forces. The experiments make it difficult to decide which effect is most important.

As an extension of our work (1, 2, 3) on deuterium kinetic isotope effects we have measured the kinetic consequences of β-deuteration for a series of compounds solvolyzing in water,

$$RX + H_2O \rightarrow ROH + H^+ + X^- . \qquad [1]$$

The kinetic effect produced by substituting deuterium for β-hydrogen in molecules undergoing solvolytic substitution has been studied by Shiner (4, 5, 6), Lewis *et al.* (7, 8, 9), Streitwieser *et al.* (10), and others (11, 12, 13). This paper presents a survey for a series of alkyl halides and sulphonates and the results of these measurements have been collected in Table I.

DISCUSSION

It will be noted that in all cases the deuterated compounds react more slowly than their protium analogues, the magnitude of the total isotope effect increasing both absolutely and relatively as the transition state becomes more ionic. Thus the effect of deuteration for a given alkyl group is greater in the sulphonates than for the halides and increases with increasing α-methylation. Since some of the compounds have been extensively deuterated, it will be necessary to consider as sources of the observed isotope effect not only those factors involved in the activation process contributing to changes in the zero-point energy such as changes in hyperconjugation and non-bonded interaction but also the consequence of mass increase. This factor has been discussed by us in an earlier paper as a "thermodynamic" effect involving changes in translational and rotational properties which affect the thermodynamic properties of the molecule independently of the zero-point energy shifts.

"Thermodynamic" Factors

Although a detailed evaluation of these elements is not yet possible, the relative values of k_H/k_D evident in Table I provide a basis for a semiquantitative discussion of the importance of possible contributors to the deuterium isotope effect.

[1]*Manuscript received August 4, 1960.*
Contribution from the Division of Pure Chemistry, National Research Council, Ottawa, Canada. Presented in part at the Chemical Institute of Canada Meeting in Ottawa, June 1960.
Issued as N.R.C. No. 5969.
[2]*National Research Council Postdoctorate Fellow.*

TABLE I

Secondary β-deuterium isotope effects in the water solvolysis of some alkyl compounds

Compound	$10^4\ k_H$ (sec^{-1})	$10^4\ k_D$ (sec^{-1})	Temp., ° C	k_H/k_D
Ethyl *p*-toluenesulphonate	3.480	3.420	59.93_5	1.01_8
Ethyl methanesulphonate	1.958	1.907	60.00_0	1.02_7
Ethyl bromide	2.722	2.636	80.00_1	1.03_3
Ethyl iodide	1.554	1.499	80.00_0	1.03_7
Isopropyl *p*-toluenesulphonate	7.664	4.942	30.00_1	1.55_1
Isopropyl methanesulphonate	3.686	2.386	30.00_1	1.54_5
Isopropyl bromide	3.448	2.580	59.93_2	1.33_6
Isopropyl iodide	3.125	2.380	60.00_2	1.31_3
t-Butyl chloride	9.860	3.840	2.07_0	2.56_8

In order to consider these effects, it is necessary to postulate models for initial and transition states of reaction. Obviously there is scope for considerable conjecture here, and it appears advisable to set limits where possible by oversimplification, and thereby obtain maximum values. For these reactions, the C—X bond (X represents the leaving group) is undoubtedly stretched almost to breaking; the number and role of the water molecules in the transition state form a field for speculation. Consider first translational changes: a simple ionization with no water involved and bond stretching in the transition state would have zero translational contribution to the isotope effect. For an extensively solvated transition state and an unsolvated initial state (almost as unrealistic a model as the first (14)), the translational differences will approximate to those in the initial state. This contribution will tend to slow the reaction for the heavy compound and a maximum value of about 86 cal/mole ($\Delta F_H^{\ddagger} - \Delta F_D^{\ddagger}$) can be calculated for *tert*-butyl chloride at 273° K. Initial-state solvation, which is undoubtedly important in these reactions, will serve to reduce this effect considerably. Rotational changes may be considered for similar models. Simple C—X extension if carried sufficiently far might produce an inverse effect ($k_H/k_D < 1$) by displacing the center of gravity in a direction away from the site of isotopic substitution. For more complicated models the expression for the rotational contribution (eq. 2) may be examined as follows in order to assess its maximum contribution

$$[2] \qquad k_H/k_D(\text{rotation}) = \left[\frac{\Pi I_D}{\Pi I_H}\frac{\Pi I_H^{\ddagger}}{\Pi I_D^{\ddagger}}\right]^{\frac{1}{2}}.$$

The maximum value for the second factor in the square bracket (referring to the transition state) is unity. Such a condition would exist for a massive, highly solvated transition state when deuteration made a negligible contribution to the mass. Thus the maximum value of the rotational contribution is now dependent on the ratio of the initial-state terms to the one-half power so that in case of a doubling of this inertial product by deuteration the maximum rotational isotope effect would be $k_H/k_D = \sqrt{2}$. Rough estimates for *t*-butyl and isopropyl halides indicate smaller effects which would again be further reduced by initial-state solvation. If rotational contributions were important, a decrease in isotope effect would be expected to follow substitution of toluenesulphonate for a halide as leaving group. Such changes do occur for the ethyl compounds, suggesting that inertial changes cannot be neglected. For the *n*-propyl series (3), and more particularly for higher members of the α-methylated series, such a change in the leaving group produces an increase in k_H/k_D, which becomes more marked as the transition state becomes more ionic indicating that other more powerful factors are determining the larger isotope effects.

As usual we neglect the thermodynamic contribution from vibrations in comparison with the zero-point energy change coming from the same source.

Zero-Point Effects

The factors involved here may be conveniently considered in three groups.

Protium–Deuterium

(a) Inductive and Hyperconjugative Differences

Halevi and co-workers have focussed attention on the fact that the mean lengths of bonds to hydrogen and deuterium are different (15). This arises as a consequence of effect of a lower ground-state potential energy for the deuterium-containing molecule, allied with the asymmetry of the potential surface describing the energy of the molecule with respect to displacements of the atoms in bond-stretching and bond-shortening directions. Since the potential surface rises more steeply for bond shortening, the mean positions of atoms for a molecule in a given vibrational state will correspond to increasing bond distances as the energy of the state increases, so that the lower potential energy deuterium compound will have effectively shorter bonds than the protium compound. As a consequence of this altered bond length, dipolar and other interactions will be altered and the behavior of C—H bonds and C—D bonds with respect to inductive and hyperconjugative effects will be different, quite apart from the consequences of altered vibrations produced by the activation process.* From experiment (16, 17, 18, 19) Halevi deduces that hyperconjugative electron release is reduced in the CD_3 group, whereas inductive release is increased in the CD_3 group, compared with the CH_3 group. It might therefore be expected that these differences would be most marked where charge separations are greatest, and vice versa. Our experiments show that the magnitude of the isotope effect k_H/k_D increases in cases where the electron deficiency is expected to be greater and hyperconjugation more powerful.

(b) Non-bonding Interactions

As a consequence of the isotopic alteration in bond length there will be differences in non-bonding forces in the two species (20) but there are other larger changes which might produce zero-point variations (3). Almost all activation processes produce alterations in the molecular geometry and the hydrolyses which have been examined involve changes in the position of the leaving group, the possible insertion of the nucleophile, and the movement of three of the groups attached to the reaction-center carbon atom from tetrahedral positions to something approaching coplanarity. This latter movement will affect intramolecular non-bonded forces between β-hydrogen atoms. If we compare the geometry about the tertiary carbon atom in *tert*-butyl chloride (21, 22, 23) with that about the central carbon in a coplanar carbonium ion we find the methyl groups are about 12% farther apart (as measured by the separation of their respective carbon atoms) even when 0.05 Å is allowed for the bond contraction for C—C sp^3–sp^2 bonding (24) in the transition state. When the high inverse power expressions for non-bonding repulsions are applied to this change in separation, it is obvious that forces affecting vibrations may be considerably reduced. The magnitude of this reduction will depend on other modifying factors such as the proximity of the nucleophile and the leaving group and it is interesting to note the qualitative inverse relationship between the

**This aspect of the secondary deuterium isotope effect has been criticized by Weston (Tetrahedron, 6, 31 (1959)), who showed that isotopic perturbation of the potential energy hypersurface is negligible. Since Halevi considers that these effects (difference in bond lengths) arise in the lowest vibrational state as a result of anharmonicity, the isotopic invariance of the potential energy hypersurface will still be consistent with his hypothesis.*

magnitude of k_H/k_D and the expected proximity of these groups, with k_H/k_D per D greatest for that system which of those examined best fits the $S_N I$ case with decreasing values as this description becomes increasingly less apt and the transition state becomes more crowded.

(c) Hyperconjugative Effects

The work of Lewis and Shiner and their respective groups has established that substitution of D for H in hyperconjugative positions usually produces kinetic isotope effects. The weakening of the C—H link, which is represented in valence bond theory by the contribution of non-bonded structures to the hybrid, is thought to decrease zero-point energy by facilitating the vibrations which involve relative extensive movement of β-hydrogens. The isotope effects which we have observed are consistent with such a hypothesis. The direction of the effect and its order of magnitude are in agreement with previous work in other solvents, e.g. 2-pentyl-βd_5 bromide and *p*-toluenesulphonate solvolyzing in formic acid have isotope rate ratios k_H/k_D 1.39 and 1.69, respectively (7), which can be composed with our values for isopropyl-βd_6 bromide ($k_H/k_D = 1.34$) and *p*-toluenesulphonate ($k_H/k_D = 1.54$) solvolyzing in water. For tertiary compounds a comparison may be made between *t*-amyl-βd_3 chloride solvolyzing in 80% aqueous alcohol with a rate ratio $k_H/k_D = 2.35$ (4) and *t*-butyl-βd_9 chloride solvolyzing in water ($k_H/k_D = 2.57$). The larger β-deuterium isotope effects in formic acid are consistent with the expectation that ionization was more advanced at the transition state in formic acid than in H_2O where some degree of nucleophilic interaction between oxygen and the reactive carbon will be expected, even for the isopropyl compounds. Although water is a better ionizing medium than 80% ethanol it is not possible to decide whether the small increase in k_H/k_D observed by us is to be attributed to increased charge development in the transition state or some other solvation effect. Experimental temperature differences will also make a minor contribution.

The increase in the stability of carbonium ions along the series ethyl, isopropyl, *tert*-butyl is usually associated with an increase in both the inductive and hyperconjugative effects. The expected increase in the β-deuterium isotope effect from ethyl to *tert*-butyl as a consequence of the increase in hyperconjugation is exemplified by the k_H/k_D rate ratios for ethyl and isopropyl bromide and *tert*-butyl chloride, which are 1.03_3, 1.33_6, and 2.56_8 respectively. Differences in the rate ratios are also found when the ease of formation of the carbonium ion is altered by changing the anionic group. Thus, isopropyl methanesulphonate, which is considered to be more easily ionized than the bromide, has a rate ratio $k_H/k_D = 1.54_5$ compared with 1.33_6 for the bromide.

In a discussion of the β-deuterium isotope effect in solvolysis the possible occurrence of an olefin-forming elimination reaction accompanying substitution must be examined. Where the mechanism of the reaction is such that the formation of the olefin takes place after the transition state (e.g. *tert*-butyl chloride) olefin production will not affect the k_H/k_D ratio. However, for reactions where this is not so (E_2) the elimination reaction would exhibit a primary deuterium isotope effect with a rate ratio k_H/k_D of the order of 4 to 6, since an isotopically substituted β-C—H bond is breaking. This would affect the measured k_H/k_D ratio to an extent depending on what fraction of the total reaction was elimination. We have measured the percentage of elimination occurring in the solvolysis of the compounds studied. These results are shown in Table II.

Even in the case of the ethyl compounds where the β-deuterium isotope effects are small, the amount of elimination which takes place concurrently with substitution is insufficient to account for the observed k_H/k_D values.

TABLE II

Olefin formation in the solvolysis in water of some alkyl compounds

Compound	Reaction time, hours	Temp., °C	% Olefin formed
Ethyl *p*-toluenesulphonate	1	100	<0.2
Ethyl methanesulphonate	1	100	~0.0
Ethyl bromide	1	100	~0.0
Ethyl iodide	1	100	<0.3
Isopropyl *p*-toluenesulphonate	16	60	2.5±0.2
Isopropyl methanesulphonate	16	60	0.7±0.2
Isopropyl bromide	16	60	0.7±0.1
Isopropyl iodide	16	60	1.5±0.2
t-Butyl chloride	<1	25	2.9±0.2

The most commonly accepted theoretical mechanism for hyperconjugation is the treatment due to Mulliken *et al.* (25), although an alternative model has been set up by Kreevoy and Eyring (26) which these authors call α-hydrogen bonding. Application of this latter model to β-deuterium isotope effects would require an interaction between the β-hydrogen orbital and the developing p orbital on the electron deficient α-carbon atom. One advantage of this treatment is its ability to explain the greater effectiveness of hydrogen in hyperconjugation as compared with carbon–carbon hyperconjugation. With this model the reduction in β-hydrogen vibration frequencies on activation can occur for bending modes and is therefore in harmony with Streitwieser's treatment of β-deuterium isotope effects (10). Kreevoy and Eyring have pointed out (26) that their model for hyperconjugation is closely related to neighboring group participation as described by Winstein and co-workers (27). Neighboring hydrogen participation, however, only occurs in situations favoring skeletal rearrangement of the reacting molecule whereas α-hydrogen bonding is much more widespread, does not involve rearrangement, and gives smaller effects.

Thus, although it is not possible to choose between Mulliken's model for hyperconjugation and that of Kreevoy and Eyring from the measurement of β-deuterium isotope effects, the latter is attractive in that it is able to link qualitatively the two fields of hyperconjugative effects and neighboring group participations.

CONCLUSION

It appears that hyperconjugative and non-bonding interactions are the principal sources of these isotope effects, with small modifications arising from rotational–translational inertia changes. The role of non-bonding interactions ("intramolecular van der Waals forces" (2, 3)) has been discussed by Bartell (20) and he has shown that they can be sufficiently large to account for a major portion of the observed effects. As far as hyperconjugation is concerned the relationships are largely qualitative since no calculations appear to have been made which would even establish the order of magnitude of the consequences of hyperconjugation on isotope effects. Despite this the evidence is moderately convincing (29), isotope rate effects usually being observed for hyperconjugative sites of substitution with magnitudes varying in the way which would be expected from considerations of hyperconjugative change. The jump in isotope effect observed on passing from an isotopically substituted group on the para position of an aromatic ring to a site adjacent to the reaction center (5, 28) seems large even allowing for the damping action of the ring. This may represent the effect of changing non-bonded forces arising

from the change from tetrahedral to trigonal configuration, which will be insignificant for the para position compared with that for the site adjacent to the reaction center. For the particular effects described in this paper it is difficult to decide which contribution is greater, hyperconjugation or intramolecular van der Waals forces, but undoubtedly both are present and make the major contribution to the isotopic rate change.

EXPERIMENTAL

Ethyl-βd_3 alcohol was prepared by a lithium aluminum hydride reduction of acetic-βd_3 acid (30). The redistilled product, boiling range 79.5–81.5° C, was converted to ethyl-βd_3 *p*-toluenesulphonate by reaction with *p*-toluenesulphonyl chloride in dry pyridine (31). The crude ester (m.p. 30.6° C) was purified by distillation under a vacuum. A comparison of the N.M.R. spectrum of this compound with that of an undeuterated sample indicated that the β-carbon atom was fully deuterated.

Ethyl-βd_3 iodide, bromide, and methanesulphonate were made from the *p*-toluenesulphonate by the methods previously described for the corresponding ethyl-αd_2 compounds (2).

Isopropyl-βd_6 alcohol was obtained by the reduction of acetone-βd_6 with lithium aluminum hydride (32). The crude product was redistilled, boiling range 83.5–84.5° C, and converted to the bromide by the phosphorus tribromide method. The N.M.R. spectrum of this compound showed that the β-carbon atom was fully deuterated.

Isopropyl-βd_6 methanesulphonate, *p*-toluenesulphonate, and iodide were prepared from the bromide by the methods used in the preparation of the deuterated ethyl compounds.

Tertiary butyl-βd_9 chloride (minimum isotopic purity 99%) was purchased from Merck and Co.

For all of the above deuterated compounds the protium analogues were prepared by parallel reactions and were used to check the rate constants which had been determined in the course of previous work under the same conditions (14). Excellent agreement was obtained in all cases.

The rate measurements were made conductometrically as described previously (3).

The following procedure was used for the olefin determinations. Water (75 ml) was placed in a 100-ml bulb fitted with a break-seal. Samples of 0.05 to 0.1 g of the sulphonate or halide were weighed in a weight pipette and introduced into the bulb. The system was then sealed and allowed to react. After reaction the break-seal side arm was fused to a distillation system consisting of a short column and condenser with an outlet passing under the absorbing solution of Byrne and Johnson (33). A slow stream of dry nitrogen was introduced through a mercury trap above the bulb. After opening the bulb, the reacted solution was boiled for 15 minutes. The amount of olefin was determined by back-titration with thiosulphate, suitable corrections being made for a blank in the presence of the alcohol produced and the original unreacted ester.

ACKNOWLEDGMENTS

Thanks are due to Dr. W. Raynes for the N.M.R. measurements, to Mr. S. Sugamori for the careful kinetic measurements, and to Mr. R. Maillet for the olefin determinations.

REFERENCES

1. J. A. Llewellyn, R. E. Robertson, and J. M. W. Scott. Can. J. Chem. **38**, 222 (1960).
2. K. T. Leffek, J. A. Llewellyn, and R. E. Robertson. Can. J. Chem. **38**, 1505 (1960).
3. K. T. Leffek, J. A. Llewellyn, and R. E. Robertson. J. Am. Chem. Soc. In press.

4. V. J. SHINER. J. Am. Chem. Soc. **75**, 2925 (1953).
5. V. J. SHINER. J. Am. Chem. Soc. **76**, 1603 (1954).
6. V. J. SHINER. J. Am. Chem. Soc. **78**, 2653 (1956).
7. E. S. LEWIS and C. E. BOOZER. J. Am. Chem. Soc. **76**, 791 (1954).
8. E. S. LEWIS and G. M. COPPINGER. J. Am. Chem. Soc. **76**, 4495 (1954).
9. E. S. LEWIS, R. R. JOHNSON, and G. M. COPPINGER. J. Am. Chem. Soc. **81**, 3140 (1959).
10. A. STREITWIESER, R. H. JAGOW, R. C. FAHEY, and S. SUZUKI. J. Am. Chem. Soc. **80**, 2326 (1958).
11. S. WINSTEIN and J. TAKAHASHI. Tetrahedron, **2**, 316 (1958).
12. M. L. BENDER, M. S. FENG, and J. M. JONES. Chem. & Ind. 1350 (1959).
13. W. H. SAUNDERS, S. ASPERGER, and D. H. EDISON. Chem. & Ind. 1417 (1957).
14. R. E. ROBERTSON. Suomen Kemistilehti, A, **33**, 63 (1960).
15. E. A. HALEVI. Intern. J. Appl. Radiation and Isotopes, **7**, 192 (1960).
16. E. A. HALEVI. Tetrahedron, **1**, 174 (1957).
17. E. A. HALEVI. Tetrahedron, **5**, 352 (1959).
18. E. A. HALEVI and N. NUSSIM. Bull. Research Council Israel, Sect. A, **5**, 263 (1956).
19. E. A. HALEVI and N. NUSSIM. Bull. Research Council Israel, Sect. A, **6**, 167 (1957).
20. L. S. BARTELL. Tetrahedron Letters, No. 6, 13 (1960).
21. J. W. COUTTS and R. L. LIVINGSTON. J. Am. Chem. Soc. **75**, 1542 (1953).
22. J. Y. BEACH and D. P. STEVENSON. J. Am. Chem. Soc. **60**, 475 (1938).
23. O. BASTIANSEN and L. SMEDVIK. Acta Chem. Scand. **7**, 652 (1953).
24. L. E. SUTTON. Tetrahedron, **5**, 118 (1959).
25. R. S. MULLIKEN, C. A. RIEKE, and W. G. BROWN. J. Am. Chem. Soc. **63**, 41 (1941).
26. M. M. KREEVOY and H. EYRING. J. Am. Chem. Soc. **79**, 5121 (1957).
27. M. SIMONETTA and S. WINSTEIN. J. Am. Chem. Soc. **76**, 18 (1954).
28. V. J. SHINER and C. J. VERBANIC. J. Am. Chem. Soc. **79**, 373 (1957).
29. E. S. LEWIS. Tetrahedron, **5**, 143 (1959).
30. R. OSTWALD, P. T. ADAMS, and B. M. TOLBERT. J. Am. Chem. Soc. **74**, 2425 (1952).
31. R. S. TIPSON. J. Org. Chem. **9**, 235 (1944).
32. V. J. SHINER. J. Am. Chem. Soc. **74**, 5285 (1952).
33. R. E. BYRNE, JR. and J. B. JOHNSON. Anal. Chem. **28**, 126 (1956).

HYDROGENOLYSIS OF CARBOHYDRATES

IX. FORMATION OF 2,6-ANHYDRO-β-D-FRUCTOFURANOSE AND ETHYL α- AND β-D-FRUCTOFURANOSIDE FROM SUCROSE[1]

H. R. GOLDSCHMID[2] AND A. S. PERLIN

ABSTRACT

A compound formed during the hydrogenolysis of sucrose in ethanol or dioxane at 180° C, in the presence of copper chromium oxide catalyst, has been characterized as 2,6-anhydro-β-D-fructofuranose (2,5-anhydro-α-D-fructopyranose), a new type of anhydro-ketose. Ethyl α- and β-D-fructofuranosides are also produced when the hydrogenolysis reaction is carried out in ethanol, and various derivatives of these anomeric ketosides have been prepared.

Earlier papers of this series have described the hydrogenolysis of alkyl glycopyranosides in the presence of copper chromium oxide catalyst (1) at moderate temperature and pressure (2, 3, 4, 5, 6). A major effect observed in these reactions is the isomerization of carbinol groups but, particularly at temperatures above 180–200° C, glycosidic linkages also become unstable and extensive hydrogenolysis of hydroxyl groups occurs. Methyl β-L-arabopyranoside, for example, is isomerized to a mixture of methyl pentopyranosides at 180° C (4), whereas at 240° C it is converted in high yield to a mixture of 1,5-anhydro-2-deoxy-DL-pentitols (2, 5). In current studies the behavior of furanose glycosides towards these conditions of hydrogenolysis is being examined, and sucrose has been selected as a readily available substrate containing a furanosyl moiety.

In ethanol at 180° C,* sucrose readily afforded three derivatives of D-fructose, each in about 10% yield (based on the fructose unit of sucrose). Detected initially on paper chromatograms as compounds having high R_F values (relative to that of sucrose) and giving a typical ketohexose test with urea oxalate (7), these products have been isolated by column chromatography on charcoal (8) and cellulose (9) and characterized as 2,6-anhydro-β-D-fructofuranose (I) (2,5-anhydro-α-D-fructopyranose), and ethyl α- and β-D-fructofuranoside (III and II).

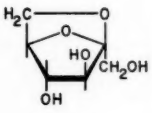

I

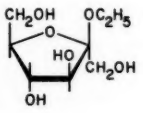

II

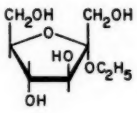

III

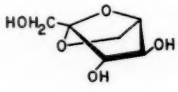

IV

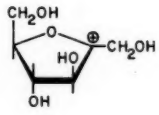

V

[1]*Manuscript received July 4, 1960.*
Contribution from the National Research Council of Canada, Prairie Regional Laboratory, Saskatoon, Saskatchewan. Presented in part to the Organic Chemistry Division, Chemical Institute of Canada, 43rd Annual Conference, Ottawa, June 13–15, 1960.
Issued as N.R.C. No. 5974.
[2]*National Research Council of Canada Postdoctorate Fellow, 1958–1960.*
**By analogy with the behavior of methyl α-D-glucopyranoside (3), the α-D-glucopyranosyl unit of sucrose was expected to be stable at 180° C.*

The anhydride, m.p. 118–119° C, was found by the isothermal distillation method (10) to be monomeric. It did not reduce hot Fehling's solution nor react with sodium borohydride and, since it was recovered unchanged after prolonged treatment with methanolic ammonia, did not appear to contain an epoxy group. At room temperature, it was easily hydrolyzed by 0.1 *N* sulphuric acid affording D-fructose as the sole product. Tritylation of the anhydride in pyridine proceeded very slowly at room temperature, and two crystalline derivatives were isolated in low yield, one being a monotrityl and the other a ditrityl ether. The compound was resistant also to tosylation but, on prolonged treatment with tosyl chloride in pyridine, yielded a syrupy diester which, however, did not react with sodium iodide. These properties suggested that only the relatively unreactive C-1-carbinol group and/or secondary hydroxyl groups of the anhydride were being substituted, and hence that the normally reactive 6-position was involved in ring formation.

Attempts to methylate the anhydride fully with dimethyl sulphate – sodium hydroxide or with methyl iodide – silver oxide were unsuccessful, but several treatments with potassium in liquid ammonia (11) followed with methyl iodide under reflux, yielded a syrupy trimethyl derivative. On acid hydrolysis this ether afforded crystalline 1,3,4-tri-*O*-methyl-D-fructose (12), showing that both the 5- and 6-hydroxyl groups of the anhydride are involved in ring formation, and hence that the anhydride is 2,6-anhydro-D-fructofuranose (2,5-anhydro-D-fructopyranose).

Since the specific rotation of the anhydride, $[\alpha]_D$ −107°, is more strongly levorotatory than D-fructose itself, the 2,6-oxygen bridge of the compound appears to possess the β-configuration. The β-assignment is strongly supported by an examination of molecular models, which shows also that the 2,6-anhydro ring assumes a boat conformation (as in IV). The eclipsing of bonds and distortion of bond angles in such a molecule could account for the observed ease of acid hydrolysis of the anhydride, as had been anticipated by Mills (13), which contrasts with the relatively high acid stability of other anhydro sugars (epoxides excepted). That the 2,6-pyranoid ring of the compound is much less stable than the five-membered 2,5-ring (see 14, 15) was indicated by the rapid formation of ethyl α- and β-D-fructofuranoside when the anhydride was treated with ethanolic hydrogen chloride at room temperature. Moreover, the α-D-anomer predominated initially, which was to be expected from scission of a β-D-anhydro ring (16), and the observed rate of formation of the mixture of furanosides (rate of rotational change) closely paralleled that found with ethyl β-D-fructofuranoside.

The anhydride consumed no periodate, although it possesses a free glycol group (the *trans*-3,4-diol group), and with lead tetraacetate in acetic acid only a slow uptake of oxidant was found, caused most probably by gradual opening of the anhydro ring. This behavior is in accord with the recent report by Angyal and Young (17) that the camphane-2,3-*trans*-diols are virtually unoxidized by glycol-cleaving agents since the structure of the anhydride is closely analogous to that of the camphane diols. Dimler (18) has suggested that the 2,3-*trans*-diol group of 1,6-anhydro β-D-gluco- and α-galactofuranose, situated on a fused bicyclic system, resists glycol scission most probably because it is fixed rigidly in an arrangement highly unfavorable for complexing by the oxidants. The *trans*-glycol groups of the camphane-*trans*-diols and the anhydrofructose appear to possess a similar spatial arrangement, and their unreactivity can therefore be interpreted in the same way.*

**Recently it has been found (H. R. Goldschmid and A. S. Perlin. Can. J. Chem. 38, 2178 (1960)) that these compounds are cleaved oxidatively by lead tetraacetate using pyridine as solvent (27).*

It may be noted, however, that some *vic–trans*-diols which are not located on bicyclic ring compounds, i.e., the 2,3-*trans*-glycol groups on internal (1 → 4)-linked units of oligosaccharides, are also resistant to attack by lead tetraacetate (19).

Several dimeric anhydrides of D-fructose are known to be formed by acid hydrolysis of D-fructans (20) and a 2,3-anhydro monomeric derivative of D-fructofuranose, as well as dimeric anhydrides, has been found recently among the products of direct nitration of D-fructose (21). The compound described here is yet another type of D-fructose anhydride. Also, it represents a class of rare anhydro-sugars, namely, that having the 1,4(2,5)-1,5(2,6)-bridged system. One other member of this class, 1,5-anhydro-β-D-ribofuranose, has been synthesized recently by Vis and Fletcher (22), and also has been converted to the 2,3-*O*-isopropylidene derivative, which proved to be indistinguishable from a compound described several years earlier but only tentatively identified (23). Derivatives of three related glycosans have been reported but incompletely characterized (see 14); these are 1,5-anhydro-2,3,6-tri-*O*-methyl-β-D-glucofuranose (24) and -α-L-idofuranose (25), and 2,3-di-*O*-acetyl-1,5-anhydro-β-L-rhamnofuranose (26).

Although 2,6-anhydro-β-D-fructofuranose cannot be regarded as a *hydrogenolysis* product derived from sucrose, it was not obtained when the reaction was carried out in the presence of argon rather than hydrogen. Considerable charring occurred under these latter conditions, however, and ethyl β-D-fructopyranoside was isolated from the reaction mixture, the furanosides being relatively minor products. Hence the hydrogenolysis conditions used may prevent decomposition of labile compounds, rather than serve directly in promoting formation of the furanose products. The occurrence together of the anhydride and of the anomeric furanosides suggests the possibility that all three products are formed from a carbonium-ion intermediate of the type encountered in the acid-catalyzed solvolysis of glycosides (see 15). A protonated form such as V, by reaction with the solvent, could yield the anomeric furanosides (II and III), and through intramolecular attack by the C-6-carbinol group give the 2,6-anhydride. Formation of an acyclic carbonium-ion intermediate (15) appears less likely in these reactions, since ethyl pyranosides would then be expected to predominate among the products at the high temperatures used. That the anhydride may be derived directly from sucrose rather than from the glycosides was shown by its formation also when the hydrogenolysis reaction was carried out in dioxane as solvent in place of ethanol. The anhydride itself undergoes ethanolysis readily by heat in the absence of added acid catalyst to yield the anomeric furanosides. Hence, the glycosides isolated from the hydrogenolysis mixture may be produced by solvolysis of the anhydride, as well as via a carbonium-ion intermediate such as V.

The α- and β-anomers of ethyl D-fructofuranoside were isolated as analytically pure syrups,* the β-anomer being readily cleaved by invertase. On tosylation, the β-glycoside furnished a crystalline diester which was converted by treatment with sodium iodide in acetone to a syrupy, monoiodo monotosyl derivative. In pyridine solution (27) the ditosylate consumed 1 mole of lead tetraacetate, in agreement with the expectation that the ester groups were located at positions-1 and -6; presumably, that at position-1 is not readily replaceable by iodide ion (28, 29). The β-anomer also furnished a crystalline 1,6-di-*O*-trityl derivative, the terminal location of the ether groups being shown by the fact that the compound, in pyridine, consumed a mole of lead tetraacetate; the ditrityl ether was characterized further as a crystalline diacetate. Tritylation of the α-glycoside

**The α-anomer of methyl D-fructofuranoside has been obtained in crystalline form (30).*

followed by acetylation afforded a crystalline di-*O*-acetyl dityrityl ether. After deacetylation the dityrityl ether was shown, also by oxidation with lead tetraacetate in pyridine, to be the 1,6-derivative.

No ethyl D-glucosides were detected among the reaction products, in accord with the expectation that the D-fructofuranosyl linkage should be cleaved preferentially. Further, as shown by the formation of D-sorbitol, the D-glucosyl unit appeared to be converted mainly to the free sugar and then reduced. The presence of D-mannitol in the mixture suggested that some D-fructose also was formed during the reaction. In addition to these products, glycerol and a small proportion of erythritol were isolated, but the origin of these fragments was not determined.

In contrast to the behavior of sucrose, the derived octaacetate was completely stable to the hydrogenolysis conditions, even at 240° C. The (2 → 6)-linked poly-D-fructan, inulin, although converted in small proportion in ethanol to the furanosides, appeared to yield none of the anhydride.

EXPERIMENTAL

Paper chromatography was carried out with butan-1-ol:ethanol:water (40:11:19) as solvent, and with urea oxalate (7) and ammoniacal silver nitrate (31) as spray reagents.

Column chromatography on cellulose was carried out using benzene:ethanol:water (500:50:1), (500:100:1) and ethanol.

Evaporations were carried out at 40–50° C, and optical rotations were measured at approximately 25° C. Melting points are corrected, and boiling points recorded are air-bath temperatures.

Hydrogenolysis of Sucrose in Ethanol and Separation of the Products

Sucrose (20 g) in absolute ethanol (75 ml) was heated at 180° C and a pressure of 1100 p.s.i. of hydrogen in the presence of copper chromium oxide catalyst (2 g) for 6 hours. The catalyst was filtered off and the filtrate concentrated, yielding a colorless syrup. Paper chromatographic examination of the syrup indicated the presence of the following components: hydroxymethylfurfural; glycerol; erythritol; ketohexose derivatives at R_F 0.60, 0.48, and 0.35; fructose; mannitol; sorbitol; sucrose; and slower-moving materials streaking to the origin.

The syrupy reaction product was chromatographed on a column of coconut charcoal (32). The glycerol (0.35 g) and erythritol (0.25 g) (m.p. 120° C, undepressed) were eluted with water.

By adding 5% ethanol to the column and then fractionating the mixture of eluted products on a cellulose column, the following were obtained: component R_F 0.60 (0.85 g), fructose (0.5 g), glucose (2.0 g), and admixed D-mannitol and D-sorbitol (1.5 g). D-Mannitol (m.p. 166° C, undepressed) was isolated by fractional crystallization, and D-sorbitol was characterized as the hexaacetate (m.p. 99° C, undepressed).

The charcoal column was washed finally with 10% ethanol yielding a mixture of products. This mixture was resolved on a cellulose column, giving component R_F 0.48 (0.9 g), component R_F 0.35 (0.85 g), and unchanged sucrose (9.5 g).

2,6-Anhydro-β-D-fructofuranose (I)

The chromatographically pure syrup (component R_F 0.35) solidified on prolonged storage, and was recrystallized from acetone, m.p. 118–119° C and $[\alpha]_D$ −107° (*c*, 1, H_2O) (no mutarotation). Calculated for $C_6H_{10}O_5$: C, 44.44%; H, 6.22%; mol. wt., 162. Found:

C, 44.49%; H, 6.37%; mol. wt., 157 (by isothermal distillation (10) in methanol at 50° C).

The compound did not reduce Fehling's solution, was unaffected by treatment under reflux for 6 hours with 1% methanolic ammonia, and also by treatment for 3 days at room temperature with aqueous sodium borohydride. With sodium metaperiodate no uptake of oxidant was found in 24 hours reaction time, and with lead tetraacetate in acetic acid the consumption of oxidant was 0.1 mole in 8 hours reaction time.

In 0.05 *N* sulphuric acid at 25° C the observed rotation of the anhydride solution (1.0%) decreased slightly from α_D −1.00° (3 minutes) → α_D −0.97° (5 hours, constant, 1 dcm tube). Paper chromatographic examination showed that most of the anhydride was hydrolyzed in 2 hours, and that conversion to fructose was complete within 5 hours; accordingly, the calculated $[\alpha]_D$ of the hydrolyzate was −89° (D-fructose shows $[\alpha]_D$ −92°). The product was characterized further by conversion to D-glucose phenylosazone, m.p. 209° C (decomp.), and indistinguishable from an authentic sample by X-ray diffraction.

The observed rotation of the anhydride in ethanolic hydrogen chloride (0.5%) at room temperature rose rapidly to $[\alpha]_D$ +0.44° (7 minutes), then decreased slowly to −0.09° (18 hours) (*c*, 1.2, 1 dcm tube). Paper chromatographic examination of the reaction mixture indicated that ethyl α-D-fructofuranoside was formed as the major product during the first 10 minutes reaction time. Under similar conditions, rotational changes shown by ethyl β-D-fructofuranoside were a rapid rise to $[\alpha]_D$ +0.32° (9 minutes), then dropping slowly to 0.03° (19 hours); ethyl α-D-fructofuranoside showed $[\alpha]_D$ +0.22° (2 minutes)→ −0.07° (20 hours), D-fructose, $[\alpha]_D$ +0.18° (14 minutes)→ −0.24° (18 hours). These values are similar to the data reported by Purves and Hudson (30, 33) for the methyl D-fructofuranosides and D-fructose.

Acetylation of the anhydride with acetic anhydride – pyridine at room temperature afforded a triacetate, b.p. 110–120° C at 0.05 mm, $[\alpha]_D$ −108° (*c*, 1.3, $CHCl_3$). Calculated for $C_{12}H_{16}O_8$: C, 50.00%; H, 5.60%; acetyl, 44.8%. Found: C, 50.17%; H, 5.79%; acetyl (sapon.), 44.4%.

Treated with benzoyl chloride and pyridine in cold chloroform, the anhydride yielded an amorphous tribenzoate, $[\alpha]_D$ −163° (*c*, 1.1, $CHCl_3$). Calculated for $C_{27}H_{22}O_8$: C, 68.35%; H, 4.67%. Found: C, 67.90%; H, 4.73%.

*1,3,4-Tri-O-methyl-*D*-fructose*

The anhydride (0.20 g) was dissolved in liquid ammonia (20 ml) and potassium was added portionwise until a stable blue color developed in the solution. After evaporation of the ammonia, methyl iodide (3 ml) was added and the solution heated under reflux for 3 hours and then stored at room temperature for 18 hours. The methyl iodide was evaporated off, the methylation procedure repeated twice, and the final reaction mixture was extracted with chloroform. The chloroform extract afforded a syrup which was distilled, b.p. 60–70° C at 0.05 mm. Paper chromatographic examination of the distillate showed the presence of a major component and a minor, slower-moving component which corresponded to 1,3,4-tri-*O*-methyl-D-fructose (below), indicative of partial hydrolysis. Calculated for $C_9H_{16}O_5$: methoxyl, 45.6%. Found: (two preparations) methoxyl, 42.9%, 41.7%.

The distillate (105 mg) was hydrolyzed with *N* sulphuric acid, the solution was neutralized with barium carbonate and extracted with chloroform. On evaporation, the aqueous layer yielded a syrup (99 mg) which consisted of a single component (paper chromatogram). Purified by distillation (b.p. 115–120° C at 0.05 mm) the product solidi-

fied, and was recrystallized from carbon tetrachloride, m.p. 72–73° C and $[\alpha]_D$ −49.6° (*c*, 1.3, H_2O) (lit. (12), m.p. 73° C and $[\alpha]_D$ −51.8° (H_2O)). Calculated for $C_9H_{18}O_6$: C, 48.36%; H, 8.3%; methoxyl, 41.89%. Found: C, 48.34%; H, 8.17%; methoxyl, 41.79%.

In acetic acid, the trimethyl D-fructose consumed no lead tetracetate in 4 hours reaction time, showing the absence of a free *vic*-diol at the 2,3-position (34) and also at the 1,2-position (35). After reduction with sodium borohydride, 1 mole of formaldehyde was produced (chromotropic acid method (36)) in 1 hour reaction time. This behavior showed the absence of methoxyl groups at positions-2, -5, and -6, and hence confirmed that the product was the 1,3,4-tri-*O*-methyl derivative.

Tritylation of 2,6-Anhydro-β-D-fructofuranose

In a preliminary experiment, using 2.2 moles of trityl chloride per mole of anhydride in pyridine at room temperature, some unchanged anhydride was present in the reaction mixture after 1 week (paper chromatogram). The anhydride (162 mg) in pyridine (4 ml) was treated at room temperature for 10 days with triphenylchloromethane (615 mg). Ice water was added, the reaction mixture was extracted with benzene, and the extract washed successively with water, sodium bicarbonate solution, and water, then dried over sodium sulphate, and the benzene was evaporated off. The oily product (720 mg) was fractionated on a column of reagent silicic acid using chloroform as the solvent. After elution of triphenylcarbinol, a ditrityl derivative (85 mg) was isolated and recrystallized from ethanol, m.p. 224–226° C and $[\alpha]_D$ −38.5° (*c*, 0.8, $CHCl_3$). Calculated for $C_{44}H_{38}O_5$: C, 81.75%; H, 5.92%; mol. wt., 643. Found: C, 81.88%; H, 6.00%; mol. wt., 621 (melting point depression in camphor).

Continued washing of the column with chloroform eluted a monotrityl derivative (145 mg) which, after recrystallization from dichloromethane – *n*-hexane, had a melting point of 150–153° C, $[\alpha]_D$ −43.7° (*c*, 1.0, $CHCl_3$). Calculated for $C_{25}H_{24}O_5$: C, 74.24%; H, 5.98%. Found: C, 74.24%; H, 5.98%.

Di-O-tosyl-2,6-anhydro-β-D-fructofuranose

The anhydride (200 mg) in pyridine (5 ml) was treated with *p*-toluenesulphonyl chloride (500 mg) at room temperature for 18 hours. A few drops of water were added, and after 30 minutes the reaction mixture was poured into ice water and extracted with benzene. After successive washings with water, sodium bicarbonate solution, and water, the benzene extract was dried and concentrated affording a glass (139 mg). The product, treated in acetone with sodium iodide in a sealed tube at 100° C, yielded only a trace of sodium *p*-toluenesulphonate in 24 hours reaction time, $[\alpha]_D$ −29.1° (*c*, 1.4, $CHCl_3$). Calculated for $C_{20}H_{22}O_9S_2$: C, 51.04%; H, 4.71%; S, 13.62%. Found: C, 51.60%; H, 4.91%; S, 14.17%.

Ethyl β-D-Fructofuranoside (II)

The syrupy, chromatographically pure glycoside had $[\alpha]_D$ −36° (*c*, 1, H_2O), was readily degraded to fructose by treatment with invertase, and was hydrolyzed to fructose at room temperature within 2 days by 0.1 *N* sulphuric acid. It consumed 1.0 mole of sodium periodate per mole.

On acetylation with acetic anhydride in pyridine at room temperature, the glycoside (200 mg) afforded a tetraacetate (310 mg), b.p. about 150° C at 0.06 mm, $[\alpha]_D$ −25° (*c*, 1.1, $CHCl_3$). Calculated for $C_{16}H_{24}O_{10}$: C, 51.06%; H, 6.43%; acetyl, 45.8%. Found: C, 51.07%; H, 6.52%; acetyl (sapon.), 46.1%.

1,6-Di-O-trityl Ethyl β-D-Fructofuranoside

The glycoside II (200 mg) in pyridine (4 ml) was treated at room temperature with trityl chloride (600 mg) for 48 hours. Isolated after treatment with ice water and extraction into benzene, the product (490 mg) was crystallized from ethanol, m.p. 180–183° C and $[\alpha]_D$ −2.3° (*c*, 1.0, $CHCl_3$). Calculated for $C_{46}H_{44}O_6$: C, 79.74%; H, 6.40%. Found: C, 79.91%; H, 6.60%.

Treated with lead tetraacetate in pyridine (27) at 0° C the ditrityl derivative consumed 1 mole of oxidant per mole in 0.5 hour.

The ditrityl glycoside (100 mg) treated with acetic anhydride – pyridine afforded a diacetate (95 mg) which, after recrystallization from ethanol, had a melting point of 207–208° C, $[\alpha]_D$ +35.8° (*c*, 1.3, $CHCl_3$). Calculated for $C_{50}H_{48}O_8$: C, 77.30%; H, 6.23%. Found: C, 77.07%; H, 6.29%.

1,6-Di-O-tosyl Ethyl β-D-Fructofuranoside

To the glycoside II (400 mg) in pyridine (5 ml) at 0° C was added a solution of *p*-toluenesulphonyl chloride (750 mg) in chloroform (10 ml). After 2 hours at 0° C and 18 hours at 25° C the reaction mixture was diluted with chloroform (30 ml), treated with a few drops of water, and 30 minutes later was washed successively with ice water, copper sulphate, sodium bicarbonate, and water. The solution was dried over sodium sulphate and concentrated, yielding a crystalline product (230 mg) which was recrystallized from ethanol – *n*-hexane, m.p. 125–127° C (decomp.), $[\alpha]_D$ −12.8° (*c*, 1.0, $CHCl_3$). Calculated for $C_{22}H_{28}O_{10}S_2$: C, 51.15%; H, 5.46%; S, 12.41%. Found: C, 51.02%; H, 5.46%; S, 12.13%.

In pyridine, the ditosyl derivative consumed 1.0 mole of lead tetraacetate per mole in 1 hour reaction time.

The ditosylate (100 mg) was heated at 100° C with sodium iodide (75 mg) in acetone (6 ml) for 24 hours. Sodium *p*-toluenesulphonate (35 mg), which crystallized out on cooling, was filtered off. After evaporation of the acetone, the residue was taken up in chloroform, washed with water, and recovered as an oil (72 mg), $[\alpha]_D$ −22.5° (*c*, 1.0, $CHCl_3$). Calculated for $C_{15}H_{21}O_7SI$: S, 6.79%; I, 26.87%. Found: S, 6.68%; I, 25.94%.

Ethyl α-D-Fructofuranoside (III)

The syrupy, chromatographically pure material showed $[\alpha]_D$ +65° (*c*, 1, H_2O), was not attacked by invertase, and was hydrolyzed to D-fructose within 15 hours at room temperature by 0.1 *N* sulphuric acid. It consumed 1 mole of sodium periodate per mole. Calculated for $C_8H_{16}O_6$: C, 46.15%; H, 7.75%; ethoxyl, 21.6%. Found: C, 45.98%; H, 8.13%; ethoxyl, 21.1%.

Acetylated at 25° C with acetic anhydride – pyridine, the glycoside yielded a tetraacetate, b.p. about 135° C at 0.01 mm, $[\alpha]_D$ +76° (*c*, 1.4, $CHCl_3$). Calculated for $C_{16}H_{24}O_{10}$: C, 51.06%; H, 6.43%; acetyl, 45.8%. Found: C, 51.22%; H, 6.65%; acetyl (sapon.), 45.8%.

3,4-Di-O-acetyl-1,6-di-O-trityl Ethyl α-D-Fructofuranoside

The glycoside III (205 mg) was treated with trityl chloride (615 mg) in pyridine (4 ml) at room temperature for 7 days, and the reaction mixture was worked up as described previously. The syrupy product (722 mg) was fractionated on a silicic acid column using chloroform as solvent, affording a crystalline ditrityl ether (260 mg) and, by continued elution, an oily product which probably was a monotrityl derivative. Despite repeated recrystallization from ethanol the ditrityl ether had a broad melting point (about

140–150° C). On acetylation at 100° C with acetic anhydride – sodium acetate, a di-*O*-acetyl di-*O*-trityl derivative was obtained, m.p. 142–144° C and $[\alpha]_D$ +44.7° (*c*, 1.4, $CHCl_3$). Calculated for $C_{50}H_{48}O_8$: C, 77.30%; H, 6.23%. Found: C, 77.32%; H, 6.32%.

The product was deacetylated with sodium methoxide in chloroform–methanol, the solvent was evaporated, and the residue treated at 0° C with lead tetraacetate in pyridine. Found: 1.0 mole of oxidant consumed per mole in 0.5 hour.

Hydrogenolysis of Sucrose in Dioxane

Sucrose (5 g) and copper chromium oxide catalyst (0.5 g) in dioxane (75 ml) were heated for 6 hours at 180° C under hydrogen at 1100 p.s.i. An oil consisting mainly of unchanged sucrose separated out on cooling, and the dioxane solution was evaporated. The residue (2.9 g) showed heavy streaking on a paper chromatogram. By chromatography on a cellulose column, a fraction corresponding (paper chromatogram) to the anhydride (I) was isolated (167 mg). After recrystallization from acetone, the product had a melting point of 118–119° C, undepressed. The X-ray diffraction powder diagram of the product was indistinguishable from that of the anhydride (I).

Ethanolysis of Sucrose

Sucrose (10 g) in dry ethanol (75 ml) was heated for 6 hours at 180° C in an atmosphere of argon (10 p.s.i.). The resulting dark-brown solution was concentrated to a syrup which, from paper chromatographic examination, appeared to contain hydroxymethylfurfural, ethyl D-fructofuranosides (II and III), a trace of anhydride (I), fructose, and sucrose. By column chromatography on cellulose the glycoside mixture was found to contain ethyl β-D-fructopyranoside (105 mg), m.p. 150–151° C and $[\alpha]_D$ −160° (*c*, 1.0, H_2O). Calculated for $C_8H_{16}O_6$: C, 46.15%; H, 7.75%. Found: C, 46.21%; H, 7.86%. The derived tetraacetate had a melting point of 83–84° C and $[\alpha]_D$ −127° (*c*, 1.2 $CHCl_3$). Calculated for $C_{16}H_{24}O_{10}$: C, 51.06%; H, 6.43%. Found: C, 51.33%; H, 6.57%.

ACKNOWLEDGMENTS

The authors gratefully acknowledge the technical assistance given by Mr. J. W. L. C. Christ, and helpful suggestions made by Dr. P. A. J. Gorin. Microanalyses were performed by Mr. M. Mazurek, and X-ray powder diagrams and infrared absorption spectra were prepared by Miss Inez Gaffney.

REFERENCES

1. W. H. Zartman and H. Adkins. J. Am. Chem. Soc. **55**, 4559 (1933).
2. H. F. Bauer and D. E. Stuetz. J. Am. Chem. Soc. **78**, 4097 (1956).
3. E. von Rudloff, H. F. Bauer, and D. E. Stuetz. Can. J. Chem. **35**, 315 (1957).
4. A. S. Perlin, E. von Rudloff, and A. P. Tulloch. Can. J. Chem. **36**, 921 (1958).
5. T. Francis and A. S. Perlin. Can. J. Chem. **37**, 1229 (1959).
6. P. A. J. Gorin. Can. J. Chem. **38**, 641 (1960).
7. E. L. Hirst, D. I. McGilvray, and E. G. V. Percival. J. Chem. Soc. 1297 (1950).
8. R. L. Whistler and D. F. Durso. J. Am. Chem. Soc. **72**, 677 (1950).
9. L. Hough, J. K. N. Jones, and W. H. Wadman. J. Chem. Soc. 2511 (1949).
10. C. E. Childs. Anal. Chem. **26**, 1963 (1954).
11. I. E. Muskat. J. Am. Chem. Soc. **56**, 693 (1934).
12. H. Hibbert, R. S. Tipson, and F. Brauns. Can. J. Research **4**, 221 (1931).
13. J. A. Mills. *In* Advances in carbohydrate chemistry. Vol. 10. Academic Press, Inc., New York. 1955. p. 1.
14. S. Peat. *In* Advances in carbohydrate chemistry. Vol. 2. Academic Press, Inc., New York. 1947. p. 37.
15. F. Shafizadeh. *In* Advances in carbohydrate chemistry. Vol. 13. Academic Press, Inc., New York. 1958. p. 9.
16. R. U. Lemieux. *In* Advances in carbohydrate chemistry. Vol. 9. Academic Press, Inc., New York. 1954. p. 1.

17. S. J. ANGYAL and R. J. YOUNG. J. Am. Chem. Soc. **81**, 5467 (1959).
18. R. J. DIMLER. *In* Advances in carbohydrate chemistry. Vol. 7. Academic Press, Inc., New York. 1952. p. 37.
19. A. S. PERLIN and A. R. LANSDOWN. Can. J. Chem. **34**, 451 (1956).
20. E. J. MCDONALD. *In* Advances in carbohydrate chemistry. Vol. 2. Academic Press, Inc., New York. 1947. p. 253.
21. M. SAREL-IMBER and J. LEIBOWITZ. J. Org. Chem. **24**, 1897 (1959).
22. E. VIS and H. G. FLETCHER, JR. J. Am. Chem. Soc. **79**, 1182 (1957).
23. P. A. LEVENE and E. T. STILLER. J. Biol. Chem. **102**, 187 (1933).
24. K. FREUDENBERG and E. BRAUN. Ber. **66**, B, 780 (1933).
25. K. HESS and F. NEUMANN. Ber. **68**, B, 1360 (1935).
26. F. MICHEEL and H. MICHEEL. Ber. **63**, 2862 (1930).
27. R. C. HOCKETT and D. F. MOWERY, JR. J. Am. Chem. Soc. **65**, 403 (1943).
28. R. S. TIPSON. *In* Advances in carbohydrate chemistry. Vol. 8. Academic Press, Inc., New York. 1953. p. 107.
29. R. U. LEMIEUX and J. P. BARRETTE. J. Am. Chem. Soc. **80**, 2243 (1958).
30. C. B. PURVES. J. Am. Chem. Soc. **56**, 1969 (1934).
31. S. M. PARTRIDGE. Nature, **158**, 270 (1946).
32. F. W. BARTH and T. E. TIMELL. Can. J. Chem. **36**, 1321 (1958).
33. C. B. PURVES and C. S. HUDSON. J. Am. Chem. Soc. **56**, 1973 (1934).
34. A. S. PERLIN and C. BRICE. Can. J. Chem. **34**, 541 (1956).
35. B. LINDBERG and B. WICKBERG. Acta Chem. Scand. **7**, 969 (1953).
36. M. LAMBERT and A. C. NEISH. Can. J. Research, B, **28**, 83 (1950).

REACTION OF OXYGEN ATOMS WITH BUTADIENE[1]

R. J. Cvetanović and L. C. Doyle

ABSTRACT

Reaction of oxygen atoms with 1,3-butadiene has been investigated at room temperature. It is found that it conforms to the general mechanism established previously for the analogous reactions of monoolefins. Only 1,2-addition occurs, and the addition products, butadiene monoxide and 3-butenal, possess excess energy when formed as a result of high heats of reaction. The pressure dependence of the formation of the addition products yields the values of the "lifetimes" of the initially produced "hot" molecules. The relative rate constants have been determined at 25 and 127° C and from these the relative values of the Arrhenius parameters have been calculated.

INTRODUCTION

The general mechanism of reaction of oxygen atoms with alkenes has recently been established in this laboratory (1) and the trends in the relative rate constants (2) demonstrated the electrophilic character of the ground-state oxygen atoms in these reactions. As an extension of this work the present study of the analogous reaction with 1,3-butadiene, as the simplest representative of conjugated diolefins was carried out.

The particular questions which the present investigation was hoped to answer are: first, whether conjugated diolefins in their reactions with oxygen atoms follow the general mechanism established for monoolefins; secondly, whether only 1,2- or also 1,4-addition products are formed; and lastly, whether the value of the rate constant of the reaction of oxygen atoms with 1,3-butadiene is such as might be expected in view of the trends and relations established in the case of monoolefins (2). Affirmative answers to these questions have been obtained and only the two 1, 2-addition products predicted on the basis of the rules formulated for the monolefins (1), butadiene monoxide and 3-butenal, the latter readily isomerizing to the more stable crotonaldehyde, have been observed. The 1,4-addition product, 2,5-dihydrofuran, is not formed.

The pronounced pressure effect observed in the present work illustrates particularly well initial formation of "hot" addition products and the consequent "pressure-dependent fragmentation" (1) in the reactions of oxygen atoms with olefins. As a result, in some of these reactions, including 1,3-butadiene itself, the addition products are essentially completely decomposed at pressures of a few millimeters and are then not observable experimentally. This feature and some other difficulties inherent in the electrical discharge method for production of oxygen atoms, as discussed recently elsewhere (3), are believed to be responsible for the entirely different conclusions from the present ones arrived at by Avramenko and Kolesnikova (4) in what seems to be the only other attempt reported in the literature to study the reaction of oxygen atoms with butadiene. These differences are of a general character and are not limited to the case of butadiene.

Oxygen atoms were generated by mercury-photosensitized decomposition of nitrous oxide, as described in the previous work (1, 2), and nitrogen liberated provided a quantitative measure of the oxygen atoms consumed in the reaction.

EXPERIMENTAL

The apparatus used in this work consisted of a cylindrical quartz reaction cell 5 cm in diameter and 10 cm long, connected in series with an all-glass vertical plunger-type

[1]*Manuscript received August 8, 1960.*
Contribution from the Division of Applied Chemistry, National Research Council, Ottawa, Canada.
Issued as N.R.C. No. 5978.

circulating pump. The circulating reaction system had a total volume of 415 ml. It was connected by means of mercury cutoffs to a constant volume burette for measuring the amounts of reactant hydrocarbons (butadiene, cyclopentene) to the analysis system and to the vacuum manifold. Nitrous oxide was measured manometrically on a volume of 1000 ml and then was frozen over into the reaction vessel.

The analysis system consisted of a Le Roy still (5), followed by a "pump-out" trap and then by a constant volume burette and outlets for transfer of samples to the gas–liquid chromatographic apparatus (GLC), mass spectrometer, and infrared spectrometer. The Le Roy still was used in particular for the separation of the more volatile fractions. The noncondensable gases, N_2, CO, CH_4, and H_2, were analyzed by the use of a copper oxide tube to oxidize CO and H_2. The CO_2 formed was measured manometrically and mass spectra were taken of the residual N_2 and CH_4. Hydrogen, the amount of which was determined by difference, was at best formed only in trace amounts in the present work. The "pump-out" trap ensured quantitative retention of C_2H_4 which, together with C_2H_6 and traces of CH_4 and N_2O, was eluted from the Le Roy still at $-180°$. This fraction was further analyzed mass spectrometrically. No appreciable amounts of methane, ethylene, or ethane were formed in the reaction of oxygen atoms with butadiene. Ethylene formed from cyclopentene served for the determination of the relative rate constants, as described before (2).

After removal of excess N_2O and a part of the butadiene, the remainder was run on a 4-ft GLC column consisting of about 4 weight per cent dimethyl sulpholane on glass beads (passing 270 mesh). Infrared and mass spectra of the major reaction products were taken after their elution from the GLC column.

An air-cooled low-pressure mercury lamp was used as source of the mercury resonance radiation. In most experiments the large excess of N_2O employed ensured only negligible quenching by butadiene and separate experiments showed that mercury-photosensitized decomposition of butadiene itself was not important under conditions of the present experiments. The reactants were of the best available grade and were degassed and bulb-to-bulb distilled *in vacuo* in the usual manner before use.

In the reaction of oxygen atoms with butadiene only two addition products were detected by GLC analysis (using dimethyl sulpholane column): butadiene monoxide and crotonaldehyde. They had GLC elution times, infrared spectra, and mass spectra identical with those of the respective commercial samples (a sample of butadiene monoxide was kindly supplied by Columbia-Southern Chemical Corp.). The GLC analysis of the condensable products showed also small amounts of what appeared to be three compounds eluting much faster than the two addition products. These were formed in too small amounts to be identified by the analytical techniques used but are believed to be the products of fragmentation of the "hot" addition products, as will be discussed in the following section. No 2,5-dihydrofuran, a potential 1,4-addition product, was detected.* The quantitative data on the products observed by GLC are based on calibrations made with butadiene monoxide and crotonaldehyde and with the assumption that the fragmentation products had equal response per unit area of the peaks to that of butadiene monoxide. Only the total sum of the fragmentation products observed by GLC is reported here since individually they were present in most cases in little more than trace amounts.

In the reaction of oxygen atoms with butadiene there was evidence for the formation

The authors are very grateful to Dr. E. C. Horswill of these laboratories for synthesizing a sample of 2,5-dihydrofuran in order that its absence in the reaction products could be verified directly.

of a deposit (referred to in the following as the "polymer") which was not removed, or was removed only extremely slowly, from the reaction vessel by evacuation or freezing out. No attempt was made to obtain qualitative and quantatitive information on this material.

RESULTS

The results of several experiments carried out at 25±2° at constant pressures of nitrous oxide and butadiene, 300 and 30 mm, respectively, but at varying exposure times are presented in Fig. 1. They show that within the investigated range the rates of formation of the products are independent of the reaction time.

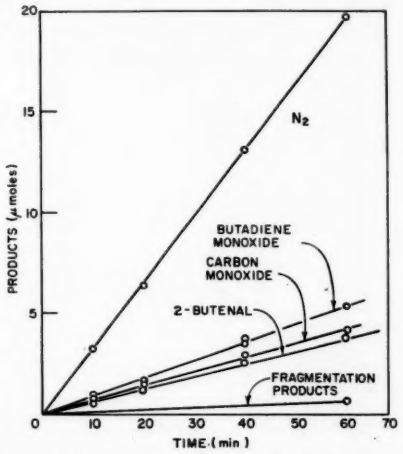

FIG. 1. Variation of the amounts of products formed with irradiation time. (Pressure of N_2O 299±2 mm, pressure of butadiene 31±2 mm, temperature 25±2° C. "Fragmentation products" refer to the unidentified condensable products of pressure-dependent fragmentation as observed by GLC.)

In the experiments shown in Fig. 1 exceptionally large amounts of butadiene were employed, about 10 times as large as in most of the other experiments. Even then no products other than those usually observed were detected. The only effect of variation in butadiene concentration reflected itself in a slight variation in the number of oxygen atoms generated (as measured by nitrogen formation) because of some competitive quenching by the diolefin. This is shown in Table I where more than fourfold increase

TABLE I

Dependence of the amounts of products formed on the initial concentration of butadiene

			Products				
Run	Butadiene, mm	Butadiene / N_2O	N_2, μmoles	CO / N_2	Epoxide / N_2	2-Butenal / N_2	Frag. products* / N_2
86	2.49	0.0073	12.8	0.22	0.27	0.19	0.04
88	5.48	0.0173	12.7	0.22	0.29	0.20	0.04
87	8.21	0.0265	12.5	0.22	0.27	0.19	0.04
85	11.10	0.0355	12.3	0.21	n.d.	0.20	0.05

NOTE: Temperature 25±1° C; irradiation time 40 minutes; N_2O pressure 303±1.5 mm.
*Condensable fragmentation products observed by GLC.
n.d. = not determined.

in butadiene concentration did not affect the rates of formation of the products per oxygen atom consumed (R/R_{N_2}) and only slightly decreased nitrogen production. This decrease is of correct magnitude to be entirely explainable as due to competitive quenching by butadiene. At the relatively high total pressures employed in the present work the energy transferred by quenching to butadiene is likely to be rapidly dissipated through collisional deactivation, as is usually the case with olefins, without causing any substantial decomposition of butadiene. Small amounts of a butadiene dimer, identified as such mass spectrometrically, were occasionally observed by GLC analysis of the products. This compound was found, however, to be present as a minor impurity in the butadiene used and was initially introduced together with the butadiene into the reaction system.

The effect of pressure on the products formed is very pronounced, as is shown in Fig. 2. In these experiments the pressure of butadiene was kept approximately constant

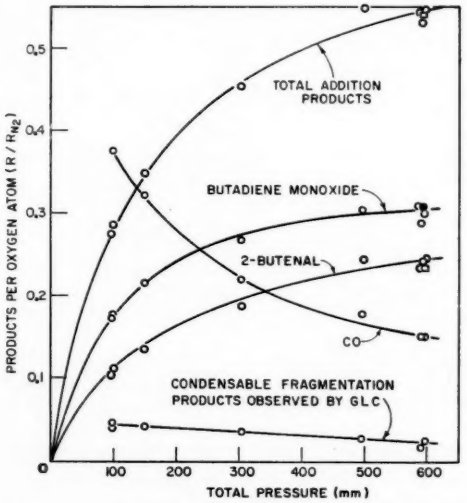

FIG. 2. Rates of product formation per oxygen atom consumed (R/R_{N_2}) at various total pressures. (Pressure of butadiene 3.0±0.5 mm, exposure 40 minutes, temperature 26±1° C. Filled circle and squares indicate initially added 3 mm of O_2.)

at about 3 mm, the exposure was 40 minutes so that between 11 and 13 μmoles of nitrogen were produced, and the temperature was 26±1°. The total pressure was varied by varying the partial pressure of nitrous oxide.

The general behavior in the case of butadiene is quite similar to that observed previously with propylene (1): with increasing pressure the amounts of the addition products, butadiene monoxide and crotonaldehyde, increase while at the same time those of the fragmentation products decrease. The reaction of oxygen atoms with butadiene provides therefore another good illustration of the pressure-dependent fragmentation in the reactions of oxygen atoms with olefins: at higher pressures greater number of the initially produced "hot" addition products is deactivated and less fragmentation of these products occurs.

An initial addition of 3 mm of molecular oxygen to 3 mm of butadiene and 587 mm

of nitrous oxide did not affect the formation of butadiene monoxide and crotonaldehyde, as shown by filled circle and squares in Fig. 2, and eliminated the condensable fragmentation products. No attempt was made to measure directly N_2 and CO in this case because of large excess of O_2 present. Nitrogen was estimated from comparable runs done in the absence of molecular oxygen.

The rate constants of the reaction of oxygen atoms with butadiene (k_B) were determined relative to those of cyclopentene (k_C) at 25.4±1° and 126.8±2° C. The experimental details and the results are given in Table II. The rate constants have been

TABLE II

Determination of the relative rate constant for butadiene and cyclopentene

Run	Butadiene / Cyclopentene	Butadiene, mm	Cyclopentene, mm	N_2O, mm	Gaseous products: N_2, mm	C_2H_4/N_2	CO/N_2	k_B/k_C
			(I) 25.4±1° C					
60	0.84	6.88	8.17	507.2	2.12	0.160	0.075	0.810
62	1.74	18.57	10.66	499.1	1.94	0.113	0.094	0.808
65	1.79	13.15	7.35	502.8	1.81	0.112	0.092	0.776
64	3.75	30.99	8.26	465.3	1.68	0.0685	0.117	0.845
61		29.73	—	503.3	1.94	—	0.143	
							Mean	0.810±.018
			(II) 126.8±2° C					
66	1.17	10.84	9.28	504.5	1.69	0.133	0.112	0.905
69	1.72	13.91	8.11	501.4	1.64	0.109	0.128	0.876
67	2.13	19.36	9.11	501.6	1.64	0.0962	0.136	0.869
71	2.63	21.64	8.23	505.5	1.62	0.0822	n.d.	0.879
68	3.07	28.64	9.34	507.5	1.54	0.0734	0.145	0.892
70		27.88	—	506.3	1.58	—	0.181	
							Mean	0.884±.011

NOTE: Exposure 60 minutes; quantities are given in millimeters in 415.1 ml at 25° C.

calculated from the rates of ethylene production in the manner described previously (2). From the mean values of the relative rate constants at the two temperatures the relative values of the Arrhenius parameters are found to be $E_B - E_C = 0.20$ kcal/mole and $A_B/A_C = 1.14$.

DISCUSSION

The products formed in the reaction of oxygen atoms with butadiene indicate that this diolefin conforms to the general mechanism established before (1) for the reaction of oxygen atoms with monoolefins. In the case of butadiene this mechanism requires the formation of butadiene monoxide and 3-butenal as the initial addition products. Actually crotonaldehyde (2-butenal) was observed after elution from the dimethyl sulpholane GLC column instead of 3-butenal. However, infrared absorption spectra of the condensable products taken *before* passage through GLC show that crotonaldehyde is not the primary product of the reaction but is formed during passage through GLC by isomerization of an aldehyde which has the carbonyl stretching absorption band at about 1745 cm^{-1} instead of a doublet at about 1720 cm^{-1} present in crotonaldehyde. Both aldehydes have the C=C stretching absorption band at about 1650 cm^{-1}. *After* GLC the infrared spectra of the products show only the presence of butadiene monoxide and crotonaldehyde, the latter at the expense of the aldehyde initially present, from which it is apparently formed by isomerization. We believe that the initially formed aldehyde

is 3-butenal. Some additional evidence for this was obtained by separating from a polypropylene glycol column a compound with an infrared spectrum similar to that of the initially formed aldehyde. This compound elutes much faster than crotonaldehyde but has a mass spectrum essentially the same as crotonaldehyde.

The isomerization of the initially produced aldehyde to crotonaldehyde apparently takes place quite readily on passage through GLC. Also there appeared to be as a rule slight and sometimes quite appreciable isomerization even in the course of the regular handling of the products in the vacuum apparatus before passage through GLC. While the information on 3-butenal available in the literature is somewhat limited, it would seem that an isomerization to the more stable 2-butenal under present conditions could readily take place.

A 1,4-addition of oxygen atoms to butadiene would produce 2,5-dihydrofuran. However, this compound is not observed so that 1,4-addition does not occur. The assumed primary intermediate in these reactions is a triplet biradical (1). There is evidence that this is extremely short-lived, since the distribution of the products differs somewhat between the two 2-butene isomers (1). Also, in view of the pronounced electronegativity of oxygen, the initial "biradical" is likely to have some zwitterion character. The formation of the 1,2- rather than 1,4-adduct with oxygen atoms in the case of 1,3-butadiene may then be understandable both on kinetic and energetic grounds.

The observed pressure effect in the reaction of oxygen atoms with 1,3-butadiene is very interesting and, together with the corresponding reaction of propylene (1), it illustrates well one of the fundamental features of these addition processes. As a result of high heats of reaction the products formed are "hot" to the extent of about 115 kcal/mole in the case of carbonyl compounds and probably about 80 to 90 kcal/mole in the case of the epoxides. Depending largely on the number of degrees of freedom available, various average time intervals will be required before sufficient excess energy is concentrated in a critical bond to break it. In the meantime the molecule will tend to become stabilized through collisional deactivation. In the case of ethylene, decomposition largely predominates at the usual pressures (6), while the products from the butenes are stabilized already at about 10 to 30 mm (7). Propylene exhibits an intermediate behavior and the same is now found to be true for 1,3-butadiene as well.

For a kinetic treatment of the observed pressure effect the following reaction scheme, based on the general mechanism of reaction of oxygen atoms with olefins, is considered.

$$N_2O + Hg(^3P_1) \rightarrow N_2 + O + Hg(^1S_0) \qquad (i)$$

$$CH_2{=}CH{-}CH{=}CH_2 + O \rightarrow (CH_2{=}CH{-}\dot{C}H{-}CH_2O\cdot) \rightarrow \alpha BO^* + \beta BA^* + X \qquad [1]$$

$$BO^* \rightarrow \gamma CO + \text{other decomposition products} \qquad [2]$$

$$BO^* + M \rightarrow BO + M \qquad [2a]$$

$$BA^* \rightarrow \delta CO + \text{other decomposition products} \qquad [3]$$

$$BA^* + M \rightarrow BA + M \qquad [3a]$$

where BO stands for butadiene monoxide, BA for butenal, X for any unknown products of reaction [1], and the asterisk indicates "hot" molecules. Steady-state treatment leads to the following expressions:

[1] $$\frac{R_{N_2}}{R_{BO}} = \frac{1}{\alpha}\left(1 + \frac{k_2}{k_{2a}(M)}\right),$$

[2] $$\frac{R_{N_2}}{R_{BA}} = \frac{1}{\beta}\left(1 + \frac{k_3}{k_{3a}(M)}\right)$$

and

[3] $$\frac{R_{CO}}{R_{N_2}} = \frac{\gamma\alpha}{1+k_{2a}(M)/k_2} + \frac{\delta\beta}{1+k_{3a}(M)/k_3}.$$

Plots of R_{N_2}/R_{BO} and R_{N_2}/R_{BA} against 1/(M) are given in Fig. 3. From these the

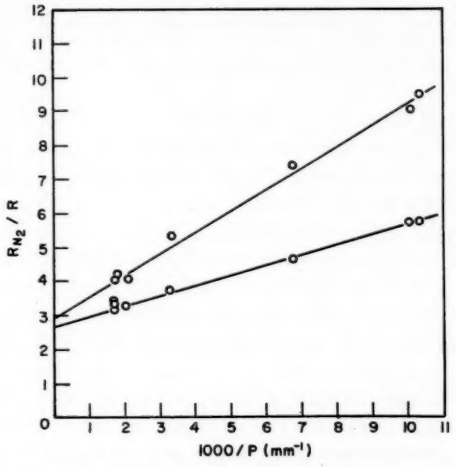

FIG. 3. Plots of R_{N_2}/R_{BO} and R_{N_2}/R_{BA} against reciprocal total pressure (equations [1] and [2]).

following values are obtained: $k_2/k_{2a} = 3.7\times10^{18}$ cc/molecule, $k_3/k_{3a} = 7.2\times10^{18}$ cc/molecule, $\alpha = 0.38$, $\beta = 0.34$.

In Fig. 4 R_{N_2}/R_{CO} is seen to be a linear function of (M) and this simple relation requires

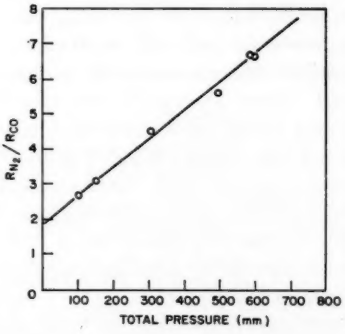

FIG. 4. Plot of R_{N_2}/R_{CO} against total pressure (equation [3a]).

simplification of equation [3]. The slope-to-intercept ratio of the plot in Fig. 4 indicates a k/k_a value of 7.3×10^{18} cc/molecule which is essentially the same as that obtained for k_3/k_{3a} from the plot in Fig. 3. In view of this it would appear that CO is produced by decomposition of "hot" butenal and not to any important extent from decomposition of "hot" butadiene monoxide, i.e., that in equation [3] $\gamma = 0$ and therefore

[3a] $$R_{CO}/R_{N_2} = \delta\beta/(1+k_{3a}(M)/k_3).$$

The plot in Fig. 4 is in agreement with equation [3*a*]. The intercept gives 0.54 for the value of $\delta\beta$, i.e. the value of R_{CO}/R_{N_2} as $P \rightarrow 0$. If CO is formed only from "hot" butenal such a high value of $\delta\beta$ is inconsistent with the value $\beta = 0.34$ from the plot in Fig. 3 since δ cannot be larger than unity. Additional CO is not produced in a pressure-independent fragmentation, as is evident from the alternative plot of equation [3*a*] in Fig. 5. The

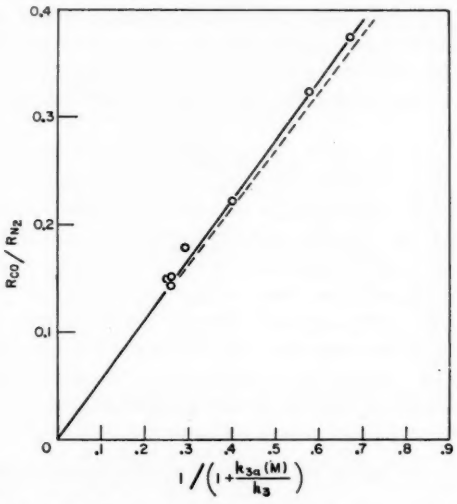

FIG. 5. Plot of R_{CO}/R_{N_2} against $1/(1+k_{3a}(M)/k_3)$ (rearranged equation [3*a*]).

values for k_3/k_{3a} have been taken as 7.2×10^{18} (broken line) as found above and 6.6×10^{18} cc/molecule (full line), the latter to show the relatively small effect of an appreciable variation in the value selected for k_3/k_{3a}. As $P \rightarrow \infty$ R_{CO}/R_{N_2} approaches zero or a value very close to it. The difficulty could be formally resolved by assuming that a constant fraction (37%) of the collisionally deactivated BA* molecules are not recovered as butenal but polymerize instead, either during the reaction or in subsequent handling of the products. This would also bring up the material balance of the oxygen atoms used in the reaction as $P \rightarrow \infty$ from about 70 to 75% to about 90 to 95%, which is satisfactory in view of the long extrapolations made to obtain the intercepts. In this connection it is of interest that Farberov and Ustavshchikov (8) have recently observed that 3-butenal resinifies rapidly on standing. However, it was not feasible in the present work to obtain quantitative estimates of the polymer formed and the suggested explanation must be regarded as only speculative.

Besides carbon monoxide only small amounts of other fragmentation products are observed. This is probably due to the scavenging action of butadiene for H atoms and free radicals with eventual formation of higher molecular weight compounds not directly observable by the analytical techniques used.

If it is assumed approximately that $k_{2a} = k_{3a} = 10^{-10}$ cc molecule^{-1} sec^{-1}, i.e. that deactivation occurs at approximately every collision, then the lifetimes of the "hot" butadiene monoxide and 3-butenal are calculated to be, respectively, $1/k_2 = 2.7\times10^{-9}$ and $1/k_3 = 1.4\times10^{-9}$ sec. From the plots in earlier work (1) the lifetime for the "hot" propanal is similarly found to be 8.0×10^{-9} and that of the "hot" propylene oxide

5.8×10^{-9} sec, although in this latter case on the basis of a very limited number of experiments the pressure dependence appeared to be more complex. For the hot addition products of the reaction of oxygen atoms with butene-1 and isobutene lifetimes an order of magnitude greater were indicated by the complete suppression of pressure-dependent fragmentation at pressures as low as 10 to 30 mm (7). The exceptionally short lifetimes of butadiene monoxide and in particular of 3-butenal considering the number of degrees of freedom available in these compounds are understandable since breakage of bonds may lead to the resonance stabilized allylic and substituted allylic radicals.

The rate constant of the reaction of oxygen atoms with butadiene is very close to that of isobutene and other two-substituted ethylene derivatives as may be expected in view of the electrophilic character of oxygen atoms in their reactions with olefins (2, 9). The temperature coefficient of the rate constant will be discussed elsewhere together with the data obtained for a number of monoolefins (10).

It is evident from the present work that at pressures as low as a fraction of a millimeter to several millimeters essentially complete decomposition of the "hot" addition products should occur and the primary step of the process, addition of oxygen atoms to the double bond, would no longer be directly observable. Under such conditions only fragmentation products would be produced and in particular their derivatives from secondary reactions with molecular oxygen, even when the latter is present only in small amounts, or with other active species which may be present. On this basis the entirely different results from the present ones obtained by Avramenko and Kolesnikova (4) are understandable, as well as the conclusions of these authors that oxygen atoms exhibit a versatility of behavior in their reactions with some organic compounds, and with olefins as well. These conclusions have not been born out by investigations in this laboratory, which show instead an electrophilic addition of the ground-state oxygen atoms to the double bond as the only primary reaction with olefins at room temperature.

ACKNOWLEDGMENTS

The authors are grateful to Dr. A. W. Tickner for mass spectrometric analyses and to the Analytical Section of this Division for the infrared analyses.

REFERENCES

1. R. J. CVETANOVIĆ. Can. J. Chem. **36**, 623 (1958).
2. R. J. CVETANOVIĆ. J. Chem. Phys. **30**, 19 (1959).
3. J. M. S. JARVIE and R. J. CVETANOVIĆ. Can. J. Chem. **37**, 529 (1959).
4. L. I. AVRAMENKO and R. V. KOLESNIKOVA. Voprosy Khimicheskoi Kinetiki Kataliza i Reaktsionnoi Sposobnosti. Akad. Nauk S.S.S.R., Moscow. 1955. p. 7; N.R.C. of Canada Technical Translation 789, Ottawa. 1959.
5. D. J. LE ROY. Can. J. Research, B, **28**, 492 (1950).
6. R. J. CVETANOVIĆ. J. Chem. Phys. **23**, 1375 (1955).
7. S. SATO and R. J. CVETANOVIĆ. Can. J. Chem. **36**, 970 (1958).
8. M. I. FARBEROV and B. F. USTAVSHCHIKOV. J. Gen. Chem. U.S.S.R. **25**, 2025 (1955). (English translation, Consultants Bureau, New York, N.Y. 1956.)
9. S. SATO and R. J. CVETANOVIĆ. J. Am. Chem. Soc. **81**, 3223 (1959).
10. R. J. CVETANOVIĆ. J. Chem. Phys. In press.

DECOMPOSITION PRESSURES OF FERRIC SULPHATE AND ALUMINUM SULPHATE[1]

N. A. WARNER[2] AND T. R. INGRAHAM[3]

ABSTRACT

The gas pressures over samples of anhydrous ferric sulphate and anhydrous aluminum sulphate have been measured in a static system, using a mercury manometer in which the exposed surface was covered with a flexible Pyrex bellows. The calculated ΔH for the decomposition of $Fe_2(SO_4)_3$ was +135.4 kcal/mole. It was not possible to calculate the ΔH for the $Al_2(SO_4)_3$ decomposition, because a discrete aluminum oxide with singular thermodynamic properties was not obtained.

In the $Fe_2(SO_4)_3$ system, the fraction of SO_3 in the gas phase was found to be almost constant over the range of temperature and pressure changes used in the study.

At any given temperature, the decomposition pressure over a ferric sulphate sample is greater than that over an aluminum sulphate sample, thus indicating that preferential decomposition of ferric sulphate should be thermodynamically feasible in mixtures of ferric sulphate and aluminum sulphate.

INTRODUCTION

When metallic sulphates are heated *in vacuo* or in a neutral atmosphere, they can be decomposed to oxides, e.g.,

$$MSO_4 \rightleftharpoons MO + SO_3,$$

$$M_2(SO_4)_3 \rightleftharpoons M_2O_3 + 3SO_3.$$

The ease with which this decomposition can be brought about varies widely with the different metallic sulphates. This variation has been utilized commercially in the separation of some sulphates. For example, copper sulphate is more stable than ferric sulphate. Hence, when some ores which contain copper and iron compounds are roasted in controlled sulphating atmospheres, it is possible to prepare copper sulphate almost selectively, while the iron is retained as oxide. Simple leaching techniques effectively separate the soluble copper sulphate from the insoluble iron oxide. The same basic principle of selective sulphate formation or decomposition has been applied industrially for the separation of cadmium and zinc compounds when they occur together in smelting dusts (1).

One of the recently patented methods for separating the constituents of clays and shales (2) would seem to depend on the fact that aluminum sulphate is more stable than ferric sulphate. Since the problem of utilizing the constituents of shale is an important one, the literature was searched to determine whether this assumption were true. Very little information is available on the stability of either compound, and the published data (3) fail to satisfy the critical tests of Kelley (4). Hence, it seemed worth while to measure the decomposition pressures of both of these compounds to determine whether the separation would be thermodynamically possible.

APPARATUS AND PROCEDURE

Because of its simplicity, a static method was chosen for measuring the equilibrium dissociation pressures of the sulphates. The apparatus assembled for the measurements

[1]*Manuscript received July 13, 1960.*

Contribution from the Extraction Metallurgy Division, Mines Branch, Department of Mines and Technical Surveys, Ottawa, Canada.

[2]*Postdoctorate Research Fellow of the National Research Council of Canada, assigned to the Mines Branch. Present address: School of Metallurgy, University of New South Wales, Australia.*

[3]*Head, Research Subdivision.*

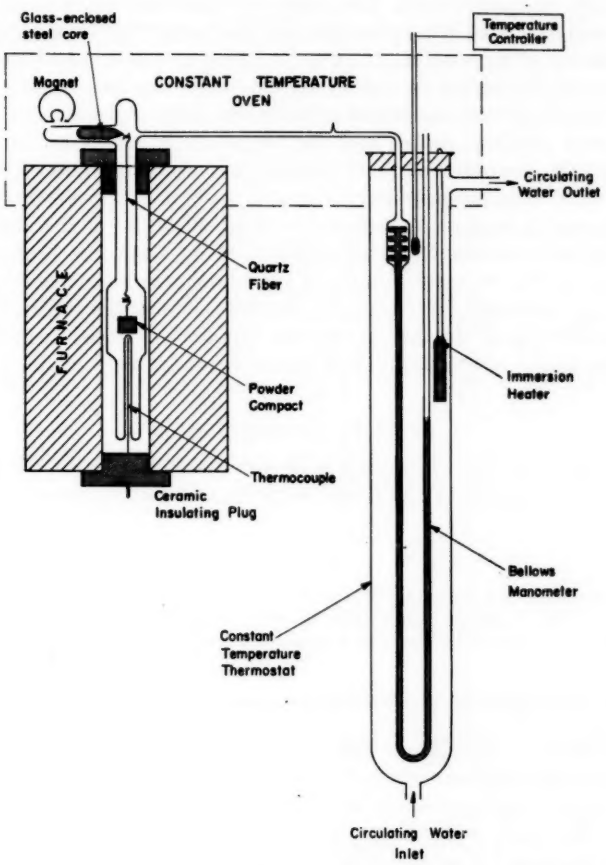

FIG. 1. Apparatus for measuring decomposition pressures of anhydrous sulphates.

is shown diagrammatically in Fig. 1. The most important feature of the apparatus is the glass-bellows mercury manometer. The design of the manometer is based on one originated by Spence (5). However, in the present version the mercury displacement has been modified from horizontal to vertical, and an appreciable increase in sensitivity has resulted (6).

The apparatus was constructed entirely from Pyrex and Vycor glass. The Vycor section extended out to the cool zone of the furnace, where it was joined through graded seals to the Pyrex part of the apparatus.

To avoid complications that might be introduced by the condensation of sulphur trioxide, the bellows manometer and the connecting tubing were thermostatically controlled at a temperature of 60° C.

For convenience in handling, powder compacts of anhydrous ferric sulphate and aluminum sulphate were pressed with a small platinum wire anchored in the pellet. The pellets were suspended by this platinum wire and a small quartz fiber which was attached

to a magnetically moveable hook. The hook was made moveable to permit free access for installing and removing the pellet through the top of the furnace tube.

After installation of each pellet, the reaction tube was sealed and the apparatus was evacuated. During the period of evacuation the pellet was heated to a temperature of about 650° C to remove the last traces of moisture. After several hours at this temperature, the vacuum line was sealed and the temperature raised to the point at which displacement of the mercury column indicated that decomposition of the sulphate had begun. Readings of the pressure were made at 24-hour intervals in the study of the ferric sulphate system, and at 48-hour intervals in the study of the aluminum sulphate system. The experiment was continued until a steady state had been reached.

Displacement of the mercury column in the manometer was observed with a cathetometer, and was corrected for changes in barometric pressure. With small changes in pressure, some sticking of the mercury in the column was noted. Sticking was relieved by rapping the manometer sharply just before readings were made.

RESULTS AND DISCUSSION

The results obtained in experiments with ferric sulphate, with aluminum sulphate, and with 1:1 mole mixtures of aluminum sulphate with iron oxide are shown in Table I.

TABLE I

Decomposition pressures over ferric sulphate, aluminum sulphate, and an aluminum sulphate – iron oxide mixture

Ferric sulphate		Aluminum sulphate		Aluminum sulphate – ferric oxide (mole ratio 1:1)	
Temp. (°C)	Pressure (cm of Hg)	Temp. (°C)	Pressure (cm of Hg)	Temp. (°C)	Pressure (cm of Hg)
				627	1.0
630*	7.3				
638	8.4				
		652*	1.4		
658	14.7				
660*	16.8				
		673*	2.4		
				679	3.2
680*	27.1	680	2.4		
685	28.6				
		694	3.6		
700	41.9				
705*	48.1				
		708	4.5		
715	61.1				
724	72.0				
				724	14.1
		730	7.8		
				736	49.6
				742	54.3
		743	13.5		
				752	71.7
		753	19.4		
		762	28.2		
		769	40.0		
		777	72.0		

*Measurements made with temperature decreasing. All other measurements made with temperature increasing.

Ferric Sulphate

When the results shown in Table I were plotted on a log p versus reciprocal of absolute temperature graph, Fig. 2 was obtained. It will be noted from Fig. 2 that the linearity

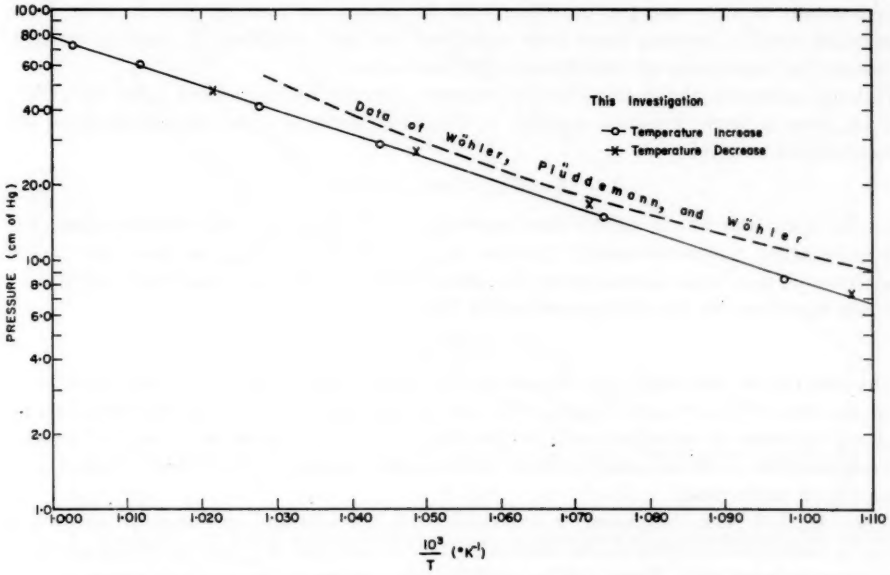

FIG. 2. Pressure vs. reciprocal temperature relationship for anhydrous ferric sulphate.

of the results is good, thus indicating that over the temperature range of the experiments there is not an appreciable change in the heat of the decomposition reaction. The linearity of the results and the demonstrated reversibility of the system indicate that true equilibrium had been reached in the experiments and that the gas phase probably contained only SO_2, SO_3, and O_2. It seems unlikely that polymers of SO_3 were present. The iron oxide product was identified as hematite.

When the static method of measuring the decomposition pressures was selected, the selection was made with some misgiving. From preliminary experiments it had been established that the dynamic method might be subject to substantial errors, because the rate of attainment of equilibrium decreases as equilibrium is approached, and it would be easy to assume that equilibrium had been reached, when in fact the reaction was still proceeding slowly.

Alternatively, the measurement of pressures in a static system containing a substantial temperature gradient and gases of different molecular weights is also subject to error. In this instance, due to thermal diffusion, the lighter molecules tend to congregate in the hotter zone. This means that the 2:1 molar ratio of SO_2:O_2, produced by the decomposition of SO_3, is reduced to somewhat less than 2:1 in the hot zone, and increased to somewhat more than 2:1 in the cold zone. This departure from exact stoichiometry can lead to errors in any quantities, e.g. degree of dissociation, etc., calculated on the basis of the 2:1 stoichiometry.

The magnitude of the error caused by thermal diffusion is difficult to assess on a purely theoretical basis (7), but the linearity of the results shown in Fig. 2 would favor the conclusion that the error is small or at least comparable with the other errors of measurement. Recently a novel method of studying sulphate equilibria, through the measurement of only one gas pressure, was developed by Kellogg (8). It is expected that when similar systems have been examined by both methods, it may be possible to assess the magnitude of the thermal diffusion error.

Having measured the decomposition pressure exerted by the mixed gases SO_3, SO_2, and O_2, over a ferric sulphate sample, it was of interest to calculate the heat of the decomposition reaction

$$Fe_2(SO_4)_3 \rightleftharpoons Fe_2O_3 + 3SO_3 \qquad [1]$$

from the variation of the equilibrium constant of the reaction with temperature. For this calculation it was necessary to know p_{SO_3}, since $K'_p = p^3_{SO_3}$ for reaction 1. The magnitude of p_{SO_3} was calculated on the assumption that p_{SO_3} satisfied both equation 1 and the equation for the decomposition of SO_3,

$$2SO_3 \rightleftharpoons 2SO_2 + O_2. \qquad [2]$$

The calculation was made by obtaining the equilibrium constant K_p, for reaction 2, from the data of Evans and Wagman (9) and converting this K_p to K_x (the equilibrium constant in terms of mole fractions) by dividing by the total pressure at each of a series of temperatures. For convenience and to minimize errors, interpolated temperatures from Fig. 2 were used.

When K_x had been calculated, it was equated to the equilibrium constant which was set up in mole fraction form on the basis that α is the fraction of 1 mole of SO_3 dissociated at a given temperature. Thus, $\{2(1-\alpha)\}/\{(2+\alpha)\}$ represents the mole fractions of SO_3, and $K_x = 4\alpha^3/(4\alpha^3-12\alpha+8)$. It should be noted that in this calculation an exact SO_2:O_2 ratio of 2:1 is implicitly assumed.

When K_x was calculated, it was found to be almost constant, with an average deviation of 1% over the temperature range 920 to 1000° K. The average K_x was used in calculations, and $\alpha = 0.538$ and a mole fraction of $SO_3 = 0.364$ were obtained.

The implications of the constancy of the mole fraction of SO_3 are of interest. Once the value 0.364 is known, the pressure of SO_3 in a system can be set very conveniently by including an excess of ferric sulphate in the system and then heating the system until the total pressure, reduced by the factor 0.364, produces the required partial pressure of SO_3.

When $\log K'_p = p^3_{SO_3}$ was plotted against reciprocal absolute temperature, a linear relationship was obtained. The relationship can be described by the equation:

$$\log K'_p = 28.34 - (29{,}600/T).$$

When this equation was used to calculate the heat of reaction for the dissociation of ferric sulphate, a ΔH of +135.4 kcal was obtained.

Aluminum Sulphate

The results obtained from a study of the decomposition of aluminum sulphate and 1:1 mole mixtures of aluminum sulphate with ferric oxide are shown in Table I and as a log P versus reciprocal temperature relationship in Fig. 3. The curvature of the relationship indicates that the type of treatment accorded the ferric sulphate results to obtain a heat of decomposition would not be valid for the aluminum sulphate systems. It would

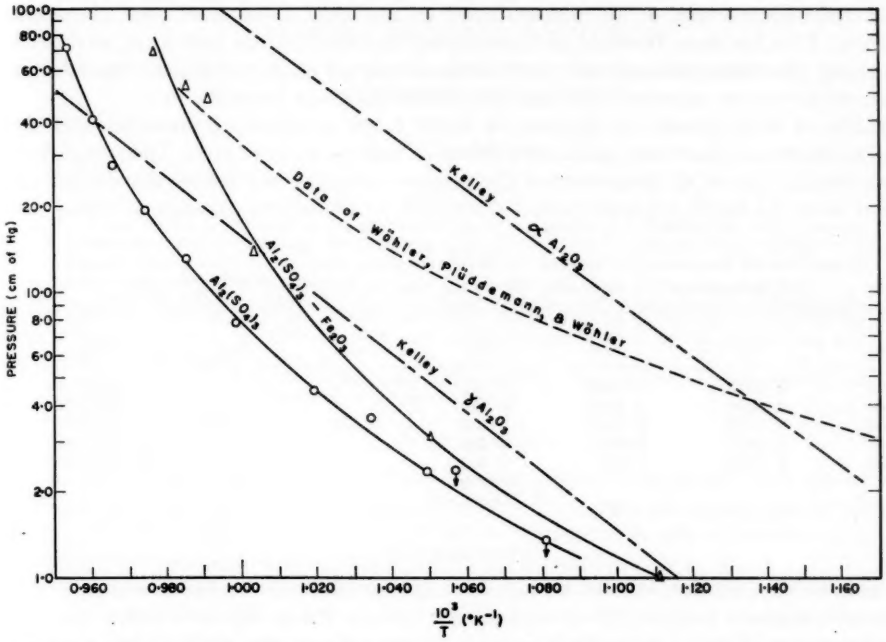

FIG. 3. Pressure vs. reciprocal temperature relationship for anhydrous aluminum sulphate and aluminum sulphate – iron oxide mixtures.

therefore seem sufficient to seek an explanation for the lack of linearity of the results, and to compare the pressures with the corresponding pressures for ferric sulphate, under similar conditions of temperature.

When the partly decomposed and completely decomposed pellets of aluminum sulphate were examined by X-ray diffraction, it was observed that gamma alumina was present. In one pellet which had been heated for a long time at a high temperature, alpha alumina was found. This is in general agreement with the observations of Kelley (10): "In actual decomposition of $Al_2(SO_4)_3$, there is not obtained Al_2O_3 (alpha) but a less stable variety usually designated Al_2O_3 (gamma). Unfortunately the latter appears not to have unique thermodynamic properties; available information indicates that there may be two varieties of Al_2O_3 (gamma) or at any rate that its properties depend upon the temperature to which it is heated and the time of heating." From the foregoing, it would seem possible that the results shown in Fig. 3 represent steady-state pressures over a metastable system of aluminum sulphate and some modification of gamma alumina. The curvature of the line in Fig. 3 could be interpreted as representing the presence of an increasingly stable modification of alumina, as the temperature of the experiments was increased. From a few experiments, there was an indication that the pressure measurements, although steady, were not readily reversible if the temperature of the specimen had previously been raised to appreciably above the temperature of the measurement. This would tend to confirm the presence of the more stable form of alumina at higher temperatures. Time did not permit a more extensive investigation of this point.

It is of interest to note, in Fig. 3, that the stable pressures over the aluminum sulphate –

ferric oxide system are, at all temperatures, greater than those over pure aluminum sulphate. This has been resolved by considering that ferric oxide acts as a catalyst in promoting the formation of the more stable forms of alumina. Higher equilibrium pressures are to be expected over the more stable forms of alumina.

Finally, it is of interest to compare, in Table I, the steady-state pressures over the ferric sulphate and aluminum sulphate systems at various temperatures. The comparison shows clearly that at all temperatures the pressure at any given temperature is always greater over the ferric sulphate system than over an aluminum sulphate system.

TABLE II

Calculations made to determine ΔH for the reaction $Fe_2(SO_4)_3 \rightleftharpoons Fe_2O_3 + 3SO_3$

T (°K)	K_p	P (atm)	K_x	α	N_{SO_3}	K'_p
920	0.0415	0.1466	0.283	0.538	0.364	1.519×10^{-4}
940	0.0706	0.2480	0.284			7.356×10^{-4}
960	0.1172	0.4046	0.290			3.194×10^{-3}
980	0.1914	0.6650	0.288			1.418×10^{-2}
1000	0.3050	1.047	0.291			5.535×10^{-2}
			Average 0.287 ± 0.003			

CONCLUSIONS

From an examination of the steady-state gas pressures over ferric sulphate and aluminum sulphate samples heated in a closed system, it has been concluded that the pressure at any given temperature is always substantially greater over a ferric sulphate sample. Hence, it would seem thermodynamically feasible to separate aluminum sulphate from ferric sulphate by roasting the compounds under conditions selected to decompose the ferric sulphate only, and then leaching the water-soluble aluminum sulphate from the roasted mixture. The practical limitations affecting the application of this approach will be discussed in a later communication.

ACKNOWLEDGMENT

The authors wish to express their thanks to Mr. George Ensell, glassblower at the National Research Council of Canada, for the construction of the bellows manometer used in this project.

REFERENCES

1. R. E. Lund and D. E. Warnes. Trans. AIME, **209**, 608 (1957).
2. R. C. Haff. U.S. Patent No. 2,551,944 (April, 1947).
3. L. Wöhler, W. Plüddemann, and P. Wöhler. Ber. deut. chem. Ges. **41**, 703 (1908).
4. K. K. Kelley. U.S. Bur. Mines, Bull. No. 406, 66, 89 (1937).
5. R. Spence. Trans. Faraday Soc. **36**, 417 (1940).
6. S. N. Flengas and T. R. Ingraham. Can. J. Chem. **38**, 813 (1960).
7. Sir James Jeans. An introduction to the kinetic theory of gases. Cambridge Univ. Press, London. 1959. p. 251.
8. H. H. Kellogg. Private communication.
9. W. E. Evans and D. D. Wagman. J. Research Natl. Bur. Standards, **49**, 141 (1952).
10. K. K. Kelley. U.S. Bur. Mines, Tech. Papers, No. 688, 58 (1946).

STUDIES ON IONIC SOLVATION

PART III. NEW THEORY FOR CALCULATING HEATS OF HYDRATION OF MONOVALENT IONS AT 25° C[1]

A. M. AZZAM

ABSTRACT

From Part I of this series, the structure of solution around a completely hydrated monovalent ion could be visualized. On the basis of this picture, the ionic heats of hydration is to be due to three terms. These three terms are critically discussed and evaluated for the case of alkali metals and halide ions.

The present theory shows that the Born–Bjerrum term contributes a significant part to the heat and that the ionic radius value included in this term must be dependent only on the charge and not on the ionic size. The most probable value is 2.4 Å for the positive ions and 2.9 Å for the negative ions.

The calculated ionic heats of hydration, which are in good agreement with the experimental values, are compared with those of previous theories.

1. INTRODUCTION

The heat of solvation of an ion, which does not combine chemically with the solvent, depends upon the difference in its potential energy in vacuum and in solution. Knowledge of values of ionic heats of solvation is of great importance in the calculation of several physical properties of ionic solutions (9, 12, 15, 37, 41, 42, 44).

Using experimental data on the heats of solution (13, 14, 31), together with the crystal lattice energy values (8, 9, 10, 11, 16), and following Born–Haber cycle, the heats of hydration of alkali halides (see Table I) had been calculated (5, 12). There is no simple

TABLE I

Heats of hydration calculated from the different experimental values of the lattice energy and the heat of solution

Salt \ Reference	(12, 19, 31)	(5)	(37)	(40)
LiF	245.9	246	241.8	
LiCl	211.3	208.8	208.6	213
LiBr	202.5	199.9	197.6	202
LiI	192.4	189.1		191
NaF	217.6	213.9	214.7	
NaCl	184.2	182.4	181.5	183
NaBr	177.6	174.9	175.3	
NaI	167.0	165.5		
KF	198.8	194.6	193.1	206
KCl	165.2	161.5	159.9	159
KBr	157.7	154.5	148	153
KI	147	145.9		
RbF	190.7	187.9		
RbCl	158.9	156.4		
RbBr	151	147.2		
RbI	142.7	138.8		137
CsF		182.4		
CsCl		147.4		
CsBr		139.7		
CsI		131.1		133

[1]*Manuscript received April 14, 1960.*
Contribution from the Chemistry Department, Faculty of Science, A'in Shams University, Cairo, Egypt.

way of dividing these sums into the hydration energies of the separate ions. However, several attempts (3, 5, 6) have been made to deduce from these experimental values the corresponding ionic heats of solvation. None of these methods is completely satisfactory (12, 19, 20, 21).

Moreover, several workers (1, 2, 3, 4, 5, 6, 29, 33) have theoretically calculated the ionic heats of solvation with widely divergent results (see Table II). However, certain features of this work are not entirely satisfactory (7, 18, 19, 24, 46).

TABLE II

Theoretical values of ionic heats of solvation as calculated by different authors

Author / Ion	Group I		Group II				
	Bernal and Fowler (4)	Eley and Evans (3)	Latimer, Pitzer, and Slansky (5)	Verwey (6)	Miscenko (29)	Average of all methods	Azzam
Li^+	136	133	121.2		125	128.8	139.0
Na^+	114	115	94.6		98	105.4	107.9
K^+	94	90	75.8	75	78	83.3	84.6
Rb^+	87	81	69.2			79.4	79.5
Cs^+	80	73	62	53		67	75.1
F^-	97	91	122.6	122		108.2	106.7
Cl^-	65	59	88.7		88	75.2	71.7
Br^-	57	52	81.4		77	66.8	68.0
I^-	47	45	72.1	72	66	60.4	63.7

Recently, the present author (7, 36) suggested a new method for the calculation of ionic solvation number by applying statistical–mechanical analysis to a postulated structure of the solution around an ion. The good agreement between the calculated values and those obtained by several experimental methods is a strong evidence for the validity of the suggested physical approach of the molecular structure of the solvent (7, 36).

The present theory is an attempt to calculate the heats of hydration of alkali metals and halide ions at 25° C.

2. ORIENTATION OF A SOLVENT MOLECULE NEXT TO AN ION

It seems to be generally agreed (3, 4, 7, 46, 47, 49) that the orientation for a water molecule next to a positive ion is as shown in case I, Fig. 1. On the other hand, it has been assumed by previous theories (3, 4, 6, 47, 49) that the orientation for a water molecule next to a negative ion is as shown in case IV, Fig. 1. This configuration was criticized and critically discussed by the present author (7, 18). Accordingly, it was suggested that the most probable structure of the solvated negative ion is as shown in case III, Fig. 1.

A similar conclusion was reached recently by Buckingham (46). In conclusion, cases I and III are energetically more favorable. Less familiar orientations (6, 26, 34) have been already criticized (19, 24).

3. STRUCTURE OF SOLUTION AROUND AN ION

The most outstanding problem, which is connected with the calculation of ionic heats of hydration, lies in the need of definite quantitative knowledge of the structure of solution around an ion. A simple model for the structure of solution around an ion could

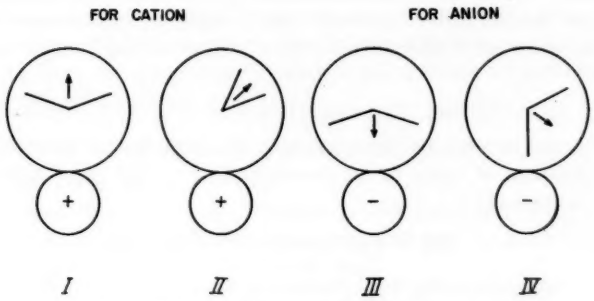

FIG. 1. Orientation of a water molecule next to an ion.

I	II	III	IV
Bernal and Fowler (4), 1933 Eley and Evans (3), 1938 Haggis *et al.* (49), 1952 Azzam (7), 1954 Buckingham (46), 1957	Verwey (6), 1941	Azzam (7), 1954 Buckingham (46), 1957	Bernal and Fowler (4),1933 Eley and Evans (3), 1938 Verwey (6), 1941 Haggis *et al.* (49), 1952

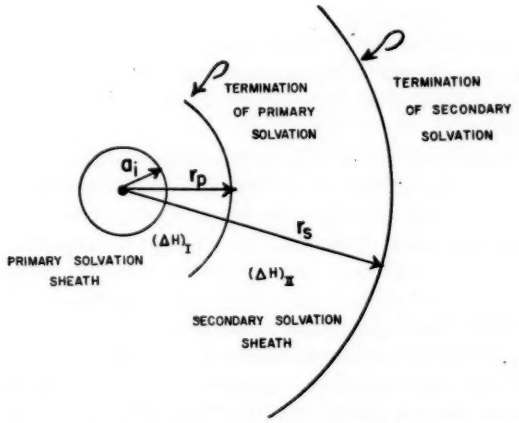

FIG. 2. The proposed structure of solution around a monovalent ion.
a_i = crystallographic radius of the ion,
r_p = radius of the primary solvated ion,
r_s = radius of the completely solvated ion.

be visualized from the present author's statistical-mechanical analysis (7) for the distribution of solvent dipoles around an ion.

The model suggested by these results is shown diagrammatically in Fig. 2. The firmly bound water molecules will be those constituting the primary solvation sheath (the innermost region). Beyond this sheath, there is the secondary solvation sheath with less firmly bound water molecules and finally there is the main bulk of the solvent (for definition see 7, 36).

Frank and Evans, from a re-analysis of the entropy of hydration (43), have developed a fundamentally similar picture. These authors claim that the ion is surrounded by three

concentric regions which are: the immobilization of water molecules, the structure-breaking and the structurally "normal" water regions. These three zones seem very probable to correspond with the three layers of the preceding model (see Fig. 2).

4. NEW THEORY FOR CALCULATING HEATS OF HYDRATION

From the proposed structure of ionic solution, the ionic heat of hydration is represented essentially by the sum of three terms corresponding to the three zones around an ion (see Fig. 2). It follows that

$$[1] \qquad \Delta H = (\Delta H)_{\mathrm{I}} + (\Delta H)_{\mathrm{II}} + (\Delta H)_{\mathrm{III}}$$

where $(\Delta H)_{\mathrm{I}}$ represents the contribution of water dipoles in the primary solvation sheath to (ΔH),

$(\Delta H)_{\mathrm{II}}$ represents the contribution of water dipoles in the secondary solvation sheath to (ΔH),

$(\Delta H)_{\mathrm{III}}$ represents the contribution of water dipoles beyond the solvation sheaths to (ΔH). In other words, it is the contribution of transferring an ion from the gas phase into solution.

The magnitudes of various contributions to ΔH for alkali metals and halide ions are discussed in Section 5 of this paper.

Concerning the structure of the primary solvation shell, a very clear physical picture, which is suitable for our purpose, is known from the present author's previous results (7). This is discussed in Section 3 of this paper. Accordingly the most probable value of $(\Delta H)_{\mathrm{I}}$ could be evaluated.

The secondary solvation layer (see Fig. 2) is the intermediate zone between the frozen water (7, 18, 19, 41, 43) region and the normal structure region. Calculation of the term $(\Delta H)_{\mathrm{II}}$ requires definite and quantitative knowledge of the structure-breaking effect (43, 48). Such a knowledge is not available. Any attempt to estimate the numerical magnitude of this structure-breaking effect must be based on rather arbitrary assumptions for which in the first instance no strict justification can be given.

As long as we consider the alkali metals and halide ions, it is not known whether or not, and to what extent, this structure-breaking effect is important in the calculation of heats of hydration. It seems very probable that such an order–disorder phenomenon is of significant importance for the calculations of entropies but not for the calculation of heats (49).

In the present theory, we will follow the most physical approach which was adopted by Buckingham (46) and treat the solvent beyond the primary solvation shell as a continuous dielectric, that is, a dielectric constant which can vary with the electric field strength.

We do not know how much error is involved in this approximation, but the effect is in any case of insignificant magnitude and could be checked in the following way.

CsI is usually regarded as having the relatively most marked structure-breaking effect (43, 45). In this case, $(\Delta H)_{\mathrm{II}}$ contributes 8.7% to the total (ΔH). Assuming, as the result of neglecting the structure-breaking effect, a maximum of 25% error in the value of $(\Delta H)_{\mathrm{II}}$, this will give rise to a maximum error of about 2.2% in the value of $(\Delta H)_{\mathrm{total}}$.

A serious difficulty in the previous theories (3, 4, 5, 6, 8) is the choice of dielectric model. This problem was treated to a first approximation on the basis that very near to the ion the dielectric constant is taken as 1 and for layers of water molecules outside the first

layer it is taken as 80. In the present theory a less approximate treatment of the dielectric constant difficulty has been attempted by the application of Webb's analysis (2). It must be pointed out here that the structure-breaking effect, which is neglected in the present theory, is either partially or completely covered on using Webb's values for the dielectric constant as a function of distance.

5. VARIOUS CONTRIBUTIONS TO (ΔH)

(a) Evaluation of the Term $(\Delta H)_{\mathrm{I}}$

Consider an element volume (dv) at a distance (r) from an ion in the primary solvation sheath. If $(ds)_r$ is the number of dipoles associated with the ion in this element volume and $(u)_r$ is the ion–dipole interaction, it follows that

$$d(\Delta H) = (ds)_r\, u_r. \qquad [2]$$

The present author's statistical–mechanical analysis (7) showed that the number of dipoles associated with the ion in a concentric shell at a uniform distance (r) from the ion and of thickness (dr) is given by

$$(ds)_r = 4\pi n_0\, e^{-[(w_r - w_0)/kT]}\, r^2\, dr \qquad [3]$$

where

n_0 is the number of water molecules per cubic centimeter in the bulk of solution,
w_0 is the potential of a water molecule in the bulk of solution,
w_r is the net potential energy of a solvent dipole at a distance (r) from the ion.

Taking into account the specific factors on which the solvation number depends (7, 18), together with the suggested structure of a solvated ion, the net interaction energy term (w_r) could be evaluated from the following equation.

$$w_r = (u_1 - u_2 - u_3)_r \qquad [4]$$

where

u_1 is the ion–dipole interaction energy,
u_2 is the electrostatic potential due to the presence of the two water molecules attached to the dipole which is associated with the ion (3, 4, 7, 36), and
u_3 is to allow for the mutual effect of the co-ordinated water molecules.

Substituting from [3] into [2]

$$d(\Delta H_{\mathrm{I}})_r = 4\pi n_0\, u_r\, e^{-[(w_r - w_0)/kT]} r^2\, dr. \qquad [5]$$

The contribution of water molecules in the primary solvation sheath could be evaluated by integrating equation [5] over the volume of the solvent that surrounds the ion from a_1 to r_p (limits of primary solvation (see Fig. 1)).

$$(\Delta H)_{\mathrm{I}} = 4\pi n_0 \int_{a_1}^{r_p} u_r\, e^{-[(w_r - w_0)/kT]}\, r^2\, dr. \qquad [6]$$

(b) Evaluation of the Term $(\Delta H)_{\mathrm{II}}$

This term could be evaluated in a similar manner as in the case of $(\Delta H)_{\mathrm{I}}$. The main differences between the two cases lie in the values of the limits of integration and also in the expression of the term (w_r). A solvent molecule in the secondary solvation sheath is no longer associated with the ion (4, 7, 12, 19) but it is only under the influence of its field.

[7] $$d(\Delta H)_{II} = 4\pi n_0 u_r e^{-\{(u_r - w_0)/kT\}} r^2 dr.$$

The integration will be carried out over the volume of the solvent that surrounds the ion from the distance at which the primary solvation ceases (r_p) to the distance at which secondary solvation terminates (r_s).

From the above discussion, it follows that

[8] $$(\Delta H)_{II} = 4\pi n_0 \int_{r_p}^{r_s} u_r e^{-\{(u_r - w_0)/kT\}} r^2 dr.$$

(c) Evaluation of the Term $(\Delta H)_{III}$

Whenever an ion passes from the gas phase into solution, the free energy of this process is best given by Born expression (1),

[9] $$\Delta G = -\frac{N(Ze)^2}{2x}\left(1-\frac{1}{D}\right),$$

where N is the Avogadro's number,
Ze is the charge of the ion,
x is the radius of the ion,
D is the dielectric constant of the medium.

The corresponding heat of hydration (Q) is obtained from the Gibbs–Helmholtz equation as

[10] $$Q = -\frac{N(Ze)^2}{2x}\left\{1-\frac{1}{D}-\frac{T}{D^2}\left(\frac{\partial D}{\partial T}\right)_p\right\}$$

(Born–Bjerrum equation) (32).

The term $(\Delta H)_{III}$ of the present theory (see equation [1]) can be evaluated from equation [10] provided that the selected value of "x" will be taken as r_s (the termination of solvation). It follows that

[11] $$(\Delta H)_{III} = -\frac{N(Ze)^2}{2r_s}\left\{1-\frac{1}{D}-\frac{T}{D^2}\left(\frac{\partial D}{\partial T}\right)_p\right\}.$$

(d) Evaluation of the Ionic Heats of Hydration

On substituting from equations [6], [8], and [11] into (1), the total ionic heat of hydration is given by

[12] $$(\Delta H)_{total} = 4\pi n_0 \int_{a_1}^{r_p} u_r e^{-\{(w_r - w_0)kT\}} r^2 dr + 4n_0 \int_{r_p}^{r_s} u_r e^{-\{(u_r - w_0)kT\}} r^2 dr + \frac{N(Ze)^2}{2r_s}\left\{1-\frac{1}{D}-\frac{T}{D^2}\left(\frac{\partial D}{\partial T}\right)_p\right\}.$$

6. METHOD OF CALCULATION

Methods of evaluations of u_1, u_2, u_3, r_p, r_s, n_0, w_0, and w_r have already been critically discussed in a previous paper (7) by the present author. It must be pointed out that in these calculations, microscopic values of the dielectric constant (2, 7) of water at different distances from the ion are used.

The integration terms of equation [12] cannot be evaluated directly. However, these integrations were solved graphically.

All data which are needed for the calculation of the term $(\Delta H)_I$ are recorded in Table III. The corresponding relation

$$u_r e^{-[(w_r - w_0)/kT]r^2} - r,$$

which is required for the graphical evaluation of $(\Delta H)_I$ (see equation [6]), is plotted in Fig. 3.

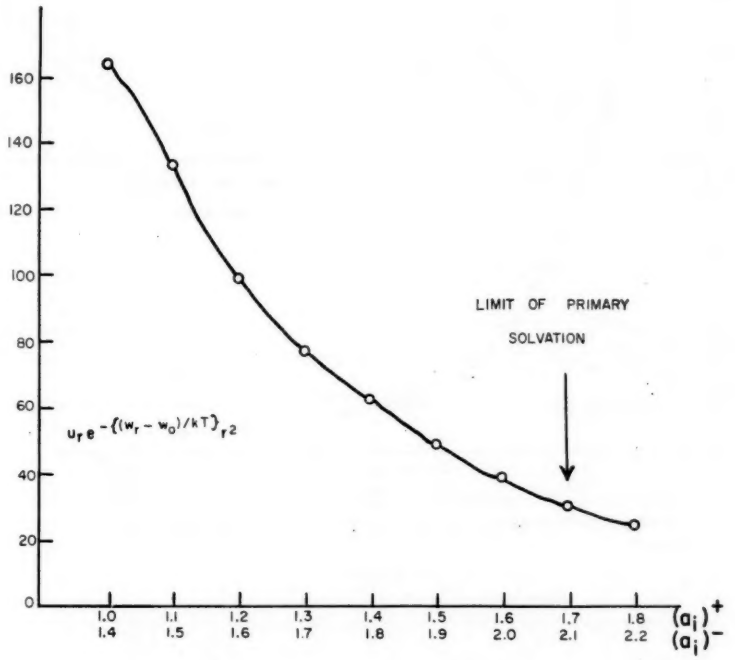

FIG. 3. The relation between $u_r e^{-[(w_r - w_0)/kT]r^2}$ and ionic radii.

TABLE III

Data needed for the calculation of $(\Delta H)_I$

a_i	u_1	u_2	u_3	$e^{-[(w_r - w_0)/kT]r^2}$	$u_r e^{-[(w_r - w_0)/kT]r^2}$, kg cal/g ion	$(\Delta H)_I$
1.0	0.1490	0.012	0.0291	76.5	164.14	6.93
1.1	0.1323	0.0116	0.0194	70.1	133.36	5.63
1.2	0.1168	0.0113	0.0138	59.5	99.74	4.22
1.3	0.1047	0.011	0.0094	51.6	77.8	3.28
1.4	0.0937	0.0107	0.0061	47.1	63.55	2.68
1.5	0.0836	0.0105	0.0044	41.2	49.6	2.09
1.6	0.0751	0.0104	0.0032	36.7	39.69	1.68
1.7	0.0667	0.0102	0.0025	32.3	31.02	1.31
1.8	0.06	0.0101	0.0019	29.6	25.58	1.08

The area underneath this curve between the specific limits is equal to $(\Delta H)_I/4\pi n_0$. Similarly, all data which are required for the evaluation of the term $(\Delta H)_{II}$ are given in Table IV and the required graphical relation is plotted in Fig. 4. The area underneath

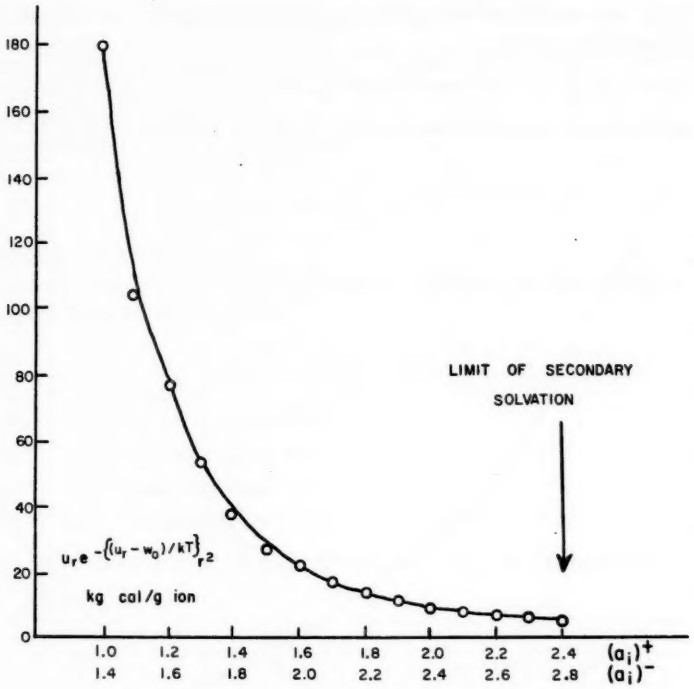

FIG. 4. The relation between $u_r e^{-\{(u_r - w_0)/kT\} r^2}$ and ionic radii.

TABLE IV

Data needed for the calculation of $(\Delta H)_{II}$

a_i	u_1	$e^{-\{(u_r - w_0)/kT\} r^2}$	$u_r e^{-\{(u_r - w_0)/kT\} r^2}$ kg cal/g ion	$(\Delta H)_{II}$
1.0	0.1490	198.0	179.3	48.6
1.1	0.1323	141.6	113.9	35.4
1.2	0.1168	109.4	77.6	25.8
1.3	0.1047	83.5	53.3	19.9
1.4	0.0937	67.0	38.1	15.2
1.5	0.0836	54.3	27.6	12.9
1.6	0.0751	49.5	22.6	9.1
1.7	0.0667	42.8	17.5	6.9
1.8	0.0600	38.7	14.1	5.2
1.9	0.0539	35.3	11.6	3.9
2.0	0.0482	32.5	9.5	2.9
2.1	0.0437	30.7	8.2	2.0
2.2	0.0399	29.7	7.2	1.2
2.3	0.0369	28.5	6.3	0.6
2.4	0.0322	27.2	5.2	0.0

this curve between the specific limits is equal to $(\Delta H)_{II}/4\pi n_0$. The theoretically calculated values of $(\Delta H)_I$, $(\Delta H)_{II}$, $(\Delta H)_{III}$, and $(\Delta H)_{total}$ for all the alkali metals and the halide ions are shown in Table V and the corresponding relationships to ionic radius are represented graphically in Fig. 5.

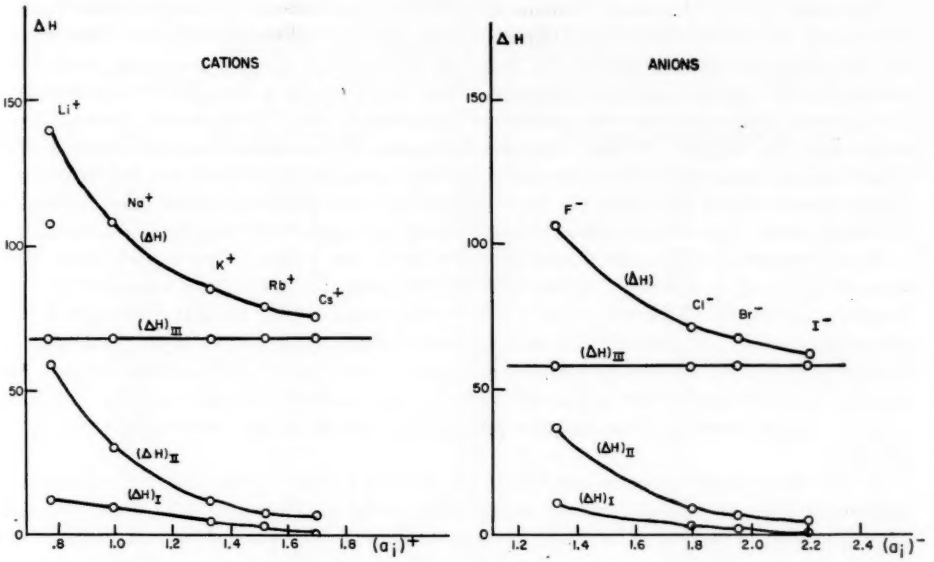

FIG. 5. Theoretically calculated values of $(\Delta H)_{\mathrm{I}}$, $(\Delta H)_{\mathrm{II}}$, $(\Delta H)_{\mathrm{III}}$, and $(\Delta H)_{\mathrm{total}}$ for the alkali metals and halide ions.

TABLE V

Theoretically calculated ionic heats of solvation using equation [12] (in kg cal/g ion at 25° C)

	Cations					Anions			
	Li^+	Na^+	K^+	Rb^+	Cs^+	F^-	Cl^-	Br^-	I^-
a_i	0.78	1.00	1.33	1.52	1.7	1.33	1.8	1.96	2.2
$(\Delta H)_{\mathrm{I}}$	12.6	9.7	4.5	2.8		11.2	3.7	2.5	
$(\Delta H)_{\mathrm{II}}$	59.0	30.0	12	7.5	6.9	37	9.5	7.0	5.2
$(\Delta H)_{\mathrm{III}}$	68.2	68.2	68.2	68.2	68.2	58.5	58.5	58.5	58.5
$(\Delta H)_{\mathrm{total}}$	139.8	107.9	84.7	78.5	75.1	106.7	71.7	68.0	63.7

7. DISCUSSION

The various theoretical calculations of ionic heats of solvation (3, 4, 5, 6, 29) do not give values which are in good agreement (see Table IV). However, some measure of agreement is obtained among the results if they are classified in such a way as to compare theories which are self-consistent. Accordingly, previous theories could be divided into two main groups:

group I: (1) Bernal and Fowler theory, (2) Eley and Evan theory;
group II: (1) Latimer *et al.* theory, (2) Verwey theory, (3) Miscenko theory.

A comparison between the results of the present theory and those of previous theories is of interest. The most important fact which arises from this analysis is that theories of group I give higher values for the positive ions, lower values for the negative ion while theories of group II show the reverse. It follows that the agreement of the present calculation with the average values of all previous theories is good (see Table II).

The numerically calculated values of ionic heats of hydration from the theories of group II (mainly that of Latimer *et al.*) disagree with those of the present theory. Their values for the positive ions are smaller by about 10–18 kg cal/g ion. On the other hand, their values for the negative ions are higher by about 10–18 kg cal/g ion. This is mainly due to an incorrect assumption in the method of calculation (19, 21). However, these authors claim that the validity of their theories rest upon the comparison of their values with experimental values which have been obtained by a procedure in which the validity of the theory under test is assumed (12, 18, 19, 20, 21, 23, 24). Moreover, their results disagree markedly with those of theories of group I which are apparently theoretically valid.

It is of interest to compare values obtained from the present theory with those from theories of group I. Table IV shows that all the group I values of the negative ions are lower by about 10–18 kg cal/g ion^{-1}. The fundamental reason for this difference is that the orientation of a water molecule near an anion, which is postulated in the present work, differs from that of authors of theories of group I (see Fig. 1) (7, 46). However, if the present author's model, which was successfully used in the calculation of ionic solvation number (7), is used in these authors procedures, values of the correct order could be obtained.

On the other hand, numerical values of Bernal and Fowler for the case of cations are in agreement with those of the present theory. The model of orientation of a water molecule near a cation is the same in both theories of Bernal and Fowler, and theories of the present author. This fact is a further supporting evidence for the explanation of the discrepancy found in the case of anions.

Using the same model as that of Bernal and Fowler, but subjecting the theory to a more vigorous treatment, Eley and Evans' calculated values show a better agreement with those of the present theory (see Table IV).

The small difference in the case of cations between the present theory and those of the theories of group I may be the consequence of the very approximate treatment given by these authors to the variation of dielectric constant with distance in which two zones were considered. The first layer near an ion is assumed to have $D = 1$ whereas the value $D = 80$ is used elsewhere. This picture is oversimplified (2, 7, 12, 18, 19, 27, 28, 35).

In conclusion, there is an essential agreement between the results of the present theory and those of the more reliable theories of group I.

It is to be stressed that some of the previous theories suffer from mixing of heat and free energy terms which may introduce an ambiguity of 3 to 30 kcal (19). However, this was avoided in the present theory (38).

The real test is to compare theoretically calculated and experimental values, but experimental values of ionic heats of hydration cannot be directly measured. The problem of evaluating individual heats of solvation depends on the assumption used in dividing up the experimental values. None of these methods can be considered as completely satisfactory (12, 19, 20, 21, 46). This difficulty hinders the checking of the theoretical values. However, the present theory can be verified by adding up the calculated ionic values to give values for the corresponding salts which can be then compared with the most reliable experimental results. This method of checking can only be applied to the present theory and to Eley and Evans' theory since all the other theories are semi-empirical ones (they depend on experimental values).

The good agreement which is shown in Table VI is a further indication of the validity of the present theory.

TABLE VI

Comparison between the theoretically calculated and experimentally determined values of heats of hydration of alkali halides

Salt	Results of experimental methods (mean of four sets (see Table I))	Theoretically calculated values	
		Azzam	Eley and Evans' theory (3)
LiF	244.4	245.7	224
LiCl	210.4	210.7	192
LiBr	200.5	207	185
LiI	190.8	202.7	178
NaF	215.4	214.6	206
NaCl	182.8	179.6	174
NaBr	175.9	175.9	167
NaI	166.3	171.6	160
KF	198.1	191.3	185
KCl	161.4	156.3	153
KBr	153.5	152.6	146
KI	146.5	148.3	139
RbF	189.3	186.2	172
RbCl	157.6	151.2	140
RbBr	149.1	147.5	133
RbI	139.1	143.2	126
CsF	182.4	181.8	164
CsCl	147.4	146.8	132
CsBr	139.7	143.1	125
CsI	132.0	138.8	118

8. "THE THIRD TERM OF EQUATION 12" BORN'S HEAT TERM

One of the most important conclusions arising from the present work is that the third term of equation [12] makes a significant contribution to the ionic heats of solvation (see Table V). Accordingly, a discussion of this term which has been used in all previous theories (1, 2, 3, 4, 5, 6) is of interest.

The main difficulty, which arises in the application of equations [9] and [10] in the calculation of ionic solvation energies, is the choice of the ionic radius (term x).

A list of the selected values of "x" in the different theories, which calculated the ionic solvation energies of alkali metal and halide ions, is as follows:

Theory	Selected value of x in Å	Remarks
Born (1)	a_i	Crystallographic radius
Latimer *et al.* (5)	$a_i+0.1$ (for anions) $a_i+0.85$ (for cations)	Assuming that $[\Delta G\ \alpha(1/r)]$
Eley and Evans (3)	$a_i+2r_{H_2O}$ ($2r_{H_2O} = 2.76$)	Arbitrary
Verwey (6)	$a_i+2r_{H_2O}$	Arbitrary
Bernal and Fowler (4)	2.9	Empirically
Azzam	2.4 (for cations) 2.8 (for anions)	Statistical–mechanical limit of solvation

With the exception of Bernal and Fowler and the present author's theories, the selected value of (x) is a function of the crystallographic ionic radii. Evidence given by these

authors in support of their selections are not completely satisfactory and have been criticized (4, 12, 19, 21, 22).

Bernal and Fowler suggested that "x" should represent the radius of the saturation sphere around the ion and pointed out that it must be dependent only on the charge and not on the ionic size. A similar picture has been given by Passynaski (39).

Bernal and Fowler suggested the value of 2.9 Å as the radius of the saturation sphere. There is an essential agreement between Bernal and Fowler's value and those of the present theory. The small differences in these values may arise from the very approximate treatment given by Bernal and Fowler (7, 19). Furthermore, Bernal and Fowler have derived their value 2.9 Å empirically while the values given in the present theory (2.4 and 2.8 Å) were calculated statistically–mechanically. Moreover, Bernal and Fowler did not differentiate between the case of cations and anions as in the present theory. However, due to the difference in the mode of orientation of water dipoles in the case of cations and the case of anions we should expect different values of the radius of the saturation sphere.

9. GENERAL REMARKS

It must be pointed out that all calculations of this kind by the author and by previous workers are beset with inherent difficulties (46, 47). The most important ones are probably the ordered structure of water, the effect of ions on it, and the time factors involved in the movement of water molecules near an ion.

This is mainly due to our incomplete state of knowledge of polar dielectrics. However, with the aid of some reasonable assumptions, it has been found possible to make successful attempts. These limitations must be borne in mind in judging the quantitative conclusions for such calculations.

10. CONCLUSIONS

1. Three layers around an ion contribute to ionic heats of solvation. These layers are:
   - (*a*) primary solvation sheath with contribution = $(\Delta H)_{\mathrm{I}}$,
   - (*b*) secondary solvation sheath with contribution = $(\Delta H)_{\mathrm{II}}$,
   - (*c*) main body of water with contribution = $(\Delta H)_{\mathrm{III}}$.
2. The following critical conditions have been derived:

Conditions	Remarks	$(\Delta H)_{\text{total}}$
Monovalent cations with radius less than 1.7 Å Monovalent anions with radius less than 2.1 Å	Primary and secondary hydrated	$(\Delta H)_{\mathrm{I}}+(\Delta H)_{\mathrm{II}}+(\Delta H)_{\mathrm{III}}$
Monovalent cations with radius less than 2.4 and greater than 1.7 Å Monovalent anions with radius less than 2.8 and greater than 2.1 Å	Secondary hydrated	$(\Delta H)_{\mathrm{II}}+(\Delta H)_{\mathrm{III}}$
Monovalent ions with radius beyond the above-mentioned limits	Unhydrated	$(\Delta H)_{\mathrm{III}}$

3. Both $(\Delta H)_{I}$ and $(\Delta H)_{II}$ can be calculated by statistical-mechanical analysis, while $(\Delta H)_{III}$ is best obtained from the Born–Bjerrum equation.

4. The effective radius term of Born–Bjerrum term is theoretically found to be 2.4 Å for cations and 2.8 Å for anions.

5. Theoretically calculated ionic heats of solvation are in good agreement with experimental values.

6. This theory supports the suggested physical approach concerning the orientation of a water molecule next to an ion and the structure of ionic solutions.

REFERENCES

1. M. Born. Verhandl. deut. physik. Ges. **21**, 13, 679 (1919).
   F. Haber. Verhandl. deut. physik. Ges. **21**, 750 (1919).
   K. Fajans. Verhandl. deut. physik. Ges. **21**, 549, 709 (1919).
   M. Born. Z. physik, **1**, 45 (1920).
2. T. J. Webb. J. Am. Chem. Soc. **48**, 2589 (1926).
3. D. D. Eley and M. G. Evans. Trans. Faraday Soc. **34**, 1093 (1938).
4. J. D. Bernal and R. H. Fowler. J. Chem. Phys. **1**, 515 (1933).
5. W. M. Latimer, K. S. Pitzer, and C. M. Slansky. J. Chem. Phys. **7**, 108 (1939).
   W. M. Latimer, K. S. Pitzer, and W. V. Smith. J. Am. Chem. Soc. **60**, 1829 (1938); J. Chem. Phys. **23**, 90 (1955).
   R. E. Powell and W. Latimer. J. Chem. Phys. **9**, 1139 (1951).
6. E. J. W. Verwey. Rec. trav. chim. **61**, 127 (1942).
   E. J. W. Verwey. Rec. trav. chim. **60**, 887 (1941).
7. A. M. Azzam. Z. Elektrochem. **58**, 889 (1954).
8. M. L. Huggins. J. Chem. Phys. **5**, 143 (1937).
9. H. Falkenhagen. Electrolyte, Leipzig. 1953.
10. E. Lange. Z. physik. Chem. **116**, 337 (1925).
11. J. Slater. Phys. Rev. **23**, 488 (1924).
12. G. Kortüm and J. Bockris. Textbook of electrochemistry. Elsevier. 1951.
13. F. Bichowski and F. D. Rossini. Thermochemistry of chemical substances. New York. 1936.
14. Landolt-Börnstein. Physikalisch-Chemische Tabellen. Springer, Berlin. p. 1505.
15. E. A. Moelwyn-Hughes. Physical chemistry. Cambridge University Press. 1947.
16. A. E. Van Arkel and J. H. de Boer. Chemical binding. Leipzig. 1931.
17. E. A. Moelwyn-Hughes. Proc. Cambridge Phil. Soc. **45**, 477 (1949).
18. A. M. Azzam. Thesis, London. 1949.
19. J. Bockris. Modern aspects of chemistry. London. 1954.
20. K. Fajans. Z. Elecktrochem. **34**, 502 (1928).
21. A. N. Frumkin. J. Chem. Phys. **7**, 552 (1939).
22. Strehlow. Z. Elecktrochem. **56**, 119 (1952).
23. D. Eley. Trans. Faraday Soc. **35**, 1281 (1939).
24. E. S. Compell. J. Chem. Phys. **20**, 1411 (1952).
25. Symposium on Hydrophobic Colloids, Utrecht. 53 (1937).
26. E. J. W. Verwey. Chem. Weekblad, **37**, 530 (1940).
27. H. Franck. J. Am. Chem. Soc. **63**, 1789 (1941).
28. J. Malsch. Z. Physik, **30**, 837 (1929).
29. K. P. Miscenko. Acta Physicochim. U.R.S.S. **3**, 693 (1935).
30. O. Klein and E. Lange. Z. Elecktrochem. **43**, 570 (1937).
31. G. Scatchord. J. Chem. Phys. **9**, 34 (1941).
    A. Eucken. Test book of chemical physics II, 2, 992. Leipzig. 1944.
    G. Scatchord. J. Am. Chem. Soc. **53**, 2037 (1931).
32. N. Bjerrum and Larsson. Z. physik. Chem. **127**, 358 (1927).
33. E. A. Moelwyn-Hughes. Proc. Cambridge Phil. Soc. **45**, 477 (1949).
34. J. Lennard-Jones and J. A. Pople. Proc. Roy. Soc. (London), A, **205**, 155, 161 (1951).
35. Debye. Marx Handbuch der Radiologie. Leipzig. 6, 618, 680. 1925.
    C. H. Collie, J. B. Hasted, and D. M. Ritson. J. Chem. Phys. **16**, 1 (1948).
    G. Schwartzenbach. Z. phys. Chem. A, **176**, 133 (1936).
36. A. M. Azzam. Can. J. Chem. **38**, 993 (1960).
37. J. A. V. Butler. Chemical thermodynamics. Macmillan, London. 1946.
38. H. Remy. Inorganic chemistry, Elsevier. 1956.
39. A. Passynsky. Acta Physicochim. U.R.S.S. **8**, 385 (1938).
40. P. Darmois. J. phys. radium, **2**, 2 (1941).
41. Interaction in Ionic Solutions. Discussions Faraday Soc. No. 24 (1957).
42. G. Milazzo. Elecktrochemie, Theoretische Grundlagen und Anwendunigen. Vienna. 1952.
    H. Harned and B. Owen. The physical chemistry of electrolytic solutions. Reinhold, New York. 1950.
43. H. S. Frank and M. G. Evans. J. Chem. Phys. **13**, 507 (1945).
    H. S. Robinson and A. L. Robinson. J. Chem. Phys. **8**, 933 (1940).
    H. S. Frank and Wen-Yang Wen. Discussions Faraday Soc. No. 24, 133 (1957).

44. R. GURNEY. Ionic processes in solution. McGraw-Hill, New York. 1953.
45. D. D. ELEY. Discussions Faraday Soc. No. 24, 219 (1957).
46. A. D. BUCKINGHAM. Discussions Faraday Soc. No. 24, 151 (1957).
47. C. A. COULSON and D. H. EVERETT. Trans. Faraday Soc. **36**, 633 (1940).
48. A. EUCKEN. Z. Elektrochem. **51**, 6 (1948).
49. G. H. HAGGIS, J. B. HASTED, and T. J. BUCHANAN. J. Chem. Phys. **20**, 1452 (1952).

2,3-*O*-ISOPROPYLIDENE-L-ERYTHROTETRURONIC ACID AND -L-ERYTHROSE, AND THE METHYL D-ERYTHRO- AND D-THREO-TETROFURANOSIDES[1]

J. N. BAXTER[2] AND A. S. PERLIN

ABSTRACT

Oxidation of 2,3-*O*-isopropylidene-β-L-rhamnose (I) with hypoiodite, followed by periodate cleavage of the derived aldonic acid, affords 2,3-*O*-isopropylidene-L-*erythro*tetruronic acid. Reduction of I with sodium borohydride and periodate oxidation of the resulting glycitol gives 2,3-*O*-isopropylidene-L-erythrose. Both products have been obtained in high yield, and are readily hydrolyzed to L-*erythro*tetruronic acid and L-erythrose, respectively.

Methyl α- and β-D-*erythro*- and D-*threo*-tetrofuranosides have been prepared by the Fischer glycoside synthesis from D-erythrose- and D-threose-formates, respectively. A notable anomeric difference in the lead tetraacetate oxidation behavior of the methyl D-threosides has been observed, the β-anomer being more reactive than the α-anomer.

In continuing earlier studies in this laboratory on the chemistry of the tetrose sugars (1, 2, 3, 4) several new tetrose derivatives have been prepared and are described in the current paper.

Stepwise degradation of D-glucuronic and D-galacturonic acids to D-*erythro*- and D-*threo*-tetruronic acids, respectively, by lead tetraacetate oxidation has been described previously (3). Since the L-isomers of these hexuronic acids are rare compounds, they do not provide practical sources of the L-tetruronic acids. The L-*threo*-isomer has been prepared by selective reduction of 2,3-di-*O*-acetyl-L-tartaric anhydride (5) and by oxidative degradation of D-glucosaccharo-γ-lactone (6), but the L-*erythro*-acid does not appear to have been reported. In the current paper a method is described for preparing L-*erythro*tetruronic acid from readily available 2,3-*O*-isopropylidene-L-rhamnose (7) (I). The latter derivative also has been utilized to prepare L-erythrose in high yield.

Acetonation of L-rhamnose in the presence of hydrogen chloride (7) appears to yield the 2,3-*O*-isopropylidene derivative almost exclusively. Two crystalline forms of monoacetone L-rhamnose have been described (8, 9) but only the β-anomer (9) has been isolated in the present study. The isopropylidene derivative (I) was oxidized with hypoiodite (10) to the L-rhamnonate (II) and the latter, which was not isolated, was degraded by periodate cleavage. From the reaction mixture crystalline 2,3-*O*-isopropylidene-L-*erythro*tetruronic acid (III) was isolated in about 75% yield. Chromatographically pure L-*erythro*tetruronic acid was readily obtained by autohydrolysis of III in aqueous solution.

Reduction of isopropylidene-β-L-rhamnose (I) to the rhamnitol derivative (IV), followed by periodate oxidation, afforded crystalline 2,3-*O*-isopropylidene-L-erythrose (V) in about 80% yield. The L-glycitol derivative (IV) was obtained as a syrup by catalytic hydrogenation but, with sodium borohydride reduction, attempts to isolate it resulted in partial hydrolysis of the isopropylidene group. For preparation of V, however, it was most convenient to carry out the reduction with borohydride and, after neutralizing the reaction mixture, to continue directly with the periodate cleavage step. Such a procedure was used by Ballou (11) in converting 3,4-*O*-isopropylidene-D-arabinose to the D-isomer

[1]*Manuscript received June 23, 1960.*
Contribution from the National Research Council of Canada, Prairie Regional Laboratory, Saskatoon, Saskatchewan. Presented in part at the 4th Western Regional Conference, Chemical Institute of Canada, Winnipeg, September 4, 1958.
Issued as N.R.C. No. 5988.
[2]*National Research Council of Canada Postdoctorate Fellow, 1956–1958.*

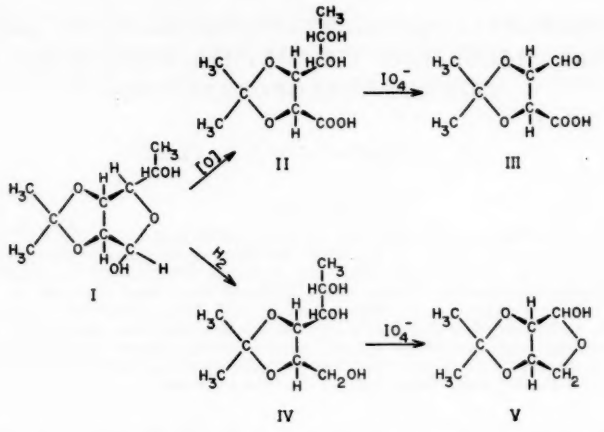

of V. Ballou's method, it will be noted, can also readily furnish V itself by starting with L-arabinose, but the required isopropylidene-pentose derivative is less readily prepared than is the monoacetone-L-rhamnose used in the current study.

Hydrolysis of 2,3-*O*-isopropylidene-L-erythrose with dilute acid afforded chromatographically pure L-erythrose. The calculated $[\alpha]_D$ of the latter sugar was +39°, somewhat higher numerically than most values reported earlier for the D- or L-isomer (see ref. 1 and references cited therein), but close to the value of $[\alpha]_D$ −41° found by Schaffer for D-erythrose derived from crystalline 2,4-*O*-ethylidene-D-erythrose dimer (12). These higher values, together with rotational data obtained by hydrolysis of the methyl D-erythrosides (see below), indicate that the specific rotation of D- or L-erythrose is −38° or +38° (±3°).

The current procedure for preparing L-erythrose may be found more satisfactory than previous means for obtaining this tetrose. Of other methods available the sulphone degradation (13) of diethyl dithio-L-arabinose affords the highest over-all yield of chromatographically pure L-erythrose (13), although the low specific rotation ($[\alpha]_D$ +23°) recorded for the syrupy product (13) suggests the presence of an undetected impurity.

Hockett and Maynard (15) found that D-erythrose reacts with methanolic hydrogen chloride (16) to form a mixture of the α- and β-furanosides (VII and VIII) rather than the dimethyl acetal or dimeric products, in this respect resembling more closely the higher-order sugars rather than DL-glycerose (17). In the current study it was of interest to isolate the isomeric tetrosides, which represent the simplest of the true glycosides. Di-*O*-formyl-D-erythrose (1), in 1% methanolic hydrogen chloride at room temperature, was rapidly deacylated and converted to a mixture of the glycosides. The anomeric compounds were readily distinguished on paper chromatograms (which showed also that

VI $R_1 = OCH_3$, $R_2 = H$ VIII $R_1 = OCH_3$, $R_2 = H$

VII $R_1 = H$, $R_2 = OCH_3$ IX $R_1 = H$, $R_2 = OCH_3$

other products were produced in only minor proportions), and were separated by chromatography on a cellulose column. The ratio of α- to β-anomer formed was about 1 to 3, whereas Hockett and Maynard found the ratio to be about 4 to 5 (15) and, recently, Ballou (18) has reported that the β-anomer is produced almost exclusively. In all three instances the reaction conditions used appear to have been similar and no explanation is offered to account for these wide variations. It may be noted, however, that the *trans*-β-glycoside always predominates in the mixtures.

Both glycosides were isolated as analytically pure syrups and characterized by optical properties and glycol-cleavage oxidation. Methyl β-D-erythroside was smoothly converted to a 2,3-cyclic carbonate, and a di-*p*-nitrobenzoate of the α-anomer was prepared. On hydrolysis with dilute aqueous acid each glycoside afforded chromatographically pure D-erythrose, the calculated specific rotation of the latter being $[\alpha]_D$ −36° to −39°.

For the preparation of methyl α- and β-D-*threo*-tetrofuranosides (IX and X), di-*O*-formyl-D-threose (2) was treated with methanolic hydrogen chloride as for the corresponding D-erythrose derivative. The specific rotation of the syrupy product and of the dialdehydes derived by periodate oxidation indicated that the α- and β-glycosides were formed in a ratio of about 3 to 2. The mixture was not well resolved on paper chromatograms and only a partial separation was effected on a cellulose column. Presence of two major components in the reaction mixture in the ratio given above was demonstrated more satisfactorily by gas–liquid chromatography* and small analytically pure samples of the α- and β-threosides were obtained by this chromatographic method. Methyl α-D-threoside was isolated also via the mixture of derived di-*p*-nitrobenzoates by fractional crystallization and deacylation.

The possibility of preparing methyl α-D-threoside by means of the Koenigs–Knorr reaction (20) was examined briefly. Extensive studies on the halides of *O*-acyl-pentofuranoses (21) have shown that the 1,2-*trans*-glycoside is generally formed starting with either the α- or β-halide. Applied to the D-*threo*furanose series, formation of the α-glycoside was to be expected. Tri-*O*-acetyl-D-threofuranose (22) was accordingly treated with hydrogen bromide in acetic acid, yielding an unstable syrupy product which appeared to contain both anomeric bromides. Reaction of this material with methanol, either in the presence or absence of silver oxide, led to formation of the mixed α- and β-glycosides, with the former predominating. Under the conditions used, therefore, the reaction was less stereospecific than usually encountered with the higher sugars and did not constitute a satisfactory preparative procedure.

The behavior of the various glycosides towards glycol scission by lead tetraacetate in acetic acid (23) was in general accord with the oxidation characteristics of related five-membered ring compounds. The steric arrangement of the *vic*-diol group of the D-erythrosides should correspond closely to that found in cyclopentane-*cis*-1,2-diol (24) and 1,4-anhydro erythritol (25) and, accordingly, these glycosides consumed oxidant extremely rapidly (Table I), as already shown for the mixed anomers (15). Similarly, as with cyclopentane-*trans*-1,2-diol (23) and 1,4-anhydro-L-threitol (26, 27), the D-threosides were attacked relatively slowly (Table I). The oxidation rates for the anomeric forms differed substantially, however, in contrast to the more uniform behavior of anomeric pyranose glycosides towards lead tetraacetate.†

**This technique has been shown to be highly effective for separating the anomeric forms of some methyl hexoside methyl ethers (19).*

†*A notable exception is the observation that the α-anomer of methyl 2-deoxy-D-erythropentopyranoside consumes lead tetraacetate almost twice as rapidly as does the β-anomer (28). In the periodate oxidation of* sterically rigid *bicyclic methyl glycosides, substantial anomeric differences have been observed (29).*

TABLE I

Properties of the methyl D-tetrofuranosides

Isomer	$[\alpha]_D^{25}$	$[\alpha]_D^{25}$ dialdehyde*	Oxidation rate (k)†
α-D-*Erythro*-(VII)	+133°	+121°	Fast (0°)‡
β-D-*Erythro*-(VIII)	−148°	−119°	Fast (0°)‡
α-D-*Threo*-(IX)	+97°	+113°	0.084 (25°)§
β-D-*Threo*-(X)	−193°	−116°	0.49 (25°)§

*D'- of L'-Methoxy-diglycolic aldehyde formed by periodate oxidation. Derived from crystalline methyl pentosides, these dialdehydes show $[\alpha]_D^{20}$ ±122–124° (37, 38).

†Rate of lead tetraacetate oxidation in mole^{-1} liter minute^{-1}. Cyclopentane-*trans*-1,2-diol gives $k_{20°}$ 12.8 (24).

‡One mole of oxidant per mole was consumed within 45 seconds.

§The compound was not hydrolyzed when kept in acetic acid at 25° C for 6 hours.

EXPERIMENTAL

Paper chromatography was carried out using as solvents (A) ethyl acetate – acetic acid – formic acid – water (18:3:1:4), (B) butan-1-ol – ethanol – water (40:11:19), and (C) ethyl acetate – pyridine – water (100:40:30).

Gas–liquid chromatography was carried out as described by Craig and Murty (30), using a succinate – ethylene glycol polyester on Chromosorb W at a column temperature of 205° and a helium flow of 60 ml/minute.

Solutions were concentrated *in vacuo* at 40° C. Melting points are corrected. Boiling points cited are air-bath temperatures. Optical rotations were measured at approximately 25°.

2,3-O-Isopropylidene-L-*rhamnose* (I)

A slight modification of the procedure of Fischer (16) was used. L-Rhamnose hydrate (30 g) was dehydrated by heating *in vacuo* at 100° C for 3 hours. Dry acetone (300 ml) was added, followed by a solution of acetone (20 ml) containing hydrogen chloride (1.5 g), and the mixture was shaken at room temperature until the solid dissolved (1–2 hours). Excess ammonia was bubbled into the solution, the ammonium chloride filtered off, and the filtrate concentrated. The syrupy residue was dissolved in water (50 ml), extracted twice with ethyl acetate (100 ml), and the extract was washed twice with water (25 ml), dried over sodium sulphate, and concentrated. Weight, 19.0 g, $[\alpha]_D$ +6° (*c*, 4.3, H_2O). Paper chromatographic examination of the syrupy product and of the aqueous fractions indicated that the former consisted almost exclusively of monoacetone L-rhamnose (R_F 0.9, solvent B) and the latter mainly of L-rhamnose. Five grams of 2,3-*O*-isopropylidene-β-L-rhamnose, m.p. 88–90° C, $[\alpha]_D$ +17° (equilibrium value) (*c*, 2, H_2O), was obtained from a solution of the syrup in ether–hexane, but prolonged storage of the mother liquor in the cold failed to yield additional crystalline material. (For further examination of the syrupy residue, see below.)

2,3-O-Isopropylidene-L-*erythruronic Acid* (III)

2,3-*O*-Isopropylidene-β-L-rhamnose (1.0 g) was dissolved in water (50 ml), 0.1 *N* iodine (110 ml containing 2.4 g of potassium iodide) was added, and the solution cooled in an ice bath. Sodium hydroxide (*N*, 17.0 ml) was added dropwise with good stirring during a period of 15 minutes. At 45 minutes, titration of a portion of the reaction mixture showed that the consumption of hypoiodite was 1.0 mole/mole. A few drops of 0.1 *N* thiosulphate was added to decolorize the solution, silver acetate (7.0 g) was added and the suspension stirred at room temperature for 15 minutes, and sodium chloride solution

then added to remove excess silver ion. The suspension was filtered, the filtrate cooled to 5° C, and powdered sodium periodate (1.0 g) added. After 30 minutes, the oxidation mixture (which gave a faint test for excess periodate) was concentrated to a volume of 200 ml, acidified with Amberlite IR-120, and the solution and resin were extracted 5 times with ethyl acetate (50 ml). The combined extract was washed twice with water (25 ml) and dried over sodium sulphate. Evaporation of the solvent afforded a syrup which rapidly solidified (weight, 0.65 g), m.p. 92–98° C. (R_F 0.85, solvent A, yellow color with *p*-anisidine hydrochloride spray (31).) Recrystallized from ethyl acetate – hexane, the product had a melting point of 103–104° C, $[\alpha]_D$ +1.4° (*c*, 1.4, H_2O). Calculated for $C_7H_{10}O_5$: C, 48.27%; H, 5.79%. Found: C, 48.05%; H, 5.76%.

L-*Erythrotetruronic Acid*

Monoacetone L-erythruronic acid (28 mg) in water (2.0 ml) was heated on the steam bath: α_D +0.02° (1 dm, initial) → α_D −0.20° (60 minutes, constant); $[\alpha]_D$ −18° (calc.). (D-Erythruronic acid has $[\alpha]_D$ +18° (3).) Chromatographic examination of the hydrolyzate indicated the presence of one component travelling at the rate of D-*erythro*tetruronic acid (R_{Gal} 1.4, solvent A) and giving an intense yellow color (which appears in the cold and intensifies on heating) with *p*-anisidine hydrochloride spray.

D-*Erythrono-γ-lactone*

Monoacetone L-erythruronic acid (0.3 g) was reduced with sodium borohydride (0.3 g) in water–methanol (2:1). The isopropylidene group of the syrupy product was hydrolyzed at 100° C in 80% acetic acid for 1.5 hours, affording D-erythrono-γ-lactone (0.1 g), which, recrystallized from ethanol, had a melting point of 100–102° C, undepressed, $[\alpha]_D$ −73° (*c*, 2.4, H_2O). (Lit. (1): m.p. 103–104° C; $[\alpha]_D$ −72°.) Calculated for $C_4H_6O_4$: C, 40.68%; H, 5.12%. Found: C, 40.69%; H, 5.16%.

2,3-O-Isopropylidene-L-*erythrose* (V)

2,3-*O*-Isopropylidene-L-rhamnose (2.0 g) in water (80 ml) was added dropwise to a well-stirred solution of sodium borohydride (0.8 g) in ice water (40 ml). After 4 hours at room temperature, acetic acid was added slowly to destroy excess borohydride and to adjust the pH to 6. The solution was cooled externally to 10° C, and powdered sodium periodate (2.2 g) was added portionwise over a period of 15 minutes. The reaction mixture was kept at 25° C for 3 hours (it then gave a faintly positive test for periodate), then concentrated to a volume of about 25 ml, and the slurry extracted 4 times with ethyl acetate (50 ml). After the extract was washed twice with water (15 ml) and dried over sodium sulphate, the solvent was evaporated off affording a clear, colorless syrup* (1.3 g) (R_F 0.8, solvent B) which solidified almost completely when stored overnight at 3° C. The crystalline material melted at 27–30° C. After distillation (60–70° C (bath) at 10 mm) the product still contained a small proportion of liquid, and the crystalline material melted at 29–31° C, $[\alpha]_D$ +72° (*c*, 2.4, CH_3OH) (no mutarotation observed). Calculated for $C_7H_{12}O_4$: C, 52.49%; H, 7.55%. Found: C, 52.53%; H, 7.56%.

2,3-O-Isopropylidene-L-*erythrose from Syrupy Monoacetone* L-*Rhamnose*

A sample (1.0 g) of the material remaining after crystallization of I (above) was treated with sodium borohydride followed by periodate oxidation, as in the preparation of V. The syrupy product (0.8 g) was distilled (50–70° C (bath) at 2 mm) affording a colorless syrup which solidified almost completely at 3° C. The melting point of the crystalline

**This product is moderately volatile, and hence should not be dried for a prolonged period in vacuo.*

material was 27–31° C. In addition to V, the product was found chromatographically to contain a minor component (R_F 0.9, solvent B) that was detected with aniline oxalate but did not give the tetrose color. Attempts to purify the monoacetone-L-erythrose by recrystallization from various solvent systems were unsuccessful.

L-Erythrose

2,3-*O*-Isopropylidene-L-erythrose (19.3 mg) in 0.1 *N* sulphuric acid (1 ml) was heated on the steam bath: α_D +1.22° (1 dm, initial) → +0.97° (30 minutes, constant); $[\alpha]_D$ +39° (calc.). After neutralization with Dowex-1 resin (bicarbonate form) the hydrolyzate was found chromatographically (solvent C) to contain a single component travelling at the rate of D-erythrose and giving the typical tetrose fluorescence under ultraviolet with aniline oxalate spray (32). The infrared absorption spectrum (potassium bromide disk) of the product was indistinguishable from that of D-erythrose. Reduction of the product with aqueous sodium borohydride yielded chromatographically pure erythritol, m.p. 118–120° C, undepressed. Calculated for $C_4H_{10}O_4$: C, 39.34%; H, 8.25%. Found: C, 39.43%; H, 8.30%.

2,3-O-Isopropylidene-L-rhamnitol

2,3-*O*-Isopropylidene-L-rhamnose (0.5 g) in absolute ethanol (10 ml) was heated at 100° C for 8 hours at a pressure of 1400 p.s.i. of hydrogen in the presence of Raney nickel catalyst (0.3 g). The catalyst was filtered off and the filtrate evaporated, affording a colorless syrup (0.5 g) which gave a single spot on a paper chromatogram (R_F 0.7, solvent B, ammoniacal silver nitrate spray (33)), $[\alpha]_D$ +5.5° (*c*, 4.1, CH_3OH). Presence of an isopropylidene group was indicated by the infrared absorption spectrum. The product consumed 1.0 mole of periodate per mole, affording 2,3-*O*-isopropylidene-L-erythrose. Acetylation and benzoylation gave amorphous products.

Reaction of Di-O-formyl-D-erythrose with Methanolic Hydrogen Chloride

Di-*O*-formyl-D-erythrose syrup (1) (3.2 g) in methanol (50 ml) (α_D +0.14°) was treated with 2.5% methanolic hydrogen chloride (35 ml) at 25° C, the observed rotation changing to α_D −1.65° (5 minutes, constant). Excess silver carbonate was added, the neutral filtrate was treated with hydrogen sulphide and again filtered, and the solution was concentrated to yield a colorless syrup (2.2 g), $[\alpha]_D$ −49° (*c*, 4.4, CH_3OH). Examined by paper chromatography (solvent B), the syrup was found to contain two main components (R_F 0.59 (major) and R_F 0.66), a small proportion of free erythrose, and two trace components (R_F 0.74 and R_F 0.79).

Methyl β-D-Erythrotetrofuranoside (II)

Methyl D-erythroside syrup (5.5 g) was chromatographed on a cellulose column using benzene–ethanol–water (500:50:1) as solvent. The component (R_F 0.59) was eluted from the column first and isolated as a colorless syrup (3.5 g), b.p. 80–90° C at 0.5 mm; n_D 1.4630, $[\alpha]_D$ −148° (*c*, 1.5, H_2O). (Ballou reports $[\alpha]_D$ −149° (*c*, 1, $CHCl_3$) (18).) Calculated for $C_5H_{10}O_4$: C, 44.77%; H, 7.52%. Found: C, 44.30%; H, 7.62%.

The glycoside was hydrolyzed with 0.1 *N* sulphuric acid at 100° C to constant rotation in 30 minutes. Calculated for chromatographically pure D-erythrose formed $[\alpha]_D$ −36° (in the acid solution, and after treatment with Dowex-1 resin (bicarbonate form)).

Oxidized with sodium periodate, the uptake by the glycoside was 1.0 mole/mole, and the observed rotation changed from α_D −2.55° (*c*, 1.75) to −2.06° (20 minutes, constant). Calculated for dialdehyde formed $[\alpha]_D$ −119°.

Methyl β-D-Erythrofuranoside-2,3-carbonate

Methyl β-D-erythroside (0.9 g) was dissolved in pyridine (30 ml) and to the stirred solution was added dropwise a solution of phosgene (0.75 g) in toluene (35 ml) (34). After 18 hours the solid pyridine hydrochloride was filtered off, the filtrate concentrated, and the residue taken up in chloroform. The chloroform solution was washed twice with copper sulphate solution, then with bicarbonate solution, twice with water, dried over sodium sulphate, and concentrated. The syrupy product (1.0 g) solidified, and recrystallization was effected from ethyl acetate – hexane, m.p. 73° and $[\alpha]_D$ −152° (*c*, 2.4, $CHCl_3$). Calculated for $C_6H_8O_5$: C, 45.00%; H, 5.01%. Found: C, 44.81%; H, 5.01%. The infrared absorption spectrum showed a major broad peak at 1790–1795 cm^{-1}, characteristic of a cyclic, rather than acyclic, carbonate group (35).

Methyl α-D-Erythrotetrofuranoside (I)

Following elution of the β-glycoside from the cellulose column, a fraction consisting mainly of the α-anomer was obtained (0.6 g), rechromatographed on the cellulose column, and distilled (b.p. 65–85° C at 0.2 mm); n_D 1.4665, $[\alpha]_D$ +133° (*c*, 1.2, H_2O). Calculated for $C_5H_{10}O_4$: methoxyl, 23.1%. Found: methoxyl, 22.8%.

On hydrolysis with 0.1 *N* sulphuric acid at 100° C to constant rotation, the observed value corresponded to $[\alpha]_D$ −37° for chromatographically pure D-erythrose formed; after neutralization with Dowex-1 (bicarbonate form), $[\alpha]_D$ −39°.

Treated with sodium periodate, the glycoside consumed 1.0 mole/mole, the observed rotation changing from α_D +1.71° → +1.48° (10 minutes, constant). Calculated for the dialdehyde formed, $[\alpha]_D$ +121°.

Methyl α-D-Erythrofuranoside Di-p-nitrobenzoate

Methyl α-D-erythroside (0.10 g) in pyridine (5 ml) was treated with *p*-nitrobenzoyl chloride (0.65 g) at 55° C for 4 hours. On addition of aqueous sodium bicarbonate, a solid product was obtained (0.30 g) and was recrystallized from ethyl acetate – hexane, m.p. 109–110° C and $[\alpha]_D$ −17.3° (*c*, 1.7, $CHCl_3$). Calculated for $C_{19}H_{16}O_{10}N_2$: C, 52.78%; H, 3.73%. Found: C, 52.84%; H, 3.60%.

Reaction of D-Threose Formate with Methanolic Hydrogen Chloride

D-Threose formate syrup (2) (4.5 g), treated with methanolic hydrogen chloride as described above, afforded a colorless syrup (2.6 g). Purified by distillation (b.p. 75–90° C at 0.2 mm) the product had $[\alpha]_D$ +7.9° (*c*, 2.4, H_2O) and, examined by paper chromatography (solvent B), was found to contain two major tetrose components (R_F 0.65 and 0.62; overlapping, with the former predominant) and a minor tetrose component (R_F 0.75). On treatment with periodate the mixture consumed 0.9 mole of oxidant per mole, the calculated value of $[\alpha]_D$ +33° for the dialdehydes formed corresponding to an α,β-mixture of about 3 to 2. Calculated for $C_5H_{10}O_4$: methoxyl, 23.1%. Found: methoxyl, 24.6%.

Methyl α- and β-D-Threotetrofuranosides

Vapor phase chromatography of the syrupy mixture of D-threosides readily separated the two major components from each other, and showed them to be present in a ratio of about 3 to 2 (α- to β-). On a preparative scale, 50–100 mg of each component was isolated by repeated chromatographic runs, and purified by distillation.

The first of the two components to emerge from the column was the *β-anomer* (R_F 0.62, b.p. 80–90°/0.2 mm), $[\alpha]_D$ −193° (*c*, 1.1, H_2O). The glycoside consumed 1.0 mole of

periodate per mole, affording a dialdehyde having $[\alpha]_D$ −116° (calculated). Calculated for $C_5H_{10}O_4$: C, 44.77%; H, 7.52%. Found: C, 44.60%; H, 7.48%.

The *α-anomer* (R_F 0.65, b.p. 85–100°/0.2 mm) had $[\alpha]_D$ +97° (*c*, 1.6, H_2O). It consumed 1.0 mole of periodate per mole, yielding a dialdehyde having $[\alpha]_D$ +113° (calculated). Calculated for $C_5H_{10}O_4$: C, 44.77%: H, 7.52%. Found: C, 44.73%; H, 7.31%.

Methyl α-D-Threofuranoside Di-p-nitrobenzoate and Methyl α-D-Threofuranoside

The mixture of α- and β-D-threosides (0.5 g) was treated with *p*-nitrobenzoyl chloride as described above, and the amorphous product (1.2 g) was taken up in ethyl acetate – hexane. Crystalline material (0.6 g) was deposited and recrystallized twice from the same solvent, m.p. 131–133° C and $[\alpha]_D$ −115° (*c*, 2.0, $CHCl_3$). Calculated for $C_{19}H_{16}O_{10}N_2$: C, 52.78%; H, 3.78%. Found: C, 52.80%; H, 3.65%.

The di-*p*-nitrobenzoate (0.3 g) suspended in methanol (20 ml) was treated under reflux with sodium methoxide (0.1 *N*, 2 ml). Acetic acid was added to neutrality, the methanol evaporated off, and the residue taken up in water and extracted three times with benzene. The aqueous layer was concentrated, and the product distilled, $[\alpha]_D$ +96° (*c*, 2.2, H_2O). The infrared absorption spectrum of the syrup was indistinguishable from that of methyl α-D-threoside and different from that of the β-glycoside.

Methyl β-D-Threofuranoside Di-p-nitrobenzoate

A syrup consisting mainly of methyl β-D-threofuranoside ($[\alpha]_D$ −165°) was obtained by partial separation of the mixed threosides on a cellulose column using benzene–ethanol–water (1000:15:0.5). Treatment with *p*-nitrobenzoyl chloride afforded a di-*p*-nitrobenzoate which, when crystallized from ethyl acetate – pentane, had a melting point of 55–57° C, $[\alpha]_D$ −213° (*c*, 1.6, $CHCl_3$). Calculated for $C_{19}H_{16}O_{10}N_2$ (containing a mole of ethyl acetate): C, 53.05%; H, 4.62%; N, 5.38%; acetyl, 8.27%. Found: C, 53.03%; H, 4.63%; N, 5.21%; acetyl, 7.81%.

Preparation of the Methyl D-Threosides via Acetobromo-D-threose

Tri-*O*-acetyl D-threose (22) (0.50 g) in chloroform (4 ml) ($[\alpha]_D$ +35°) was treated with hydrogen bromide (2 ml, 40% in acetic acid). Within 5 minutes the observed rotation was constant, giving a calculated value of $[\alpha]_D$ −10°. The solution was quickly concentrated, toluene being added 4 times in completing the evaporation of solvent, affording a pale yellow syrup (0.54 g). (Attempts to dry a portion thoroughly for analysis resulted in rapid darkening, and no crystalline product could be isolated from cold ether–hexane.)

The syrup (0.1 g) in methanol (5 ml) was shaken for 18 hours with silver oxide (0.3 g) and Drierite (0.7 g). Found: $[\alpha]_D$ −5° (calculated for methyl tetroside). In the absence of silver oxide and Drierite the observed rotation of the solution was constant in 10 minutes, $[\alpha]_D$ −6° (calculated for methyl tetroside). Both products were deacylated with sodium methoxide, and found by paper chromatography to contain mainly methyl threoside, $[\alpha]_D$ +25° (*c*, 1, H_2O). The infrared absorption spectra of the deacetylated products were closely similar to that of methyl α-D-threoside. Examined by vapor phase chromatography the α- and β-anomers were detected in the products in a ratio of about 3 to 1.

Lead Tetraacetate Oxidations

The methyl D-erythrosides (40 mg) in 5 ml of acetic–propionic acid mixture (75:25) (2) were each treated at 0° C with lead tetraacetate solution (50 mg in 4 ml of the same solvent). Oxidation of the methyl D-threosides was carried out in acetic acid at 25° C,

using the same concentration of reactants. Reaction rates were measured as described by Criegee (36).

ACKNOWLEDGMENTS

The authors are grateful to Dr. B. M. Craig for carrying out the vapor phase chromatographic separations reported, and to Mr. J. W. L. C. Christ for technical assistance. Microanalyses were carried out by Mr. M. Mazurek, and infrared absorption spectra were prepared by Miss Inez Gaffney.

REFERENCES

1. A. S. Perlin and C. Brice. Can. J. Chem. **33**, 1216 (1955).
2. A. S. Perlin and C. Brice. Can. J. Chem. **34**, 85 (1956).
3. P. A. J. Gorin and A. S. Perlin. Can. J. Chem. **34**, 693 (1956).
4. J. N. Baxter, A. S. Perlin, and F. J. Simpson. Can. J. Biochem. and Physiol. **37**, 199 (1959).
5. H. J. Lucas and W. Baumgarten. J. Am. Chem. Soc. **63**, 1653 (1941).
6. O. T. Schmidt and P. Günthert. Ber. **71**, 493 (1938).
7. E. Fischer. Ber. **28**, 1145 (1895).
8. K. Freudenberg and A. Wolf. Ber. **59**, 836 (1926).
9. P. A. Levene and J. Compton. J. Biol. Chem. **114**, 9 (1936).
10. R. Willstäter and G. Schudel. Ber. **51**, 780 (1918).
11. C. E. Ballou. J. Am. Chem. Soc. **79**, 165 (1957).
12. R. Schaffer. J. Am. Chem. Soc. **81**, 2838 (1959).
13. D. L. Macdonald and H. O. L. Fischer. J. Am. Chem. Soc. **74**, 2087 (1952).
14. L. Hough and T. J. Taylor. J. Chem. Soc. 1212 (1955).
15. R. C. Hockett and C. W. Maynard, Jr. J. Am. Chem. Soc. **61**, 2111 (1939).
16. E. Fischer. Ber. **26**, 2400 (1893).
17. H. O. L. Fischer and C. Taube. Ber. **60**, 1706 (1927).
18. C. E. Ballou. J. Am. Chem. Soc. **82**, 2585 (1960).
19. A. G. McInnes, D. H. Ball, F. P. Cooper, and C. T. Bishop. J. Chromatog. **1**, 556 (1958).
20. W. Koenigs and E. Knorr. Ber. **34**, 957 (1901).
21. R. K. Ness and H. G. Fletcher, Jr. J. Am. Chem. Soc. **80**, 2007 (1958); and references cited therein.
22. R. C. Hockett. J. Am. Chem. Soc. **57**, 2260 (1935).
23. R. Criegee. Ber. **64**, 260 (1931).
24. R. Criegee, E. Büchner, and W. Walther. Ber. **73**, 571 (1940).
25. R. E. Reeves. J. Am. Chem. Soc. **72**, 1499 (1950).
26. H. Klosterman and F. Smith. J. Am. Chem. Soc. **74**, 5336 (1952).
27. J. S. Brimacombe, A. B. Foster, M. Stacey, and D. H. Whiffen. Tetrahedron, **4**, 351 (1958).
28. R. E. Deriaz, W. G. Overend, M. Stacey, and L. F. Wiggins. J. Chem. Soc. 2836 (1949).
29. J. Honeyman and C. J. G. Shaw. J. Chem. Soc. 2454 (1959).
30. B. M. Craig and N. L. Murty. Am. Oil Chemists' Soc. **36**, 549 (1959).
31. L. Hough, J. K. N. Jones, and W. H. Wadman. J. Chem. Soc. 1702 (1950).
32. R. H. Horrocks. Nature, **164**, 444 (1949).
33. S. M. Partridge. Nature, **158**, 270 (1946).
34. B. J. Ludwig and E. C. Piech. J. Am. Chem. Soc. **73**, 5779 (1951).
35. L. Hough, J. E. Priddle, R. S. Theobald, G. R. Barker, T. Douglas, and J. W. Spoors. Chem. & Ind. London, 148 (1960).
36. R. Criegee. Ann. **495**, 211 (1932).
37. E. L. Jackson and C. S. Hudson. J. Am. Chem. Soc. **59**, 994 (1937).
38. F. Smith and J. W. van Cleve. J. Am. Chem. Soc. **77**, 3901 (1955).

CHEMICAL SHIFTS IN THE N.M.R. SPECTRA OF SUBSTITUTED XYLENES[1]

ROBERT R. FRASER

ABSTRACT

The complete results of analysis of the N.M.R. spectra of twelve 2,6-dimethyl-1-substituted benzenes are reported. The results are interpreted as evidence that the ability of the substituent to donate or withdraw electrons by resonance interaction with the benzene ring is a major factor in determining the position of absorption of the protons attached to the ring. The chemical shifts and coupling constants for nitroethylene are also reported.

The study of the effect of a substituent on the position of absorption in the N.M.R. spectra of protons attached to a benzene ring has been greatly hindered by the complexity of the spectra of monosubstituted benzenes. These spectra generally fall in the classification AB_2C_2 following the nomenclature of Bernstein, Pople, and Schneider (1). Analysis of such a five-spin system is extremely tedious even in the case of pyridine, which belongs to the slightly simpler AB_2X_2 system (2). For this reason little work has appeared in the literature on the correlation of chemical shifts of protons on a benzene ring with substituents since the first report by Corio and Dailey (3). These authors reported the values δ_o, δ_m, δ_p for the chemical shifts of the ortho, meta, and para protons in the N.M.R. spectra of 22 monosubstituted benzenes. Their analysis was of a qualitative nature on spectra whose resolution was limited by the use of a transmission frequency of 30.00 Mc/sec. Furthermore Bothner-By and Glick subsequently showed that solvent effects were responsible for inaccuracies of as much as 0.07 p.p.m. in the values for δ_p (4). Correlation of their δ values with Hammett's σ constants gave only rough agreement although Taft later showed that agreement to within 0.07 p.p.m. could be obtained employing the equation* $\delta_p = +0.40\sigma_I + 1.04\sigma_R^0 + 0.02$ (5). In this equation σ_I is the inductive substituent constant of Taft (6) and σ_R^0 is the resonance substituent constant corrected for isovalent conjugation (5). Taft has interpreted this agreement to be an indication that polarization effects in the transition state are sufficiently similar to those in the ground state to give the correlation between σ and δ_p (7).

An alternative theory of the origin of chemical shift differences in the ring protons of monosubstituted benzenes has been suggested in a recent article by Buckingham (8). He proposes that the screening constant for each proton is determined by the "internal electric field" of the molecule. In addition polarization of the surrounding solvent by the solute produces a "reaction field" whose effect combines with that of the electric field to give the total effect on the screening constants. He has derived expressions for these two fields in terms of the dipole moment of the solute, its refractive index, and the dielectric of the solution from which screening constants can be directly calculated. Calculations for nitrobenzene gave values of -0.69, -0.40, and -0.51 p.p.m. relative to benzene for the ortho, meta, and para protons in fair agreement with the values -0.97, -0.30, and -0.42 observed by Corio and Dailey. In order to provide data which might aid in the elucidation of the cause of chemical shift differences with different substituents, a series

[1]*Manuscript received June 29, 1960.*
Contribution from the Department of Chemistry, University of Ottawa, Ottawa, Ontario. This paper was presented at the 43rd Annual Conference of the Chemical Institute of Canada, Ottawa, June 13–15, 1960.

**It should be noted that Corio and Dailey employ $\delta_p = 10^6\{(H_{ref}-H)/H_{ref}\}$, which causes negative signs to represent shifts to higher field.*

of 2,6-dimethyl-1-substituted-benzenes were synthesized and their spectra obtained with a Varian V-4302 spectrometer using a 60 Mc/sec r.f. unit. These xylene derivatives were selected for study since they provide spectra which can be accurately analyzed.

RESULTS AND DISCUSSION

The results of analysis of the spectra of 12 substituted xylenes are given in Table I.

TABLE I

Results of analysis of twelve 2,6-dimethyl-1-substituted benzenes (substituent σ values are also given)

Substituent	$\Delta\nu_m$*	$\Delta\nu_p$*	$\Delta\nu_m'$	σ_m	σ_p	σ_R	τ_{CH_3}†
CN	12.9	0.3	2.6	0.62	0.68	0.10	7.52
Br	16.8	16.8	6.5	0.39	0.23	−0.22	7.61
I	18.4	14.4	8.1	0.35	0.28	−0.11	7.54
F	22.5	26.5	12.2	0.35	0.08	−0.44	7.76
D	24.8	14.5	14.5	0.00	0.00	0.00	7.73
OH	25.8	39.0	15.5	0.08	−0.35	−0.60	7.88
NH_2	29.0	47.2	18.7	−0.15	−0.66	−0.76	7.89
NO_2	12.5	5.2	2.2			+0.05	7.68
COOH	16.0	7.0	5.7			+0.06	7.55
OCH_3	23.5	29.0	13.2			−0.20	7.75
$NHCH_3$	25.5	35.8	15.2			−0.39	7.76
$N(CH_3)_2$	26	26	15.7			−0.21	7.76

NOTE: All the σ values for the first seven substituents are taken from R. W. Taft, Jr., N. C. Deno, and A. S. Skell. Ann. Rev. of Phys. Chem. **9**, 292 (1958). The σ_R values for the last five substituents are calculated from normal σ_R values by correcting for the percentage of steric inhibition of resonance. The percentage inhibition was taken from the following sources: R. W. Taft, Jr. and H. D. Evans. J. Chem. Phys. **27**, 1427 (1957), who reported NO_2 (67%), OCH_3 (59%), and $N(CH_3)_2$ (75%); B. M. Wepster. Rev. trav. chim. **76**, 335, 357 (1957), who found NO_2 (69%), $N(CH_3)_2$ (80%), and $NHCH_3$ (60%); A. Burawoy and J. T. Chamberlain. J. Chem. Soc. 2310 (1952), from whose results the value 62% is calculated for OCH_3; and G. M. Moser and A. I. Kohlenburg. J. Chem. Soc. 805 (1957), from whose data the value 50% is estimated for COOH. For a discussion of steric inhibition of resonance in these compounds see B. M. Wepster. Progress in stereochemistry. Vol. 2. *Edited by* W. Klyne and P. B. D. de la Mare. Butterworths Scientific Publications, London. 1958.

*$\Delta\nu_m$ and $\Delta\nu_p$ are the chemical shifts in cycles/sec at 60 Mc/sec relative to the internal reference benzene for the meta and para protons.

†τ_{CH_3} gives the chemical shift of the ortho methyls expressed as parts per million with tetramethylsilane assigned a value 10.00.

The protons attached to the aromatic ring appeared in all but three cases as an AB_2 pattern whose general solution has been reported in reference 1. The spectrum consists of eight transitions whose energies and intensities are dependent only on the ratio $J_{AB}/\Delta\nu_{AB}$.* In Fig. 1 the spectra of 2,6-dimethylphenol, 2,6-dimethylanisole, and N,N-dimethyl-2,6-dimethylaniline are shown. They illustrate cases where the ratio is less than one, about one, and much greater than one, respectively. In 2,6-dimethylphenol, as in all AB_2 systems, line 3 gives the position of chemical shift for the A nucleus, unmodified by spin coupling. The corresponding position for the B nuclei is the mean of transitions 5 and 7. Thus $\Delta\nu_{AB} = \Delta\nu_p - \Delta\nu_m$ can be obtained directly from the spectrum. In the spectrum of this compound transitions 5 and 6 could not be resolved. To insure accurate results, theoretical spectra were calculated for various ratios of $J/\Delta\nu_{AB}$ until agreement with the observed spectra to within 0.4 cycle/sec for each transition was obtained. In most spectra the agreement was within 0.2 cycle/sec for each transition. In all spectra J_{AB} was found to be 7.7 cycles/sec. The spectra of N,N-dimethyl-2,6-dimethylaniline and 2,6-dimethylbromobenzene showed only a single observable peak under high gain and it is estimated that the chemical shift of the meta and para protons in these two compounds is the same to within 3.0 cycles/sec.

**J_{AB} is the coupling constant between the para (A) and meta (B) protons. $\Delta\nu_{AB} = \nu_A - \nu_B$ represents the chemical shift between the meta and para protons. The symbol $\Delta\nu$ is used to denote chemical shifts in units of cycles per second as recommended by Pople, Schneider, and Bernstein (11).*

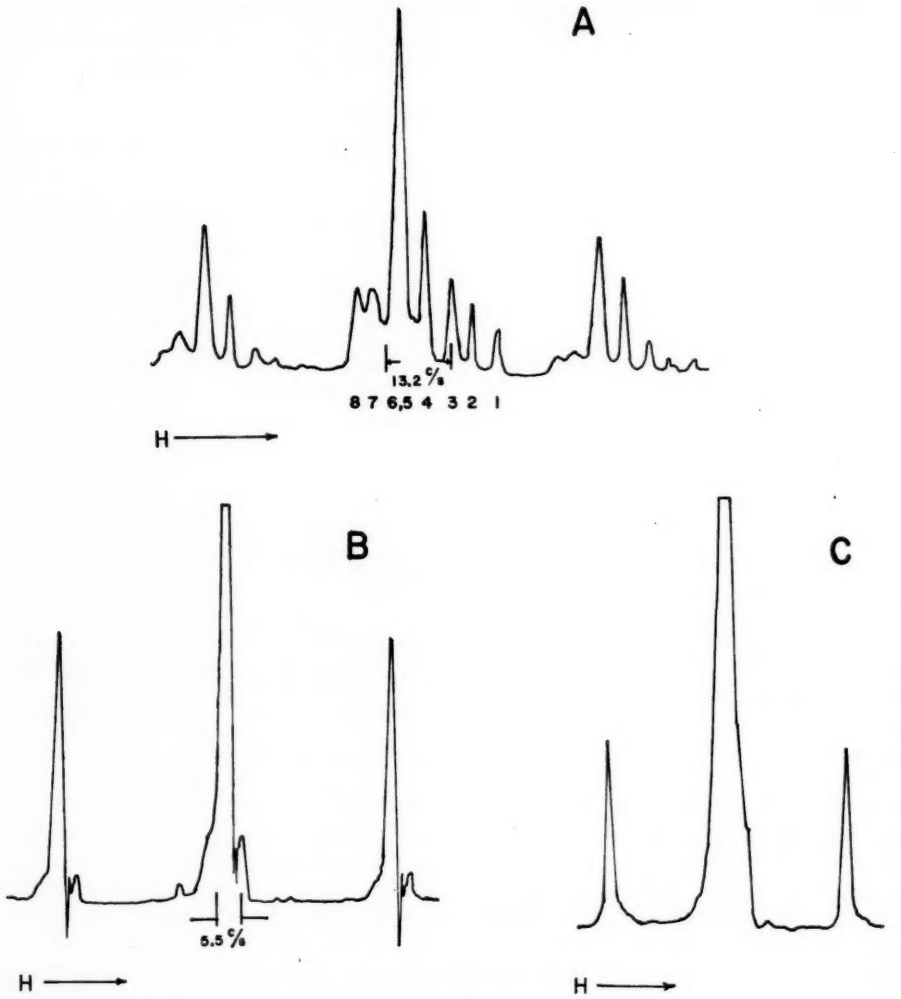

FIG. 1. (A) Aromatic proton absorption of 2,6-dimethylphenol (side bands at 40.0 cycles/sec) as a 10% solution in carbon tetrachloride. (B) Aromatic protons of 2,6-dimethylanisole (side bands at 35.1 cycles/sec) and (C) N,N-dimethyl-2,6-dimethylaniline (side bands at 25.0 cycles/sec) as 10% solutions in carbon tetrachloride.

In 2,6-dimethylfluorobenzene coupling of the fluorine atom with the meta and para protons resulted in the more complex spectrum shown in Fig. 2. By neglecting coupling of the methyl groups with the ring protons we can classify the aromatic protons and the fluorine nucleus as an AB_2X system. In order to simplify the calculations we have considered the aromatic proton spectrum as the sum of two AB_2 systems. This type of simplification has been employed previously by Anet in the analysis of the 2,3-dibromobutanes (9). When the X nucleus, fluorine, has a spin of $+1/2$ the aromatic protons will form one AB_2 system. When fluorine has a spin of $-1/2$ the aromatic protons comprise

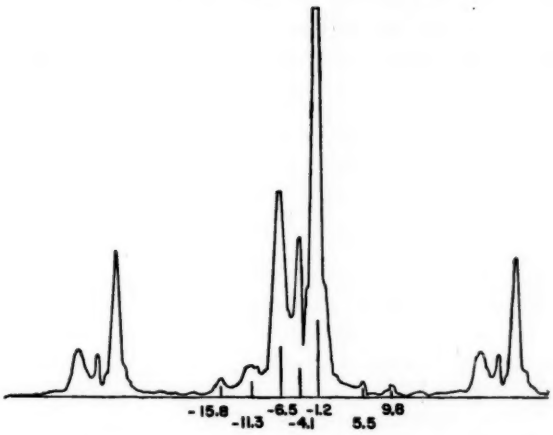

FIG. 2. Aromatic absorption of 2,6-dimethylfluorobenzene (side bands at 30.0 cycles/sec) as a 10% solution in carbon tetrachloride.

a second AB_2 system of equal total intensity. From the experimentally determined spectrum we found the chemical shift for the widely separated AB_2 system to be 8.6 cycles/sec. Using the values $J_{FH_B} = 7.0$ cycles/sec, $J_{FH_A} = \pm 2.2$ cycles/sec, and $J_{AB} = 7.7$ cycles/sec, it was then possible to calculate the complete spectrum for the aromatic protons. Two solutions were obtained, one for the case where the coupling constants between fluorine and the meta and para protons are of opposite sign (Fig. 3A) and one where the coupling constants are of the same sign (Fig. 3B). The numerical values for the fluorine–hydrogen coupling constants were chosen from the results of Gutowsky, Holm, Saika, and Williams, who observed the coupling between the ring protons and fluorine in fluoromesitylene to be 7.0 cycles/sec and the coupling between fluorine and a para proton to be 2.2 cycles/sec in several fluorinated benzenes (10). The line width of the strongest peak in the observed spectrum suggests that it is due to an AB_2 system having a very large ratio of $J/\Delta\nu_{AB}$ as depicted in Fig. 3A. In addition failure to observe the transition at +2.2 cycles/sec shown in Fig. 3B further indicates that the observed spectrum is due to a system in which the two fluorine–proton coupling constants are of opposite sign. Unfortunately an element of doubt remains as the differences between the two theoretical spectra are not large. The spectrum of 2,6-dimethylfluorobenzene was also measured in acetone, methylene iodide, dimethylsulphoxide, and aqueous methanol. Only in acetone was the spectrum altered significantly, $\Delta\nu_{AB}$ for the well-resolved AB_2 system being increased to 10.1 cycles/sec. Again better agreement between observed and calculated spectra was obtained assuming the fluorine–hydrogen coupling constants to be of opposite sign. With the values chosen in Fig. 3A, the chemical shift difference between the meta and para protons is found to be 4.0 cycles/sec with the para proton at higher field. The alternative assumption increases the difference to 6.2 cycles/sec. The methyl groups in 2,6-dimethylfluorobenzene appeared as a doublet of spacing 2.05 cycles/sec due to coupling with the fluorine nucleus.

Before the results are examined it is necessary to make a correction in the $\Delta\nu_m$ values. The spectrum of 2,6-dimethyldeuterobenzene shows that the meta protons are shifted 10.3 cycles/sec more to high field than the para ones by the methyl groups. Whatever

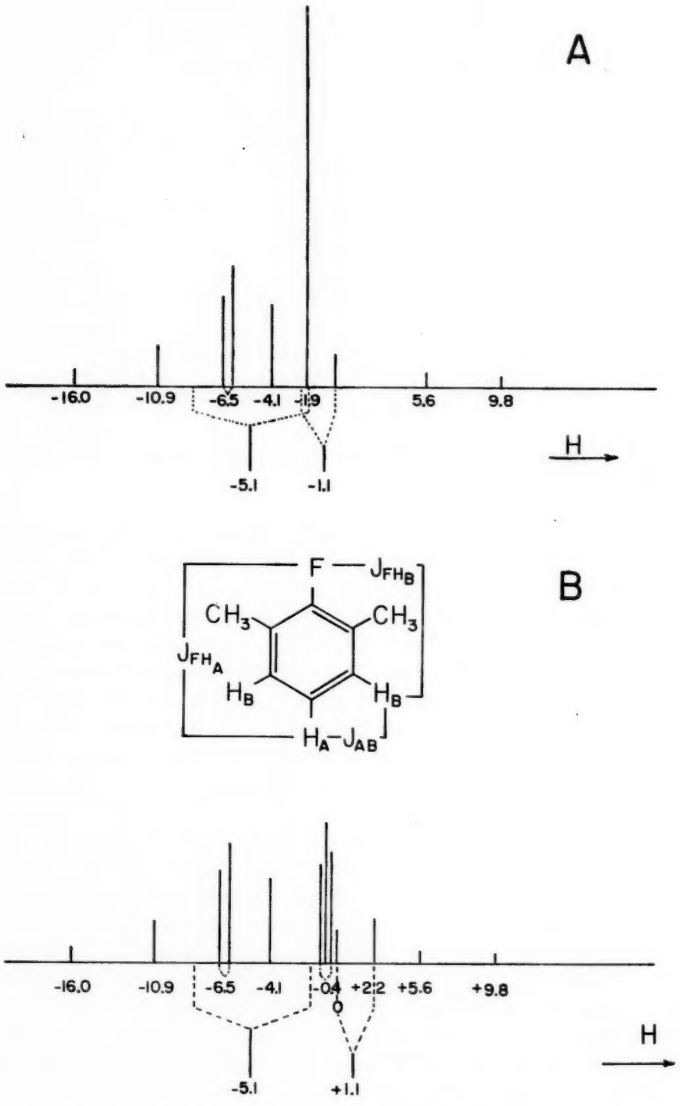

FIG. 3. Theoretical spectra of aromatic protons in 2,6-dimethylfluorobenzene.
(A) For $J_{AB} = 7.7$ cycles/sec, $J_{F-H_B} = 7.0$ cycles/sec, $J_{F-H_A} = -2.2$ cycles/sec, $\Delta\nu_{obs} = 8.6$ cycles/sec.
(B) For $J_{AB} = 7.7$ cycles/sec, $J_{F-H_B} = 7.0$ cycles/sec, $J_{F-H_A} = 2.2$ cycles/sec, $\Delta\nu_{obs} = 8.6$ cycles/sec.
In this diagram transitions of intensity less than 40% of band at +5.6 are not included. The positions of the *A* and *B* nuclei in the absence of coupling are shown below the abscissa.

the origin of this preferential shift, it is necessary to assume that it remains constant throughout the series of compounds measured. If this is true we can assign $\Delta\nu_m'$ values = $\Delta\nu - 10.3$ to the meta protons. Now the effect of the methyls is removed and the substituent

effect of a deuterium atom appears the same at the meta and para positions. The $\Delta\nu_m'$ values are also given in Table I. Let us now consider the chemical shifts observed in 2,6-dimethylaniline and its N,N-dimethyl derivative. The para proton in 2,6-dimethylaniline occurs at 47.2 cycles/sec relative to benzene, the meta proton at 29.0 cycles/sec relative to benzene. The value $\Delta\nu_p - \Delta\nu_m'$ shows that the amino substituent causes the para proton to be shifted 28.5 cycles/sec to higher field relative to the meta, which is corrected for the effect of the methyl group. On the other hand the dimethylamino substituent can be seen to cause only a 10.3 cycles/sec preferential shift of the para proton to higher field. It has been established by ultraviolet spectroscopy and by chemical reactivity (see references 1 and 2 in Table I) that two methyl groups ortho to a dimethylamino group greatly inhibit its resonance interaction with the benzene ring by preventing it from attaining coplanarity with the ring. The large difference in chemical shifts in 2,6-dimethylaniline can be explained by a resonance effect. That is to say the nitrogen atom donates its electrons to the para position more than to the meta position in the ground state and the increase in electron density results in a shift to higher field. The resonance interaction of the dimethylamino group with the ring is greatly decreased and so the effect on the shielding of the para and meta protons is also greatly diminished. The screening at the meta and para positions in the two compounds was calculated from the equations derived by Buckingham. The values 1.62 and 0.94, which Fischer found (12) for the dipole moments of 2,6-dimethylaniline and N,N-dimethyl-2,6-dimethylaniline, were used in the calculation. The dielectric constants for 5% solutions in carbon tetrachloride were estimated to be 2.5 and 2.4 respectively.

For 2,6-dimethylaniline the equations of Buckingham give values for $\Delta\nu_m'$ and $\Delta\nu_p$ of 6.4 cycles/sec and 7.2 cycles/sec. For the N,N-dimethyl derivative values of 3.7 and 4.1 cycles/sec were obtained. When these are compared with our experimental results it can be seen that the agreement is very poor.

A more obvious contradiction of the electric field effect is seen in the data for 2,6-dimethylfluorobenzene. Its dipole moment will most certainly be greater than zero with the negative end directed away from the ring.* Electric field theory then predicts that the para protons will be less screened than the meta when, in fact, the opposite situation has been found.

A plot of $\Delta\nu_m'$ and $\Delta\nu_p$ against the Hammett sigma constants for each substituent is shown in Fig. 4. No linear relationship is seen as the strongly electron-donating substituents appear at too high field. The same type of behavior was found for the F^{19} chemical shifts determined by Gutowsky (14). However, Taft later showed that the observed chemical shifts could be correlated with the inductive and resonance substituent constants σ_I and σ_R (7). The measured chemical shifts for the seven compounds whose substituents are free of steric inhibition of resonance were tested for correlation by the equation $\Delta\nu = \alpha\sigma_I + \beta\sigma_R + \gamma$ where α and β represent the susceptibility of the chemical shift to inductive and resonance effects of the substituent, respectively, and γ represents the constant methyl group effect. The chemical shifts for the meta protons are correlated by the equation $\Delta\nu_m' = 14.5 - 17\sigma_I - 10\sigma_R$, with the maximum error being 2.4 cycles/sec in the case of the bromo compound. The equation $\Delta\nu_p = 14.5 - 17\sigma_I - 46\sigma_R$ gives a better correlation, the maximum error being 1.7 cycles/sec in the iodo compound. As an illustration of the greater susceptibility of the para protons to σ_R, the value $\Delta\nu_p - \Delta\nu_m'$ for each

**The only available dipole moment data on fluorobenzenes is that of Everard, Kumar, and Sutton (13), who found the dipole moment of fluorobenzene to be 1.48 Debye units. The introduction of two methyl groups could lower the dipole moment by no more than 0.6 Debye unit which would lead to a minimum estimate of 0.88 Debye unit for 2,6-dimethylfluorobenzene.*

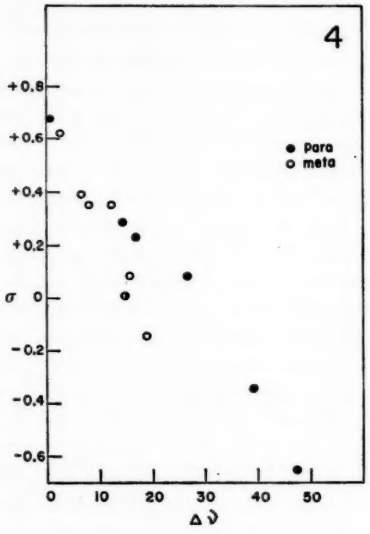

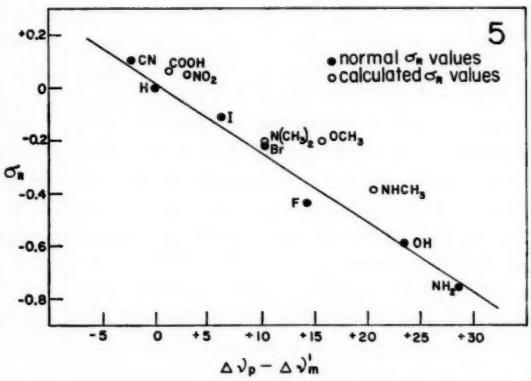

FIG. 4. Correlation of the shielding of the meta and para protons expressed in cycles per second at 60 Mc/sec from benzene by Hammett's σ's.

FIG. 5. Correlation of the separation in cycles per second at 60 Mc of the meta and para protons by Taft's σ_R.

compound is plotted against the σ_R value of the substituent in Fig. 5.* The linear relationship is obeyed to within 2.5 cycles/sec for those substituents free from resonance inhibition by the adjacent methyl groups. The substituents for which there is experimental evidence of steric inhibition of resonance are also plotted on the graph using σ_R values corrected for the percentage of inhibition as listed in Table I. The points for these substituents do not give a good linear plot, which might be interpreted as failure of the spectral and chemical methods to give a quantitative measure of the steric inhibition of resonance. Indeed the theoretical interpretation of the observed decrease in intensity of the ultraviolet absorption spectrum with increasing resonance inhibition, which was proposed by Braude, Sondheimer, and Forbes (15), has been invalidated by the recent work of Waight and Erskine (16). They observed no change in intensity of the ultraviolet spectra of a series of ortho-methylacetophenones with a 216° temperature change, a finding which contradicts Braude and co-worker's theory. It would be too presumptuous on the basis of our limited findings to propose corrected values for resonance inhibition by assuming the linear relationship to be valid for our compounds. It is sufficient to say that the deviation of these compounds from linearity does not refute the proposal that chemical shifts are determined by the inductive and resonance effects of the substituents.

Our findings can be compared with those of Corio and Dailey for the meta and para protons. The absence of ortho protons in our spectra is unimportant as Jackman has pointed out that the ortho shieldings are in many instances misleading (17). Jackman has found that each of the groups CN, Br, COOH, COCl, $COCH_3$, CHO in 2-substituted-1-propenes causes a shift of the proton cis to it to lower field relative to the trans proton.

*$If\ \Delta\nu_m' = \alpha\sigma_I+\beta\sigma_R+\gamma\ and\ \Delta\nu_p = \alpha\sigma_I+\beta'\sigma_R+\gamma\ then\ \Delta\nu_p-\Delta\nu_m' = (\beta'-\beta)\sigma_R\ and\ so\ a\ linear\ relationship\ between\ \Delta\nu_p-\Delta\nu_m'\ and\ \sigma_R\ should\ be\ found.$

The magnitude of the effect varies from 0.05 to 0.5 p.p.m. We have found that the nitro group has an even greater effect. Nitroethylene as a 10% solution in carbon tetrachloride gave a spectrum with well-separated absorption peaks. Assignments were made by assuming the coupling to be greater between protons trans to one another than cis and the results of analysis by first-order perturbation theory are given in Fig. 6. The

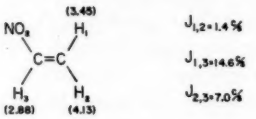

FIG. 6. Chemical shifts (τ values) and coupling constants for nitroethylene.

proton cis to the nitro group appears 0.68 p.p.m. to lower field than the proton trans to the nitro group. This effect of substituents will undoubtedly also be present in monosubstituted benzenes and will result in ortho protons appearing to lower field than in the absence of the effect. In instances where the effect is large, e.g. nitro, it could also be significant in the meta position even though it should fall off with the cube of the distance (11, p. 176). Our results are generally in agreement with those of Corio and Dailey although they show much greater sensitivity. For example, phenol showed no resolvable fine structure at 30 Mc/sec whereas 2,6-dimethylphenol showed signals for the meta and para protons separated by 13.2 cycles/sec. There is a discrepancy in the case of the iodo substituent. The values assigned to the para and meta protons in iodobenzene were +.10 and +.17 p.p.m. or 6.0 and 10.2 cycles/sec at 60 Mc/sec respectively. By subtracting the effect of the methyl groups our results for iodobenzene would be −0.1 and −6.4 cycles/sec respectively. Presumably, the discrepancy is due to those factors mentioned earlier, solvent effects and approximate analysis.

In conclusion it can be stated that our findings are not explainable by the Buckingham electric field theory. They are in agreement with the proposal of Taft that the observed shifts at the meta and para positions are determined by both the inductive and resonance effects of the substituent. The theoretical basis for such a relationship has been clearly discussed by Taft (7). In spite of our findings it should be emphasized that the quantitative value of the correlations is questionable. The meta protons are subject to only small shifts which could easily be overwhelmed by solvent or anisotropy effects. Indeed the recent work of Schneider (18) points out the need for caution. He found that the chemical shifts of the C^{13} nuclei in monosubstituted benzenes show appreciable variation due to resonance at the para position and even larger variation due to resonance and anisotropy effects at the ortho positions. At the meta position the variation in chemical shift was extremely small and not interpretable by resonance effects.

EXPERIMENTAL

The spectra were measured with a Varian V-4302 high-resolution N.M.R. spectrometer. Every result reported is the average of at least three determinations. Peak separations were determined by the side-band technique (11, p. 74) employing a Hewlett–Packard wide-range oscillator. The frequency of the side band was counted after each determination with a Hewlett–Packard 521C frequency counter with an accuracy of ±0.1 cycle/sec. If a broad peak was being measured the calibration was carried out by superposition of the reference signal on the desired peak. Alternatively, several of the spectra were calibrated by recording the spectrum of the reference and aromatic compound and their

side bands, then measuring the separation by interpolation. Both methods were used on 2,6-dimethylphenol and were found to agree to within 0.2 cycle/sec. All calibrations with respect to the internal reference were made employing 5% solutions of the aromatic compound in carbon tetrachloride containing 1% of benzene as internal reference. Measurements of the aromatic proton absorption of 2,6-dimethylanisole were made on 20%, 10%, and 5% solutions in carbon tetrachloride. From complete analysis of the multiplet system it was found that the chemical shift between the meta and para protons changed only 0.4 cycle/sec over the range studied. The check on effect of dilution was made since it was necessary to employ a concentration of 10% of some compounds in order to get reproducible measurements of the AB_2 system. For analysis of the deutero, dimethylamino, carboxyl, bromo, and methoxy compounds 5% solutions were employed. It is estimated from the average standard deviation for all compounds that the measured chemical shift between meta and para protons is accurate to within 0.4 cycle/sec and that the same accuracy was obtained for reference measurements. This would lead to a maximum possible error of ±0.8 cycle/sec for the chemical shifts in Table I. The τ values for the methyl groups as listed in the table were obtained from measurements on 5% solutions in carbon tetrachloride containing 1% of tetramethylsilane. The nitroethylene spectrum was obtained from a 10% solution in carbon tetrachloride containing 1% of tetramethylsilane.

2,6-Dimethylaniline

Reagent grade 2,6-dimethylaniline (Eastman Kodak Co.) was freshly distilled from zinc dust to give a liquid, b.p. 79–80°, 6 mm, n_D^{25} 1.5588 (literature b.p. 216°, 747 mm, n_D^{20} 1.5602 (19)).

2,6-Dimethylnitrobenzene

Practical grade 2,6-dimethyl-1-nitrobenzene (Eastman Kodak Co.) was distilled before use to give a light yellow liquid, b.p. 81°, 7 mm, n_D^{25} 1.5203 (literature b.p. 225°, 744 mm (20, Vol. 3, p. 815)).

2,6-Dimethylphenol

Reagent grade 2,6-dimethylphenol (Eastman Kodak Co.) was twice sublimed before use to give white crystals, m.p. 43–44.5° (literature m.p. 49° (20, Vol. 4, p. 680)).

2,6-Dimethylanisole

Methylation of 2,6-dimethylphenol with dimethyl sulphate in alkali (21, p. 58) gave 69% of product from which a portion was redistilled to give a colorless liquid, b.p. 54°, 6 mm, n_D^{23} 1.5024 (literature b.p. 66–67°, 11 mm, n_D^{25} 1.5003 (22)).

N-*Methyl-2,6-dimethylaniline*

A mixture of 2.55 g (0.021 mole) of 2,6-dimethylaniline and 3.2 g (0.023 mole) of methyl iodide was heated under reflux for 30 minutes. The solid which formed was recrystallized from chloroform and acetone. The purified solid, 2.7 g, was then dissolved in 10% sodium bicarbonate and the solution extracted twice with ether. The ether extracts were dried over magnesium sulphate, then filtered, and the filtrate was distilled to remove the ether. The residue, 1.1 g (37%), was distilled through a Holtzmann column to give N-methyl-2,6-dimethylaniline, b.p. 73.5–74°, 6 mm, n_D^{25} 1.5347 (literature b.p. 87°, 13 mm (12)).

N,N-*Dimethyl-2,6-dimethylaniline*

Following the procedure of Brown and Grayson (19), N,N-dimethyl-2,6-dimethylaniline was prepared in 41% yield. The product distilled at 64–64.5°, 5 mm, n_D^{24} 1.5136 (literature b.p. 195°, 740 mm, n_D^{25} 1.5133 (19)).

2,6-Dimethylbenzonitrile

The nitrile was obtained in 37% yield from 2,6-dimethylaniline by diazotization and treatment with cuprous cyanide (21, p. 514). The product melted from 88–89.3° (literature m.p. 90–91° (23)).

2,6-Dimethylbenzoic Acid

The nitrile was converted to the amide by treatment with concentrated sulphuric acid and thence to the acid by heating with 100% phosphoric acid as described by Berger and Olivier (24). The acid after recrystallization from benzene melted from 115.5–116.5° (literature m.p. 115–116° (24)).

2,6-Dimethyliodobenzene

Following the procedure used for the preparation of iodobenzene (25, p. 351), 2,6-dimethylaniline was converted to the iodo compound in 14% yield. The product was a liquid, b.p. 98–99°, 9 mm (literature b.p. 228–230° (20, Vol. 3, p. 49)). Calc. for C_8H_9I: C, 41.4; H, 3.9. Found: C, 41.6; H, 3.7.

2,6-Dimethylbromobenzene

The procedure used for the conversion of *o*-toluene to *o*-bromotoluene (21, p. 135) was employed to convert 2,6-dimethylaniline into 2,6-dimethylbromobenzene in 15% yield. The product was a liquid, b.p. 74.5–75°, 7 mm, n_D^{25} 1.5532 (literature b.p. 206° (20, p. 379)). Calc. for C_8H_9Br: C, 51.8; H, 4.9. Found: C, 52.4, 51.9; H, 5.0, 5.0.

2,6-Dimethylfluorobenzene

This compound, although not previously prepared, was readily obtained from 2,6-dimethylaniline following exactly the procedure for the conversion of aniline to fluorobenzene (25, p. 295). The product was obtained in 40% yield as a liquid, b.p. 85°, 115 mm, n_D^{28} 1.4762. Calc. for C_8H_9F: C, 77.4; H, 7.3. Found: C, 77.6; H, 7.4.

2,6-Dimethylbenzene-1-d

The procedure for the preparation of this compound was kindly provided by Dr. L. C. Leitch (26). A mixture of 5 g of 2,6-dimethylaniline and 8 ml of heavy water (99.9%) containing a pellet of sodium hydroxide was stirred for 8 hours at 80°. The heavy water was separated in a separatory funnel and the exchange procedure was repeated twice more with fresh heavy water. The amine, 4.18 g (0.035 mole), was added to 12.1 ml of completely deuterated 50% hypophosphorous acid and 6.2 ml of heavy water and the mixture was cooled to −5° in an ice–salt bath. To this was added dropwise a solution of 2.38 g (0.035 mole) of sodium nitrite in 4.2 ml of heavy water keeping the temperature below 0°. The resultant solution was kept at 0° for 20 hours then extracted with ether. The extracts were dried over magnesium sulphate, filtered, and after removal of the ether under reduced pressure, distillation of the residue gave 0.7 g of colorless liquid, b.p. 65° (80 mm), whose N.M.R. spectrum gave no indication of contamination by other products.

Nitroethylene

This compound was prepared by the sequence recommended by Noland (27). The product was a lachrymatory yellow liquid, b.p. 43°, 90 mm, (literature b.p. 38–39°, 80 mm (28)).

ACKNOWLEDGMENTS

The author is grateful to Dr. W. G. Schneider for his helpful discussions. The author wishes to thank Dr. L. C. Leitch for providing the method of preparation of 2,6-dimethylbenzene-1-*d* and for a gift of deuterated hypophosphorous acid. The financial assistance

of the National Research Council of Canada is gratefully acknowledged. The author is also indebted to Mrs. V. Nicolson for technical assistance and to Miss E. Busk for the microanalyses.

REFERENCES

1. H. J. BERNSTEIN, J. A. POPLE, and W. G. SCHNEIDER. Can. J. Chem. **35**, 65 (1957).
2. W. G. SCHNEIDER, H. J. BERNSTEIN, and J. A. POPLE. Ann. N.Y. Acad. Sci. **70**, 806 (1958).
3. P. L. CORIO and B. P. DAILEY. J. Am. Chem. Soc. **78**, 3043 (1956).
4. A. A. BOTHNER-BY and R. E. GLICK. J. Chem. Phys. **26**, 1651 (1957).
5. R. W. TAFT, JR., S. EHRENSON, J. C. LEWIS, and R. E. GLICK. J. Am. Chem. Soc. **81**, 5352 (1959).
6. R. W. TAFT, JR. *In* Steric effects in organic chemistry. *Edited by* M. S. Newman. John Wiley and Sons, Inc., New York. 1956. p. 594.
7. R. W. TAFT, JR. J. Am. Chem. Soc. **79**, 1045 (1957).
8. A. D. BUCKINGHAM. Can. J. Chem. **38**, 300 (1960).
9. F. A. L. ANET. Proc. Chem. Soc. 327 (1959).
10. H. S. GUTOWSKY, C. H. HOLM, A. SAIKA, and G. A. WILLIAMS. J. Am. Chem. Soc. **79**, 4596 (1957).
11. J. A. POPLE, W. G. SCHNEIDER, and H. J. BERNSTEIN. High-resolution nuclear magnetic resonance. McGraw-Hill Book Co., Inc., New York. 1959. p. 88.
12. I. FISCHER. Acta Chem. Scand. **4**, 1197 (1950).
13. K. B. EVERARD, L. KUMAR, and L. E. SUTTON. J. Chem. Soc. 2807 (1951).
14. H. S. GUTOWSKY, D. W. MCCALL, B. R. MCGARVEY, and L. H. MEYER. J. Am. Chem. Soc. **74**, 4809 (1952).
15. E. A. BRAUDE, F. SONDHEIMER, and W. F. FORBES. Nature, **173**, 117 (1954).
16. E. S. WAIGHT and R. L. ERSKINE. Absorption spectra of conjugated carbonyl compounds. *In* Steric effects in conjugated systems. Butterworths Scientific Publications, London. 1958. p. 75.
17. L. M. JACKMAN. Applications of nuclear magnetic resonance spectroscopy in organic chemistry. Pergamon Press, New York. 1959. p. 123.
18. W. G. SCHNEIDER. To be published.
19. H. C. BROWN and M. GRAYSON. J. Am. Chem. Soc. **75**, 20 (1953).
20. I. HEILBRON and H. M. BUNBURY. Dictionary of organic compounds. Eyre and Spottiswoode Ltd., London. 1953.
21. ORGANIC SYNTHESES. Coll. Vol. I, p. 58.
22. D. Y. CURTIN and R. R. FRASER. J. Am. Chem. Soc. **80**, 6016 (1958).
23. R. SCHOLL and F. KACER. Ber. **36**, 327 (1903).
24. G. BERGER and S. C. J. OLIVIER. Rec. trav. Chim. **46**, 600 (1927).
25. ORGANIC SYNTHESES. Coll. Vol. II. p. 351.
26. L. C. LEITCH. Private communication.
27. W. E. NOLAND, H. I. FREEMAN, and M. S. BAKER. J. Am. Chem. Soc. **78**, 188 (1956).
28. N. LEVY and C. W. SCAIFE. J. Chem. Soc. 1471 (1947).

THE MECHANISMS OF PERMANGANATE OXIDATION

VI. THE OXIDATION OF CYANIDE ION[1, 2]

ROSS STEWART AND R. VAN DER LINDEN[3]

ABSTRACT

Kinetic and oxygen-18 tracer experiments have been used in an attempt to elucidate the mechanism(s) of permanganate oxidation of cyanide. From pH 12 to 14.6 the oxidation is represented by the equation,

$$2MnO_4^- + CN^- + 2OH^- \rightarrow 2MnO_4^{=} + NCO^- + H_2O.$$

From pH 12 to 6 the reaction was found to be complex and unstoichiometric yielding cyanate, carbon dioxide, cyanide ion, and finally cyanogen at pH 9 to 6.

The rate of reduction of permanganate, as followed iodometrically and spectrophotometrically, is found to be markedly dependent on the pH of the medium and reactant concentration. The rate is negligible in acid solution but rapid in basic media.

At pH greater than 12 two parallel processes are indicated which have been designated as reaction A and reaction B. Reaction A appears at low reactant concentrations <0.0004 M cyanide and higher hydroxyl ion concentrations >pH 13 and is represented by the kinetic expression

$$\left(-\frac{d[MnO_4^-]}{dt}\right)_A = k_2[MnO_4^-][CN^-]$$

where k_2 is independent of hydroxyl ion concentration and is insensitive to the presence of manganate and barium ions. A positive salt effect is observed and labeling experiments using permanganate enriched in oxygen[18] showed that the oxygen introduced into the product cyanate comes mainly from the oxidant (70%–80% oxygen-18 transferred).

The existence of a second process reaction B was indicated by the changing kinetics at higher reactant concentrations and lower basicities, by the non-linear Arrhenius plots, and by the observation that only 15–25% oxygen-18 transfer from permanganate to substrate had occurred at pH 13. The rate of this latter process is approximately represented by the kinetic expression

$$\left(-\frac{d[MnO_4^-]}{dt}\right)_B = \frac{k_3[MnO_4^-][CN^-]^2}{[OH^-]}.$$

These reactions are discussed in terms of mechanism.

INTRODUCTION

The permanganate oxidation of cyanide ion in basic solution is known to be a quantitative reaction and has been used by Drummond and Waters (5) in their studies of the oxidation of organic compounds by various compounds of manganese. Little is known about the mechanism of this reaction, however. Preliminary work in these laboratories (6) indicated that a transfer of oxygen occurs since oxidation with permanganate enriched in oxygen-18 produced cyanate containing an excess of oxygen-18. The present work was undertaken to elucidate the mechanism of this reaction.

After this work was completed a report of a kinetic study of the permanganate–cyanide reaction by Freund appeared (7). He studied the reaction in the 0.035–0.18 M hydroxyl ion region and obtained the rate law

$$-d[MnO_4^-]/dt = k_2[MnO_4^-][CN^-]$$

with an energy of activation of 9.0 kcal/mole^{-1}.

[1]*Manuscript received June 27, 1960.*

Contribution from the Department of Chemistry, University of British Columbia, Vancouver, B.C. From part of the thesis presented by R. V. der L. in partial fulfillment of the requirements for the Ph.D. degree, 1960.

[2]*The paper "The mechanism of the permanganate oxidation of fluoro alcohols in aqueous solution" by Ross Stewart and R. Van der Linden, Discussions Faraday Soc.* **29** *(1960), should be considered as Part V of this series. For earlier papers see references 1 to 4.*

[3]*Present address: Imperial Oil Co., Sarnia, Ontario.*

EXPERIMENTAL

Product Analysis

1. Cyanogen

A method developed by Rhodes (8) for detecting cyanogen was used. Nitrogen gas was bubbled through the cooled, acidified reaction mixture after the oxidation displacing the gaseous cyanogen. This was washed free of hydrocyanic acid by passing the gas flow through two tubes containing acidified 10% silver nitrate solution, and then was passed into two tubes containing 0.5 *M* sodium hydroxide which can hydrolyze cyanogen quantitatively to cyanide and cyanate (9). Cyanide was then determined by a Liebig titration (10). Yields of cyanogen were much lower if the permanganate oxidation was carried out at room temperature or if the reaction mixture was allowed to stand for any length of time before acidification, owing mainly to extensive hydrolysis under these conditions. If the oxidation was carried out at pH 9 at room temperature no cyanogen was found nor was cyanogen found when freshly precipitated manganese dioxide was used as the oxidizing agent. Paracyanogen or cyanogen polymer could not be observed when the reaction mixture after oxidation was slightly acidified and the manganese dioxide reduced with sodium bisulphite to obtain a clear solution.

2. Cyanate

(*a*) Cyanic acid was converted quantitatively (11) to carbon dioxide and ammonia by acid hydrolysis and the latter was determined by the usual Kjeldahl method. Cyanogen was removed from the reaction solutions before carrying out the Kjeldahl analysis.

(*b*) A gravimetric method, found to be reliable, involved the precipitation of cyanate as the silver salt after neutralization of the alkaline reaction mixtures to pH 5. This method cannot be used when the oxidation is carried out below pH 11, since cyanide, recovered in the reaction mixture, is precipitated as silver cyanide.

3. Carbon Dioxide

The total CO_2 content of the reaction mixtures was determined by using the same technique as for the analysis of cyanogen. Nitrogen was bubbled through the acidified oxidation mixture in which the cyanate has been hydrolyzed to CO_2, then through an acidified 10% silver nitrate solution into two tubes containing standard barium hydroxide solution. The unneutralized barium hydroxide was then titrated with standard acid. The amount of carbon dioxide which is produced in the oxidation at a given pH is the total amount minus the amount produced by cyanate hydrolysis.

4. Cyanide

Cyanide was analyzed by the usual Liebig titration. Below pH 12, where a 2:3 molar ratio of permanganate–cyanide is used, the precipitated MnO_2 was first removed by filtration. Above pH 12, where a 2:1 molar ratio is used, barium nitrate was added initially to the reaction mixture to precipitate insoluble barium manganate, which was then removed by filtration.

Reagents

Reagent grade chemicals were used. Potassium permanganate–O^{18} was prepared as previously described (1).

Alkaline manganate solutions were prepared by the method of Pode and Waters (12). The oxidizing power and alkalinity of the solutions were determined by an iodometric and hydrochloric acid titration methods respectively. A small correction to the alkalinity is required due to disproportionation of manganate. When manganate solutions were diluted, the solution was not allowed to become less basic than 0.01 *M* sodium hydroxide.

Kinetic Methods

Iodometric and spectrophotometric methods were used to follow the rate of reduction of permanganate and an argentimetric method was used to follow the rate of oxidation of cyanide.

1. Iodometric Method

In a typical kinetic run 50-ml samples were pipetted into 125-ml glass-stoppered Erlenmeyers and the Erlenmeyers brought to a temperature of 25±0.05° in a constant temperature bath. After addition of the permanganate these aqueous solutions became 0.1 *M* in KOH, 0.00024 *M* in KCN, 0.0005 *M* in $KMnO_4$, and 0.0363 *M* in K_2SO_4 ($\mu = 0.2$).

The reaction was initiated by introducing 4.73 ml of 0.00574 *M* permanganate solution with manual stirring from a rapid delivery pipette. The reaction was quenched at a given time interval with an acidified potassium iodide solution and the liberated iodine was titrated immediately with thiosulphate solution. In most cases at least eight points were obtained for the kinetic plots. The procedure for following the rate of manganate oxidation of cyanide was similar except that equimolar concentrations of reactants were used.

2. Spectrophotometric Method

This was essentially the same as that previously described with light absorption measurements being made at 522 and 426 mμ (3).

3. Argentimetric Method

In a typical kinetic method for following the rate of oxidation of cyanide the solutions were made up as for the iodometric method. Then 4.92 ml of 0.0116 *M* permanganate solution was added to each solution to start the reaction. The reaction was timed and then quenched with 1 drop of 30% hydrogen peroxide and the manganese dioxide filtered off. The clear solution was then titrated for cyanide by the Liebig method using 0.05 *M* silver nitrate solution.

4. Fast Reaction Kinetics

For very fast reactions the disappearance of permanganate was followed with the aid of an automatic quenching and timing device like that described by Sheppard and Wahl (13).

Oxygen-18 Tracer Techniques

1. Oxidation of Cyanide with Permanganate-O^{18}

Procedure (a): Silver cyanate obtained under stoichiometric reaction conditions.—A typical experiment was performed as follows. Over-all conditions: volume of solution 55 ml; approximate alkalinity 4 *M*; $[CN^-]_0 = 0.0195$ *M*. To a 125-ml glass-stoppered Erlenmeyer was added 0.304 gram of potassium permanganate (0.00192 mole; 1.114% enriched in O^{18}) dissolved in 25 ml boiled distilled water, 10 ml of 0.2 *M* barium nitrate solution, and 14 ml of 15.8 *M* sodium hydroxide carbonate free solution. The solution was cooled and immediately 5.5 ml of 0.195 *M* (0.00107 mole) potassium cyanide solution was pipetted into the stirred alkaline permanganate solution. The reaction mixture was allowed to stand for approximately 5 minutes at room temperature. The solution was centrifuged and the supernatant liquid filtered through a sintered glass funnel to remove the remaining insoluble barium manganate. The clear alkaline solution was then neutralized to pH 5 with dropwise addition of 4 *M* nitric acid. The neutralizing mixture was cooled in an ice bath while the solution was vigorously stirred with a magnetic stirring arrangement. Four milliliters of 0.5 *M* silver nitrate solution was added, silver cyanate was allowed to

settle and filtered on a sintered glass funnel, washed, and then dried over P_2O_5 under vacuum.

Procedure (b): Silver cyanate obtained using a twofold excess permanganate-O^{18}.—When a twofold excess of labeled permanganate was used, the excess permanganate was reduced with a few drops of 30% hydrogen peroxide after the reaction mixture was allowed to stand for 2 minutes. After filtration and centrifugation of the managanese dioxide – barium manganate precipitate, the solution was neutralized and the silver cyanate precipitated as in the previous procedure.

Procedure (c): Silver cyanate obtained under dilute reaction conditions.—Over-all conditions: volume of solution 500 ml of water; alkalinity 0.2 *M*; $[CN^-]_0 = 2.2\times10^{-3}$ *M*; $[MnO_4^-]_0 = 2.27\times10^{-3}$ *M*. To a 1000-ml stoppered Erlenmeyer was added 0.172 (0.00109 mole) of labeled permanganate dissolved in 300 ml of water, 5.6 grams of barium nitrate dissolved in 150 ml of water, than 49 ml of 2.04 *M* sodium hydroxide solution. To the vigorously stirred mixture was added 10 ml of 0.1088 *M* (0.00109 mole) potassium cyanide solution. The reaction mixture was allowed to stand until the permanganate color had disappeared (approximately 15 minutes) and then the combined silver cyanide – silver cyanate precipitate was obtained as before.

2. Determination of Oxygen Exchange Between Cyanate and H_2O^{18}

A typical experiment was performed as follows: A sample of recrystallized potassium cyanate (0.092 gram, 0.00113 mole) was weighed into a 4-ml stoppered flask and dissolved with 2 ml of water (>1.4% enriched in O^{18}). The pH of the solution, as measured on a Beckman Model G pH meter, was varied by addition of concentrated sodium hydroxide or dilute nitric acid. The solution was allowed to stand in a constant temperature bath at 25° for 30 minutes. The acidified solution was transferred to a 5-ml centrifuge tube and the cyanate precipitated with silver nitrate solution. The precipitate was centrifuged, the liquid decanted, and the solid washed with water. The wet precipitate was transferred to a 5-ml beaker, dried over calcium chloride and then over P_2O_5 under vacuum.

3. O^{18} *Analysis of Silver Cyanate*

Two methods, sulphuric acid decomposition and pyrolysis, were found suitable for converting silver cyanate to carbon dioxide which could be conveniently analyzed for O^{18} content by mass spectrometric analysis.

Method (a).—The silver cyanate was dropped on to concentrated sulphuric acid and the evolved carbon dioxide was collected. This method is similar to that previously used (12) except that break seals were used to transfer the gas to the mass spectrometer. The amount of excess O^{18} found in the silver cyanate can be calculated using the following equation (1); natural abundance of O^{18} = 0.204%.

$$\% \text{ O from permanganate} = \frac{2y-0.408}{x-0.204}\times100,$$

where

$$2y = \frac{I_{\text{mass}}46}{I_{\text{mass}}44+I_{\text{mass}}46},$$

$$x = \% \text{ O}^{18} \text{ in } KMnO_4 = 1.114.$$

Method (b).—The silver cyanate samples were decomposed under a low flame using the same apparatus as for the previous method. The carbon dioxide produced was collected and analyzed in a mass spectrometer. Other gases were produced in the decomposition as

observed by scanning the mass spectrum of the gaseous material but unlabeled silver cyanate on decomposition gave the expected normal isotopic abundance for O^{18}. The amount of O^{18} found in the silver cyanate can be calculated using a similar equation except that now all the oxygen in the carbon dioxide comes from the silver cyanate.

$$\% \, O^{18} \text{ from permanganate} = \frac{y-0.204}{x-0.204} \times 100,$$

where

$$2y = \frac{I_{\text{mass}}46}{I_{\text{mass}}46 + I_{\text{mass}}44},$$

$$x = \% \, O^{18} \text{ in } KMnO_4 = 1.114.$$

Similar results were obtained when samples of silver cyanate were subjected to analysis by both methods.

RESULTS

Kinetic Results

The rate constants were calculated using the following equations (1). For the iodometric method

$$k_2 = \frac{1}{[CN^-]_0 \times t} \times \frac{V_0 - V_t}{V_t - 4/5 V_0}$$

where V is the volume of thiosulphate solution required in the titration. When $(V_0 - V_t)/(V_t - 4/5 V_0)$ was plotted against time, linear plots were obtained over a limited reactant and hydroxyl ion concentration range. Linear second-order rate plots were obtained in some cases to 70% completion of the reaction although most plots were taken to 50% completion. Second-order rate constants (k_2, liter mole^{-1} sec^{-1}) were calculated from the slopes.

For the spectrophotometric method the following equation was used, where D is optical density at the indicated wavelength (3):

$$[MnO_4^-] = \frac{D_{522} - 0.282 D_{426}}{2248}.$$

The usual integrated second-order rate expression was applied to the rate data.

Plots of reciprocal of the permanganate concentration versus time were found to be linear up to approximately 50% reaction (Fig. 1) and second-order rate constants were calculated. The plots become non-linear and variable if the reaction was taken beyond 50% completion of the reaction possibly from light scattering due to precipitation of manganese dioxide caused by disproportionation of manganate.

The rate expression

$$-\frac{d[MnO_4^-]}{dt} = k_2[CN^-]\,[MnO_4^-]$$

is in agreement with the observed kinetics over a limited reactant and hydroxyl ion concentration range. The second-order rate constants k_2, liter mole^{-1} sec^{-1}, obtained by both spectrophotometric and iodometric kinetic methods are in good agreement and indicate that the rate constants, calculated from the rate plots, are reliable (Table I).

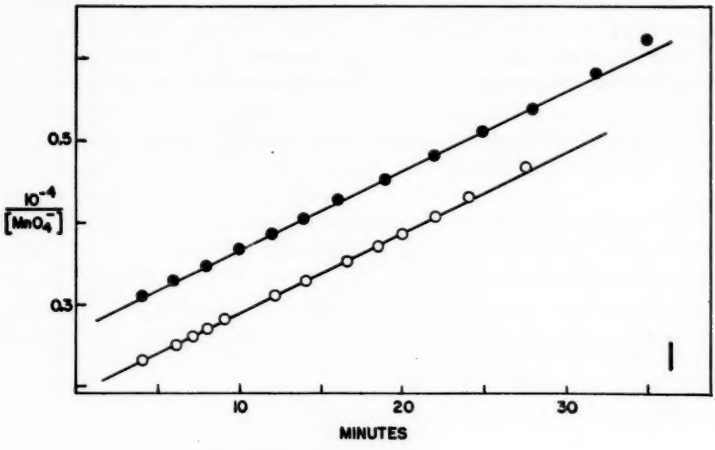

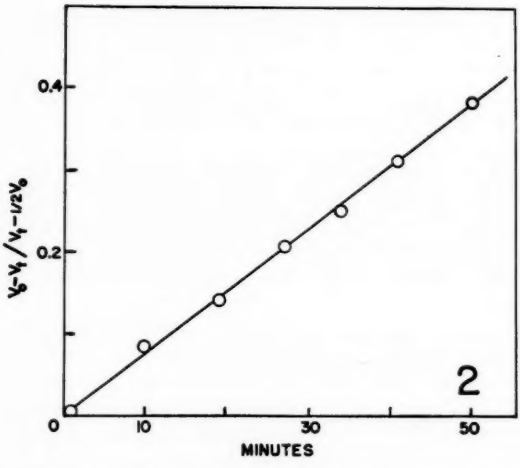

FIG. 1. Second-order rate plots for the permanganate–cyanide reaction by the spectrophotometric method.
$[OH^-] = 0.1\ M$, $T = 25°$, $k_2 = 3.20$ l. mole^{-1} sec^{-1}. ● $[MnO_4^-]_0 = 2[CN^-]_0 = 3.67\times10^{-4}$ mole/l.; ○ $[MnO_4^-]_0 = 2[CN^-]_0 = 5.13 \times 10^{-4}$ mole/l.

FIG. 2. Second-order rate plot for the manganate–cyanide reaction.
$[MnO_4^-]_0 = [CN^-]_0 = 3.27\times10^{-3}$ mole/l., $[OH^-] = 0.125\ M$, $T = 25°$, $k_2 = 0.039$ l. mole^{-1} sec^{-1}.

Observation of Table II with reference to Table I indicates that the second-order rate constants are relatively insensitive to additions of initial amounts of manganate ions and barium ions. Strontium nitrate was used to replace barium nitrate in one experiment in order to keep the ionic strength constant. Addition of initial amounts of manganate to the reaction mixture was possible since this species oxidizes cyanide 80 times slower than permanganate (Fig. 2).

TABLE I

Table of second-order rate constants for the permanganate–cyanide reaction under various conditions

Method	$[CN^-]_0$, M	$[OH^-]$, M	μ	k_2, l. mole^{-1} sec^{-1}
S	1.84×10^{-4}	0.1	0.1	3.2
S	2.57×10^{-4}	0.1	0.1	3.2
I	2.44×10^{-4}	0.1	0.1	2.9*
I	4.50×10^{-4}	0.1	0.2	4.0†
I	2.44×10^{-4}	0.1	0.2	3.9*
S	1.74×10^{-4}	0.2	0.2	3.7
I	2.44×10^{-4}	0.2	0.2	3.7‡
I	2.53×10^{-4}	0.06	0.1	3.0†
S	1.84×10^{-4}	0.06	0.1	3.4

NOTE: I = iodometric method, S = spectroscopic method, $[MnO_4^-]_0 = 2[CN^-]_0$; temperature = 25±0.05°.

*Average of two determinations.

†Rate constant obtained from the linear portion of the plot.

‡Average of three determinations.

TABLE II

Effect of initial amounts of manganate and barium nitrate on the second-order rate constants

$[CN^-]_0$, M	$[MnO_4^-]_0$, M	$[OH^-]$, M	μ	k_2,* l. mole^{-1} sec^{-1}
1.84×10^{-4}	1.78×10^{-4}	0.1	0.1	2.60
1.84×10^{-4}	3.55×10^{-4}	0.1	0.1	2.60
2.20×10^{-4}	2.13×10^{-4}	0.1	0.1	2.90
$[CN^-]_0$, M	$[Ba(NO_3)_2]$, M	$[OH^-]$, M	μ	k_2,† l. mole^{-1} sec^{-1}
2.53×10^{-4}	0.005	0.2	0.215	4.10
2.53×10^{-4}	—	0.2	0.215	3.50‡
2.53×10^{-4}	0.005	0.2	0.215	3.70

*Spectrophotometric kinetic method.

†Iodometric kinetic method; $[MnO_4^-]_0 = 2[CN^-]_0$; temperature = 25±0.05°.

‡0.005 M $Sr(NO_3)_2$ used in this experiment.

Data from Table I and Table III indicate that the second-order reaction is independent of the hydroxyl ion concentration under constant ionic strength conditions. For example, a 25-fold change in hydroxyl ion concentration does not change k_2 appreciably.

If increasing amounts of an inert electrolyte (potassium sulphate or potassium nitrate) are added to the reaction mixtures an increase in rate is observed at 0.1 M potassium hydroxide (Table IV and Table III). A primary positive salt effect is observed when log k_2 is plotted against $\sqrt{\mu}$ giving a straight line of slope +1 (Fig. 3). This agreement with the value expected from the Brönsted–Debye–Hückel relationship is rather surprising since this is a region of high ionic strength.

In order to determine the activation parameters a temperature study was done at 0.1 M and 0.2 M potassium hydroxide (Fig. 4 and Table V). When Arrhenius-type plots were made, linear plots were not obtained indicating that a more complex process was taking place than was implied by the simple rate expression given previously.

Since the kinetics indicate the presence of more than one mode of oxidation of cyanide by permanganate, the reaction conditions under which the second-order process (referred

TABLE III

Table of second-order rate constants for the permanganate–cyanide reaction under saturated salt* conditions

$[CN^-]_0$, M	$[OH^-]$, M	k_2, l. mole^{-1} sec^{-1}	
4.04×10^{-4}	0.1†	8.2	
2.02×10^{-4}	0.1*†	6.4	
4.04×10^{-4}	0.2†	8.3	
2.02×10^{-4}	0.2†	6.4	
4.04×10^{-4}	0.53†	6.0	
4.04×10^{-4}	1.55†	6.6	
4.04×10^{-4}	2.41	7.8	
4.04×10^{-4}	3.36	13.7±10%	
4.04×10^{-4}	3.65	20.0±20%	
4.04×10^{-4}	0.03†	16.5	Initial rates taken from the non-linear plots
4.04×10^{-4}	0.03	16.5	

*Use of 2 M KNO_3 gave a limiting reaction rate, i.e. further increases in salt concentration did not increase rate of reaction. Iodometric method, procedure 4; temperature = 25±0.05°.

†Ionic strength = 2.0; $[MnO_4^-]_0 = 2[CN^-]_0$.

TABLE IV

Rate constant as a function of ionic strength

Ionic strength	k_2, l. mole^{-1} sec^{-1}
0.1	2.90
0.1	2.80
0.133	3.20
0.166	3.40
0.166	3.67
0.200	3.90
0.200	3.90

NOTE: $[OH^-] = 0.1$ M; $[CN^-]_0 = 2.44\times10^{-4}$ M; $[MnO_4^-]_0 = 2[CN^-]$; potassium sulphate used to vary μ; temperature = 25±0.05; iodometric method.

TABLE V

Table of second-order rate constants at various temperatures

Temperature	0.1 M KOH k_2, l. mole^{-1} sec^{-1}	0.2 M KOH k_2, l. mole^{-1} sec^{-1}
10°±0.05	—	1.84
10°±0.05	—	1.88
15°±0.05	2.30	2.20
15°±0.05	2.20	2.16
20°±0.05	2.60	2.62
20°±0.05	—	2.64
30°±0.05	3.50	4.40
35°±0.05	4.3	5.80
35°±0.05	5.0	5.76

NOTE: $[MnO_4^-]_0 = 2[CN^-]_0 = 2.44\times10^{-4}$ M. Refer to Table I for 25° temperature points.

to herein as reaction A) is observed are summarized as follows:

when (*a*) $[MnO_4^-] = 2[CN^-]$ is less than 8×10^{-4} M;

(*b*) $[OH^-]$ is greater than or equal to 0.1 M;

(*c*) temperature is 25°.

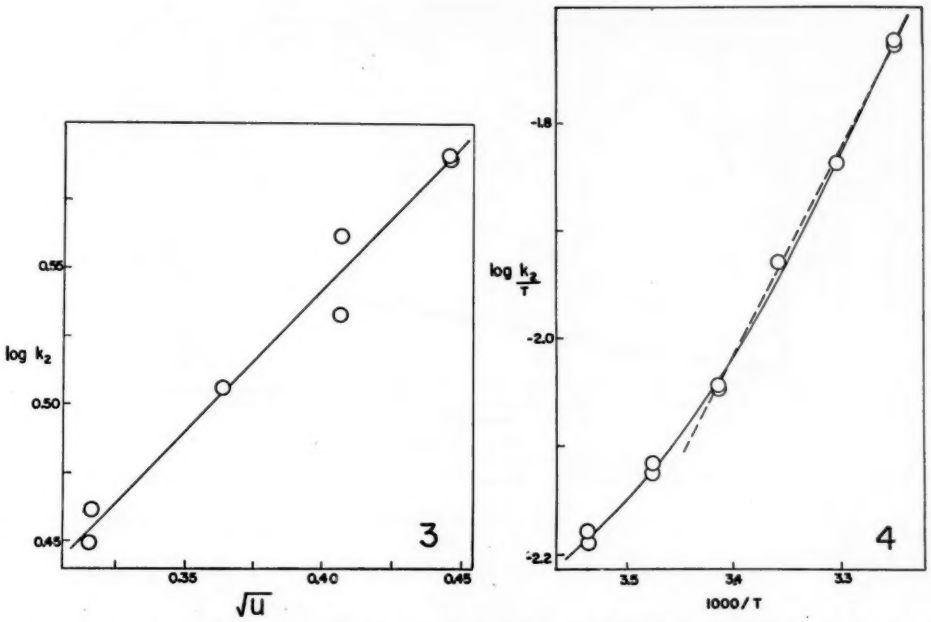

FIG. 3. Log k_2 vs. the square root of the ionic strength for the alkaline permanganate oxidation of cyanide. Slope = 1.0.

FIG. 4. Effect of temperature change on the rate of the permanganate–cyanide reaction in 0.2 *M* KOH. The straight line gives $\Delta H^{\ddagger} = 8.7$ kcal mole^{-1} and $\Delta S^{\ddagger} = -27$ e.u.

If second-order rate plots are attempted at higher concentration of reactants at the *same alkalinity* (Fig. 5) or lower alkalinities at the *same concentration of reactants* (Fig. 6), non-linear second-order rate plots are obtained and the rate was found to decrease with time. Under intermediate conditions (Fig. 6) the initial second-order rate plots are non-linear, becoming linear when the concentration of the reactants has been reduced.

The presence of a second mode of oxidation of cyanide is indicated (reaction B). Its rate appears to be a different function of concentration than the second-order process observed at lower concentrations and its rate is inhibited by high hydroxyl ion concentration. In an attempt to separate the two suspected reactions, concentration versus time plots were made for the rate data (Fig. 7) which gave non-linear second-order kinetics. These curves were smoothed and the slopes $(-d[MnO_4^-]/dt)_{A+B}$ obtained at various times.

Consider two parallel reactions contributing to the over-all rate,

$$\left(-\frac{dMnO_4^-}{dt}\right)_{A+B} = \left(-\frac{dMnO_4^-}{dt}\right)_A + \left(-\frac{dMnO_4^-}{dt}\right)_B,$$

where

$$\left(-\frac{dMnO_4^-}{dt}\right)_A = \tfrac{1}{2}k_2[MnO_4^-]^2,$$

and

$$\left(-\frac{d[MnO_4^-]}{dt}\right)_B \propto [MnO_4^-]^n.$$

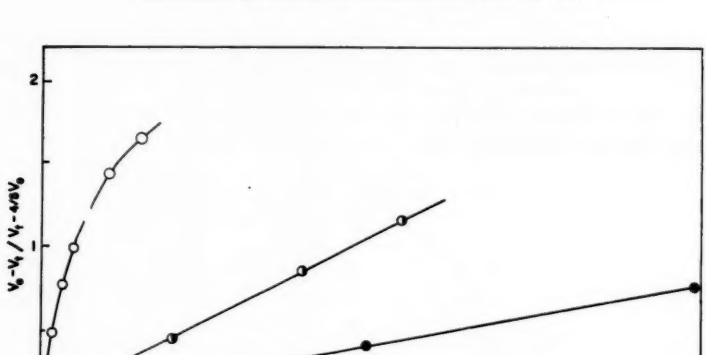

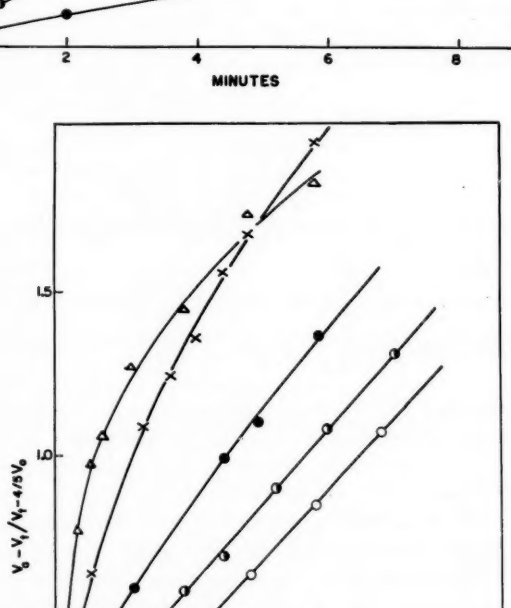

FIG. 5. Variation of the second-order rate function with reactant concentration in 0.1 M NaOH. $T = 25°$, $\mu = 2(KNO_3)$, $[MnO_4^-]_0 = 2[CN^-]_0$. ○ $[CN^-]_0 = 7.49 \times 10^{-4}$; ◑ $[CN^-]_0 = 4.04 \times 10^{-4}$; ● $[CN^-]_0 = 2.02 \times 10^{-4}$ mole/l.

FIG. 6. Variation of the second-order rate function with hydroxyl ion concentration. $[MnO_4^-] = 2[CN^-]_0 = 5.06 \times 10^{-4}$ mole/l., $\mu = 0.1$ (K_2SO_4), $T = 25°$. Δ = 0.01 M KOH; × = 0.02; ● = 0.04; ◑ = 0.06; ○ = 0.10.

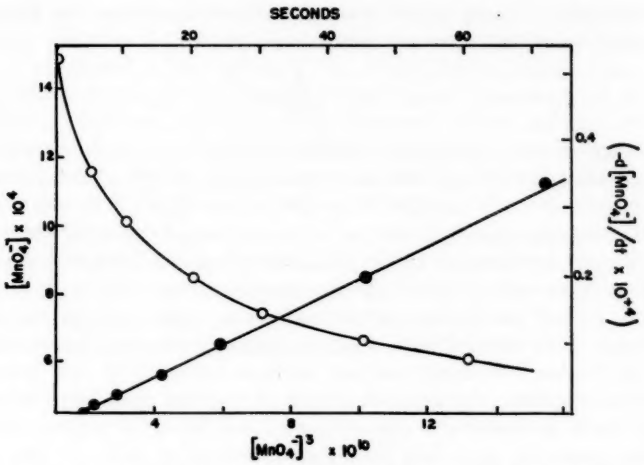

FIG. 7. Concentration vs. time (○) and the third-order rate plot (●) for the permanganate–cyanide reaction.
$[CN^-]_0 = 7.49\times10^{-4}$ mole/l., $[OH^-] = 0.1\ M$, $\mu = 2.0$.

Substituting for reaction A in the above equation and rearranging

$$\left(-\frac{d[MnO_4^-]}{dt}\right)_B = \left(-\frac{d[MnO_4^-]}{dt}\right)_{A+B} - \tfrac{1}{2}k_2[MnO_4^-]^2.$$

Therefore if k_2 is known at the same ionic strength and temperature and since reaction A is found to be independent of hydroxyl ion concentration, the rate of reaction A can be subtracted from the over-all rate.

A plot of $(-d[MnO_4^-]/dt)_B$ versus $[MnO_4^-]^3$ gives a straight line (Fig. 7). This technique was applied to a number of rate plots which gave non-linear second-order kinetics. The results although qualitative indicated that the reaction is third order and that the reaction is inhibited by hydroxyl ions.

Thus
$$\left(-\frac{d[MnO_4^-]}{dt}\right)_B = k_3[MnO_4^-]^3.$$

In order to determine the dependence of rate of reaction B on hydroxyl ion concentration more accurately, another plot using initial rates as obtained from the rate data from pH 12 to 13 was made. The initial point of the concentration–time plot was used to obtain $(-d[MnO_4^-]/dt)_{A+B}$ (Table VI).

TABLE VI

Initial rate as a function of hydroxyl ion concentration*

$[OH^-]$, M	$(-d[MnO_4^-]/dt)_{A+B\ (initial\ rate)}$	$[OH^-]\times$initial rate
0.01	0.034×10^{-4}	3.4×10^{-6}
0.02	0.021×10^{-4}	4.2
0.04	0.012×10^{-4}	4.8
0.05	0.0082×10^{-4}	4.1
0.06	0.0053×10^{-4}	3.2
0.10	0.0033×10^{-4}	3.3

*$[CN^-]_0 = 2.53\times10^{-4}$ mole/l.; $\mu = 0.1$; temperature = 25°.

The data in Table VI show that the initial rate multiplied by the hydroxyl ion concentration is very roughly a constant indicating that

$$k_3 \approx \frac{k_3'}{[OH^-]}.$$

The next stage in the investigation of this third-order process (reaction B) was to examine the kinetics of the very fast reaction when a 10-fold excess cyanide was used. Though the results are only qualitative a plot of log $[MnO_4^-]$ versus time (Fig. 8) at 0.03 *M* NaOH was approximately first order in permanganate after the first 5 seconds.

In an attempt to determine whether manganate was involved in a prior equilibrium step barium ions were added initially to the kinetic mixture. No marked change in rate was observed at 0.01 *M* and 0.04 *M* sodium hydroxide when insoluble barium manganate was precipitated. Also checks were made under various conditions using strontium nitrate to keep the ionic strength constant with no variation in rate being observed.

The spectrophotometric kinetic method led to marked non-linear second-order rate plots only at lower hydroxyl ion concentration, e.g. (0.02 *M* sodium hydroxide, μ = 0.1), since the permanganate and cyanide concentration used in this method were necessarily lower than those concentrations used in the iodometric method. It was observed that reaction B was greatly accelerated by increases in ionic strength.

Reduction of manganese to a lower valence state was considered as a possible cause for the observed faster reactions at lower alkalinities and higher reactant concentrations. If a deep-seated oxidation was taking place reducing permanganate or manganate to

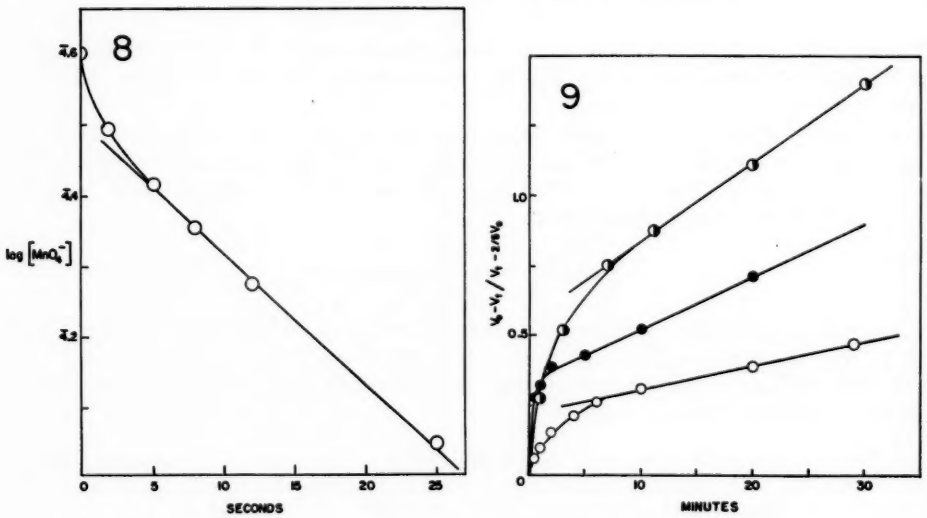

FIG. 8. Rate of disappearance of permanganate in presence of excess cyanide.
$[CN^-]_0 = 20.3 \times 10^{-4}$ mole/l., $[MnO_4^-]_0 = 4.03 \times 10^{-4}$ mole/l., $[OH^-] = 0.03$ mole/l., $T = 25°$, $k_1 = 0.0336$ sec^{-1}.

FIG. 9. Second-order rate function vs. time for the permanganate–cyanide reaction in weakly basic solution.
$[MnO_4^-]_0 = 2/3[CN^-]_0$, $\mu = 0.1$ (K_2SO_4), $T = 25°$, ○ pH = 10.4, $[CN^-]_0 = 2.67 \times 10^{-4}$ mole/l., $k_2 = 0.54$ l. mole^{-1} sec^{-1}; ● pH = 10.4, $[CN^-]_0 = 5.43 \times 10^{-4}$ mole/l., $k_2 = 0.59$ l. mole^{-1} sec^{-1}; ◑ pH = 9.8, $[CN^-]_0 = 2.52 \times 10^{-4}$ mole/l., $k_2 = 1.92$ l. mole^{-1} sec^{-1}.

lower oxidation states, an excess of cyanide over permanganate should be observed as reaction proceeds. Therefore, the argentimetric method for following the rate of oxidation of cyanide was developed. Observation of the concentration–time plots, obtained by both argentimetric and iodometric methods for the faster process at 0.1 M and 0.01 M sodium hydroxide, indicate that the stoichiometric concentrations (in this case $[MnO_4^-]$:$[CN^-]$ 2:1 molar ratio) holds throughout a major portion of the plot.

Early in the kinetic study a number of rate plots were obtained for the reaction at low pH's, and a few of these plots are presented (Fig. 9). Since the kinetics were more complex than those studied in more basic solution, a relative rate study was undertaken. This was accomplished by measuring the rate of the permanganate–cyanide reaction over a wide pH range, stopping the reactions at a given time interval. The extent of the reduction of permanganate was determined in an iodometric titration and $V_0 - V_t$ plotted against pH for a number of reaction conditions (Fig. 10).

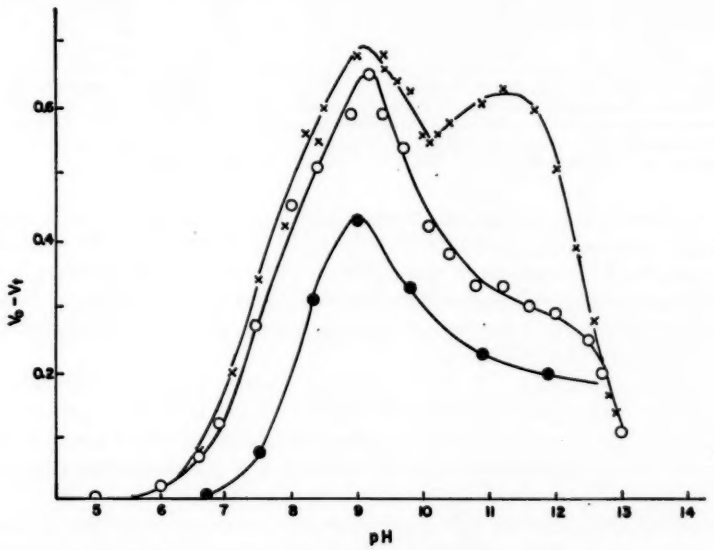

FIG. 10. Volume of thiosulphate consumed in a fixed time interval for the permanganate–cyanide reaction.

$T = 25°$, $\mu = 0.1$. ● $[CN^-]_0 = 3/2[MnO_4^-]_0 = 2.53\times10^{-4}$ mole/l., time interval = 2 minutes; ○ $[CN^-]_0 = 3/2[MnO_4^-]_0 = 2.09\times10^{-4}$ mole/l., time interval = 5 minutes; × $[CN^-]_0 = \frac{1}{2}[MnO_4^-]_0 = 2.09\times10^{-4}$ mole/l., time interval = 2 minutes.

Two important results might be noted:

(*a*) The rate of the permanganate–cyanide reaction is negligible in acid solution and increases markedly with increasing basicity.

(*b*) The maximum rate of the relative rate plots appears at the pK_a of HCN (pH = 9).

Oxygen-18 Tracer Results

Observation of Table VII shows that a transfer of oxygen has occurred from the oxidizing agent permanganate to the substrate cyanide. The percentage of O^{18} transferred appears to depend on the molar ratio and concentration of reactants as well as the alkalinity used in the experiments.

TABLE VII

Percentage O^{18} transferred from permanganate to cyanide under various reaction conditions

Alkalinity, *M*	$[MnO_4^-]_0/[CN^-]_0$	% O^{18} transferred (mean)	% O^{18} transferred (maximum)*
6	2/1†	—	80
4	2/1	70‡	78§, ‖
3	2/1	60¶	70
1.5	2/1	—	55
1	2/1	—	31
0.4	2/1	22**	25
0.1	2/1	20¶	23††
0.4	2/1	—	20
4	4/1	—	71‡‡
0.1	4/1	—	49‡‡
0.5	1/1	—	47§§
0.02	1/1	—	16§§
pH = 11.2	2/3	—	14
= 10	2/3	—	19
= 8	2/3	—	10

*$[CN^-]_0$ = 0.019 *M*; CO_2 obtained by pyrolysis of AgOCN. †Approximately 5% excess cyanide used in these experiments. ‡Average of five determinations. §76% obtained by the sulphuric acid method with the same sample. ‖82% transferred when the reaction was carried out at 50°. ¶Average of two determinations. **Average of three determinations. †† 26% transferred under saturated salt conditions, i.e., ionic strength 4, KNO_3. ‡‡$[CN^-]_0$ = 0.013 *M*. §§$[CN^-]_0$ = 0.0023 *M*.

In order to determine whether the product cyanate exchanges its oxygen with the solvent, cyanate was equilibrated with H_2O^{18} (<1.4% enriched) for 30 minutes at 25° at various acidities (six experiments were performed over a pH range from 5 to 14.6). In all experiments a negligible amount of O^{18} (0 to 2%) was found in the cyanate recovered as the silver salt, indicating that cyanate does not exchange its oxygen with the solvent in the time required to perform the oxidation.

The variation in the amount of O^{18} transferred under apparently similar conditions (e.g., 4 *M* sodium hydroxide) is difficult to explain but it should be pointed out that exchange reactions (14) can serve only to decrease the apparent transfer of O^{18} and, therefore, the maximum percentage transfer at any given pH can be used as a criterion of mechanism.

The O^{18} tracer and kinetic data will be discussed in terms of mechanism further in the paper, but the important features of the tracer data might be itemized as follows:

(*a*) The maximum percentage of O^{18} transferred in any experiment was 82% in 4 *M* sodium hydroxide at 50°.

(*b*) A general increase in percentage of O^{18} transferred is observed as the alkalinity is increased from 0.04 *M* to 6 *M* sodium hydroxide, i.e., fourfold increase (Fig. 11).

(*c*) The low percentage of O^{18} transferred at 0.1 *M* sodium hydroxide is not affected when the reaction is carried out at high ionic strength, i.e., $\mu = 4$.

(*d*) Almost a twofold increase in O^{18} transfer occurred on diluting the reaction mixture by eightfold at 0.4–0.5 *M* sodium hydroxide whereas at 0.02–0.04 *M* sodium hydroxide no change in percentage transfer took place.

(*e*) No further increase in O^{18} transfer is observed when the reaction is carried out with excess permanganate–O^{18} at 4 *M* base whereas an approximate twofold increase is observed at 0.1 *M* sodium hydroxide.

(*f*) In weakly basic solution, pH <12, only a small percentage of the oxygen introduced into cyanate originates from the oxidant.

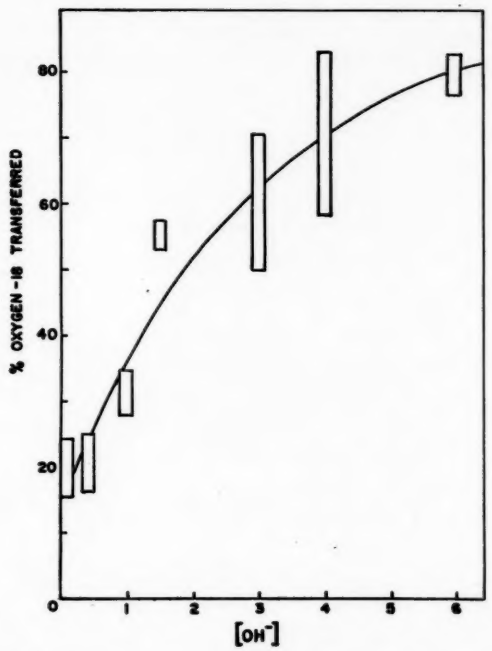

FIG. 11. Percentage of oxygen-18 transferred from permanganate to cyanide as a function of the molarity of hydroxyl ion.
$[MnO_4^-]_0 = 2[CN^-]_0$. The bar heights represent the variations found in different experiments.

DISCUSSION

The correlation of kinetic, oxygen-18 tracer, and analytical data which were of necessity obtained under different reaction conditions presents considerable difficulty. The kinetic data could only be conveniently obtained under low reactant concentration conditions where the rate was relatively small, whereas oxygen[18] tracer and analytical experiments necessitated in most cases considerably higher reactant concentrations.

The main features of the analytical data obtained for the permanganate–cyanide reaction over the pH range 6 to 14.6 are the following: Above pH 12 the sole product of the reaction is cyanate in almost quantitative yield; below pH 12 the reaction becomes increasingly unstoichiometric, yielding cyanate, carbon dioxide, cyanide, and finally cyanogen, which is isolated at pH 9 to 6. Cyanogen is presumably formed at higher basicities in these reaction mixtures but hydrolysis is very rapid at any pH greater than 9.

A fair material balance was obtained for the reaction over most of the pH range studied except for nitrogen (Table VIII). The presence of cyanogen in the reaction mixture (15) gives a ready explanation for the production of carbon dioxide through a deep-seated oxidation with permanganate and consequent recovery of cyanide, since cyanogen is known to hydrolyze readily in aqueous solutions to a number of easily oxidizable compounds (16, 17). As a consequence most of the kinetic and oxygen-18 tracer experiments were performed in alkaline solution above pH 12.

The rate of permanganate oxidation of cyanide is found to be markedly dependent on

TABLE VIII

Product yields for the permanganate–cyanide reaction

pH	13	12	11	10	9	8	7
% OCN^- Kjeldahl method	94		84	40	35	30	12
% OCN^- as AgOCN	98	96					
% Total CO_3*		99	96	71	50		46
% CO_3 produced in the reaction*		—	12	31	15†		24
% CN^- recovered			—	27	41		46
$\%(CN)_2$	—	—	—	—	Trace	11	28

NOTE: Cyanide concentration approximately 0.02 *M* in the analytical experiments; 3:2 molar ratio of cyanide to permanganate used below pH 12; 1:2 molar ratio used at pH 12 and above.

*Total CO_3 includes that formed by complete hydrolysis of cyanate during the analysis plus that formed by the oxidation reaction. (See experimental section.)

†Weighed as barium carbonate.

the pH of the medium and on the reactant concentrations. Thus the rate of reaction is negligible in acid solution at pH 6 or less, and above pH 7 the rate increases rapidly as the solution becomes more alkaline, reaching a maximum rate at pH 9.1. At this point the rate decreases again as the alkalinity is increased and at pH 13 (depending on reactant concentration) the rate levels off and becomes independent of pH except for an ionic strength effect (Fig. 29).

Two reaction paths, A and B, are indicated. Since the experimental evidence for reaction A is more clear-cut, this process will be discussed first.

Route A

(1) Second-order kinetics are observed over a limited reactant and hydroxyl ion concentration range indicating that the rate expression

$$\left(-\frac{d[MnO_4^-]}{dt}\right)_A = k_2[MnO_4^-]\,[CN^-]$$

holds for reaction A.

(2) A primary positive salt effect was observed indicating that the slow step was between two like singly charged ions, presumably permanganate and cyanide ions. This result is surprising in this case in view of the fact that the Brönsted–Debye–Hückel relationship normally holds for reactions carried out under more dilute aqueous conditions. Though the result is qualitatively correct, the close correlation to theory may be the result of an increased contribution from reaction B which is strongly ionic strength dependent.

(3) At constant ionic strength or under saturated salt conditions k_2 is found to be independent of the hydroxyl ion concentration, i.e., from 0.1 *M* to 2.4 *M* sodium hydroxide at low reactant concentrations. An increase in rate is observed at high alkalinities but in this region the effect of various electrolytes on the activity coefficients of the reacting molecules is difficult to predict and this effect will not be considered further here.

(4) The rate is not affected by the presence of initial quantities of manganate or barium ions. If an equilibrium was present such as

$$MnO_4^- + CN^- \rightleftharpoons MnO_4^{=} + CN\cdot,$$

an initial concentration of manganate should retard the reaction whereas the presence of barium ions would precipitate barium manganate and thereby increase the rate of reaction.

(5) The oxygen introduced into the product cyanate comes predominantly *from* the oxidizing agent rather than from the solvent. The maximum percentage of O^{18} transferred,

80%, occurred when the tracer experiments were carried out at high alkalinities, e.g., 4 *M* sodium hydroxide. An explanation is necessary at this point. Most of the kinetic data was obtained in the low hydroxyl ion concentration region, 0.1 to 0.2 *M* potassium hydroxide, where only 15 to 25% O^{18} transfer was observed. The discrepancy between the kinetic and O^{18} results at low base concentrations is probably due to the large reactant concentration difference which exists between the two series of experiments, e.g., 0.02 *M* cyanide for the tracer experiments and 0.0004 *M* cyanide for the kinetic experiments. When the alkalinity is increased in the O^{18} tracer experiments, a gradual increase in percentage of O^{18} transfer is observed (Fig. 11) whereas k_2 remains essentially constant (Table III) for the same increase in base concentration, thus indicating that reaction A (the second-order process) involves the oxygen transfer mechanism. The changing kinetics at higher reactant concentrations at 0.1 to 0.2 *M* potassium hydroxide tends to confirm these ideas. In this connection a twofold increase in percentage of O^{18} transferred was observed at 0.5 *M* sodium hydroxide when the reactants were diluted eightfold as would be expected if reaction A was favored at the lower reactant concentrations.

(6) Though Arrhenius-type plots were made using the rate constants obtained under conditions where apparently only one reaction process was present, non-linear plots were observed. Approximate values of $\Delta H^{\ddagger} = 8.7$ kcal/mole and $\Delta S^{\ddagger} = -27$ e.u. were obtained for the study at 0.2 *M* potassium hydroxide. This enthalpy of activation corresponds very closely to that calculated from Freund's results (7), and the entropy of activation is reasonable for a reaction between two anions. The significant curvature observed in the plots further indicates the possibility that two processes are present each with a different activation energy.

A mechanism which fits most of the data for reaction A is the following:

$$MnO_4^- + CN^- \xrightarrow{k_2} (NC\text{---}O\text{---}MnO_3)^- \rightarrow MnO_3^- + {}^-OCN,$$

$$MnO_3^- + MnO_4^- + 2OH^- \xrightarrow{\text{fast}} 2MnO_4^- + H_2O.$$

The existence of a Mn(V) species as a reaction intermediate in permanganate oxidations has been well established (18).

Route B

Although the kinetic data for reaction B is of a qualitative nature certain aspects of this study, in particular, the O^{18} tracer experiments and the observation that cyanogen was produced in the reaction at lower pH, suggest a reasonable reaction path.

Linear third-order kinetic plots were obtained for some of the rate data. In some instances a much faster decrease in rate with time was observed for the initial portions of the rate plots than would be predicted for a third-order process, thus indicating that still more complex processes were occurring.

If the third-order kinetic relation is assumed to be due to a first-order dependence on permanganate ion and a second-order dependence on cyanide ion and if the approximately inverse dependence on hydroxyl ion is indeed correct the following relations hold for route B:

$$(-d[MnO_4^-]/dt)_B = k_3[MnO_4^-][CN^-]^2$$

$$= k_3' \frac{[MnO_4^-][CN^-]^2}{[OH^-]} \qquad \text{since } k_3 = k_3'/[OH^-]$$

$$= \frac{k_3' K_a}{K_w} [MnO_4^-][HCN][CN^-],$$

where K_a and K_w are the ionization constant and ion product of hydrocyanic acid and water, respectively.

A possible mechanism for route B is the following:

$$MnO_4^- + HCN + CN^- \xrightarrow{\text{slow}} MnO_4^{=} + (CN)_2^- + H^+$$

$$(CN)_2^- + MnO_4^- \xrightarrow{\text{fast}} (CN)_2 + MnO_4^{=}$$

$$(CN)_2 + 2OH^- \xrightarrow{\text{fast}} CN^- + NCO^- + H_2O$$

In this connection Adamson (19) has suggested that $(CN)_2^-$ is present as an intermediate in the ferricyanide oxidation of cyanide.

It is worth comparing the behavior of permanganate towards cyanide ion and towards formate ion. The latter has been shown by Taylor and Halpern to be oxidized by permanganate about 2000 times faster at room temperature than the neutral formic acid molecule (20). This is a rather similar situation to the cyanide reaction, the difference being that for the latter a path involving both a HCN molecule and a cyanide ion appears to exist (route B). If a species $H(CN)_2^-$ is in equilibrium with HCN and CN^- it could be oxidized by permanganate by a hydride transfer mechanism which would produce Mn (V) and cyanogen, which would then yield the observed reaction products.

$$HCN + CN^- \rightleftharpoons H(CN)_2^-$$

$$MnO_4^- \overset{\curvearrowleft}{H}\text{—}(CN)_2^- \rightarrow HMnO_4^{=} + (CN)_2 \rightarrow \text{products}$$

The hypothetical species $H(CN)_2^-$ might have either of the following structures,* the second being merely a hydrogen-bonded form.

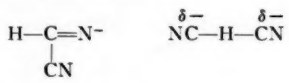

An electron transfer from cyanide ion to permanganate ion is probably not an energetically reasonable step although electron transfer from hydroxyl ion to permanganate ion appears to take place in strongly basic solution (21, 22).

Finally it should be mentioned that hydrogen cyanide can be added to the list of compounds for which the anion reacts very much faster with permanganate ion than does the neutral molecule (23). These include alcohols (3, 24), formic acid (2, 20), and water (21, 22).

ACKNOWLEDGMENT

The financial assistance of the National Research Council is gratefully acknowledged. One of us (R. V. der L.) is grateful for the award of the Cominco Fellowship and the Shell Oil Fellowship.

REFERENCES

1. K. B. WIBERG and R. STEWART. J. Am. Chem. Soc. **77**, 1786 (1955).
2. K. B. WIBERG and R. STEWART. J. Am. Chem. Soc. **78**, 1214 (1956).
3. R. STEWART. J. Am. Chem. Soc. **79**, 3057 (1957).

*A dimer of HCN exists. It hydrolyzes in water and is believed to be iminoformyl isocyanide with structure

(25).

4. K. B. WIBERG and K. A. SAEGEBARTH. J. Am. Chem. Soc. **79**, 2822 (1957).
5. A. Y. DRUMMOND and W. A. WATERS. J. Chem. Soc. 435 (1953).
6. R. I. CARLSON, W. A. BRYCE, and R. STEWART. Unpublished results.
7. T. FREUND. J. Inorg. & Nuclear Chem. **13** (1960).
8. F. H. RHODES. Ind. Eng. Chem. **4**, 652 (1912).
9. B. RICCA. Ann. chim. appl. **16**, 83 (1926).
10. A. I. VOGEL. Quantitative inorganic analysis. Longmans, Green & Co., Inc., Toronto. 1951. p. 263, 275.
11. A. R. AMELL. J. Am. Chem. Soc. **78**, 6234 (1956).
12. J. S. F. PODE and W. A. WATERS. J. Chem. Soc. 717 (1956).
13. J. C. SHEPPARD and A. C. WAHL. J. Am. Chem. Soc. **79**, 1021 (1957).
14. M. C. R. SYMONS. J. Chem. Soc. 3676 (1954).
15. B. RICCA and F. PIRRONE. Ann. chim. appl. **18**, 550 (1928).
16. V. MIGRDICHIAN. The chemistry of organic cyanogen compounds. Reinhold Publishing Corp., New York. 1947. p. 10.
17. H. E. WILLIAMS. Cyanogen compounds. Edward Arnold and Co., London. 1948. p. 3.
18. J. S. F. PODE and W. A. WATERS. J. Chem. Soc. 3373 (1956).
19. A. W. ADAMSON. J. Phys. Chem. **56**, 858 (1952).
20. S. M. TAYLOR and J. HALPERN. J. Am. Chem. Soc. **81**, 2933 (1959).
21. M. C. R. SYMONS. J. Chem. Soc. 3956 (1956).
22. K. A. K. LOTT and M. C. R. SYMONS. Discussions Faraday Soc.
23. J. W. LADBURY and C. F. CULLIS. Chem. Revs. **58**, 403 (1958).
24. R. STEWART and R. VAN DER LINDEN. Discussions Faraday Soc. **29** (1960).
25. L. E. HINKEL and R. J. DUNN. J. Chem. Soc. 1834 (1930).

THE ROLE OF REACTION PRODUCTS IN THE SILVER-CATALYZED OXIDATION OF ETHYLENE[1]

KENNETH E. HAYES[2]

ABSTRACT

Initial-rate studies of the kinetics of the silver-catalyzed oxidation of ethylene oxide and carbon dioxide in a flow system have been made. It was found that, using carefully purified reactants, the effect of added carbon dioxide was to suppress the formation of ethylene oxide only. The initial rate of the formation of ethylene oxide is given by the equation

$$r = r^0\left(m + \frac{n}{1+kP_{CO_2}}\right) = r^0\left(\frac{1+mkP_{CO_2}}{1+kP_{CO_2}}\right)$$

where r^0 is the initial rate in the absence of CO_2; m, n, and k are constants with $m+n = 1$.

These results together with the results of oxygen exchange reactions between O^{18} and $C_2H_4O^{16}$, CO_2^{16} and H_2O^{16} are interpreted mechanistically.

INTRODUCTION

The silver-catalyzed oxidation of ethylene has been investigated by a large number of workers in the last 10 years: the researches of Twigg (1), Murray (2), and Orzechowski and MacCormack (3) should particularly be mentioned. At the time that this investigation was started there was no quantitative information regarding the influence of the reaction products on the reaction. This investigation was undertaken with a view to rectifying this omission, and also with the hope of obtaining a more detailed knowledge of the mechanism of the reaction.

EXPERIMENTAL

The apparatus used to investigate the role of carbon dioxide and water vapor on the rates of formation of ethylene oxide and carbon dioxide was essentially a conventional flow system as shown schematically in Fig. 1.

The nitrogen, oxygen, and ethylene, all of a nominal purity of 99.5% or better, were passed from their respective cylinders through purification trains consisting of (A) anhydrous magnesium perchlorate (anhydrone), (B) activated charcoal, (C) KOH pellets, (D) silver turnings, and then through U-tubes immersed in solid carbon dioxide/isopropyl alcohol at −80° C. From the purification trains the gases passed through their respective capillary flowmeters, the flow being controlled by "Edward's LB2" fine control needle valves; through more silver turnings; and then through a further set of U-tubes at −80° C. The oxygen and nitrogen were mixed and passed through a preheater filled with silver turnings before entering the reactor. The ethylene was admitted to the reactor at the same gas inlet.

The carbon dioxide was passed through a similar purification train except for the omission of the KOH and the first cold trap. After the carbon dioxide was passed through a flowmeter, it was admitted to the nitrogen stream at a point prior to the second cold trap in the nitrogen line.

Water vapor was admitted to the system by passing the purified ethylene through a

[1]*Manuscript received in original form June 29, 1959, and, as revised, June 1, 1960.*
Contribution from the Division of Applied Chemistry, National Research Council, Ottawa, Canada. Presented at the annual meeting of the Chemical Institute of Canada, Halifax, May 1959.
Issued as N.R.C. No. 6010.
[2]*National Research Council Postdoctorate Fellow 1954–1956. Assistant Research Officer 1956–1958. Present address: Chemistry Department, Dalhousie University, Halifax, N.S.*

series of large bubblers containing triple-distilled water. These bubblers were immersed in two thermostats, the first held approximately 1° C above the temperature of the second which was maintained within ±0.01° C of the temperature required to give the desired partial pressure of water vapor.

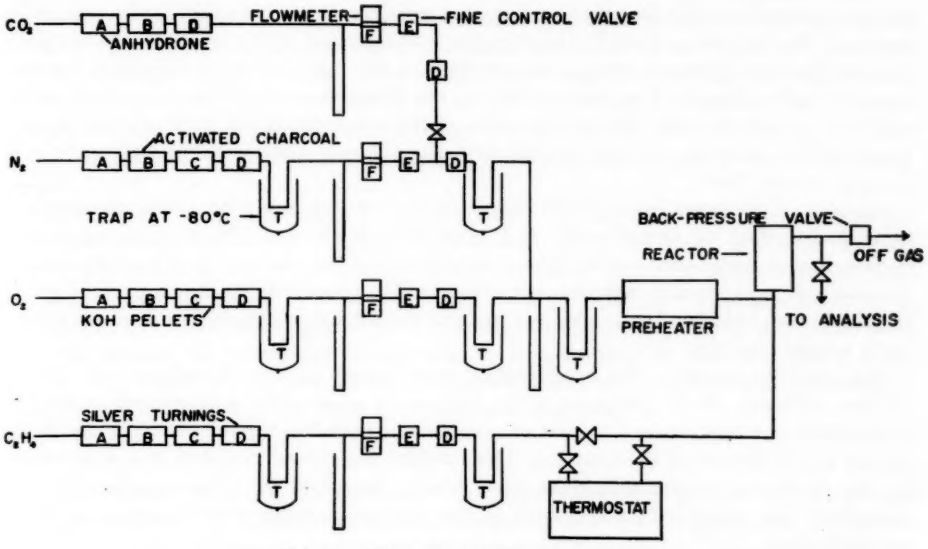

FIG. 1. Schematic diagram of apparatus.

The reactor is shown in detail in Fig. 2. For the preliminary experiments and for the comparison of various alloy catalysts, Part 2 was fabricated entirely from No. 304

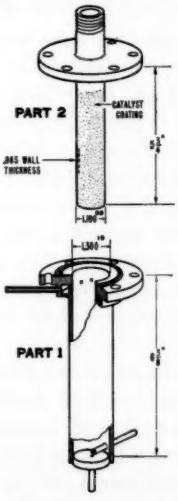

FIG. 2. Reactor in detail.

stainless steel, as was Part 1. For the detailed examination of the effect of CO_2 and H_2O on the reaction, the steel barrel of Part 2 was replaced by a sealed tube of "Mint Grade" silver. A 0.030-in. ring of annealed silver was used as a gasket between the two portions of the reactor. Temperature control was maintained by a mixture of Dowtherm A and E boiling under a pressure of nitrogen inside Part 2, heat being supplied by a sealed cartridge heater immersed in the Dowtherm. A copper condenser was attached to the reactor by means of the threads on Part 2. The temperatures reported in this work are the temperatures of the heat exchange medium measured by a chromel alumel thermocouple inserted into the boiling liquid. The temperature of the Dowtherm could be maintained within $\pm 1°$ C of a desired value. The temperature of the gas entering the reactor could also be measured by inserting a thermocouple into the thermocouple well situated right over the gas inlet of Part 1.

Samples of the gases issuing from the reactor were withdrawn by a similar technique to that described by Orzechowski and MacCormack (3) and the ethylene oxide and carbon dioxide were estimated in the customary manner by absorption in Lubatti reagent (4) and sodium hydroxide solution respectively. The absorbing solutions were added to the absorption bubblers by weight pipettes and the subsequent back titrations performed using weight burettes.

The catalysts used in this investigation were based on the "Cambron" (5) silver–calcium catalyst; 40- to 200-mesh 8.5% calcium in silver alloy was sprayed, under an atmosphere of nitrogen, onto the external surface of Part 2 of the reactor, this part being turned in a lathe during the spraying. The catalyst was cooled and then it was activated by the steam and acetic acid treatment already described (6). The reactor was then assembled and sealed into the system in the shortest possible time to avoid air-borne contamination.

Two other catalysts were examined in this investigation: a 1 wt.% gold in silver–8.5% calcium and a 1 wt.% antimony in silver – 8.5% calcium alloy. In each case the percentage of either gold or antimony was based on the amount of silver present and not on the combined silver–calcium weight. Both of these catalysts were sprayed and activated in the same manner as normal calcium–silver alloys.

The flow rates used in the investigation were multiples of 2/10/20 and 2/10/25 liters at S.T.P./hour for ethylene/oxygen/nitrogen. The maximum flow rates that could be conveniently handled were 7/35/70 and 6/30/75 liters at S.T.P./hour. Hence, for those experiments involving the catalyst deposited on the silver tube, the degree of reaction could be measured for values of M/F (where M is catalyst mass and F the total flow rate), varying between 0.191 and 0.669 and 0.193 and 0.578 g hour per liter for the two feeds, since the catalyst mass was 21.4 g and contained 0.083% calcium. When CO_2 was added to the feed it was added at the expense of the nitrogen thus maintaining the total flow rates at standard levels. The amount of CO_2 added to the feed was based on the ethylene in the feed. It then follows that when we speak of those experiments involving 10% CO_2 for example, the gas flow rates will be multiples of 2/10/19.8/0.2 and 2/10/24.8/0.2 liters at S.T.P./hour for $C_2H_4/O_2/N_2/CO_2$.

As has been shown by previous authors (3) the silver–calcium catalysts require approximately 75–100 hours operation under standard conditions before settling down to steady values of ethylene oxide and carbon dioxide produced. All of the results reported in this communication are for catalysts conditioned at standard flow rates of 2/10/20 liters at S.T.P./hour for at least 100 hours. It required a minimum of 3 hours for a

catalyst to settle down to a steady state after the flow conditions had been altered.

The preliminary experiments were performed at a total pressure of 1200 mm Hg; the experiments involving CO_2 and H_2O additions to the feed were made at both 1200 mm Hg and 850 mm Hg. The series of experiments involving CO_2 additions were made in one continuous operation—the reactor was not shut down for any purpose until the conclusion of the series; the same tank of ethylene was used throughout this series and necessary replacement of oxygen or nitrogen tanks was made at such times as coincided with the necessary changes in flow conditions. All of these experiments were made using the bracketing technique. At the end of the CO_2 series the reactor was shut down under a gas stream of 2/10/20 and then stored under nitrogen for a few days. The experiments on the addition of water vapor were then started and carried out in one continuous operation.

The exchange reactions between ^{18}O and C_2H_4O, CO_2, and H_2O were carried out in the same conventional high-vacuum apparatus that was used in the study of the decomposition of nitrous oxide on these silver–calcium catalysts (6). Ten millimeters of $^{18}O_2$-enriched oxygen, prepared by the electrolysis of H_2O^{18} (10%), was admitted to 10 g of an activated silver–calcium powder containing 0.43% calcium, and, after sufficient time had elapsed for adsorption equilibrium to be attained, 10 mm of either C_2H_4O, CO_2, or H_2O vapor (all purified by repeated distillation) was added, small gas samples being removed periodically for mass spectrographic analysis.

RESULTS

The preliminary experiments indicated that the results obtained for the percentage ethylene converted to ethylene oxide and carbon dioxide were reproducible to better than 3%, both for repeated experiments at a constant flow rate and for experiments at this flow after operations at different flows. This is shown for a typical catalyst in Table I.

In addition to illustrating the reproducibility obtainable in this system, Table I

TABLE I

$C_2H_4/O_2/N_2$ flow rates in liters at S.T.P./hour	Run No.	% C_2H_4 converted to:	
		C_2H_4O	CO_2
2/10/20	1	47.4	21.8
2/10/20	2	47.7	21.3
4/10/40	3	28.4	12.5
4/10/40	4	28.2	12.3
3/15/30	5	33.6	15.4
3/15/30	6	34.1	15.9
2.5/12.5/25	7	40.6	—
2.5/12.5/25	8	41.0	17.0
2.5/12.5/25	9	40.4	17.4
5/25/50	10	24.7	10.4
5/25/50	11	24.4	9.7
2/10/20	12	45.4	23.0
2/10/20	13	45.1	22.7
4/20/30	14	26.4	12.8
4/20/30	15	26.4	12.9
3/15/30	16	33.0	15.9
5/25/50	17	22.2	11.6
2/10/20	23	45.7	22.7

NOTE: Preliminary runs with 20 g of silver catalyst, % calcium, 0.1. Total pressure = 1200 mm Hg. Temperature, 250° for runs 1–11. Temperature, 245° for runs 12–23 after shutdown for major repairs. All analyses performed at 24-hour intervals.

also shows how easily the reaction level may be altered by uncontrolled changes in operating conditions. After run No. 11, a broken N_2 line resulted in a high concentration of ethylene and oxygen in the reactor leading to a runaway temperature and presumably causing sintering of the catalyst surface.

Table II compares the results obtained with normal calcium–silver catalysts and the special 1% gold–silver–calcium and 1% antimony–silver–calcium alloys. All of the results are for fully conditioned catalysts operating at 1200 mm Hg pressure, under standard conditions of 2/10/20 liters at S.T.P./hour.

TABLE II

The effect of alloying constituents on selectivity

Catalyst	% Calcium	Temp., °C	Cat. wt., g	% C_2H_4 converted to:		% Selectivity
				C_2H_4O	CO_2	
1% Sb–Ag	<0.01	243	20.0	15.4	35.5	30
1% Au–Ag	<0.01	225	17.0	19.8	57.7	25
Ag (1)	Appr. 0.1	250	20.0	47.4	21.3	69
Ag (2)	Appr. 0.1	250	20.0	40.4	14.9	72

It is seen from Table II that the presence of small quantities of gold or antimony in the silver alloy causes a marked decrease in the selectivity, although a high total activity is maintained. It is to be noted that the calcium content of these two catalysts is very low; as will be shown later, we would expect that the selectivity for these two "binary" catalysts containing calcium as the "impurity" should be low. However, if the calcium content is increased, the effect of the gold or antimony will be masked. Unpublished data of the author have shown that gold- and antimony-containing silver catalysts, containing also appreciable quantities of calcium, act as catalysts in the N_2O decomposition as though they were binary calcium–silver alloys containing less calcium, e.g. a 1% gold – 0.43% calcium in silver alloy acts as a calcium–silver alloy containing approximately 0.3% calcium.

Preliminary studies of the effect of CO_2 on the reaction showed that, within the limits of experimental error, added CO_2 had only a limited effect on the production of ethylene oxide, and no effect at all on the production of carbon dioxide. The quantitative results for the effect of CO_2 on ethylene oxide production are given in Table III and are illustrated in Fig. 3. The data of Table III are for four separate series of experiments, with flows which were multiples of 2/10/20, and 2/10/25 liters at S.T.P./hour for $C_2H_4/O_2/N_2$ and total pressures of 1200 and 850 mm Hg.

In Table IV the results of the effect of water vapor on the reaction are given. The temperatures refer to the temperature of the water in the saturators. Room temperature was between 25 and 27° during these runs; consequently, 22° C was the highest practical saturation temperature that could be used without heating the gas lines. It is apparent that, within the limits of experimental error, the addition of water vapor to the feed gas has no effect on the production of either ethylene oxide or carbon dioxide.

In Fig. 4, the results of the exchange between $^{18}O_2$-enriched oxygen chemisorbed in a silver catalyst and ethylene oxide, carbon dioxide, and water vapor are illustrated. It will be observed that the exchange involving ethylene oxide is much more rapid than that involving either of the other two gases. Of far greater importance is the fact that,

under similar experimental conditions, no oxidation of the ethylene oxide was observed until a temperature of 220° C had been reached, some 150° C above the temperature at which exchange takes place readily.

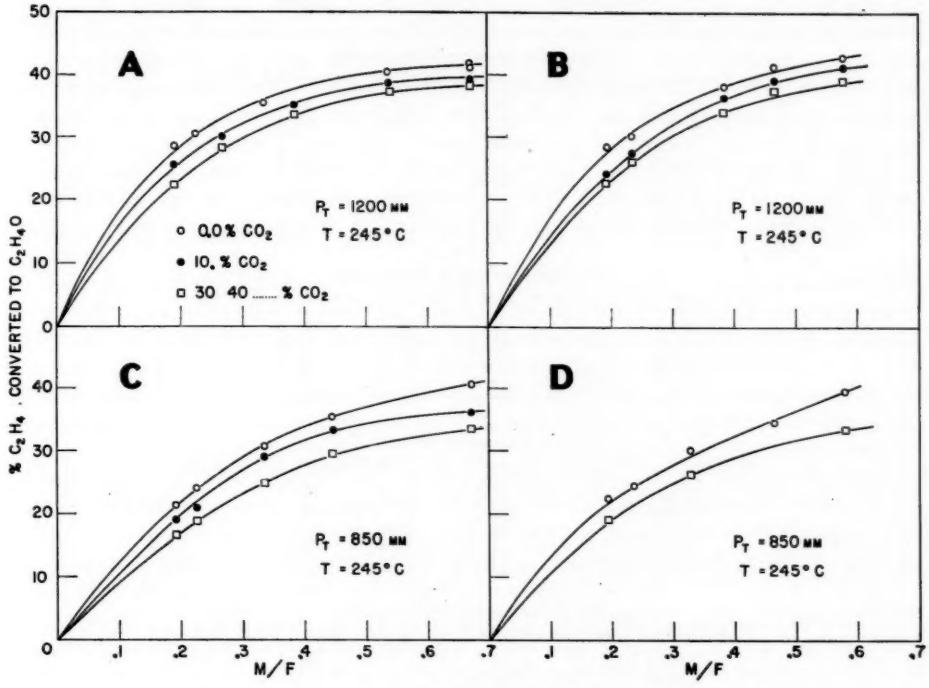

FIG. 3. Percentage conversion of C_2H_4 to C_2H_4O in the presence of CO_2.

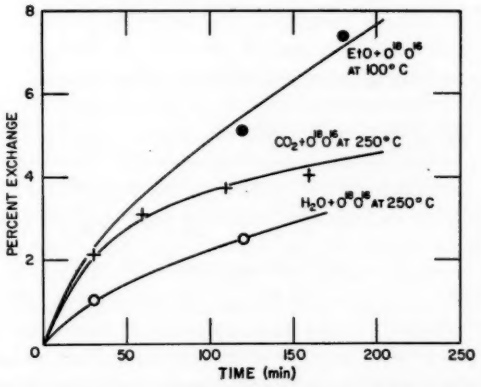

FIG. 4. Exchange between C_2H_4O, CO_2 and H_2O and O^{18} on silver–calcium alloy.

TABLE III

The effect of CO_2 on ethylene oxide production
(% conversion of ethylene to ethylene oxide)

$\frac{M}{F}$ \ $\frac{100\ CO_2}{C_2H_4}$ in feed	0	10	30	40
(A) Total pressure 1200 mm Hg				
M/F obtained from flow rates of X (2/10/20) liters at S.T.P./hour				
0.669	41.6	39.4	38.6	
0.535	40.3	38.9	37.4	37.9
0.446	38.4			
0.382		35.2	33.6	
0.334	35.3			
0.268		30.0	28.2	
0.223	30.0			
0.191	28.4	25.8	22.2	22.0
(B) Total pressure 1200 mm Hg				
M/F obtained from flow rates of X (2/10/25) liters at S.T.P./hour				
0.578	42.5	41.5	39.0	
0.463	41.2	39.3	37.5	
0.386	38.2	36.6	34.0	
0.231	31.9	27.6	26.3	
0.193	27.8	24.1	22.8	
(C) Total pressure 850 mm Hg				
M/F obtained from flow rates of X (2/10/20) liters at S.T.P./hour				
0.669	40.6	36.0	33.6	
0.446	35.3	33.2	29.4	
0.334	30.5	28.9	24.9	
0.223	23.9	21.0	18.9	
0.191	21.4	19.2	16.6	
(D) Total pressure 850 mm Hg				
M/F obtained from flow rates of X (2/10/25) liters at S.T.P./hour				
0.578	39.6		33.2	
0.463	34.4		—	
0.331	31.1		26.1	
0.231	24.6		—	
0.193	22.5		19.1	

NOTE: Catalyst, 21.4 g of 0.083% calcium in silver. Temperature, 245° C.

TABLE IV

The effect of water vapor on ethylene oxide production

$C_2H_4/O_2/N_2$ flow rates in liters at S.T.P./hour	No H_2O added	10° C	22° C
(A) % Ethylene converted to ethylene oxide			
2/10/20	38.5	38.5	38.7
7/35/70	23.6	24.4	24.0
(B) % Ethylene converted to CO_2			
2/10/20	35.8	—	35.3 (after 80 hours)

DISCUSSION

The experimental results of the silver-catalyzed oxidation of ethylene have been interpreted by two postulated mechanisms. The first, due to Twigg (1), assumed that ethylene oxide was formed by the interaction of ethylene with a single oxygen adatom;

and that deep oxidation was caused by the interaction of ethylene with a pair of suitably disposed oxygen adatoms. Orzechowski and MacCormack (3), on the other hand, interpreted their results on the basis of interaction between ethylene and chemisorbed oxygen atoms alone.

In 1952, DeBoer and Fortiun postulated (7) the existence of oxygen molecule ions O_2^- chemisorbed on silver, to account for the silver-catalyzed oxidation of cumene to cumene hydroperoxide. It was later postulated in this laboratory that chemisorbed O_2^- ions might be responsible for the deep oxidation of ethylene, with chemisorbed O^- ions being responsible for the formation of ethylene oxide. This viewpoint has subsequently been put forward by workers in this field. The conductivity measurements of Ljuburskij (8) have shown that oxygen abstracts electrons from a silver surface and this has been confirmed by the surface potential measurements of Kummer (9). In this latter paper, Kummer has also presented direct evidence for the existence of chemisorbed O_2^- ions on silver.

If oxygen is chemisorbed on silver, initially in the form of O_2^- ions, and subsequently as two O^- ions, we would expect that the addition of other components to the silver to decrease the work function would result in an increase in selectivity for the ethylene oxidation. A lowering of the work function would enhance the dissociation of O_2^- ions into O^- ions. Increasing the work function, on the other hand, would be expected to give the opposite effect, resulting in a lowering of the selectivity. The author has already shown (6), as a part of this investigation, that the addition of gold to silver increases the activation energy of the silver-catalyzed decomposition of N_2O. Since the rate-determining step in this decomposition involves the donation of an electron from the catalyst to the N_2O, an increase in activation energy is equivalent to an increase in work function. This same investigation also showed that by increasing the residual calcium in the catalyst (the silver–calcium alloys) the work function could be lowered.

The results in Table II show how the selectivities of the 1% gold in silver and 1% antimony in silver catalysts are markedly lower than the selectivities obtained from normal calcium–silver alloys. It is to be regretted that lowering the work function will not bring about as great an increase in selectivity under normal flow conditions, as we postulate that O^- ions are also responsible for the further oxidation of ethylene oxide to CO_2 and H_2O. A forthcoming publication (10) dealing with *initial-rate studies* on the silver-catalyzed oxidation of ethylene in a circulating system, in which the products are removed from the gas phase as they are formed, will show how the selectivity may be increased from 45% for pure silver to 65% for a 0.1% calcium in silver alloy.

If we now consider the poisoning of the reaction by added CO_2, we see from Fig. 4 that increasing the CO_2/C_2H_4 ratio in the feed gas over 0.30 has no further effect on the production of ethylene oxide. This means in effect that the initial rate of C_2H_4O formation in the presence of CO_2 falls to a steady value, greater than zero, as the partial pressure of CO_2 is increased. The data were analyzed in a manner similar to that used by Orzechowski and MacCormack, i.e., by considering the steady-state concentrations of the various adsorbed species (3). The two simplest assumptions regarding the adsorption of CO_2 are that CO_2 is either adsorbed on the free surface, at the expense of oxygen, or that it is adsorbed on top of the chemisorbed oxygen film at the expense of ethylene. Neither of these assumptions leads to a rate equation which fits our experimental data, since both derived rate equations require that the rate of production of C_2H_4O shall fall to zero if the CO_2 pressure is sufficiently high. If, on the other hand, it is assumed that the adsorption of CO_2 requires both a free surface site and an adsorbed O^- ion, leading

to a CO_3^- ion as the adsorption complex, then the initial-rate equation may be shown to be of the form

$$r_{EtO} = r^0_{EtO}\left(m+\frac{n}{1+kP_{CO_2}}\right) = r^0_{EtO}\left(\frac{1+k'P_{CO_2}}{1+kP_{CO_2}}\right)$$

where m, n, and k are constants, with $m+n = 1$ and $k' = mk$.

r_{EtO} = initial rate of C_2H_4O production in the presence of CO_2,

r^0_{EtO} = initial rate of C_2H_4O production in the absence of CO_2.

The rates, r, are given by the relation

$$r = \left(\frac{dx}{d(M/F)}\right)V_E$$

where x = fraction of ethylene converted to C_2H_4O,

M = catalyst weight in grams,

F = total flow rate in liters at S.T.P./hour,

and V_E = volume fraction of ethylene in the feed.

The constants m, n, and k were obtained from the data given in Table III(A). Values of $[dx/d(M/F)]V_E$ were then computed for the experimental conditions of Table III, (B), (C), and (D). The results are shown in Fig. 5, where the solid lines were calculated from the fitted points of A, the circles represent the experimentally determined points. The agreement is satisfactory.

Although the effect of added ethylene oxide on the production of ethylene oxide was not determined in this investigation, it has been shown by Roginskii and Margulis (11) that added C_2H_4O decreases the rate of production of C_2H_4O. This result could have been inferred from the exchange behavior of ethylene oxide with chemisorbed ^{18}O. We may visualize the exchange taking place as follows:

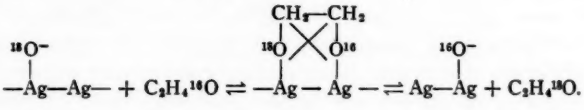

In view of the exchange behavior of water vapor, in which exchange possibly takes place via the formation of two OH^- ions in the surface, it is perhaps surprising that added water vapor has no apparent effect on either C_2H_4O and CO_2 production. It is possible, however, that water does inhibit the formation of ethylene oxide, in a manner analogous to that shown by CO_2, but the effect of water is so small that the water formed in the normal course of the reaction is sufficient to saturate the surface with respect to water vapor. We can summarize the basic postulates of this paper in the following reaction schemes:

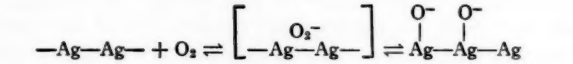

[1]

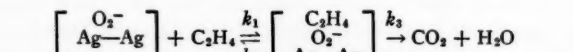

[2]

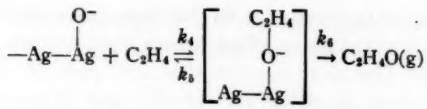

[3]

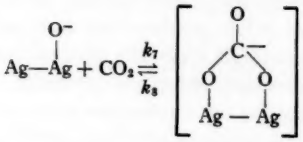

[4]

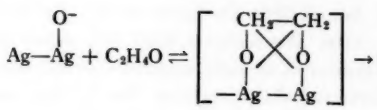

[5]

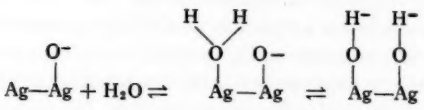

[6]

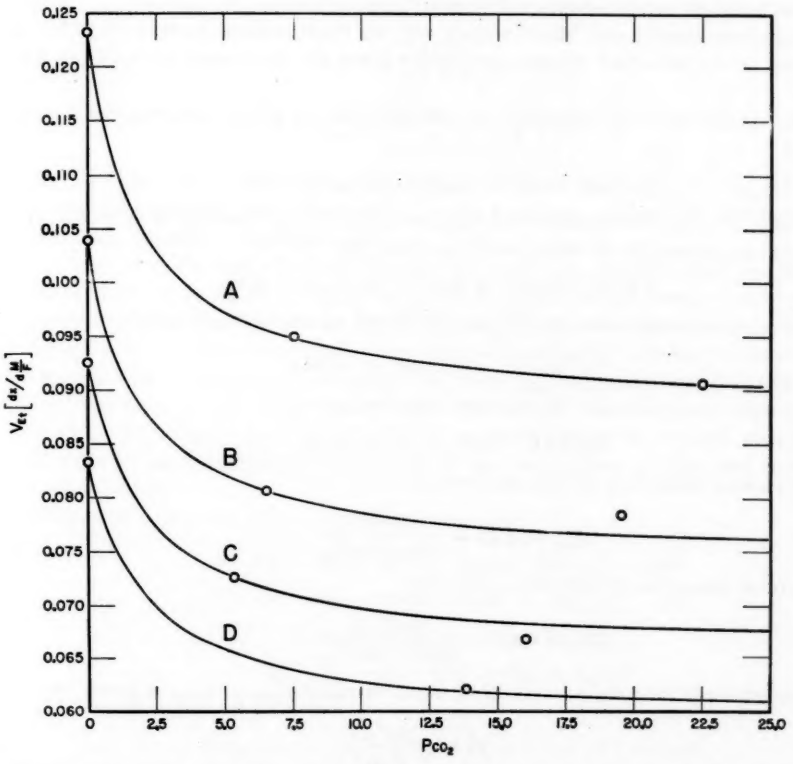

FIG. 5. Initial rates for the conversion of C_2H_4 to C_2H_4O as a function of the partial pressure of CO_2.

In applying the steady-state treatment to this postulated mechanism it is possible to treat the surface in two ways; this in effect means that we can treat the adsorption of oxygen in two ways. The first is to assume that any part of the surface is capable of holding the adsorbed oxygen as either O_2^- or O^-, and the second is to assume that, because of marked a priori heterogeneity, only certain portions of the surface can hold adsorbed oxygen as O_2^- and that other portions can hold adsorbed oxygen as O^-. The first treatment is far more complicated than the second, and while it shows that the selectivity of the reaction is a function of oxygen pressure (10), it also shows that the effect of added CO_2 under *all possible* circumstances is to reduce the rate of production of both CO_2 and EtO to zero if the pressure of CO_2 is sufficiently high.

The second treatment, while being perhaps more naive, satisfactorily accounts for most of the data published to date. We assume that the rates of formation of both adsorbed O_2^- and O^- may be considered as independent of each other and that the two species are found on different portions of the surface. We further assume that *all* of the CO_2 produced in the *early stages of the reaction* comes from interaction between ethylene and adsorbed O_2^-, i.e., there is no formation of CO_2 by a secondary oxidation of EtO.

Let θ be fraction of surface covered by O_2^- and θ' be fraction of surface covered by O^- under steady-state conditions. Further, let α be the fraction of the O_2^--covered surface covered by adsorbed ethylene, and β be the fraction of the O^--covered surface covered by adsorbed ethylene under steady-state conditions.

Following Orzechowski and MacCormack (3), we shall assume further that the rates of formation of the adsorbed oxygen species are given by the simple form of the Elovic equation.

Then the steady-state concentration of adsorbed O_2^- is given, ignoring desorption of oxygen, by

$$[1] \qquad jP_O(1 - m\theta) + k_2\alpha\theta = k_1P_{Et}(1 - \alpha)\theta,$$

where P_O and P_{Et} are the pressures of oxygen and ethylene respectively. Similarly the steady-state concentration of adsorbed O^- is given by

$$[2] \qquad j'P_O(1 - m'\theta') + k_5\beta\theta' = k_4P_{Et}(1 - \beta)\theta'.$$

The steady-state concentration of ethylene adsorbed on the O_2^- is given by

$$[3] \qquad k_1P_{Et}(1 - \alpha)\theta = (k_2 + k_3)\alpha\theta.$$

and steady-state concentration of ethylene adsorbed on the O^- by

$$[4] \qquad k_4P_{Et}(1 - \beta)\theta' = (k_5 + k_6)\beta\theta'.$$

Hence the rate of formation of CO_2 is given by

$$[5] \qquad r^0_{CO_2} = k_3\alpha\theta = \frac{k_3\alpha jP_O}{(k_3\alpha + jmP_O)}.$$

and the rate of formation of ethylene oxide by

$$[6] \qquad r^0_{EtO} = k_6\beta\theta' = \frac{k_6\beta j'P_O}{(k_6\beta + j'm'P_O)}.$$

We see immediately that the selectivity S, equal to $r^0_{EtO}/(r^0_{EtO} + r^0_{CO_2})$ is given by

$$[7] \qquad S = \frac{j'\left(1 + \frac{jmP_O}{k_3\alpha}\right)}{\left[j\left(1 + \frac{jmP_O}{k_3\alpha}\right) + j'\left(1 + \frac{j'm'P_O}{k_6\beta}\right)\right]}$$

or at constant ethylene pressure, as α and β are constants, the selectivity is a function of the oxygen pressure. From equations 5 and 6 we see that

[8] $$r^0_{EtO} = \frac{k_6 j' B P_O P_{Et}}{k_6 B P_{Et} + j' m' P_O + j' m' B P_O P_{Et}}$$

and

[9] $$r^0_{CO_2} = \frac{k_3 j A P_O P_{Et}}{k_3 A P_{Et} + j m P_O + j m A P_O P_{Et}}$$

where

$$A = \frac{k_1}{k_2 + k_3}$$

and

$$B = \frac{k_4}{k_5 + k_6}.$$

Equations 8 and 9 will then apply to those situations where the rate of oxygen adsorption is of the same order of magnitude as the rate of production of CO_2 and EtO. If now the rate of adsorption of oxygen becomes the limiting rate of the reaction it is permissible to suppose that in this case θ and θ' will be very small and that α and β both approach unity so that the rate of production of EtO will be independent of P_{Et} and,

[10] $$r^0_{EtO} = \frac{k_6 j P_O}{k_6 + j' m' P_O} \sim K P_O^{1/n}$$

[11] $$r^0_{CO_2} = \frac{k_3 j P_O}{k_3 + j P_O m} \sim K' P_O^{1/m}$$

Similarly, if the rate of adsorption of oxygen is faster than r^0_{EtO} or $r^0_{CO_2}$, then we can expect that the over-all rate, r^0_{EtO} or $r^0_{CO_2}$, to be functions only of the ethylene pressure; this has been found by Kurilenko (12).

If we now consider the effect of CO_2 on r^0_{EtO} and $r^0_{CO_2}$, we find that the postulate of adsorption of CO_2 on either O^-(ads.) or on the free surface will lower the activity to zero at sufficiently high CO_2 pressures. Similarly, in general, two point attachment of CO_2 involving both O^- adsorption and a free site will lower the activity to zero. However, for a special case, two point attachment will lower r_{EtO} only, and that to a limiting value greater than zero.

Let us suppose that a fraction γ of the O^--covered surface is covered with CO_2 under steady-state conditions, then a fraction $\gamma\theta'$ of the free surface will be used to obtain two point attachment.

The general equations 1, 2, 3, and 4 now become

[12] $$jP_O(1 - m\theta - \gamma\theta') + k_2\alpha\theta = k_1 P_{Et}(1 - \alpha)\theta$$

[13] $$j' P_O(1 - m'\theta' - \gamma\theta') + k_5\beta\theta' = k_4 P_{Et}(1 - \beta)\theta'$$

[14] $$k_1 P_{Et}(1 - \alpha)\theta = (k_2 + k_3)\alpha\theta$$

[15] $$k_4 P_{Et}(1 - \beta - \gamma)\theta' = (k_5 + k_6)\beta\theta'$$

and for the adsorption of CO_2

[16] $$k_7 P_{CO_2}(1 - \beta - \gamma)\theta'(1 - (\theta' + \theta) - \gamma\theta') = k_8\gamma\theta'.$$

The equations are difficult to solve (without making assumptions as to the relative value of second and third degree terms), but predict that the effect of CO_2 in general

will be to inhibit both CO_2 and EtO production. A similar series of equations predict the same behavior for both added EtO and H_2O. This type of behavior, namely complete inhibition by reaction products, in the order $EtO > CO_2 > H_2O$, would have been predicted on the basis of the isotope-exchange studies and has been found by Kurilenko (12) and more recently by Gorokhovatskii (13).

The results of this paper may be rationalized by assuming, (*a*) two-site adsorption of CO_2; (*b*) that the amount of adsorbed CO_2 is sufficiently small that no sites on which O_2^- (ads.) may be formed are destroyed, and (*c*) that the adsorption of CO_2 on the O^- (ads.) layer does not effect the adsorption of ethylene on this layer. The steady-state equations comparable to 13, 15, and 16 then become

$$j'P_O(1 - m'\theta' - \gamma\theta') + k_5\beta\theta' = k_4P_{Et}(1 - \beta)\theta', \quad [17]$$

$$k_4P_{Et}(1 - \beta)\theta' = (k_5 + k_6)\beta\theta', \quad [18]$$

$$k_7P_{CO_2}(1 - \gamma)\theta'(1 - \theta' - \gamma\theta') = k_8\gamma\theta'. \quad [19]$$

On solving these equations, with the further assumption that $(\theta')^2$ and $\gamma^2(\theta')$ may be neglected, we find that r_{EtO} is given by

$$r_{EtO} = \frac{k_6\beta j'P_O\left[1+\frac{k_7}{k_8}P_{CO_2}\right]}{k_6\beta\left(1+\frac{k_7}{k_8}P_{CO_2}\right)+j'm'P_O\left[1+\frac{k_7}{k_8}\left(\frac{m'+1}{m'}\right)P_{CO_2}\right]}. \quad [20]$$

For given values of P_O and P_{Et} equation 6 may be transformed to

$$\frac{1}{r^0_{EtO}} = \frac{k_6\beta+j'm'P_O}{k_6\beta j'P_O} = \frac{a}{r^0_{EtO}}+\frac{b}{r^0_{EtO}} \quad [21]$$

where a and b are fractions and $a+b = 1$. Comparison of 20 and 21 then gives, after some rearranging,

$$r_{EtO} = r^0_{EtO}\left[\frac{\left(1+\frac{k_7}{k_8}P_{CO_2}\right)}{\left\{1+\frac{k_7}{k_8}\left(\frac{m'+b}{m'}\right)P_{CO_2}\right\}}\right]. \quad [22]$$

Equation 22 then satisfactorily accounts for the data of this paper.

REFERENCES

1. G. H. Twigg. Proc. Roy. Soc. A, **188**, 92, 105, 123 (1946).
2. K. E. Murray. Australian J. Sci. Research, A, **3**, 433 (1950).
3. A. Orzechowski and K. E. MacCormack. Can. J. Chem. **32**, 388, 415, 432, 443 (1954).
4. O. F. Lubatti. J. Soc. Chem. Ind. (London), **51**, 361 (1933).
5. A. Cambron and F. L. W. McKim. U.S. Patent No. 2, 563,857 (1951); Can. Patent No. 475, 366 (1951).
6. K. E. Hayes. Can. J. Chem. **37**, 583 (1959).
7. J. H. DeBoer. Advances in catalysis. Vol. 8. Academic Press, Inc., New York, p. 79.
8. G. D. Ljuburskij. Doklady Akad. Nauk S.S.S.R. **110**, 112 (1956).
9. J. T. Kummer. J. Phys. Chem. **63**, 460 (1959).
10. J. B. Chenier, R. J. Cvetanović, and K. E. Hayes. To be published.
11. S. Z. Roginskii and L. Y. Margulis. Doklady Akad. Nauk S.S.S.R. **89**, 515 (1953).
12. A. I. Kurilenko *et al.* Zhur. Fiz. Khim. **32**, 797 (1958).
13. Ya. B. Gorokhovatskii *et al.* Doklady Akad. Nauk S.S.S.R. **125**, 171 (1959).

NOTES

ON THE EXISTENCE OF TERNARY COMPOUNDS IN THE SYSTEM NH_3–H_2O_2–H_2O

K. E. MIRONOV

Recently a note was published in this Journal (1) on the existence of ternary compounds in the system NH_3–H_2O_2–H_2O. On the basis of appearance of maxima in the melting-point curve along the plane $H_2O_2 \cdot 2H_2O$–NH_3 it was concluded that two compounds are formed, namely $NH_3 \cdot 3H_2O_2 \cdot 6H_2O$, m.p. −28.9° C, and $(NH_4)_2O_2 \cdot 2H_2O$, m.p. around 15° C. That this conclusion is erroneous may be gathered from an investigation of the whole liquidus surface of that system (2).

Indeed, there are two maxima in the above-mentioned plane (Fig. 1, p. 2270), but these maxima provide no evidence for ternary compounds since the said plane is not a singular or stable one (3). The first maximum at −29° C comes from intersection of the ridge in crystallization field of ice, while the second maximum comes from crystallization of the the compound $NH_3 \cdot H_2O_2$.

There were indications (1) from the infrared spectrum of the presumed compound at 32% NH_3 that it contained the NH_4^+ ion as well as water of crystallization. As may be judged from Fig. 1, the infrared investigation is consistent with the presence in that solid of the compound $NH_3 \cdot H_2O_2$ (4, 5) together with ice. On the other hand, the conclusion (1) regarding the non-ionic nature of the compound $2NH_3 \cdot H_2O_2$ seems correct in view of its limited range of existence, from −93.5° to −107° C (6). There are no ternary compounds in the system NH_3–H_2O_2–H_2O.

The author is grateful to I. I. Vol'nov for drawing his attention to paper (1).

1. P. A. GIGUÈRE and D. CHIN. Can. J. Chem. **37**, 2064 (1959).
2. K. E. MIRONOV. Dissertation. The diagram of phase conversions in the system NH_3–H_2O_2–H_2O and characteristics of compound $NH_3 \cdot H_2O_2$. (In Russian.) Referat. Zhur. Khim. No. 3 (1953). Ref. 2835D.
3. V. YA. ANOSOV and S. A. POGODIN. Fundamental principles of physico-chemical analysis. (In Russian.) Moscow, Leningrad. 1947. p. 576.
4. A. SIMON and A. KRIEGSMANN. Naturwiss. **42**, 14 (1955).
5. O. KNOP and P. A. GIGUÈRE. Can. J. Chem. **37**, 1794 (1959).
6. K. E. MIRONOV. Zhur. Neorg. Khim. **4**, 153 (1959).
7. A. G. ROLLET and G. VUILLARD. Compt. rend. **243**, 383 (1956).

RECEIVED MAY 30, 1960.
CANDIDAT OF CHEMICAL SCIENCES,
SIBERIAN DIVISION OF THE ACADEMY OF SCIENCES OF U.S.S.R.,
NOVOSIBIRSK, 49, KRASNY PROSPEKT,
U.S.S.R. DOM 163, KW. 114.

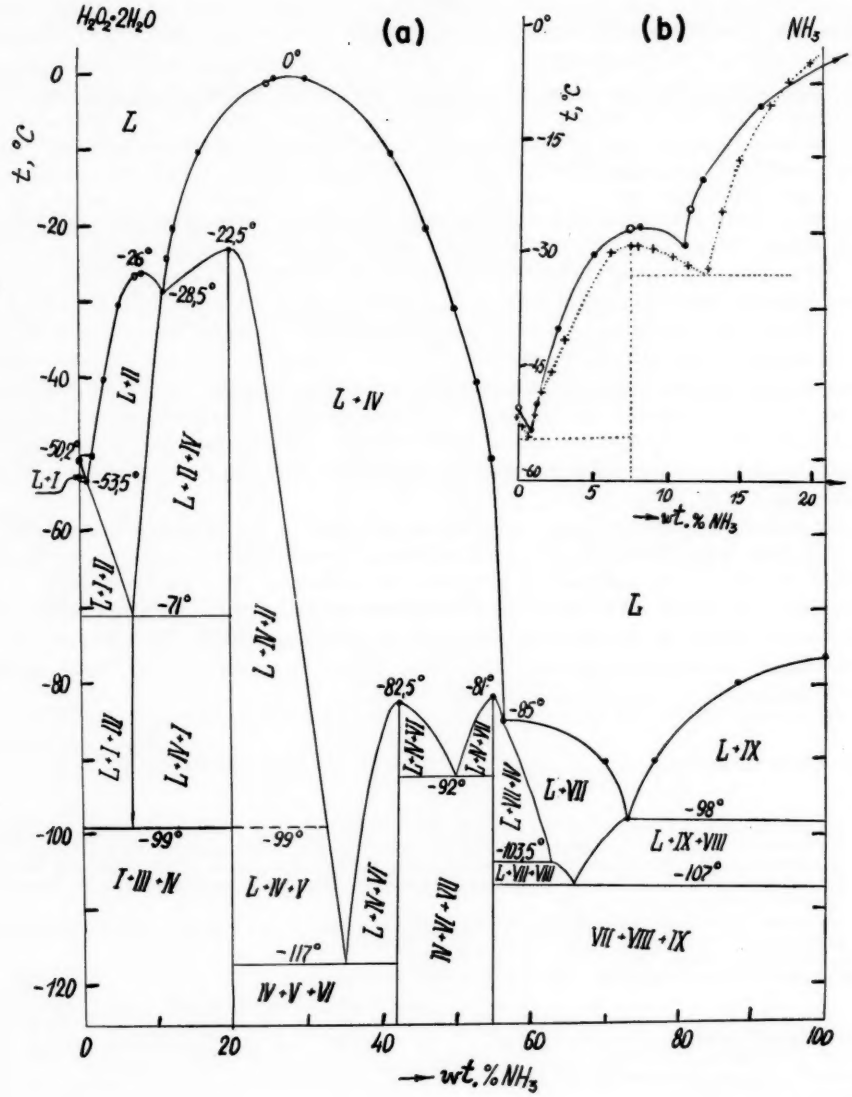

FIG. 1. (*a*) Melting-point diagram in the plane $H_2O_2 \cdot 2H_2O$–NH_3. (*b*) Comparison of liquidus diagrams in that plane.

Symbols: ○ liquidus from experimental data, ● liquidus from isotherms in the ternary system (2), + liquidus from the data of reference 1, ··· liquidus and solidus from reference 1, – – – more precise liquidus data from reference 7. L, liquid; I, $H_2O_2 \cdot 2H_2O$; II, ice; III, H_2O_2; IV, $NH_3 \cdot H_2O_2$; V, $NH_3 \cdot 2H_2O$; VI, $NH_3 \cdot H_2O$; VII, $2NH_3 \cdot H_2O$; VIII, $2NH_3 \cdot H_2O_2$; IX, NH_3.

APPLICATION OF THE HAMMETT EQUATION TO THE HYDROLYSIS OF SUBSTITUTED BENZAMIDES

J. T. EDWARD,* H. S. CHANG,* K. YATES,† AND ROSS STEWART†

The hydrolysis of amides is believed to take place by the two-stage mechanism (1, 2, 3):

$$RCONH_2 + H^+ \overset{\text{fast}}{\rightleftharpoons} RCONH_3^+ \qquad [1]$$

$$RCONH_3^+ + H_2O \xrightarrow[\text{slow}]{k_2} RCO_2H_2^+ + NH_3 \qquad [2]$$

Recently Leisten (4), by working with acid solutions which he considered concentrated enough to have all the amide present as $RCONH_3^+$, has attempted to obtain the rate constants k_2 for various substituted benzamides in the second rate-determining step:

$$\text{rate of reaction } v = k_2[RCONH_3^+].$$

(The concentration of water was not included in the kinetic equation since it was effectively constant in the experiments carried out in any one acid concentration.)

Leisten used 5.86 *M*, 7.19 *M*, and 8.54 *M* perchloric acid at 95° C. He gives reasons for believing that the pK_{BH^+} values of amides at this temperature will be about the same as at room temperature. On the basis of early estimates (3) of the basicities of benzamides, these concentrations of acid were assumed to be sufficient for essentially complete protonation of the compounds listed in Table I. However, the pK_{BH^+} values

TABLE I

Corrected rate constants k_2 (in hr^{-1}) for the hydrolysis of substituted benzamides in perchloric acid

	Acid concentration		
Substituent	5.86 *M*	7.19 *M*	8.54 *M*
p-Methoxy	0.238	0.073	0.026
p-Methyl	0.437	0.131	
m-Methyl		0.192	0.057
Hydrogen	0.805	0.234	0.073
p-Bromo		0.410	
m-Bromo		0.627	0.174
p-Nitro		1.77	0.545
m-Nitro	6.33	1.34	0.455

now reported for these compounds (5) show this assumption to be incorrect. Consequently, the experimental rate constants k_e (3), based on the stoichiometric concentration of amide and defined by

$$v = k_e([RCONH_2]+[RCONH_3^+]),$$

are not equal to k_2, which in fact is given by

$$[3] \qquad k_2 = k_e([RCONH_2]+[RCONH_3^+])/[RCONH_3^+]$$
$$= k_e(K_{BH^+}+h_0)/h_0$$

*McGill University, Montreal, Que.
†University of British Columbia, Vancouver, B.C.

where $K_{BH^+} = -\text{antilog } pK_{BH^+}$ and h_0 is Hammett's acidity function in its non-logarithmic form. The values of k_2 obtained from Leisten's results using eq. 3 are given in Table I.

The slopes of the least-squares plots of log k_2 against the σ values of the substituents (Fig. 1) give the values of the reaction constant ρ_2 for eq. 2 (6). These are listed below,

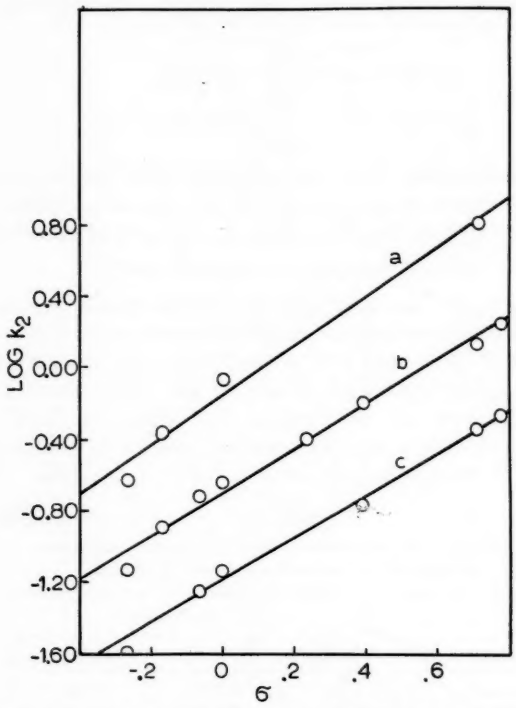

FIG. 1. Plots against Hammett's σ constants of log k_2 for substituted benzamides in the following concentrations of perchloric acid: *a*, 5.86 *M*; *b*, 7.19 *M*; *c*, 8.54 *M*.

with the number of results from which ρ_2 was determined (n), the standard deviation (s), and the correlation coefficient (r).

$HClO_4$ (M)	ρ_2	n	s	r
5.86	1.39	4	0.162	0.916
7.18	1.23	8	0.057	0.992
8.54	1.19	6	0.070	0.989

These values, slightly different from those of Leisten, are in better agreement with the value (1.42) calculated from the equation

[4] $$\rho_{0_2} = \rho_1 + \rho_2$$

where ρ_{0_2} is the reaction constant for the rates of hydrolysis of substituted benzamides in dilute acid (0.118, ref. 6), and ρ_1 (= −1.30) is the reaction constant recently determined (5) for eq. 1 in the direction shown.

1. C. K. INGOLD. Structure and mechanism in organic chemistry. Bell & Sons, Ltd., London. 1953. p. 785.
2. M. L. BENDER and R. D. GINGER. J. Am. Chem. Soc. **77**, 348 (1955).
3. J. T. EDWARD and S. C. R. MEACOCK. J. Chem. Soc. 2000 (1957).
4. J. A. LEISTEN. J. Chem. Soc. 765 (1959).
5. J. T. EDWARD, H. S. CHANG, K. YATES, and R. STEWART. Can. J. Chem. **38**, 1518 (1960).
6. L. P. HAMMETT. Physical organic chemistry. McGraw-Hill Book Co., Inc., New York. 1940. p. 184.

RECEIVED JULY 26, 1960.
DEPARTMENT OF CHEMISTRY,
MCGILL UNIVERSITY,
MONTREAL, QUE.,
AND
UNIVERSITY OF BRITISH COLUMBIA,
VANCOUVER, BRITISH COLUMBIA.

TRYPTAMINES, CARBOLINES, AND RELATED COMPOUNDS
PART VII. INTERNUCLEAR CYCLIZATION ONTO A PYRIDINE RING*†

R. A. ABRAMOVITCH

On the basis of two examples of internuclear cyclization of the Pschorr type onto a pyridine ring (1, 2) (one involving predominant electrophilic attack at the ring nitrogen) it was suggested (3) that the pyridine ring is more difficult to attack than a benzene ring in such reactions. The cyclization of 2-amino-*N*-methyl-*N*-3′-pyridylaniline (I) was studied to examine whether this was indeed so, as well as to provide a route to the δ-carboline ring system. Also, some evidence might thus be obtained to suggest a mechanism for the Pschorr reaction when carried out under such conditions, for the pyridine ring is known to be deactivated towards electrophilic substitution under mild conditions, but not towards homolytic attack. Should cyclization occur readily it was of interest to determine the orientation of the products since the isomer ratios for free radical phenylation of pyridine are in the order $\alpha > \beta > \gamma$ (4).

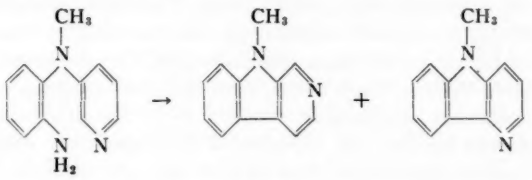

(I) (II) (III)

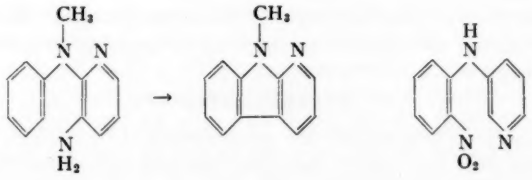

(IV) (V) (VI)

*Presented at the Atlantic City Meeting of the American Chemical Society on September 14, 1959.
†Part VI: Can. J. Chem. **38**, 557 (1960).*

Decomposition of the aqueous diazonium sulphate of 2-amino-*N*-methyl-*N*-3′-pyridylaniline (I) with copper powder at room temperature resulted in a good yield of a mixture of cyclized products which was separated into *ind*-*N*-methyl-δ-carboline (III) (47.5% yield) and *ind*-*N*-methyl-β-carboline (II) (25.5% yield) by chromatography on a column of alumina. The structure of (III) was confirmed by the analytical results and by its infrared spectrum, which showed no monosubstituted phenyl bands, thus eliminating the possibility that the substance isolated was the deaminated product. Its ultraviolet absorption spectrum was very similar to that of an authentic specimen of δ-carboline obtained by an unambiguous synthesis (5). The structure was finally proved by comparison with an authentic specimen whose preparation from δ-carboline is described in the next part of this series (5). The total yield of cyclized product (73%) is comparable with that obtained (78%) when *N*-(3-amino-2-pyridyl)-*N*-methylaniline (IV) is ring-closed to *ind*-*N*-methyl-α-carboline (V) (2), i.e. a similar cyclization, with similar internuclear separation (6), onto a benzene ring. This clearly indicates that in the present case the pyridine ring is not deactivated towards nuclear attack and that under these very mild reaction conditions free radical intermediates (perhaps bound in some way with the copper catalyst) may be involved. An amino substituent in the pyridine is known to facilitate electrophilic attack of the ring due to the mesomeric effect of the electron pair of the amino nitrogen atom. Phenyl substitution at the 3-amino group is expected, however, to decrease the activating effect of this group and *o*-diazotization to decrease it still further. An attempt to eliminate this possible source of ambiguity by replacing the *N*-methyl group in (I) by an acyl grouping was made. 2-Nitro-*N*-3′-pyridylaniline (VI), however, resisted all attempts at acetylation, tosylation, or mesylation, so that the required starting material could not be obtained.

It is very likely (7) that in the absence of copper powder and at the boiling point of the aqueous acid the cyclization involves cationic intermediates so that in such a case, though the reaction conditions are more severe than in the one where copper powder is used, the yield of cyclized product would be expected to fall due to the resistance of the pyridine ring to electrophilic substitution. This was indeed found to be the case, the over-all yield of carbolines being 47.2%: *ind*-*N*-methyl-δ-carboline (33%), *ind*-*N*-methyl-β-carboline (14.2%). A product, whose picrate analyzed for that of the deaminated product, was also obtained under these conditions. It is to be noted, however, that in contrast to the above results ring closure of 2-amino-*N*-methyldiphenylamine under both sets of conditions gave comparable yields of *N*-methylcarbazole (6). Thus, by the action of copper powder on the cold solution of the diazonium sulphate a 66% yield of cyclized product was obtained; the action of heat upon the aqueous diazonium sulphate solution in the absence of copper resulted in a 60% yield of *N*-methylcarbazole. Here there is no decrease in yield on passing from a heterolytic to a presumably homolytic process since the benzene, unlike the pyridine ring, is not deactivated towards electrophilic attack. These observations also support the suggestion that the side-chain tertiary amino group is probably not activating the ring towards electrophilic attack in such aqueous acid solutions.

EXPERIMENTAL

Melting points and boiling points are uncorrected. Ultraviolet absorption spectra were measured on a Beckman DK 2 recording spectrophotometer. For the chromatographic separations alumina supplied by Peter Spence and Sons, Ltd., as activated alumina type H, 100/200 mesh, was used.

N-Methyl-2-nitro-N-3'-pyridylaniline

A mixture of 3-bromopyridine (3.2 g), *N*-methyl-*o*-nitraniline (2.3 g), anhydrous potassium carbonate (2 g), and copper bronze (100 mg) in nitrobenzene (12 ml) was boiled under reflux for 24 hours. The suspension was steam-distilled and the residue extracted with chloroform, the extract dried ($MgSO_4$) and evaporated. The residue was distilled *in vacuo* giving a red viscous oil (1.4 g), b.p. 140–150°/2×10^{-2} mm, which formed a glass on cooling. The product was analyzed as *the picrate* which crystallized from ethanol as yellow needles, m.p. 168°. Found: C, 46.90; H, 2.99. Calc. for $C_{12}H_{11}O_2N_3$, $C_6H_3O_7N_3$: C, 47.17; H, 3.06.

2-Amino-N-methyl-N-3'-pyridylaniline

The above nitro compound (2.7 g), Raney nickel (1 g), and 100% hydrazine hydrate (10 ml) in alcohol (50 ml) were boiled under reflux for 15 minutes, the suspension filtered, and the filtrate evaporated to dryness leaving an oil (1.77 g) which slowly solidified. Vacuum distillation gave the *amine* as a colorless oil, b.p. 140–143°/0.4 mm, which solidified to a colorless solid. This was recrystallized from benzene – light petroleum (b.p. 60–80°) giving colorless needles, m.p. 93–94°. Found: C, 71.98; H, 6.24; N, 20.60. Calc. for $C_{12}H_{13}N_3$: C, 72.33; H, 6.57; N, 21.10.

Decomposition of the Aqueous Diazonium Sulphate of 2-Amino-N-methyl-N-3'-pyridylaniline

(i) With Copper Powder at Room Temperature

The amine (1.9 g) in concentrated sulphuric acid (4 ml) and water (50 ml) was diazotized at 0–5° with sodium nitrite (2 g) in water (20 ml), stirring at 0–5° being continued for ½ hour. Urea (1.5 g) was added to the clear solution to decompose the excess nitrous acid, and then copper powder (2 g) was gradually stirred in. The decomposition was complete in ½ hour as indicated by the cessation of effervescence and a negative alkaline β-naphthol test. The suspension was stirred at room temperature for a further ½ hour and then it was filtered from the copper, made alkaline with an excess of concentrated ammonia, and extracted with chloroform (2×200 ml). The dried ($MgSO_4$) extract was evaporated and the tarry black residue was taken up in benzene and chromatographed on a column of alumina (70 g). Elution with benzene first gave a colorless oil (0.82 g, 47%) which soon solidified, and had a melting point of 73–74°. Recrystallization from light petroleum (b.p. 60–80°) gave *ind-N-methyl-δ-carboline* as colorless plates, m.p. 74°. Found: C, 78.75; H, 5.72. Calc. for $C_{12}H_{10}N_2$: C, 79.09; H, 5.53. λ_{max} 263, 267, 306 mμ; λ_{infl} 235, 249 mμ; $\epsilon\times10^{-3}$ 18.92, 18.80, 11.83, 13.35, 10.62 (in ethanol). Infrared spectrum (Nujol mull) (main peaks only): 1628 (m), 1595 (m), 774 (m), 750 (m), 727 (s). The *picrate* separated from alcohol and was recrystallized from dioxane giving fine yellow needles, m.p. 229–230°. Found: C, 52.60; H, 3.0. Calc. for $C_{12}H_{10}N_2$, $C_6H_3O_7N_3$: C, 52.56; H, 3.19.

Further elution with benzene gave a brown oil which solidified very slowly. The solid was recrystallized from light petroleum (b.p. 60–80°) giving *ind-N*-methyl-β-carboline as colorless plates, m.p. 97° (0.45 g, 25%), undepressed on admixture with an authentic sample (8). Further recrystallization from light petroleum raised the melting point to 106–107°. Found: C, 79.03; H, 5.4. Calc. for $C_{12}H_{10}N_2$: C, 79.09; H, 5.53. The picrate separated from alcohol and was recrystallized from acetone giving fluffy yellow needles, m.p. 258°. Found: C, 52.31; H, 3.20. Calc. for $C_{12}H_{10}N_2$, $C_6H_3O_7N_3$: C, 52.56; H, 3.19. (Lit. (8) gives a melting point of 258°.)

(ii) By Boiling Without Copper Powder

The amine (2.0 g) was diazotized as before and the filtered diazonium solution was boiled under reflux for 10 hours. The cold solution was made just alkaline with aqueous sodium hydroxide and extracted with chloroform. The dried ($MgSO_4$) chloroform extract was evaporated, the residue taken up in benzene, and chromatographed on alumina as before. Elution with benzene gave first *ind-N*-methyl-δ-carboline (0.60 g, 33%), m.p. 73°, and then *ind-N*-methyl-β-carboline (0.26 g, 14.2%) as a very crude oil characterized as the picrate, m.p. and mixed m.p. 258°. Elution with ether gave a brown oil (0.10 g) which formed a picrate from alcohol. This picrate was recrystallized from acetone giving small yellow needles, m.p. 202–203° (decomp.), which analyzed for the *picrate* of *N*-methyl-*N*-3′-pyridylaniline. Found: C, 52.09; H, 3.14; N, 17.30. Calc. for $C_{12}H_{12}N_2$, $C_6H_3O_7N_3$: C, 52.21; H, 3.32; N, 16.94.

2-Nitro-N-3′-pyridylaniline

3-Aminopyridine (0.94 g), *o*-bromonitrobenzene (2.02 g), anhydrous potassium carbonate (2 g), and copper bronze (0.05 g) in xylene (20 ml) were boiled under reflux for 6 hours. The solvent was decanted off and the residue extracted repeatedly with boiling benzene, the combined extracts were treated with dilute hydrochloric acid, the acid solution made alkaline, saturated with sodium chloride, and extracted with benzene. The benzene solution was chromatographed on a short column of alumina. Elution with ether gave *2-nitro-N-3′-pyridylaniline* (0.62 g) as a dark red solid, m.p. 90°, which crystallized from water containing a little ethanol in slender orange-red needles, m.p. 95–96°. Found: C, 61.50; H, 4.51. Calc. for $C_{11}H_9O_2N_3$: C, 61.39; H, 4.42.

Attempted Tosylation of 2-Nitro-N-3′-pyridylaniline

The nitro compound (60 mg) and tosyl chloride (60 mg) in 2 ml of redistilled pyridine were boiled under reflux for 24 hours. Addition of water and recovery of the solid which precipitated gave unchanged starting material, m.p. 95–96°.

Similar results were obtained on attempted mesylation and acetylation (even in the presence of perchloric acid).

ACKNOWLEDGMENTS

Part of this work was carried out during the tenure of an I.C.I. Research Fellowship at King's College, London, England. The author is grateful to Dr. I. D. Spenser for an authentic specimen of *ind-N*-methyl-β-carboline and to Dr. L. Vining for the use of a recording Beckman DK 2 spectrophotometer.

1. D. H. Hey and J. M. Osbond. J. Chem. Soc. 3164 (1949).
2. R. A. Abramovitch, D. H. Hey, and R. D. Mulley. J. Chem. Soc. 4263 (1954).
3. H. Plieninger and M. Schach von Wittenau. Ber. **91**, 1903 (1958).
4. D. H. Hey, C. J. M. Stirling, and G. H. Williams. J. Chem. Soc. 3936 (1955).
5. R. A. Abramovitch, K. A. H. Adams, and A. D. Notation. Can. J. Chem. **38**, 2152 (1960).
6. D. H. Hey and R. D. Mulley. J. Chem. Soc. 2276 (1952).
7. D. F. Detar. Organic reactions. Vol. IX. John Wiley & Sons, Inc., New York. 1957. p. 409.
8. E. Späth and E. Lederer. Ber. **63**, 2102 (1930).

Received April 20, 1960.
Chemistry Department,
University of Saskatchewan,
Saskatoon, Saskatchewan,
and
King's College,
London, W.C.2, England.

THE CONDENSATION OF GLYOXAL WITH *p*-CRESOL

ALEX ROSENTHAL AND ALEC ZAIONCHKOVSKY

The preparation of condensation products from glyoxal and phenolic substances has been of considerable interest in the past decade. Chwala and Bartek (1) reported the condensation of glyoxal sulphate with phenol in the presence of mineral acids to yield a resin. At about the same time, Stevens and Dubbs (2) found that the reaction of 2-*tert*-butyl-4-methylphenol with glyoxal in the presence of acetic acid, hydrochloric acid, and zinc chloride afforded water-insoluble compounds. They also isolated, in unspecified yield, a substituted benzofuro[2,3-*b*]benzofuran. Groote and Keiser (3) have reported that the condensation of glyoxal with a phenol yielded low-stage resins.

In our investigation on the condensation of glyoxal with *p*-cresol, we employed two different reaction media. In the first runs, the reactants were condensed in an aqueous system using acetic acid and sulphuric acid as catalyst, whereas in later experiments the condensations were carried out in bis-(2-ethoxyethyl) ether using *p*-toluenesulphonic acid as catalyst.

When equimolar ratios of glyoxalmonohydrate and *p*-cresol were heated in aqueous acetic acid containing sulphuric acid as catalyst, a 70% yield of a crystalline material was obtained. Recrystallization of this substance from ethanol afforded 5,5¹-dimethyl-coumarano-3¹,2¹,2,3-coumaran (I). The structure of compound I was confirmed by direct comparison with an authentic sample (4).

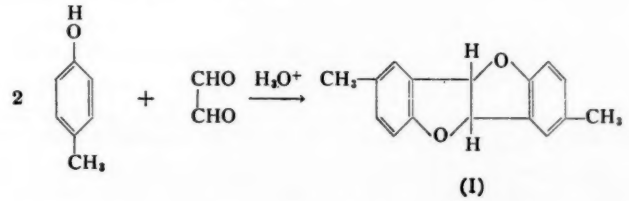

(I)

It is interesting to compare the prominent infrared spectral bands of 5,5¹-dimethyl-coumarano-3¹,2¹,2,3-coumaran (listed in the experimental) with those of other cyclic as well as straight-chain ethers. The fact that the coumarano-coumaran exhibited pronounced absorption at 1250 cm^{-1} provides additional confirmation for the generalization that the C—O—C of ring compounds probably absorbs at something like the same frequency as it does in open-chain products (5, 6). The band at 1095 cm^{-1} is ascribed to the asymmetrical ring stretching vibration (7).

Repeated attempts to condense anhydrous glyoxal with *p*-cresol in bis-(2-ethoxyethyl) ether using *p*-toluenesulphonic acid as catalyst, under various temperatures and in closed and open systems, were unsuccessful. Almost quantitative conversion of glyoxal into polymeric form occurred.

EXPERIMENTAL

Anhydrous glyoxal was prepared by heating glyoxalmonohydrate with phosphorus pentoxide in a dry all-glass apparatus fitted with a condensing trap cooled in dry ice.

Condensation of Glyoxal with p-Cresol

Procedure A.—Glyoxal monohydrate (2.6 g) dissolved in 15 ml water, and *p*-cresol

(3.6 g) dissolved in 10 ml glacial acetic acid, were mixed and placed in an apparatus fitted with a condenser. To the stirred preheated mixture, 5 ml of concentrated sulphuric acid was added dropwise. The voluminous precipitate was removed by filtration, washed with hot water, and dried: yield, 3.5 g. The material was recrystallized several times from ethanol, m.p. 192–194° C; mixed m.p. with an authentic sample of 5,5¹-dimethyl-coumarano-3¹,2¹,2,3-coumaran (4), 191–194° C; infrared data in Nujol: 1600 (w), 1495 (s), 1330 (w), 1250 (m), 1195 (w), 1130 (w), 1095 (w), 990 (s). Anal. Calc. for $C_{16}H_{14}O_2$: C, 80.65; H, 5.88. Found: C, 80.66; H, 6.26.

Procedure B.—Glyoxal monohydrate (5.3 g), *p*-cresol (7.1 g), and *p*-toluenesulphonic (0.25 g) were heated in a sealed Carius tube at 102° C for 14 hours. The product was extracted with acetone and precipitated by addition of water. Recrystallization of the product from ethyl alcohol gave 0.85 g of 5,5¹-dimethylcoumarano-3¹,2¹,2,3-coumaran.

Procedure C.—Fusion of the same reactants as described in procedure B at 130–140° C for 10 minutes gave 0.2 g of the coumaran.

Procedure D.—A solution of anhydrous glyoxal (0.72 g), *p*-cresol (1.30 g), and *p*-toluenesulphonic acid (0.050 g) dissolved in 15 ml of anhydrous bis-(2-ethoxyethyl) ether was allowed to react at 0° C in a sealed Carius tube for 24 hours. Addition of petroleum ether (200 ml) to the reaction mixture caused a precipitate (0.72 g) to form, m.p. 140–150° C (decomp.). This material showed strong absorption in the infrared at about 3400 cm^{-1}. The product, when heated to a temperature above 170° C, gave off yellowish fumes of glyoxal. When anhydrous gloxal was reacted with *p*-cresol in bis-(2-ethoxyethyl) ether at elevated temperatures only polymerized glyoxal was obtained.

ACKNOWLEDGMENT

The authors are indebted to the National Research Council of Canada for support of this research.

1. A. Chwala and W. Bartek. Monatsh. **82**, 652 (1951); Chem. Abstr. **47**, 7443 (1953).
2. D. R. Stevens and A. C. Dubbs. U.S. Patent No. 2,515,909 (July 1950); Chem. Abstr. **44**, 94, 83 (1950).
3. M. De Groote and B. Keiser. U.S. Patent No. 2,564,192 (August 1951); Chem. Abstr. **45**, 9254 (1951).
4. O. Anselmino. Ber. **41**, 621 (1908).
5. L. J. Bellamy. Infrared spectra of complex molecules. Methuen & Co. Ltd., London. 1958. p. 119.
6. R. Norman Jones and Camille Sandorfy. Chemical applications of spectroscopy. Interscience Publishers, New York. 1956. p. 438.
7. G. M. Barrow and S. Searles. J. Am. Chem. Soc. **75**, 1175 (1953).

Received July 18, 1960.
Department of Chemistry,
The University of British Columbia,
Vancouver, British Columbia.

NUCLEAR MAGNETIC RESONANCE SPECTRA OF SOME MODEL INDOLINE DERIVATIVES*

Stewart McLean†

The nuclear magnetic resonance spectra of three model indoline derivatives have been analyzed in order to obtain support for the assignment of certain N.M.R. peaks to particular structural features in dihydroindole alkaloids under investigation.

*Issued as N.R.C. No. 6012.
†National Research Council Postdoctorate Fellow. Present address: Department of Chemistry, University of Toronto, Toronto, Ontario.

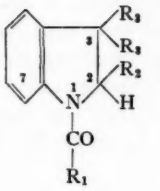

I (*a*) $R_1 = CH_3$; $R_2 = R_3 = H$
(*b*) $R_1 = CH_3CH_2$; $R_2 = R_3 = H$
(*c*) $R_1 = R_2 = R_3 = CH_3$

The aromatic protons of N-acetylindoline (I*a*) appeared in two parts of the spectrum, the C_7 proton (split by the other protons in the ring) as a doublet centered at −0.93 p.p.m. (spacing of 8.5 c.p.s.) and the remaining ring protons as a complex multiplet centered at about 0.22 p.p.m.* The corresponding peaks in N-propionylindoline (I*b*) were at −0.94 p.p.m. (spacing of 8.5 c.p.s.) and at about 0.27 p.p.m., and in N-acetyl-2,3,3-trimethylindoline (I*c*) at −0.52 p.p.m. (unresolved) and at about 0.35 p.p.m. The appearance of the C_7 proton signal at low field is potentially diagnostic for the absence of other substitution at the equivalent position in alkaloids of this partial structure. The protons at positions 2 and 3 in both I*a* and I*b* gave rise to the pair of triplets predicted for an A_2B_2 system approaching the A_2X_2 limit (2). The low-field signal was centered at 3.27 p.p.m. in the former and at 3.43 p.p.m. in the latter, and the high-field signals were centered at 4.15 p.p.m. and 4.28 p.p.m., respectively (the spacing was 8.5 c.p.s. for both). The proton at position 2 in I*c* gave rise to the *A* part of an AX_3 system (the C_2—CH_3 is the *X* part) and appeared as a quartet centered at 3.28 p.p.m. ($J = 6.5$ c.p.s.), supporting the assignment made to the corresponding proton in aspidocarpine (3).

The acetyl protons of I*a* and I*c* gave rise to single sharp peaks at 5.10 and 5.08 p.p.m., respectively. The propionyl protons of I*b* produced the expected quartet (two protons of CH_2) centered at 5.00 p.p.m. and triplet (three protons of CH_3) centered at 6.13 p.p.m. ($J = 8$ c.p.s.).

The methyl groups at positions 2 and 3 of I*c* produced three sharp peaks (total area equivalent to nine protons) at 6.05, 6.18, and 6.30 p.p.m. with relative intensities 2:3:1, which could be accounted for in the following way. The C_2 methyl group split by the C_2 proton formed a doublet at 6.18 and 6.30 p.p.m., one peak of which accidentally overlapped the peak at 6.18 p.p.m. produced by one of the C_3 methyl groups. The second C_3 methyl group produced the peak at 6.05 p.p.m.

EXPERIMENTAL

N-Acetylindoline— m.p. 106–106.5°, was prepared from indoline and acetic anhydride (4).

N-Propionylindoline— white needles, m.p. 104.5–105° from 95% ethanol, was prepared from indoline and propionic anhydride. Anal. Calc. for $C_{11}H_{13}ON$: C, 75.40; H, 7.48; N, 7.99. Found: C, 75.68; H, 7.49; N, 8.26.

N-Acetyl-2,3,3-trimethylindoline.—2,3,3-Trimethylindolenine (Aldrich Chemical Co.) (232 mg) was hydrogenated with pre-reduced platinum oxide catalyst in acetic anhydride. One mole of hydrogen was taken up rapidly. The catalyst was removed by filtration and

**Spectra were obtained with a Varian Associates high-resolution nuclear magnetic resonance spectrometer operating at 60 Mc/sec frequency. Chloroform was employed both as a solvent and as an internal reference; its proton resonance was assigned a value of zero part per million and the scale was fixed from the position of the associated C^{13} (natural abundance) peaks which were shown to have a value of ±1.75 p.p.m. Solutions were approximately 0.5 M and solvent effects were neglected. Accuracy to ±0.04 p.p.m. was anticipated on this scale. Chloroform has the value 2.75 p.p.m. on the Tiers scale (1).*

the filtrate was warmed and evaporated under reduced pressure. A chloroform solution of the residue was washed with dilute sulphuric acid and then with dilute sodium carbonate solution. The solution was dried (sodium sulphate) and evaporated. The residue, a yellow oil, distilled under reduced pressure, yielded an almost colorless oil (230 mg), b.p. 70–72°/10^{-1} mm, showing strong absorption at 1644 cm^{-1} in the infrared. Anal. Calc. for $C_{13}H_{17}ON$: C, 76.81; H, 8.43; N, 6.89. Found: C, 76.98; H, 8.43; N, 6.84.

ACKNOWLEDGMENT

Helpful discussion with Dr. H. J. Bernstein is acknowledged.

1. G. V. D. Tiers. J. Phys. Chem. **62**, 1151 (1958).
2. J. A. Pople, W. G. Schneider, and H. J. Bernstein. Can. J. Chem. **35**, 1060 (1957).
3. S. McLean, K. Palmer, and L. Marion. Can. J. Chem. **38**, 1547 (1960).
4. G. M. Bennet and M. M. Hafez. J. Chem. Soc. **287** (1941).

Received August 15, 1960.
Division of Pure Chemistry,
National Research Council,
Ottawa, Canada.

SCISSION OF STERICALLY HINDERED *vic*-DIOLS*

H. R. Goldschmid† and A. S. Perlin

The scission of *vic*-diols by lead tetraacetate (1) and periodic acid (2, 3) is strongly rate dependent on the stereochemistry of the glycol group attacked. This property has led to the view (4), now generally accepted, that the reaction usually involves formation of a coplanar cyclic intermediate complex between the glycol and oxidant. Complexing of this type is unlikely to occur if the projected valency angle of the glycol group is held rigidly in the region of 120–180° (5, 6, 7). Such a steric arrangement is found in several compounds that contain a *trans*-glycol group situated in a fused or bridged ring system, and the fact that these compounds fail to react with lead tetraacetate or periodate is in excellent agreement with the concept of the cyclic intermediate.‡ In this group of sterically hindered glycols are 1,6-anhydro-β-D-glucofuranose and -α-D-galactofuranose (8), the two *trans*-2,3-camphanediols (9), cholestane-3β,6β,7α-triol (10), 4,6-*O*-benzylidene methyl α-D-altropyranoside (11), and 2,6-anhydro-β-D-fructofuranose (12).

Steric effects that are strongly evident for oxidations with lead tetraacetate in acetic acid were noted by Hockett and Mowery (13) to be much less marked when pyridine was used as solvent. This observation suggested that the steric requirements for lead tetraacetate oxidation are less critical in pyridine than under the more usual reaction conditions, and prompted us to test the stability of the sterically hindered glycols towards lead tetraacetate in pyridine. Several of these compounds have now been examined and found, in fact, to be oxidized readily (Table I). That the reactions constitute true glycol cleavage is indicated by the degradation of 4,6-*O*-benzylidene methyl α-D-altropyranoside (I) (as well as the corresponding D-glucoside) to the dialdehyde isolated, as the hemialdal hydrate

*Issued as N.R.C. No. 5978.
†*National Research Council of Canada Postdoctorate Fellow, 1958–1960.*
‡*Trans-9,10-Decalindiol also appears unable to attain such a transition state but is nevertheless oxidized by lead tetraacetate, possible via an acyclic pathway (7). However, this compound resists attack by periodate (10).*

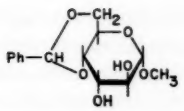

I

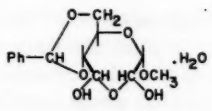

II

TABLE I

Scission of *vic*-diols by lead tetraacetate in pyridine (moles of oxidant consumed/mole at 0° C)

Time (minutes)	2,6-Anhydro-β-D-fructofuranose		*trans*-2-Exo-3-endo-camphanediol*	
	(2 moles)†	(4.5 moles)	(3 moles)	(4.5 moles)
15	0.11	0.60	0.35	0.83
30	0.19	0.69	0.42	0.93
60	0.29	0.81	0.50	1.00
180	0.44	1.02	—	1.06
480	0.57	1.30	—	1.08

	4,6-*O*-Benzylidene methyl α-D-glycopyranoside	
	D-Altro-	D-Gluco-
	(5 moles)	
5	0.51	1.01
15	0.71	1.02
30	0.82	1.07
60	1.03	—
180	1.04	1.16

	Ethyl β-D-fructofuranoside and derivatives			
	1,6-Di-*O*-trityl-‡		1,6-Di-*O*-tosyl-	Glycoside‡
	(1.6 moles)§	(5 moles)	(1.7 moles)§	(2.0 moles)
15	0.54	1.02	—	0.88
30	0.63	0.98	0.95	1.03
60	0.72	1.00	0.96	1.18
90	0.74	—	1.04	1.21

*Closely similar data were obtained for the 2-endo-3-exo-isomer.
†Figures in parentheses give the number of moles of lead tetraacetate used per mole of substrate.
‡Closely similar data were obtained for the α-anomer.
§Temperature, 25° C.

(II) (14), formed by periodate oxidation of 4,6-*O*-benzylidene methyl α-D-glucopyranoside* (14, 15, 16).†

A normally "slow" diol (17), *trans*-1,2-cyclopentanediol, was very rapidly oxidized, the observed uptake being 0.9 to 1.0 mole of lead tetraacetate per mole in 5 minutes reaction time, irrespective of whether the excess of oxidant used was 0.25, 1.0, or 3.0 moles per mole. By contrast, the rate of oxidation of the hindered diols fell off sharply at well below

*4,6-*O*-Benzylidene methyl α-D-glucopyranoside is oxidized at an unusually slow rate by periodate (11, 16). It also is extremely resistant to attack by lead tetraacetate in acetic acid, a property that is exhibited also by e,e trans-diols situated on 1,4-bonded central units of oligosaccarides (18). In pyridine, however, the benzylidene derivative is rapidly oxidized by lead tetraacetate (Table I and Experimental section).*

†*Cholestane-3β,6β,7α-triol (10) (a sample of which was kindly provided by Prof. S. J. Angyal) is more resistant to oxidation than the other compounds examined: the observed rate of lead tetraacetate uptake (mole/mole(min)) was 0.34 (15), 0.55 (90), and 0.80 (360). This result contrasts strongly with the behavior of I (Table I), which also contains a diaxal glycol group, and may be related to the greater rigidity of ring B in the cholestane derivative than of the pyranoside ring in I.*

the theoretical level if an excess of only 1 to 2 moles of lead tetraacetate was used (Table I). With an excess of 3 to 4 moles the data were much more satisfactory (Table I). The marked drop in reaction rate at the lower level of concentration may possibly be related to Criegee's suggestion (4) that acetic acid, formed in the reduction of lead tetraacetate to the diacetate, can depress the rate of oxidation in a solvent other than acetic acid by a mass-action effect. Such an effect would be most readily apparent with the most highly hindered glycols.

Although the stoichiometry of the various reactions examined is close to the theoretical value under suitable conditions, slow overoxidation is always evident (Table I). Because of this non-specific overoxidation several hydroxylated compounds, other than 1,2-glycols, were examined. In this group were 1,2,3,4- and 2,3,4,6-tetra-*O*-acetyl-D-glucopyranose; 1,3-dihydroxypropane; 1,3-dihydroxy-2,2-dimethylpropane; pentaerythritol; 1,6-dihydroxyhexane; 2,5-dihydroxyhexane; and 1,3,6-trihydroxyhexane. Of these compounds, only 1,3-dihydroxypropane was attacked to a significant degree during the period of 1 to 2 hours (Table I) required for complete oxidation of the hindered glycols, the consumption in 2 hours reaction time being 0.12 mole of lead tetraacetate per mole. With a more prolonged oxidation period (8 to 24 hours), several of the compounds reduced a small proportion of oxidant (0.1 to 0.2 mole/mole), and with pentaerythritol the consumption reached a value of 0.6 mole/mole in 24 hours. It is clear, therefore, that in testing for the presence of a 1,2-diol group in an unknown compound with lead tetraacetate in pyridine, prolonged reaction periods should be avoided.

Pyridine is particularly suitable for the glycol-cleavage oxidation of certain classes of compounds which might be unstable or poorly soluble in media used more commonly. Hockett and co-workers (13, 19) first employed this solvent for lead tetraacetate oxidation of sucrose and trityl ethers of methyl D-arabopyranoside, compounds unstable in acetic acid. Similarly, we have found these conditions of oxidation useful for determining the structure of trityl- and tosyl-derivatives of ethyl α- and β-D-fructofuranoside (12). The 1,6-ditrityl ether of these glycosides exhibited behavior that is characteristic of the highly hindered diols described above, in that their oxidation rates dropped sharply when a small excess of lead tetraacetate was used (Table I). As shown by Smith and co-workers (20), periodate oxidation may be inhibited when a trityl or phenyl group is in close proximity to the *vic*-diol, the effect being attributed to steric interference. However, interference by bulky substituents does not appear to account fully for the retarded oxidation rate of the ditrityl-D-fructofuranosides, because the corresponding 1,6-ditosyl derivative reacts readily and quantitatively (Table I).

EXPERIMENTAL

Lead tetraacetate was dried *in vacuo* over solid potassium hydroxide, and pyridine was freshly distilled over solid potassium hydroxide.

Measurement of Lead Tetraacetate Uptake

The stopping solution (1) used (per milliliter of reaction mixture) contained potassium iodide (1.0 g), sodium acetate (2.7 g, anhydrous) in water (10 ml). Acetic acid (3 ml) was added to the stopping solution immediately before an aliquot of the oxidation mixture in order to complete the liberation of iodine. A bulky yellow precipitate is formed when lead tetraacetate in pyridine is mixed with the stopping solution; determination of the iodine with thiosulphate was facilitated by adding starch indicator at the outset, the suspension being titrated until the pea-green color was discharged.

In a typical experiment, 2,6-anhydro-β-D-fructofuranose (13.0 mg) in pyridine (4 ml) was treated at 0° C with a solution of lead tetraacetate (160 mg) in pyridine (6 ml). (The solution of lead tetraacetate in pyridine is deep brown in color, and the intensity of the color diminishes as oxidant is used up.) At chosen intervals, 1-ml portions of the reaction mixture were transferred to the stopping solution, and the liberated iodine was titrated immediately with thiosulphate.

Oxidation of 4,6-O-Benzylidene Methyl α-D-Altropyranoside (I)

To a solution of the benzylidene glycoside (282 mg) in pyridine (15 ml), lead tetraacetate (1.32 g) was added. After 25 minutes at room temperature the reaction mixture was treated with oxalic acid dihydrate (4.0 g) and a few drops of water. The precipitate was filtered off, the filtrate concentrated *in vacuo* at 45° C, and the residue obtained was taken up in hot aqueous acetone. A crystalline product (201 mg) was deposited from the cooled solution, and after recrystallization from aqueous acetone the product II (14) had a melting point of 130–133° C and $[\alpha]_D^{27}$ +62.8° (*c*, 1.9, pyridine). Calculated for $C_{14}H_{18}O_7 \cdot H_2O$: C, 53.16%; H, 6.37%. Found: C, 53.25%; H, 6.44%.

On treatment with hot phenylhydrazine acetate the product yielded glyoxal bis-phenylhydrazone, m.p. 164–166° C, undepressed.

The above hemialdal hydrate furnished a bis-cyclohexylamine derivative (14) with a melting point of 115–117° C and $[\alpha]_D^{27}$ −32.6° (*c*, 1.2, pyridine). Calculated for $C_{26}H_{38}O_4N_2$: C, 70.55%; H, 8.65%. Found: C, 70.48%; H, 8.86%.

Oxidation of 4,6-O-Benzylidene Methyl α-D-Glucopyranoside

The benzylidene glycoside (282 mg) was treated in pyridine (10 ml) with lead tetraacetate (618 mg) for 15 minutes at room temperature. Excess oxidant was reduced with oxalic acid, and the reaction mixture was worked up, affording compound II (14), m.p. 130–133° C, undepressed, and $[\alpha]_D^{27}$ +63.0° (*c*, 1.8, pyridine). Calculated for $C_{14}H_{18}O_7 \cdot H_2O$: C, 53.16%; H, 6.37%. Found: C, 53.54%; H, 6.16%.

On treatment with hot phenylhydrazine acetate the product yielded glyoxal bis-phenylhydrazone, m.p. 164–166° C, undepressed.

The derived bis-cyclohexylamine derivative (14) had a melting point of 115–117° C, undepressed and $[\alpha]_D^{27}$ −31.9° (*c*, 1.2, pyridine). Calculated for $C_{26}H_{38}O_4N_2$: C, 70.55%; H, 8.65%. Found: C, 70.56%; H, 8.59%.

The X-ray powder diagrams obtained from the above hemialdal hydrate and its bis-cyclohexylamine derivative were indistinguishable from the corresponding materials obtained from 4,6-*O*-benzylidene methyl α-D-altropyranoside.

The authors gratefully acknowledge a gift of *trans*-2-exo-3-endo- and -2-endo-3-exo-camphanediol from Prof. S. J. Angyal, and of 4,6-*O*-benzylidene methyl α-D-altropyranoside from Dr. A. C. Neish. They also thank Mr. J. W. L. C. Christ for technical assistance. Microanalyses were performed by Mr. M. Mazurek and X-ray powder diagrams were prepared by Miss Inez Gaffney.

1. R. CRIEGEE. Ber. **64**, 260 (1931).
2. L. MALAPRADE. Bull. soc. chim. France, **39**, 325 (1926).
3. P. F. FLEURY and J. LANGE. Compt. rend. **195**, 1395 (1932).
4. R. CRIEGEE, L. KRAFT, and B. RANK. Ann. **507**, 159 (1933).
5. R. E. REEVES. *In* Advances in carbohydrate chemistry. Vol. 6. Academic Press, Inc., New York. 1951. p. 107.
6. R. J. DIMLER. *In* Advances in carbohydrate chemistry. Vol. 7. Academic Press, Inc., New York. 1952. p. 37.

7. R. CRIEGEE, E. HÖGER, G. HUBER, P. KRUCK, F. MARKTSCHEFFEL, and H. SCHELLENBERGER. Ann. **599**, 81 (1956).
8. R. J. DIMLER, H. A. DAVIS, and G. E. HILBERT. J. Am. Chem. Soc. **68**, 1377 (1946).
9. S. J. ANGYAL and R. J. YOUNG. J. Am. Chem. Soc. **81**, 5467 (1959).
10. S. J. ANGYAL and R. J. YOUNG. J. Am. Chem. Soc. **81**, 5251 (1959).
11. J. HONEYMAN and C. J. G. SHAW. J. Chem. Soc. 2454 (1959).
12. H. R. GOLDSCHMID and A. S. PERLIN. Can. J. Chem. This issue.
13. R. C. HOCKETT and D. F. MOWERY, JR. J. Am. Chem. Soc. **65**, 403 (1943).
14. R. D. GUTHRIE and J. HONEYMAN. J. Chem. Soc. 2441 (1959).
15. J. W. ROWEN, R. E. REEVES, and F. H. FORZIATI. J. Am. Chem. Soc. **73**, 4484 (1951).
16. J. BADDILEY, J. G. BUCHANAN, and L. SZABO. J. Chem. Soc. 3826 (1954).
17. R. CRIEGEE, E. BÜCHNER, and W. WALTHER. Ber. **73**, 571 (1940).
18. A. S. PERLIN and A. R. LANSDOWN. Can. J. Chem. **34**, 451 (1956).
19. R. C. HOCKETT and M. ZIEF. J. Am. Chem. Soc. **72**, 2130 (1950).
20. E. F. GARNER, I. J. GOLDSTEIN, R. MONTGOMERY, and F. SMITH. J. Am. Chem. Soc. **80**, 1206 (1958).

RECEIVED JULY 25, 1960.
NATIONAL RESEARCH COUNCIL OF CANADA,
PRAIRIE REGIONAL LABORATORY,
SASKATOON, SASKATCHEWAN.

Recueil des travaux chimiques des Pays-Bas

FONDÉ EN 1882 PAR

W. A. VAN DORP, A. P. N. FRANCHIMONT, S. HOOGEWERFF, E. MULDER ET A. C. OUDEMANS

EDITED BY THE ROYAL NETHERLANDS CHEMICAL SOCIETY

Generally the "Recueil des travaux chimiques des Pays-Bas" only accepts papers for publication from members of the Royal Netherlands Chemical Society who are also subscribers to the Recueil. Applications for membership of this society should be sent to The Secretariate, Lange Voorhout 5 The Hague.

The Recueil contains papers written in English, French or German and appears if possible monthly (the 15th of each month) except in August and September, in issues of varying size. It is obtainable from D. B. Centen's Uitgeversmaatschappij, 1e Weteringplantsoen 8, Amsterdam, or through any bookseller in Holland or abroad. The subscription is 30.— guilders for Holland and 32.50 guilders abroad. Authors receive 75 reprints of their papers free of charge.

Editorial Office: Lange Voorhout 5, The Hague.

NOTES TO CONTRIBUTORS

Canadian Journal of Chemistry

MANUSCRIPTS

General.—Manuscripts, in English or French, should be typewritten, double spaced, on paper 8½×11 in. **The original and one copy are to be submitted.** Tables and captions for the figures should be placed at the end of the manuscript. Every sheet of the manuscript should be numbered. Style, arrangement, spelling, and abbreviations should conform to the usage of recent numbers of this journal. Greek letters or unusual signs should be written plainly or explained by marginal notes. Characters to be set in bold face type should be indicated by a wavy line below the characters. Superscripts and subscripts must be legible and carefully placed. Manuscripts and illustrations should be carefully checked before they are submitted. Authors will be charged for unnecessary deviations from the usual format and for changes made in the proof that are considered excessive or unnecessary.

Abstract.—An abstract of not more than about 200 words, indicating the scope of the work and the principal findings, is required, except in Notes.

References.—These should be designated in the text by a key number and listed at the end of the paper, with the number, in the order in which they are cited. The form of the citations should be that used in this journal; in references to papers in periodicals, titles should not be given and only initial page numbers are required. The names of periodicals should be abbreviated in the form given in the most recent *List of Periodicals Abstracted by Chemical Abstracts.* All citations should be checked with the original articles and each one referred to in the text by the key number.

Tables.—Tables should be numbered in roman numerals and each table referred to in the text. Titles should always be given but should be brief; column headings should be brief and descriptive matter in the tables confined to a minimum. Vertical rules should not be used. Numerous small tables should be avoided.

ILLUSTRATIONS

General.—All figures (including each figure of the plates) should be numbered consecutively from 1 up, in arabic figures, and each figure referred to in the text. The author's name, title of the paper, and figure number should be written in the lower left corner of the sheets on which the illustrations appear. Captions should not be written on the illustrations.

Line drawings.—Drawings should be carefully made with India ink on white drawing paper, blue tracing paper, or co-ordinate paper ruled in blue only; any co-ordinate lines that are to appear in the reproduction should be ruled in black ink. Paper ruled in green, yellow, or red should not be used. All lines must be of sufficient thickness to reproduce well. Decimal points, periods, and stippled dots must be solid black circles large enough to be reduced if necessary. Letters and numerals should be neatly made, preferably with a stencil (**do NOT use typewriting**), and be of such size that the smallest lettering will not be less than 1 mm high when the figure is reduced to a suitable size. Many drawings are made too large; originals should not be more than 2 or 3 times the size of the desired reproduction. Wherever possible two or more drawings should be grouped to reduce the number of cuts required. In such groups of drawings, or in large drawings, full use of the space available should be made; the ratio of height to width should conform to that of a journal page (5½×7¾ in.) but allowance must be made for the captions. **The original drawings and one set of clear copies (e.g. small photographs) are to be submitted.**

Photographs.—Prints should be made on glossy paper, with strong contrasts. They should be trimmed so that essential features only are shown and mounted carefully, with rubber cement, on white cardboard, with no space between those arranged in groups. In mounting, full use of the space available should be made. **Photographs are to be submitted in duplicate;** if they are to be reproduced in groups one set should be mounted, the duplicate set unmounted.

REPRINTS

A total of 100 reprints of each paper, without covers, are supplied free. Additional reprints, with or without covers, may be purchased at the time of publication.

Charges for reprints are based on the number of printed pages, which may be calculated approximately by multiplying by 0.5 the number of manuscript pages (double-space typewritten sheets, 8½×11 in.) and including the space occupied by illustrations. Prices and instructions for ordering reprints are sent out with the galley proof.

Contents

S. Hartman and R. E. Robertson—Nucleophilic displacement of methyl sulphonic esters by hydroxide ion in water - - - - - - - - 2033

R. K. Brown and A. M. Eastham—The chemistry of ethylene oxide. VI. The acid-catalyzed reaction of ethylene oxide with ethanol–water mixtures 2039

A. F. McKay, D. L. Garmaise, G. Y. Paris, S. Gelblum, and R. J. Ranz—The preparation of substituted thionocarbamates - - - - - - - - 2042

G. A. Olah and A. A. Oswald—Organophosphorus compounds. VIII. O-Alkyl, O′-aryl phosphorofluoridothioates and O-aryl N-alkyl phosphoramidofluoridothioates - 2053

John C. Bartlet and D. Morison Smith—The determination of the areas of resolved and partially resolved chromatography peaks - - - - - - 2057

T. Schaefer and W. G. Schneider—Solvent effects as an aid in the analysis of the proton magnetic resonance spectrum of vinyl bromide - - - 2066

R. A. Bailey and L. Yaffe—Some factors affecting the zone mobility of inorganic ions during electromigration in paper - - - - - - - - 2074

F. Bruderlein, H. Bruderlein, H. Favre, R. Lapierre, and Y. Lefebvre—La réaction de Reformatsky appliquée à l'oxo-2 cyclohexane-propionitrile et à des céto-nitriles analogues - - - - - - - - - - - - - - 2085

F. W. Parrish, A. S. Perlin, and E. T. Reese—Selective enzymolysis of poly-β-D-glucans, and the structure of the polymers - - - - - - - - 2094

E. Whalley—Structure of Bridgman's black carbon disulphide - - - - - 2105

H. J. Campbell and J. T. Edward—Ionization of organic compounds in acid. I. Aliphatic ketones - - - - - - - - - - - - - - - - - - 2109

Richard F. W. Bader—The use of the Hellmann–Feynman theorem to calculate molecular energies - - - - - - - - - - - - - - - - - 2117

S. J. W. Price and K. O. Kutschke—The reactions of perfluoroethyl radicals with hydrogen and methane - - - - - - - - - - - - - - 2128

Owen H. Wheeler—Étard reaction. III. Nature of the complex - - - 2137

Denys Cook—The solid–liquid equilibrium between anhydrous magnesium chloride and N,N-dimethylformamide - - - - - - - - - - - - 2143

A. P. Baerg, R. M. Bartholomew, and R. H. Betts—Search for independent formation of Cs^{135m} in fission - - - - - - - - - - - - - 2147

R. A. Abramovitch, K. A. H. Adams, and A. D. Notation—Tryptamines, carbolines, and related compounds. Part VIII. δ-Carboline - - - - - - 2152

J. F. Henderson and E. W. R. Steacie—The photolysis of deuterated acetone and of deuterated acetone–hydrogen mixtures - - - - - - - - 2161

K. T. Leffek, J. A. Llewellyn, and R. E. Robertson—Some deuterium kinetic isotope effects. IV. β-Deuterium effects in water solvolysis of ethyl, isopropyl, and *tert*-butyl compounds - - - - - - - - - - - - 2171

H. R. Goldschmid and A. S. Perlin—Hydrogenolysis of carbohydrates. IX. Formation of 2,6-anhydro-β-D-fructofuranose and ethyl α- and β-D-fructofuranoside from sucrose - - - - - - - - - - - - - - - - - - 2178

R. J. Cvetanović and L. C. Doyle—Reaction of oxygen atoms with butadiene 2187

N. A. Warner and T. R. Ingraham—Decomposition pressures of ferric sulphate and aluminum sulphate - - - - - - - - - - - - - - - - - - 2196

A. M. Azzam—Studies on ionic solvation. Part III. New theory for calculating heats of hydration of monovalent ions at 25° C - - - - - - - - - 2203

J. N. Baxter and A. S. Perlin—2,3-*O*-Isopropylidene-L-*erythro*tetruronic acid and -L-erythrose, and the methyl D-*erythro*- and D-*threo*-tetrofuranosides - 2217

Robert R. Fraser—Chemical shifts in the N.M.R. spectra of substituted xylenes 2226

Ross Stewart and R. Van der Linden—The mechanisms of permanganate oxidation. VI. The oxidation of cyanide ion - - - - - - - - - 2237

Kenneth E. Hayes—The role of reaction products in the silver-catalyzed oxidation of ethylene - - - - - - - - - - - - - - - - - - 2256

Notes:

K. E. Mironov—On the existence of ternary compounds in the system NH_3–H_2O_2–H_2O - 2269

J. T. Edward, H. S. Chang, K. Yates, and Ross Stewart—Application of the Hammett equation to the hydrolysis of substituted benzamides - - 2271

R. A. Abramovitch—Tryptamines, carbolines, and related compounds. Part VII. Internuclear cyclization onto a pyridine ring - - - - - 2273

Alex Rosenthal and Alec Zaionchkovsky—The condensation of glyoxal with *p*-cresol - 2277

Stewart McLean—Nuclear magnetic resonance spectra of some model indoline derivatives - 2278

H. R. Goldschmid and A. S. Perlin—Scission of sterically hindered *vic*-diols 2280

Printed in Canada by University of Toronto Press